NNIN Research Highlights

August 2011

NNIN Site at Cornell University

Cornell Nanoscale Facility

Giant Proximity Effects in Confined Superfluid ^{4}He

Previous measurements of the specific heat of superfluid helium in confined structures have exhibited anomalous behavior thought to be related to coupling between neighboring cells through the channels by which they are filled. The Gasparini group from the Univ. or Buffalo has tested this hypothesis by using the etching and wafer bonding capabilities of the CNF to make extremely uniform and well-characterized confinement cells coupled by a uniform film of helium 31.7 nm thick. They quantified the effects of coupling between the confinement cells and also observed enhanced superfluidity in the 2-d film of Helium due to coupling with the confinement cells. Surprisingly, these proximity effects can occur over distances of order 100 times the superfluid correlation length, a puzzle the group is working to understand.

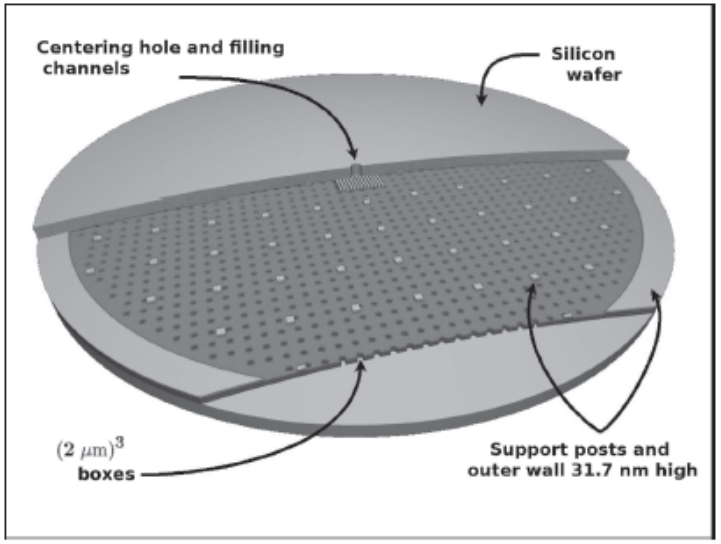

Diagram of the cell used to confine liquid helium.

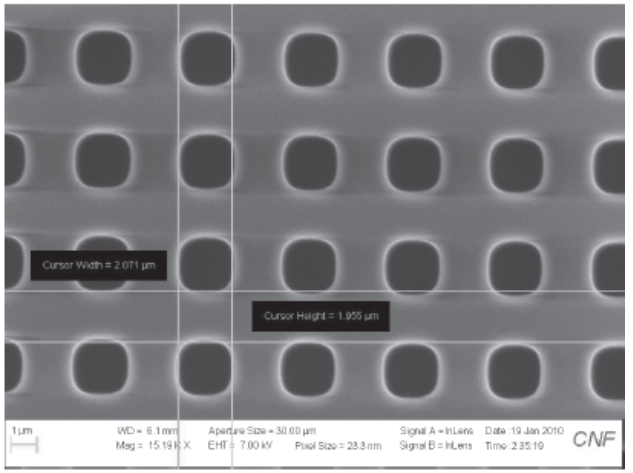

An array of (2 µm)^3 boxes etched from SiO_2.

J. K. Perron and F. M. Gasparini, Univ. Buffalo
Work performed at Cornell NanoScale Facility

Nature Physics ***6****, 499 (2010).*

Ultrafast Switching in Magnetic Tunnel Junction Based Orthogonal Spin Transfer Devices

Orthogonal spin-transfer magnetic random access memory (OST-MRAM) uses a spin-polarizing layer magnetized perpendicularly to a free layer to achieve large spin-transfer torques and ultrafast energy efficient switching. The Kent group from NYU has used the CNF to fabricate OST-MRAM devices that incorporate a perpendicularly magnetized spin-polarizing layer to apply a spin torque to a magnetic free layer together with a magnetic tunnel junction on top of the free layer to read out its orientation. They measured reliable magnetic switching at room temperature with 0.7 V amplitude pulses of 500 ps duration. The switching is bipolar, occurring for positive and negative polarity pulses, consistent with a precessional reversal mechanism, and requires an energy of less than 450 femtoJoules.

H. Liu, D. Bedau, D. Backes, P. Manandhar, S. Nanda, and A. D. Kent (New York Univ.)
Work performed at Cornell NanoScale Facility

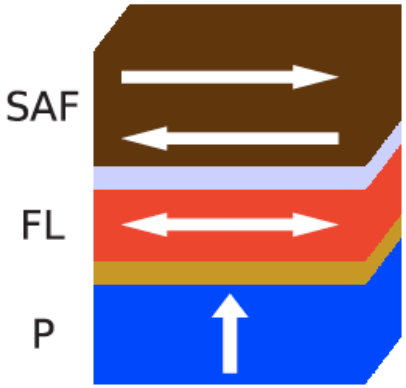

Diagram of the magnetic layer stack. A perpendicularly-magnetized polarizer (P) generates a spin torque to control an in-plane-polarized magnetic free layer (FL). The other electrode, a reference layer, consists of a synthetic antiferromagnet (SAF).

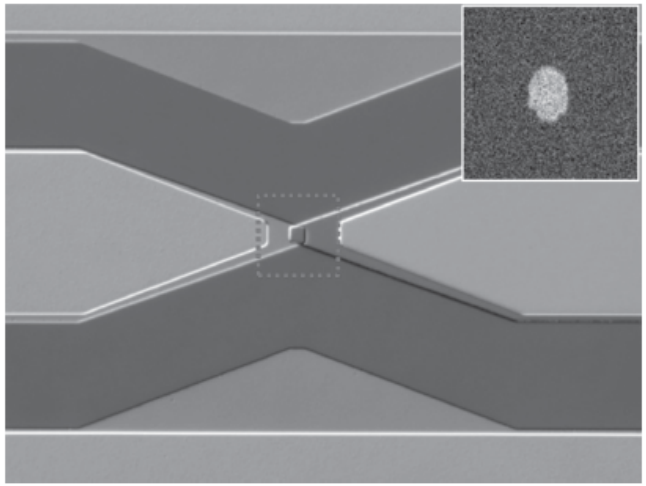

Optical microscopy image showing the top and bottom electrodes for a MRAM device. Inset: SEM image of a 100 x 150 nm^2 elliptical nanopillar cross section.

Applied Physics Letters ***97****, 242510 (2010).*

Microstrip SQUID Amplifiers with Submicron Josephson Junctions

The Plourde (Syracuse Univ.) and McDermott (Univ. of Wisconsin, Madison) research groups have used the CNF to develop amplifiers based on a dc superconducting quantum interference device (SQUID) with submicron Al–AlO_x–Al Josephson junctions. The small junction size reduces their self-capacitance and enhances the SQUID performance compared to SQUIDs with micron-scale junctions. This allows greatly improved amplifier gain at gigahertz frequencies compared to the previous state of the art. Measurements at 310 mK exhibit gain of 32 dB at 1.55 GHz.

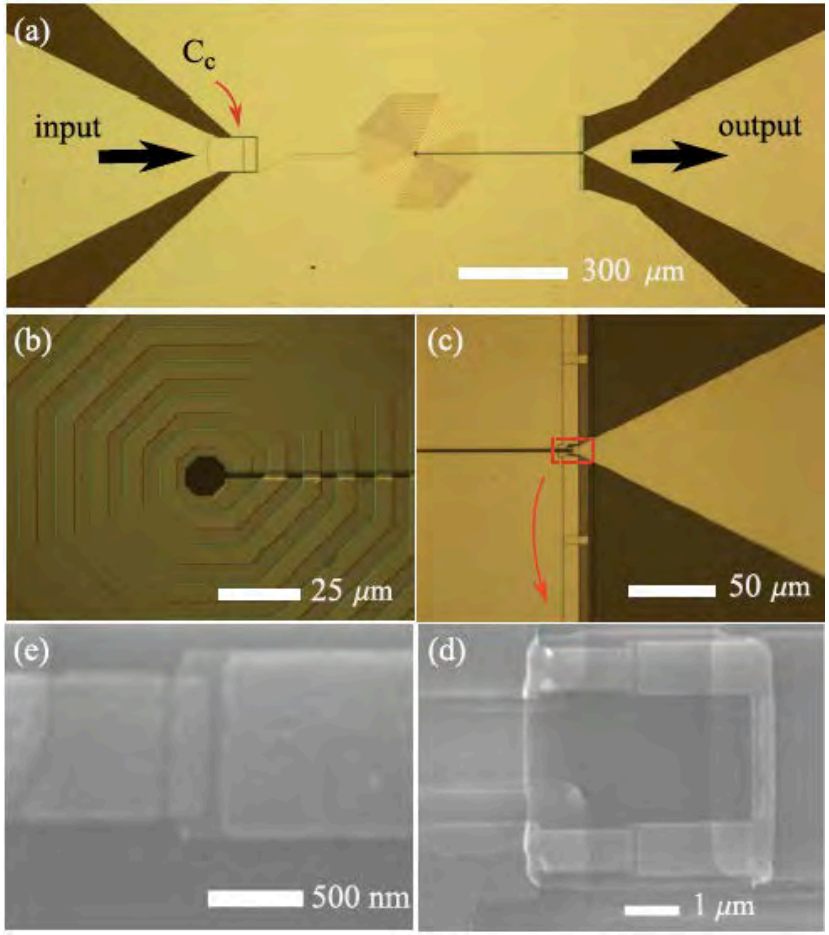

(a) Optical micrograph of the superconducting amplifier, showing coil, input and output ports, and input coupling capacitor. (b) Closeup of input coil. (c) Closeup of junction and shunt region. (d) Scanning electron micrograph of junctions. (e) Closeup of a single junction.

B. L. T. Plourde group (Syracuse Univ.) and R. McDermott group (Univ. of Wisconsin, Madison)
Work performed at Cornell NanoScale Facility

Applied Physics Letters ***97****, 092507 (2010).*

Persistent Currents in Normal Metal Rings

Measurements of persistent currents in micron-scale metal rings at cryogenic temperatures can be used to test the validity of the theory that explains electronic diffusion in metallic systems. The values of these currents are a random function of the disorder profile in the metal ring, and thus different from sample to sample. By measuring persistent currents in 8 different rings as a function of magnetic field using Si cantilever magnetometers made at the CNF, the research group of Jack Harris at Yale has characterized the statistical distributions of variations in the persistent currents for the first time. The measurements are in good agreement with predictions for the quantum mechanics of electrons in metals.

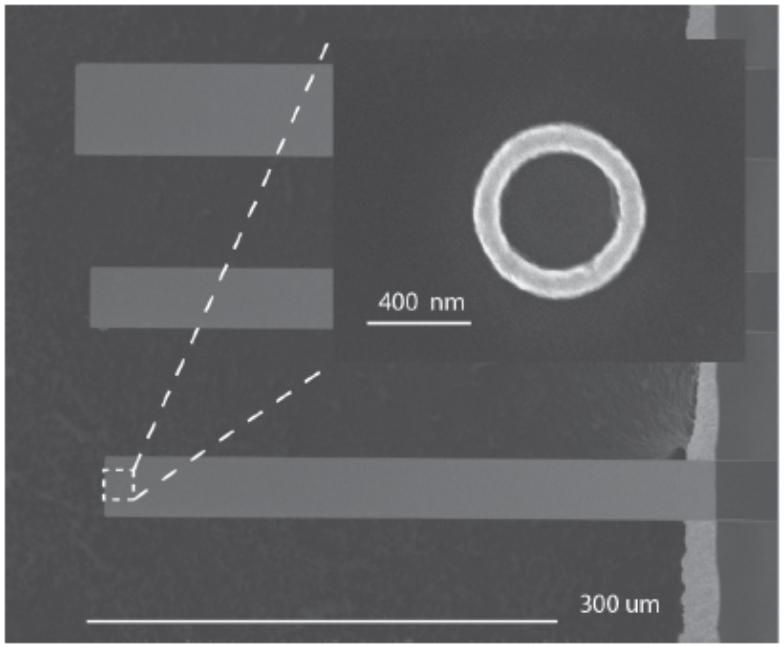

Main picture: Several Si cantilevers similar to those used in the experiment. Inset: An individual metal ring fabricated on one cantilever.

M. A. Castellanos Beltran, E. Ginossar, W. E. Shanks, and J. G. E. Harris, Yale University
Work performed at Cornell NanoScale Facility

Physical Review B **81**, 155448 (2010) [selected as an Editor's Suggestion]

Dynamical Bifurcation and Quantum Coherence in Arrays of Superfluid Josephson Junctions

Yuki Sato from the Rowland Institute at Harvard has used the CNF to make arrays of nanoscale apertures in silicon nitride membranes to study the quantum-mechanical flow of superfluid helium through the array. By applying a variable phase difference across the array using a heat gradient, he observed patterns of constructive and destructive interference for superfluid flow through different apertures. He also studied the dynamics of the superfluid flow under sufficiently strong AC driving to enter a nonlinear dynamical regime, where he observed a dynamical bifurcation – an abrupt transition between two different flow states.

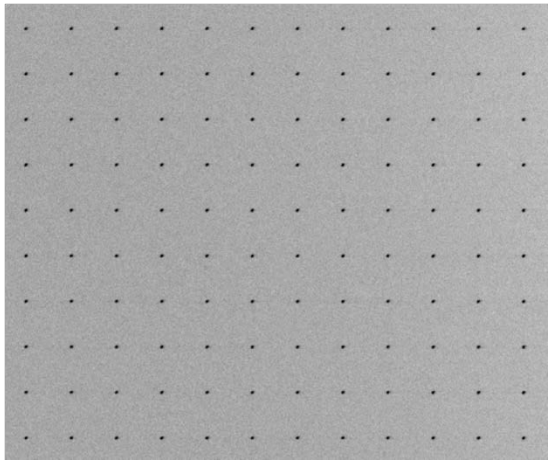

Aperture array: 60 nm apertures spaced by 2 μm in a 60 nm thick silicon nitride membrane

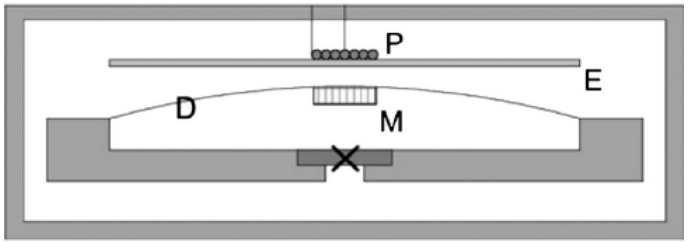

Experimental apparatus to measure superfluid He flow through the aperture array, by detecting the displacement of the thin membrane.

Y. Sato, The Rowland Institute at Harvard, Harvard University
Work performed at Cornell NanoScale Facility

Physical Review Letters **105**, 205302 (2010)
Physical Review Letters **106**, 055302 (2011)

Grains and Grain Boundaries in Single-Layer Graphene Atomic Patchwork Quilts

The Park, McEuen, and Muller groups at Cornell have used the facilities of the CNF to help develop new techniques to characterize and optimize the properties of single-atom thick graphene sheets made by chemical vapor deposition. By mounting graphene on silicon nitride scaffolds and imaging in a scanning transmission electron microscope, they determined the location and identity of every atom at graphene grain boundaries. They also used diffraction-filtered imaging to rapidly map the location, orientation, and shape of hundreds of grains and boundaries simultaneously. They were able to show that grain boundaries severely weaken the mechanical strength of graphene membranes but do not as drastically alter their electrical properties.

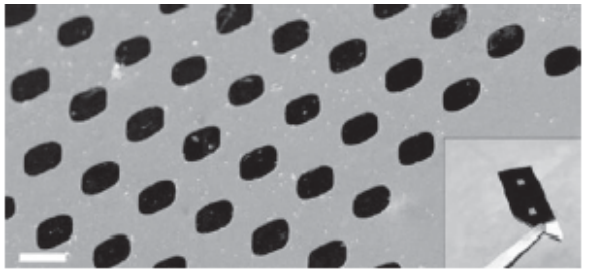

An array of graphene membranes suspended on a silicon nitride scaffold.

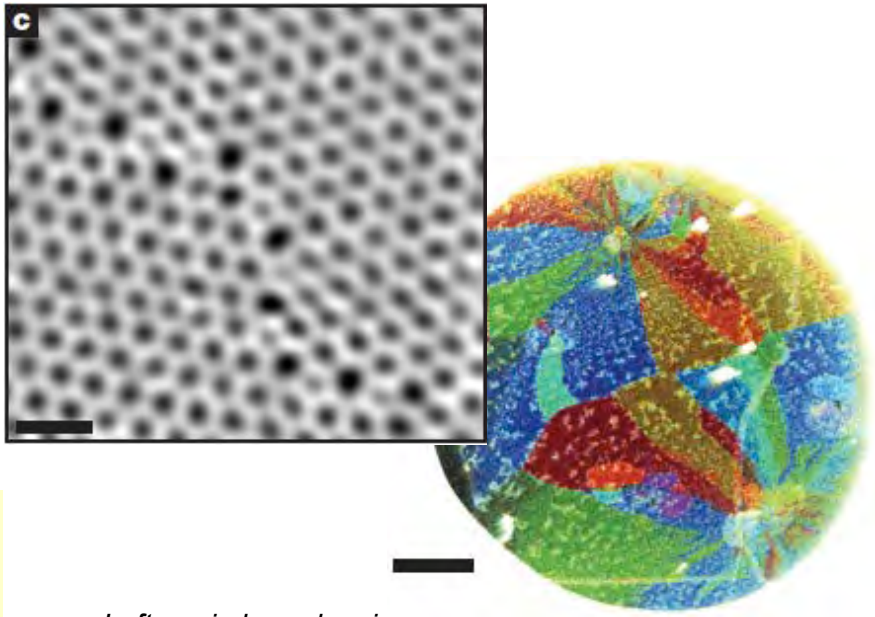

Left: grain boundary imaged within a graphene membrane. Left scale bar 0.5 nm. Right: color-coded depiction of grain orientations within one graphene membrane. Right scale bar 500 nm.

J. Park, P. L. McEuen, and D. A. Muller groups, Cornell University
Work performed at Cornell NanoScale Facility

Nature **469**, 389 (2011)

Single Crystal Homo- and Heteroepitaxial Nanostructures Made by Self Assembly within Block Copolymers

One of the key challenges in the field of inorganic solids is the development of epitaxial single-crystal nanostructures. The Wiesner, Thompson, and Muller groups at Cornell have used the facilities of the CNF to make nanoporous templates using block copolymers within which single-crystal nanostructures can be grown. They place the templates on a silicon substrate, fill the templates with amorphous silicon or NiSi, and then use a laser pulse to melt and crystallize the added material. The nanoscale confinement in the template allows for controlled growth of single-crystal epitaxial nanostructures. These results suggest a general strategy for growing single-crystal nanostructures for a wide variety of applications, including energy conversion and storage.

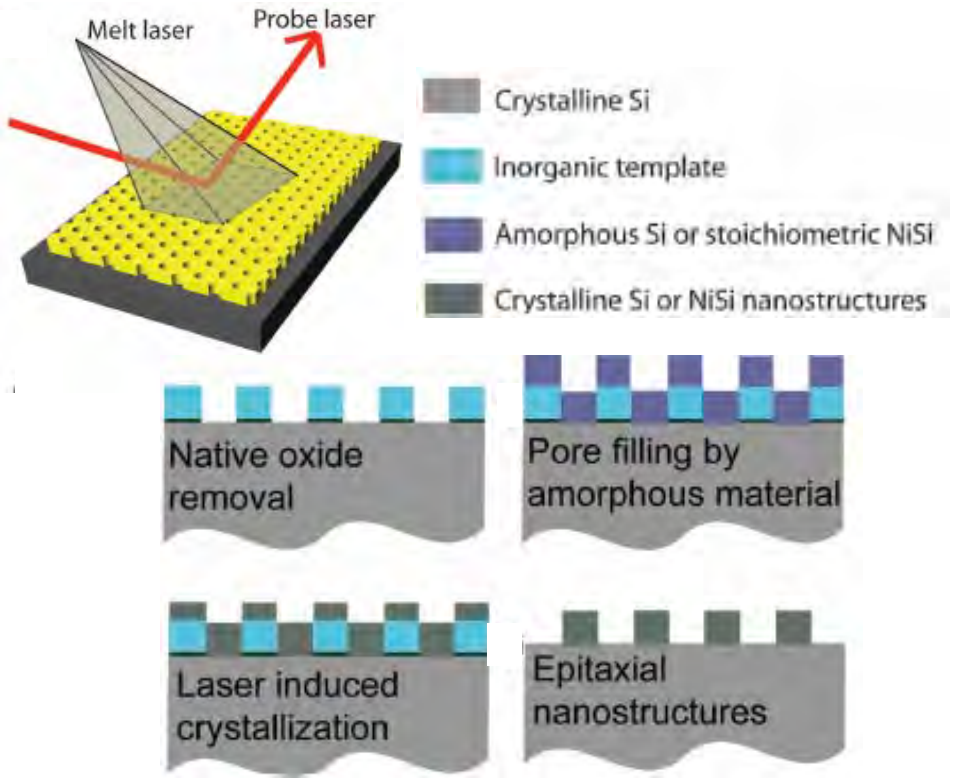

U. Wiesner, M. O. Thompson, and D. A. Muller groups, Cornell University
Work performed at Cornell NanoScale Facility

Science **330**, 214 (2010)

Large-Scale Arrays of Single-Layer Graphene Resonators

The Parpia, Craighead, and McEuen groups at Cornell used the CNF to fabricate large arrays of suspended, single-layer graphene membrane resonators made using chemical vapor deposition (CVD) growth followed by patterning and transfer. They found that the resonators can be modeled as flat membranes under tension, and that clamping the membranes on all sides reduces the variation in frequency between identical resonators. The quality factors improve dramatically with cooling, reaching values up to 9000 at 10 K. These measurements show that it is possible to produce large arrays of CVD-grown graphene resonators with reproducible properties and the same excellent electrical and mechanical properties previously reported for exfoliated graphene.

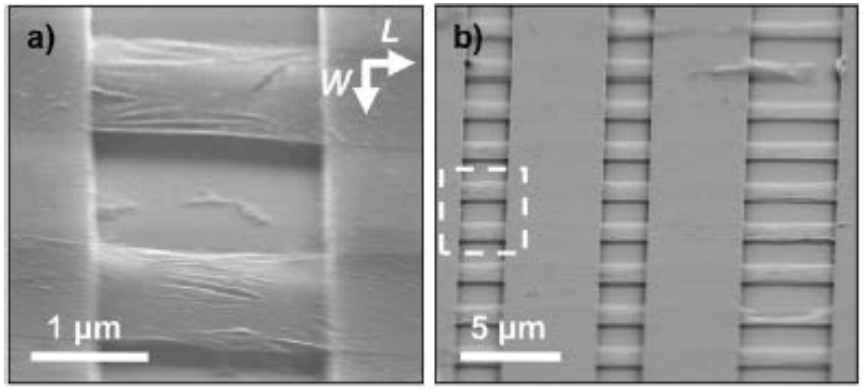

Angled scanning electron microscope pictures of arrays of graphene resonators.

J. M. Parpia, H. G. Craighead, and P. L/. McEuen groups, Cornell University
Work performed at Cornell NanoScale Facility

Nano Letters **10**, 4869 (2010)

Single-Walled Carbon Nanotubes as Excitonic Optical Wires

The Jiwoong Park group at Cornell has used the CNF to make carbon nanotube devices optimized for optical studies. By measuring the absolute intensity of Rayleigh scattering of light from individual nanotubes, they showed that single-walled carbon nanotubes act as ideal optical wires. The nanotubes display a uniform peak optical conductivity of ~8 e^2/h, suggesting universal behavior similar to that observed in the low-frequency electrical conductance of nanotubes.

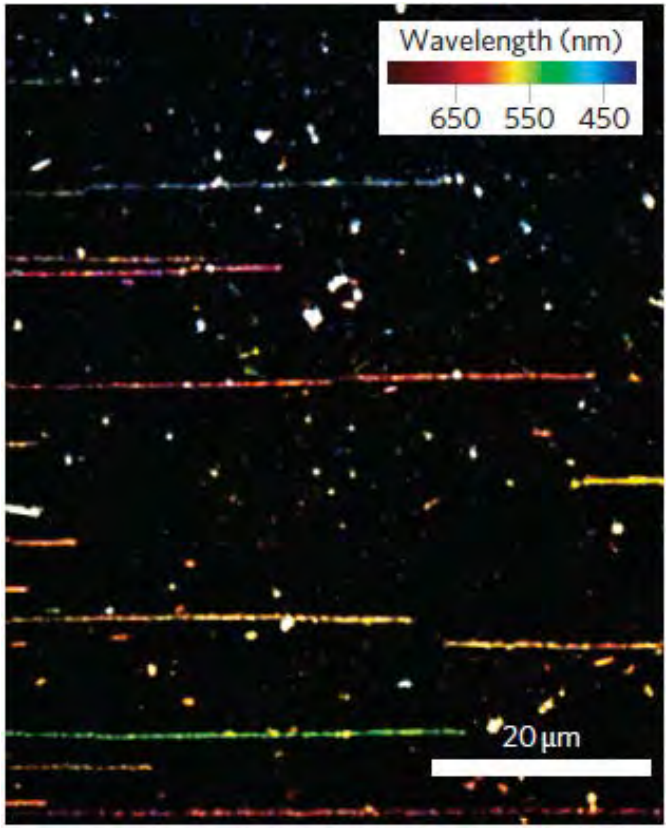

Spatial Rayleigh scattering image showing signals from more than 10 carbon nanotubes simultaneously (in false color, corresponding to the peak scattered wavelengths)

Jiwoong Park group, Cornell University
Work performed at Cornell NanoScale Facility

Nature Nanotechnology **6**, 51 (2011)

Spin-Torque Ferromagnetic Resonance Induced by the Spin Hall Effect

The Buhrman and Ralph groups at Cornell have used the CNF to make devices to investigate a new mechanism for manipulating the magnetization direction in nanoscale magnetic devices. They fabricated Pt/permalloy bilayers designed so that when electrons flow through the Pt they generate a perpendicular flow of electron spin current (due to the Spin Hall Effect, arising from spin-orbit scattering in the Pt) that travels to the permalloy layer and applies a torque to it. They demonstrated that this torque arising from the Spin Hall Effect is sufficiently strong to excite magnetic precession in the ferromagnetic film. They also were able to use this technique to make an accurate measurement of the strength of the Spin Hall Effect.

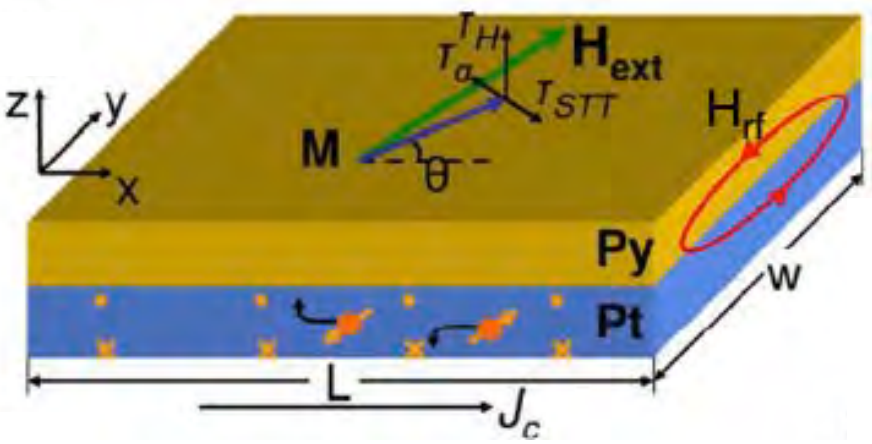

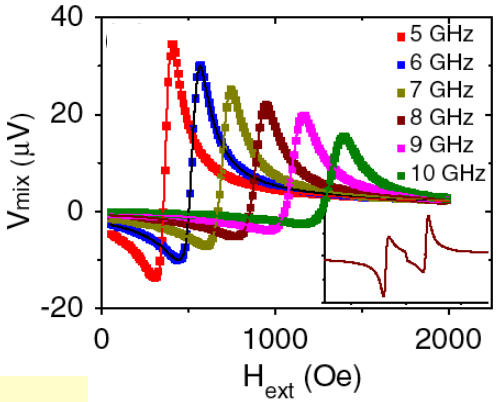

Top: Diagram depicting how the scattering of oppositely-pointing spins in Pt by the Spin Hall Effect generates a net flow of spin current perpendicular to the charge current. Bottom: magnetic resonance curves excited by the spin Hall torque in a Pt/permalloy bilayer.

R. A. Buhrman and D. C. Ralph groups, Cornell University
Work performed at Cornell NanoScale Facility

Physical Review Letters **106**, 036601 (2011)

Time-Resolved Measurement of Spin Torque in Magnetic Tunnel Junctions

The bias dependence of the torque that a spin-polarized current exerts on ferromagnetic elements is important for understanding fundamental spin physics in magnetic devices and for applications. However, previous techniques have provided only indirect measures of the torque and their results regarding the bias dependence are contradictory. Using the device fabrication facilities of the CNF, the Buhrman and Ralph groups at Cornell have developed time-domain techniques to measure the bias dependence of spin torque in nanoscale magnetic tunnel junctions by directly detecting the amplitude of magnetic precession in response to an oscillating spin torque. At high bias they found that the spin-torque vector differs markedly from the approximations commonly assumed.

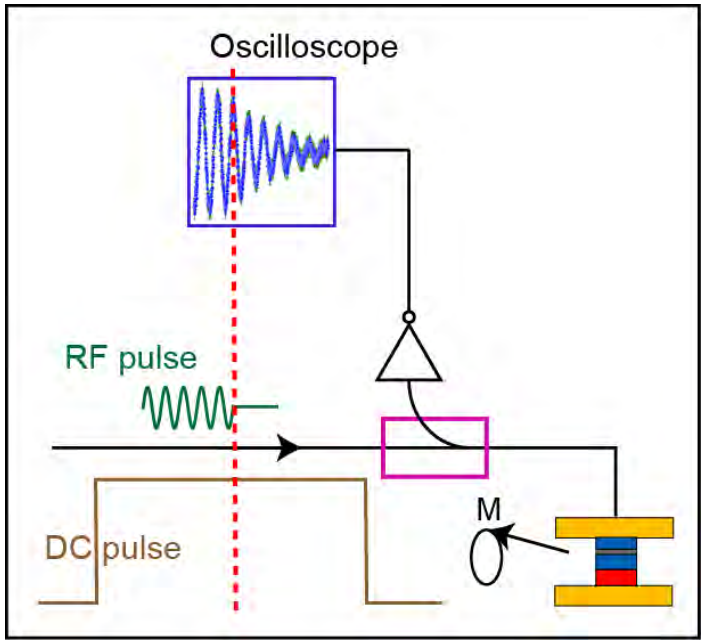

Schematic of the measurement strategy to detect current-induced magnetic precession in a nanoscale magnetic tunnel junction.

R. A. Buhrman and D. C. Ralph groups, Cornell University
Work performed at Cornell NanoScale Facility

Nature Physics **7**, 496 (2011)

Ultra-low Voltage, Ultra-small Mode Volume Silicon Microring Modulator

Low voltage operation of nanophotonic modulators is an important condition for providing the future bandwidth needs via nanophotonic-electronic integration. In particular, the operating voltage of silicon nanophotonic modulators must scale aggressively as rail voltages (Vdd) for digital nano-electronics scale to 600 mV in future CMOS platforms. a high speed, low voltage modulator remains to be demonstrated on silicon. This work demonstrates GHz modulation in a **2.5 μm radius** silicon micro-ring, with only **150 mV** peak to peak drive voltage and an electro-optic modal volume of only 2 μm^3. Low drive voltage and ultra low switching energy operation by biasing the modulator near the optimum charge injection efficiency point of the electro-optic device. This feature is unique to carrier injection modulators enabling ultra low voltage operation in contrast with other techniques for electro-optic structures. The swing voltage and the micro-ring modulator are the smallest demonstrations so far in silicon. This approach lays the ground work for a new class of high-speed low-voltage modulators enabling seamless integration of nanophotonics with low voltage CMOS nano-electronics.

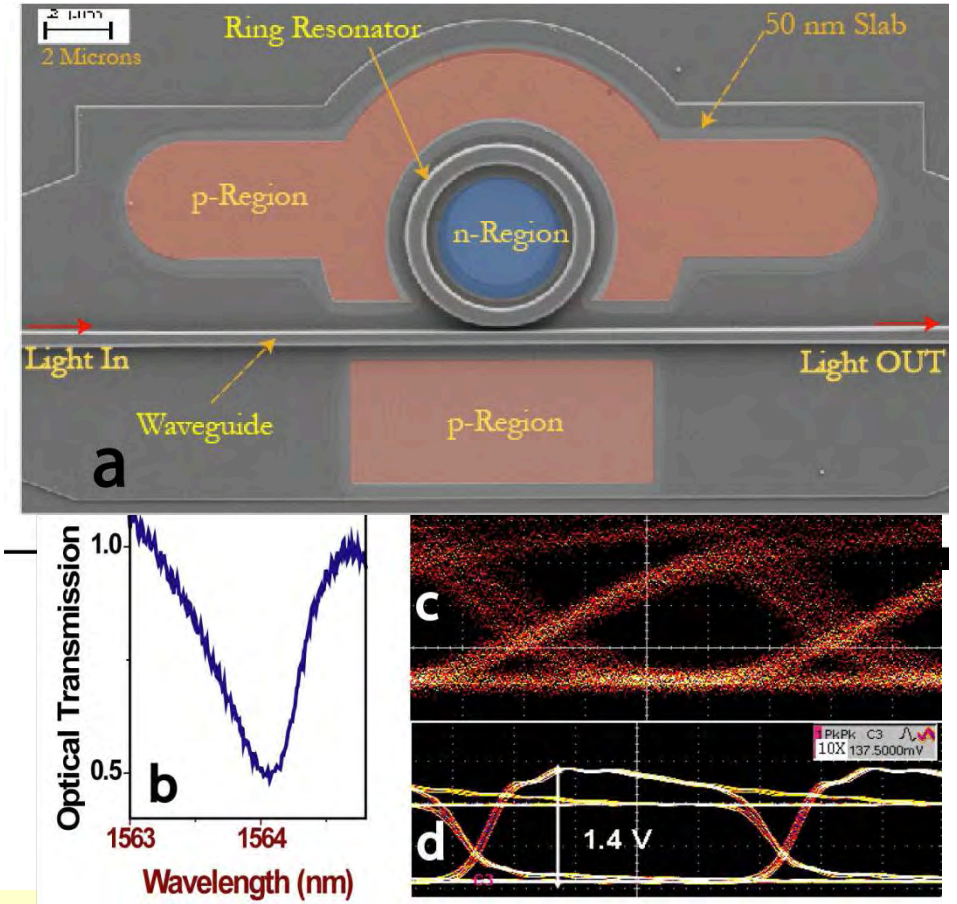

S. Manipatruni, K. Preston, Long Chen, and Michal Lipson,
Cornell University
Work performed at Cornell NanoScale Facility

2010 / Vol. 18, No. 17 / OPTICS EXPRESS

Transformation Optics on a Silicon Platform

Transformation optics (TO) reveals that the geometry of space and its constitutive parameters (i.e., permittivity and permeability tensors) affect electromagnetic waves equivalently. In reality TO allows the implementation of virtual geometries in the real universe through specially designed, inhomogeneous dielectrics. Because TO generally creates devices with continuous, highly inhomogeneous constitutive parameters, their fabrication must be precisely controlled on the scale of the wavelength. wavelength bandwidth. This work concentrates on developing designs in silicon and compatible materials for their scalability to optical wavelengths. Maxwell's fish eye at the right is an in-plane lens capable of perfect imaging without the use of negative refraction. Any source point on the surface of the lens produces a perfect image of itself on the opposite side of the lens. The fish eye is based on the conformal mapping of a spherical surface into a plane, thus it does not present any anisotropy. an SEM of the fabricated lens on the silicon platform. The images obtained also show that the discretization of the gradient index into nanometer size structures produces backscattering and is ultimately responsible for the focusing limit of the fish eye.

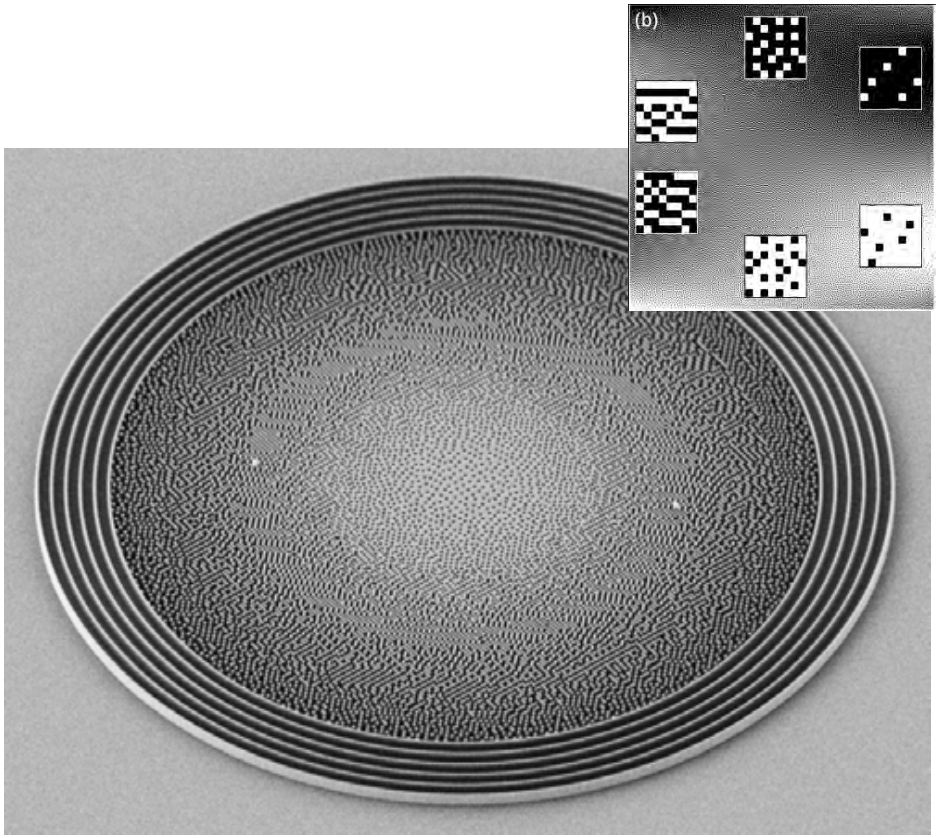

SEM of the fabricated Maxwell's fish eye with a distributed Bragg reflector surrounding it. The source and drain (where the image is formed) are based on gold dots used to scatter light into and out of the device layer.

Lucas H Gabrielli and Michal Lipson, Cornell University
Work performed at Cornell NanoScale Facility

J. Optics, V. 13, Nov. 2010.

CMOS-Compatible Temperature Insensitive Silicon Microring Modulator

This work demonstrates a passively temperature stabilized silicon electro-optic modulator, consisting of a ring resonator coupled to a Mach-Zehnder interferometer with tailored mode confinement. It has shown 2 GHz modulation over a 40° C temperature range. The basic photonic structure consists of a ring resonator overcoupled to a balanced Mach-Zehnder interferometer (MZI) that counteracts the thermal drift of the ring. The ring has an integrated p-i-n diode around it for injection and extraction of electrons and holes. The additional degree of freedom in the choice of waveguide widths, apart from just the lengths, enables one to set the thermal dependence of the MZI to be equal and opposite to that of the ring. The waveguide widths and lengths are chosen in the two arms of the MZI to give a balanced transmission while having a strong negative temperature sensitivity. The ring has a large enough waveguide width to enable highly confined single mode operation, and consequently strong positive temperature sensitivity. The relative temperature sensitivities of the ring and the MZI are designed to be equal and opposite to cancel each other out.
The fabricated device shows athermal-like behaviour over a wide temperature range (~40 degrees). This is approximately 40 times the operating temperature range of 1° C for a standard resonator modulator with Q = 10,000.

.

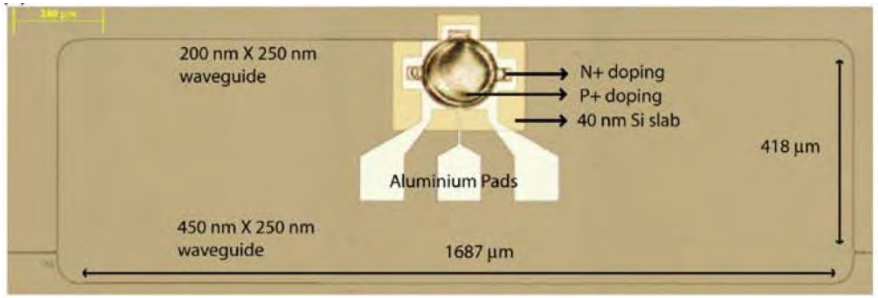

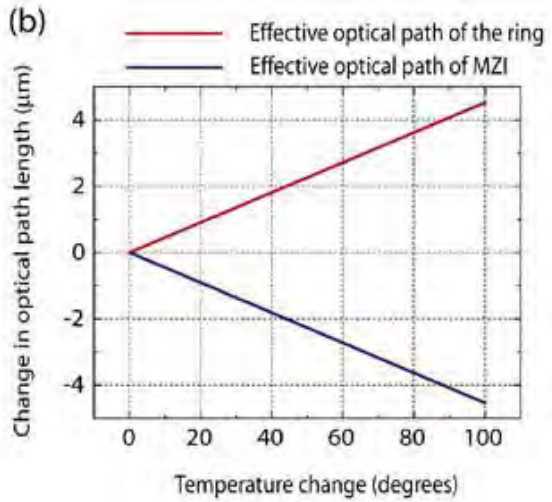

Biswajeet Guha, Michal Lipson, Cornell University

Work performed at Cornell NanoScale Facility

Optics Express, Vol. 18, 2010

Nanofountain Probes for the Delivery of Molecular Inks

The Nanofountain Probe functions as a highly miniaturized fountain pen that can be used to deliver a variety of materials with precision in the 50 nm to 1 μm range. As in a conventional fountain pen, the liquid material to be delivered (the “ink”) is contained in a reservoir and flows through a channel to an apertured dispensing tip (Figure 1). Past demonstrations of direct-write nanopatterning include proteins and DNA in buffer solution, gold nanoparticles in aqueous suspension, thiols, and drug-coated nanodiamonds. Piezoelectric positional control of the NFP by an AFM enables ultra-precise prescription of pattern geometry. The accuracy of the NFP combined with the broad range of molecular delivery capabilities enable studies at a truly single cell level through two modes of delivery: direct write nanopatterning, and direct in vitro injection.

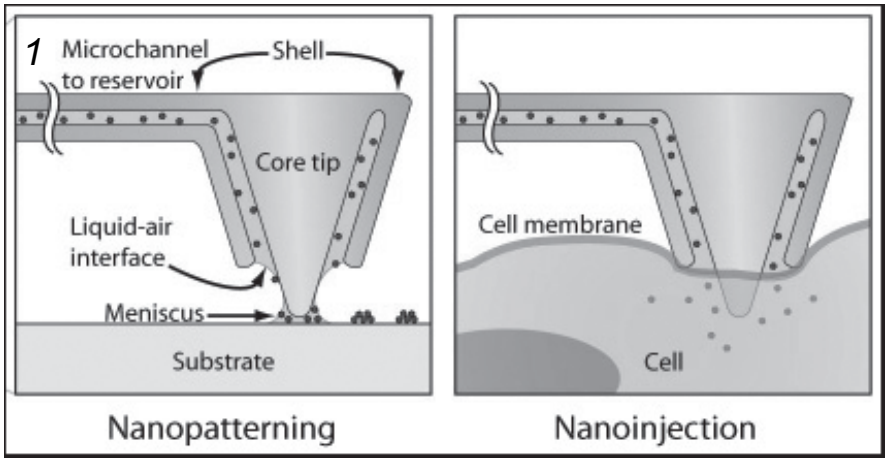

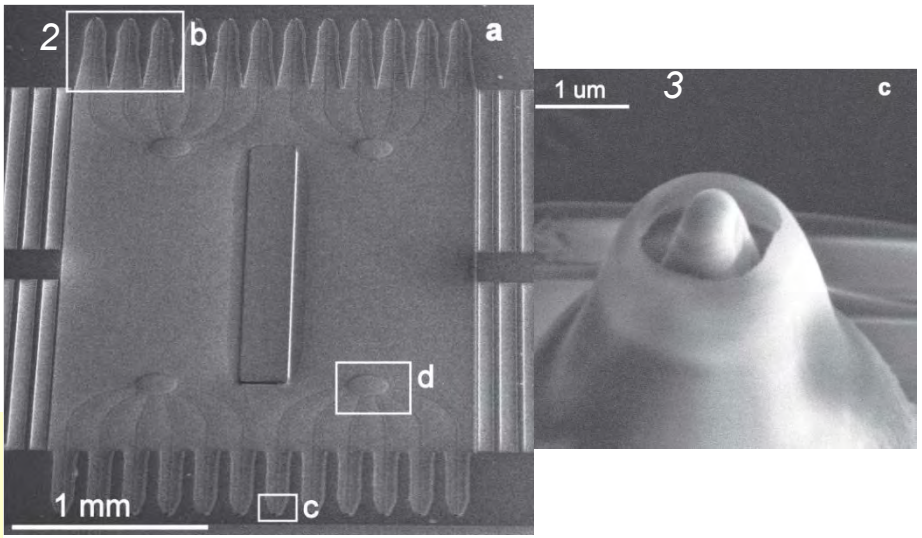

H. D. Espinosa , A. Safi, O. Loh, N. Moldovan,
Northwestern University
Work performed at Cornell NanoScale Facility

3rd IEEE International Nanoelectronics Conference, Vol. 1-2

Electron waveguide "Y-Branch Switch"

The y-branch switch was first proposed in 1992 and was shown that when operating under single mode coherent transport, there was no theoretical thermal limit for switching energy. The switching voltage is related to the transient time of the electron through the branching region. In this switching mode, the voltage required to turn the device ON and OFF is in the mV range. These devices show promising characteristics that may be capable of a variety of low-power logic applications. The device layout of the YBS has a one dimensional channel that branches off into two drain output channels. By applying a transverse external gate voltage across the central branching region, electrons can be guided into either of the two drain outputs depending on the direction of the field. This device consists of a GaAs/AlGaAs quantum well heterostructure grown on a GaAs substrate. Switching characteristics of the YBS are shown in the figure at the lower right. A voltage difference was applied between the central stem waveguide and the two drain waveguides. A transverse gate potential was applied between the two adjacent two dimensional gas reservoirs which were creased during the central waveguide isolation plasma etch. Although the current ratio between the two drain waveguides is minimal, the concept of the Y-Branch Switch operation is observed

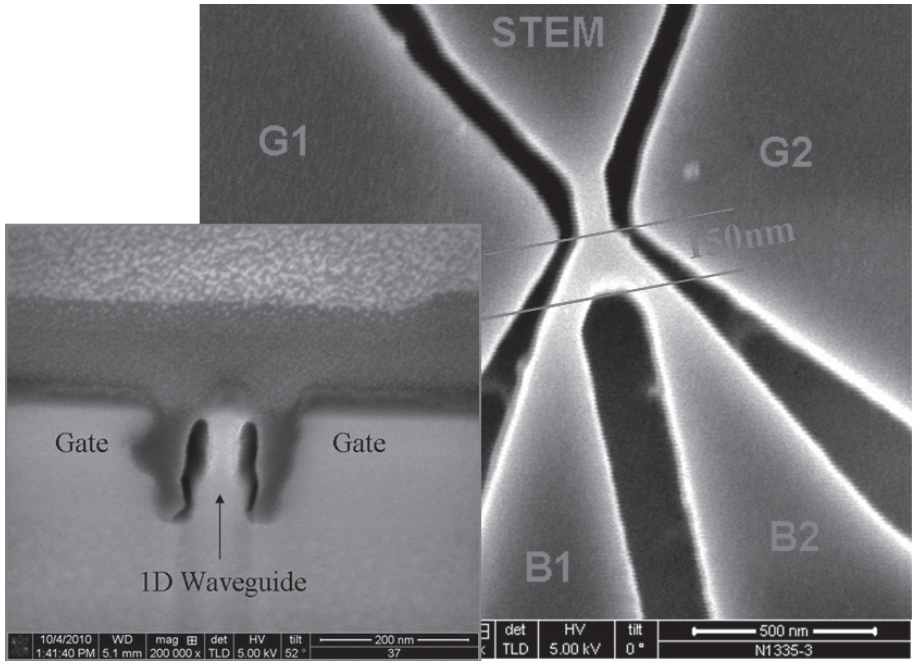

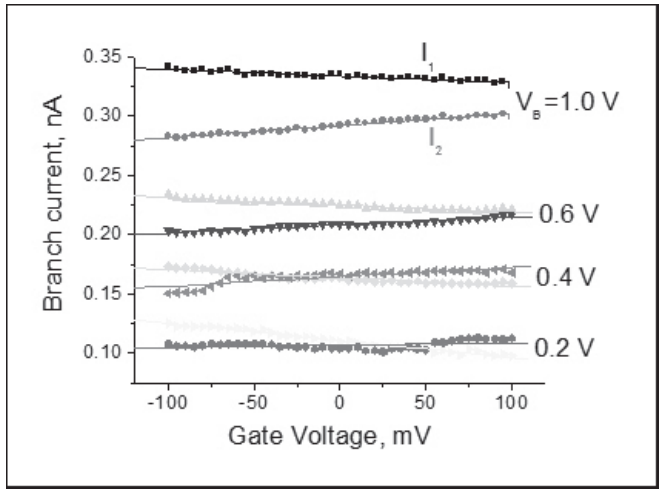

Andrew Greene, Serge Oktyabrsky
CNSE, State University of New York at Albany University
Work performed at Cornell NanoScale Facility

Multicomponent Biomolecular Arrays Generated By Aligned Printing With Parylene Peel-Off

The Craighead group at Cornell has used the CNF to develop a high-throughput "Print-and-Peel" method to generate multicomponent biomolecular arrays with sub-100 nm nanoscale feature widths. An inkjet printer is first aligned to a parylene template containing nanoscale openings. After printing, the parylene is peeled off to reveal uniformly patterned nanoscale features, despite the imperfect morphologies of the original inkjet spots. The researchers further patterned combinatorial nanoarrays by performing a second print-run superimposed over the first, thereby extending the multiplexing capability of the technique.

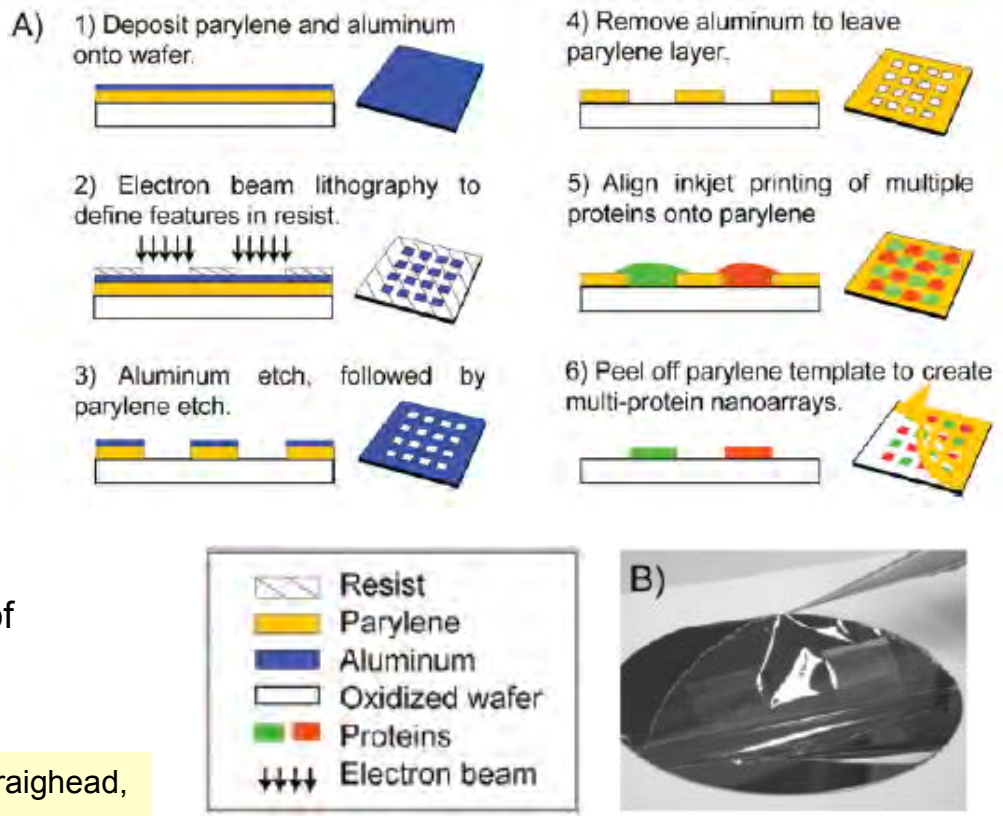

C. P. Tan, B. R. Cipriany, D. M. Lin, and H. G. Craighead,
Cornell University
Work performed at Cornell NanoScale Facility

Nano Letters ***10****, 719 (2010).*

Fabrication of a Nanomechanical Mass Sensor Containing a Nanofluidic Channel

Nanomechanical resonators operating in vacuum are capable of detecting and weighing single biomolecules, but their application to the life sciences has been limited by viscous forces that impede their motion in liquid environments. A promising approach to avoid this problem is to encapsulate the fluid completely within a mechanical resonator that is surrounded by vacuum. The Parpia and Craighead groups at Cornell have used CNF to fabricate and evaluate the performance of doubly clamped beam resonators that contain a filled nanofluidic channel and have a mass of less than 100 pg. These nanochannel resonators when filled with fluid have quality factors as high as 800, two orders of magnitude higher than comparable resonators operating in fluid. The group's analysis suggests that realistic improvements in the quality factor and frequency stability of nanochannel resonators should render these devices capable of sensing attogram masses from liquid.

A suspended nanofluidic channel 20 µm long.

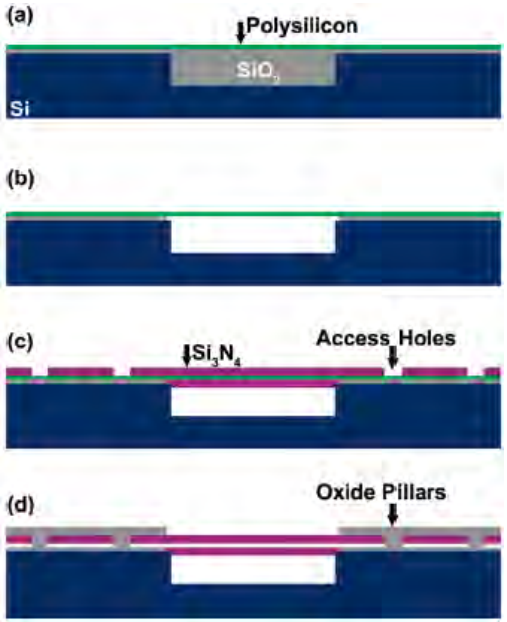

Fabrication process to form the suspended nanofluidic channel.

J. M. Parpia and H. G. Craighead groups, Cornell Univ.
Work performed at Cornell NanoScale Facility

Nano Letters ***10****, 2058 (2010).*
NNIN Research Highlights 2011

Batch Fabrication of Cantilevered Magnets on Attonewton-Sensitivity Mechanical Oscillators

The Marohn group at Cornell has used the CNF to batch-fabricate atomic-force-microscope cantilevers with ~100 nm diameter nickel nanorod tips and force sensitivities of a few attonewtons at 4.2 K. The magnetic nanorods were engineered to overhang the leading edge of the cantilever, and consequently the cantilevers experience the lowest surface noise ever achieved in a scanned probe experiment. Cantilever magnetometry indicates that the tips are well magnetized. The cantilevers were used to achieve the first demonstration of scanned probe detection of electron-spin resonance from a batch-fabricated tip.

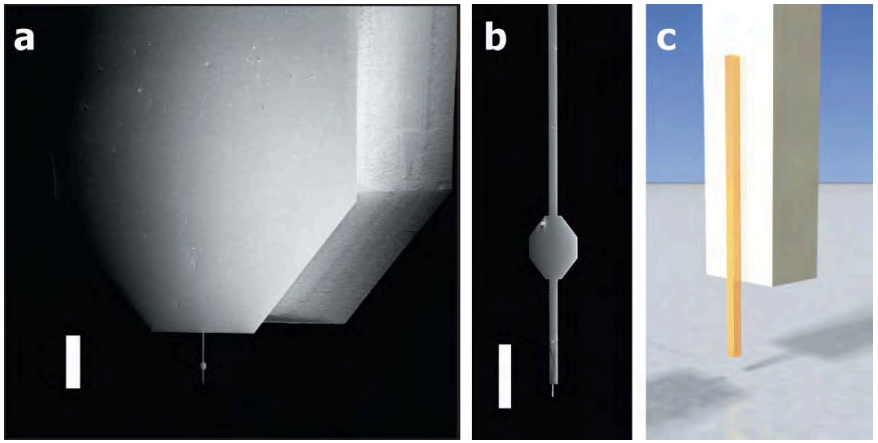

(a) ultrasensitive force microscope cantilever (scale bar 200 μm); (b) magnified view of the cantilever showing a reflective pad for interferometric detection of cantilever motion (upper) and a narrowed leading edge (lower) to minimize cantilever-sample interactions (scale bar 30 μm); and (c) sketch of a 100 nm wide magnetic nanorod tip overhanging the cantilever's leading edge.

J. A. Marohn group, Cornell University
Work performed at Cornell NanoScale Facility

ACS Nano ***4****, 7141 (2010).*

Optofluidic Waveguides for Reconfigurable Photonic Systems

The Erickson group at Cornell has used the CNF to make reconfigurable optical switches based on the principle of using flowing liquids to dynamically change the optical index of refraction. By controlling the flow of two liquids with different indices of refraction within a microfluidic device, they can create liquid-core/liquid cladding optical waveguides. By adjusting the relative pressure of the flows, they can steer the liquid core to switch between different channels, thereby also switching the path of the flow of light traveling within the waveguide. The chip-based geometry allows external optical fibers to be coupled efficiently to reconfigurable fluidic devices to make complex reconfigurable photonic systems.

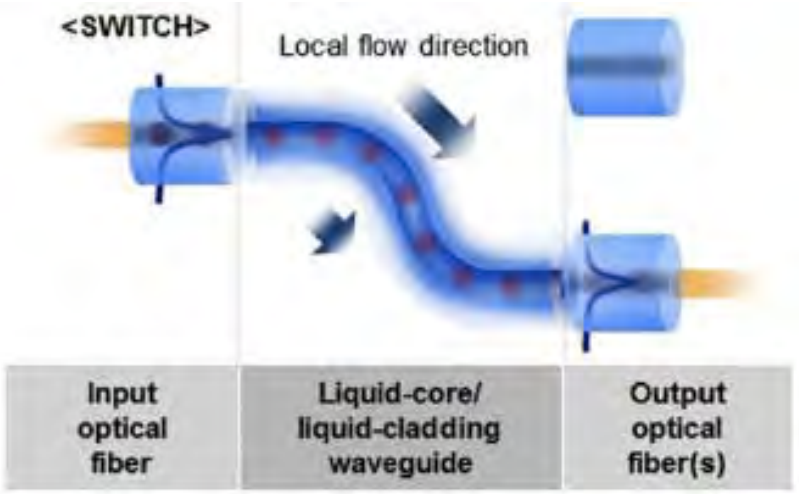

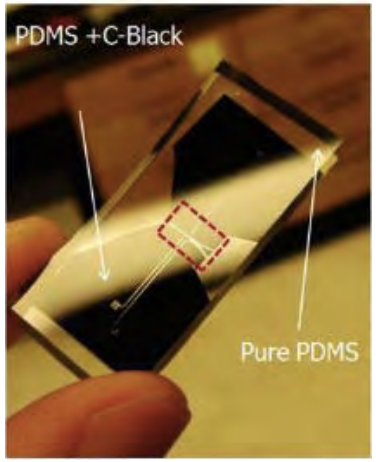

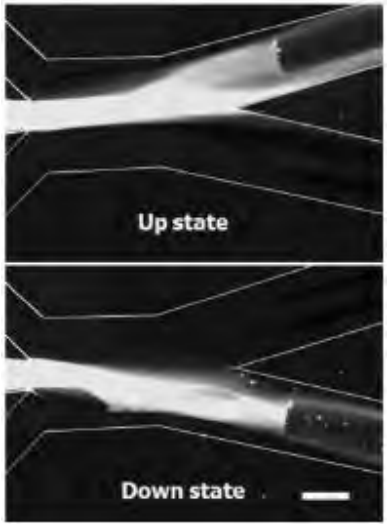

A. J. Chung and D. Erickson, Cornell University
Work performed at Cornell NanoScale Facility

Optics Express **19**, 8602 (2011)

Monolithically Integrated Junction FETs and NEMS

This group accomplished the first-ever monolithic integration of junction FETS with SOI-NEMS for enhanced signal transduction and signal processing. Monolithic integration is preferred to hybrid integration due to reduced parasitics and mismatches. The JFET was integrated directly into a SOI MEMS cantilever to form an extra-tight integration between sensing and electronic integration. When a cantilever connected to the JFET is electrostatically actuated, its motion directly affects the current in the JFET. The devices were realized in 2μm thick SOI cross-wire beams, with a novel $MoSi_2$ contact metallization for stress minimization and ohmic contact. The pull-in voltage for the NEMS cantilever was 21V and the pinch-off voltage of the JFET was -19V. Fabrication included 3 electron beam lithography steps.

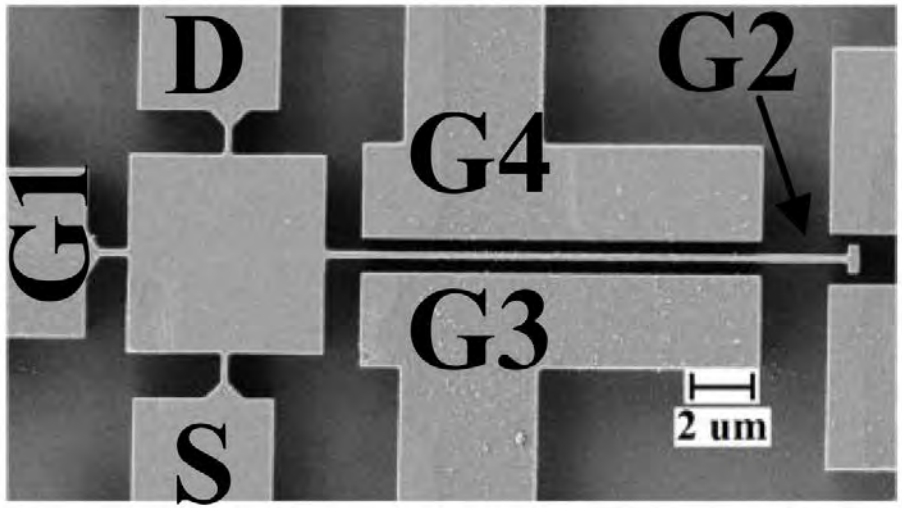

SEM micrograph of the JFET-MEMS device

Kwame Amponsah and Amit Lal, Cornell University,
Work performed at Cornell NanoScale Facility

Micro Electro Mechanical Systems (MEMS), 2011 IEEE 24th International Conference

Probing the invasiveness of prostate cancer cells in a 3D microfabricated landscape

Metastasis is a three-dimensional invasion process where cells spread from their site of origin and colonize distant microenvironmental niches. It is critical to be able to assess quantitatively the metastatic potential of cancer cells. We have constructed a microfabricated chip with a three dimensional topology consisting of lowlands and isolated square highlands (Tepuis), which stand hundreds of microns above the lowlands, in order to assess cancer cell metastatic potential as they invade the highlands. The metastatic prostate cancer cells (LNCaP and PC-3) under study exhibit strikingly different motility and proliferation in Tepui structures. The experiments reveal that highly metastatic PC-3 cells have a faster invasion rate compared to LNCaP cells. Interestingly, LNCaP cells fail to populate all Tepui tops and form dense three-dimensional structures that are not observed in two dimensional cell culture. We argue that this phenomenon is due to cell contact inhibition. Combined with confocal microcopy, this microfabricated device shows promise to be a real-time platform for in vitro quantitative studies of cell invasion for a broad arrange of cancer cells.

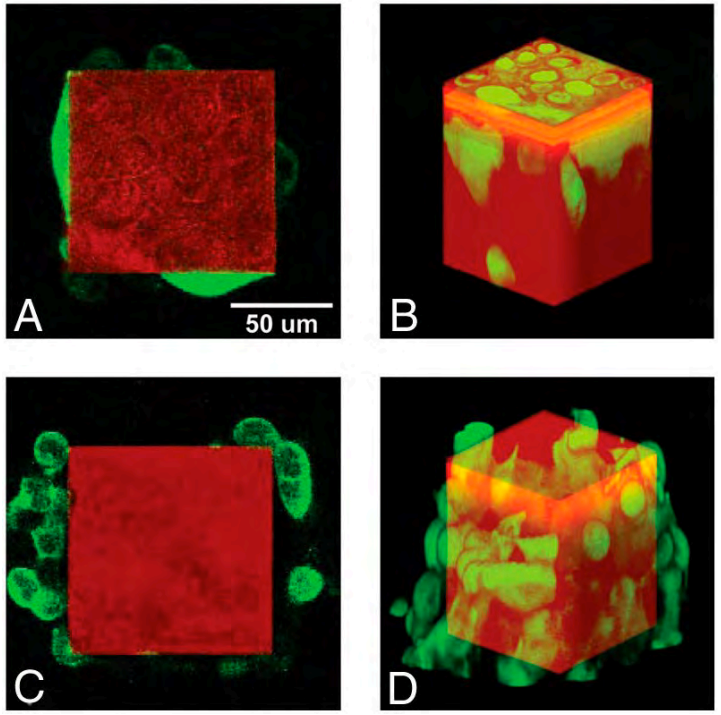

Confocal images and the corresponding three-dimensional reconstructions showing the cell-chip system after reaching steady state. The green channel represents fluorescence of GFP expressed within the cells, and the red channel represents the direct reflection from the surface of the chip. (A) A confocal z-slice of PC-3 cells cultured on the microchip. (B) The three-dimensional reconstruction shows PC-3 cells attached to the sides and densely packed on the top. (C) A confocal z-slice of LNCaP cells cultured on an identical microchip. (D) The three-dimensional reconstruction of LNCaP cells attached to the surface, showing that they barely reached the top.

L. Liua, B. Sunc, J. N. Pedersen, K-M Yongd, R. H. Getzenberg, H. A. Stone, and R. H. Austin, Princeton University
Work performed at Cornell NanoScale Facility

PNAS ***April 7, 2011***

Retinal Implant Project

The purpose of the Retinal Implant Project is to restore useful vision to patients who are blind with degenerative retinal diseases. The primary illnesses we hope to treat are retinitis pigmentosa and age-related macular degeneration. Both these diseases cause the eventual destruction of the photoreceptor cells – rods and cones – in the retina, leaving intact the ganglion cells which transmit electrical impulses (and hence visual information) to the brain. The ganglion cells may be stimulated, however, with biphasic current pulses from a microfabricated electrode array.

Blind surgical volunteers have consistently described visual percepts that resulted from such stimuli, and this has led our team to develop a wireless, implantable retinal prosthesis with 200+ electrodes (Figure 3). To develop more advanced and higher fidelity retinal implant systems, we are pursuing 3D structures to improve electrode-cell coupling. We have recently develop a microfabricated polyimide-based subretinal penetrating electrode array, a SEM image of one 'post' is shown in Figure 4. This structure penetrates the retinal tissue so that the electrode is very close to the target cells. These new structures have been electrochemically evaluated and the performance has been found to compare well with traditional planar electrodes.

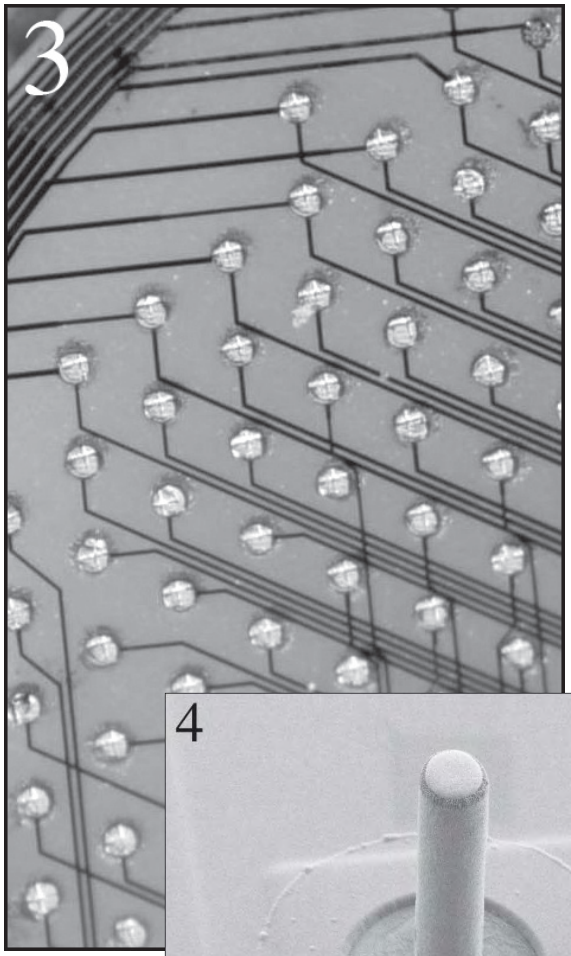

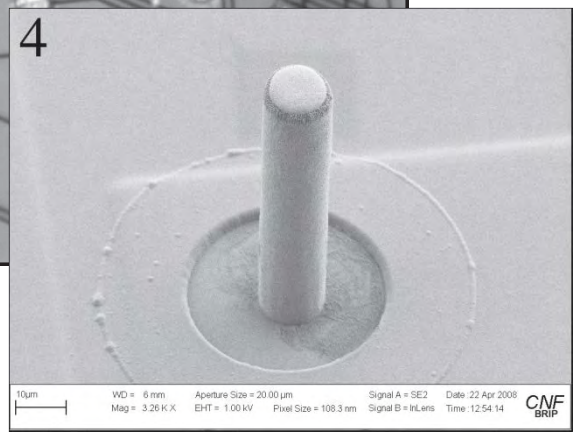

Douglas Shire, John Wyatt, Marcus Gingerich, Bruce McKee,
Cornell University, MIT, Veterans Administration
Work performed at Cornell NanoScale Facility

Microfluidic Cell Culture Analog Devices to Mimic Animal Exposures to Toxins and Drugs

Our group has developed microfluidic in vitro devices that mimic the response of humans or animals to drugs, toxins, or nanoparticles. Each device, or cell culture analog (CCA), contains an array of pseudo tissues that are interconnected by microfluidic channels. The recirculation of blood surrogate through the microchannels allows us to study tissue-tissue interactions, such as the breakdown of a parent compound in the liver and subsequent transport and reaction in the lung. We combine these in vitro device experiments with physiologically-based pharmacokinetic model simulations to predict toxin and drug dynamics in humans.

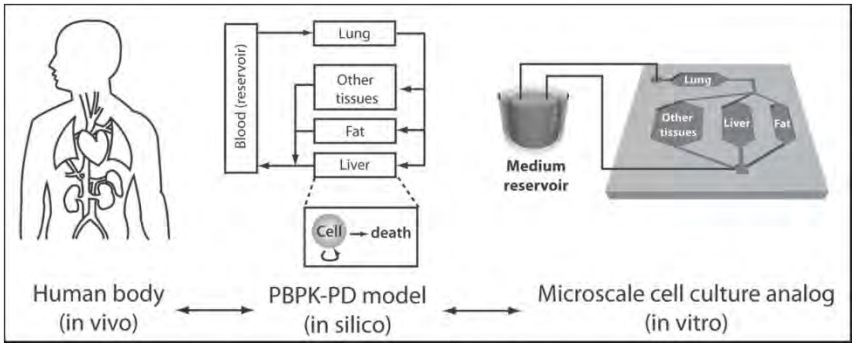

Figure 1: Schematic of the μCCA concept. The human body can be described as a series of interconnected compartments. On a μCCA device, microfluidic chambers physically represented these compartments in physiologically relevant order and with physiologically relevant fluid flow rates and residence times.

We have used micro cell culture analogs (μCCAs) to test the toxicity of nanoparticles. Because of their small size and surface to volume ratio, nanoparticles possess unique properties, which can be utilized in diagnostics and drug delivery. However, little is known of the particle's fate within the body and tissues. We have recently developed a μCCA that combines cell culture models of the liver and the intestinal epithelium of the gastrointestinal tract in a physiologically realistic way to simulate the oral uptake of nanoparticles and other drugs. To obtain more detailed information from simulations with first pass metabolism μCCAs, we have developed a microfabricated gastrointestinal tract model that incorporates an on-chip membrane and integrated electrodes for transepithelial resistance measurements.

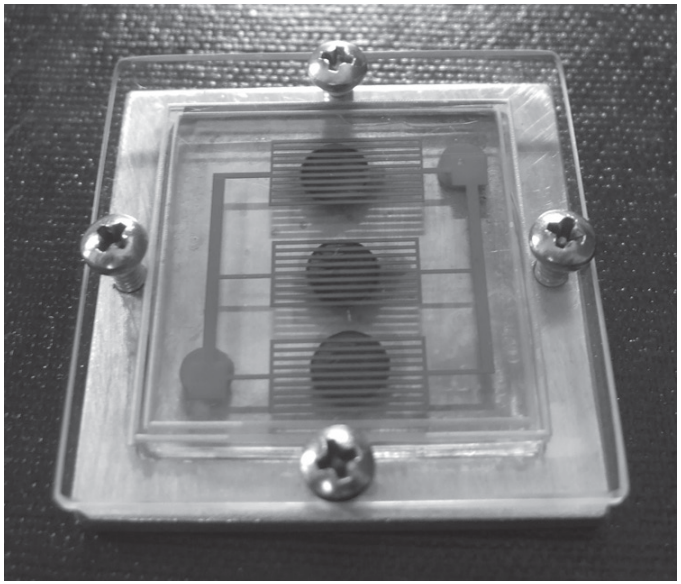

M. Esch, M. Shuler, Cornell University
Work performed at Cornell NanoScale Facility

The Evolutionary Dynamics of Drug Resistance by Grug-induced Stress Gradients

Emergence of resistance to antibiotics by bacteria is a growing problem, yet not well understood. In a microfluidic device designed to mimic naturally occurring bacterial niches. Evolution proceeds most rapidly with just the right combination of a large number of mutants and rapid fixation of the mutants (Goldilocks point). Using a two-dimensional micro-ecology it is possible to fix resistance to the powerful antibiotic ciprofloxacin (Cipro) in wild-type E. coli in 10 hours through a combination of extremely high population gradients, which generate rapid fixation, convolved with the "just right" level of antibiotic which generates a large number of mutants and the motility of the organism. The design of the micro-ecology is unique in that it provides two overlapping gradients, one an emergent and self generated bacterial population gradient due to food restriction and the other a mutagenic antibiotic gradient. Further, it exploits the motility of the bacteria moving across these gradients, to drive the rate of resistance to Cipro to extraordinarily high rates. Whole genome sequencing of the resistant organisms revealed four functional single nucleotide polymorphisms attained fixation. Rapid emergence of antibiotic resistance in the heterogeneous conditions prevailing in the mammalian body may also apply to the emergence of drug resistance during cancer chemotherapy.

G. Lambert, R. H. Austin, Princeton University
Work performed at Cornell NanoScale Facility

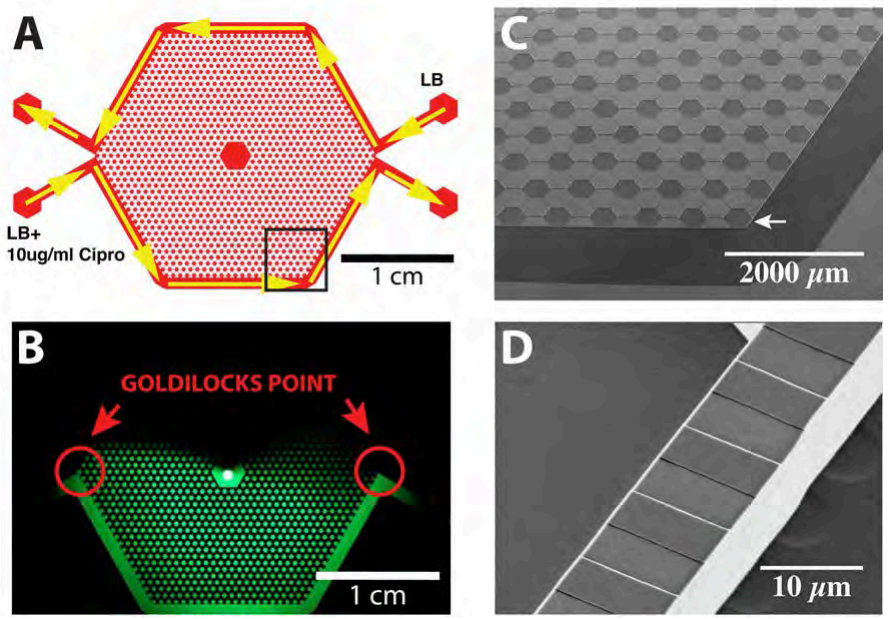

(A) An overview of the entire micro-ecology, showing the flow of the nutrient streams and the nutrient+Cipro containing streams. The nutrient stream is x1 LB broth, while the nutrient+Cipro stream is x1 LB broth + 10 μg/mL Cipro. (B) Image of the expected Cipro concentration using the dye fluorescein as a marker. The asymmetry of the pattern at the Goldilocks points is due to the direction of the flow. (C) Scanning electron microscope (SEM) image of the area of the array in (A) outlined by the box. Each hexagon is etched down 10 microns, the interconnecting channels are 10 microns deep and 10 microns wide. (D) SEM image of the nanoslits at the micro-ecology periphery. The nanoslits are etched down 100 nm and are 6 microns wide and 10 microns long.

Proc. of SPIE Vol. 7929 (2011)

Fluorine-Containing Block Copolymers Designed for Top-Down and Bottom-Up Lithography

A new series of fluorine-containing block copolymers of poly(styrene-block-2,2,2-trifluoroethyl methacrylate) (PS-b-PTFEMA) and poly[styrene-block-(methyl methacrylate-co-2,2,2-trifluoroethyl methacrylate)] (PS-b- (PMMA-co-PTFEMA)), which can be used for both top-down and bottom-up lithography, were developed. Integrated patterns such as “dots in lines” were successfully obtained through combination of degradation of the fluorine-containing block by e-beam exposure and lateral ordering of the crosslinked PS block’s self assembly. Lateral ordering of arrays of dots was observed in thin films of PS-b-PTFEMS in which polystyrene (PS) was the minor block, and in thin films of PS-b-(PMMA-co-PTFEMA) in which PS was the major block. These thin films were then exposed as in conventional e-beam and deep-UV lithography to generate integrated patterns. Both positive and negative tone processes have been demonstrated.

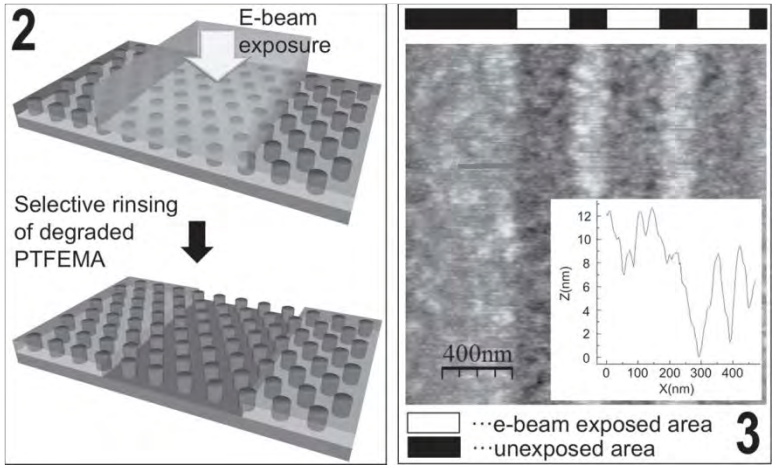

left: Schematic image of PS-b-PTFEMA after exposure by e-beam and development in a methyl isobutyl ketone/isopropanol mixture.
right: AFM height image of PS-b-PTFEMA after exposure by e-beam and development in a methyl isobutyl ketone/isopropanol mixture. The z scale is 32 nm for the AFM image.

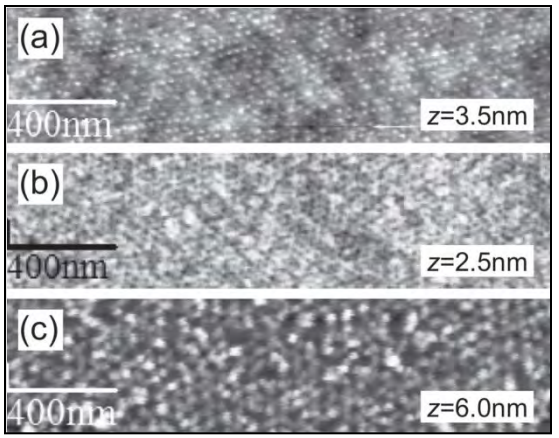

AFM height images of the PS-b-(PMMA-co-PTFEMA) (a) after annealing in toluene (b) after deep-UV exposure and (c) after rinsing with methanol to selectively remove the degraded PTFEMA.

R. Maeda, C. Ober, Cornell University
Work performed at Cornell NanoScale Facility

Interaction of DNA and Single Layer Graphene

Because it has the “ultimate” surface-to-volume ratio, graphene shows a great sensitivity to elements in close proximity to it. We would like to exploit this feature to utilize graphene as a biologically sensitive membrane. In order to convert promises into actual devices, graphene functionalization with biologically active molecules has to be solved.This work demonstrates grafting single stranded DNA onto graphene and sensing the electrical modification of the graphene’s conductivity correlated to the adsorption of these macromolecules. Whereas many biomolecules don’t show affinity to graphene (a strongly hydrophobic material) the nucleobases of a single strand of DNA form with the basal plane of graphene a strong non-covalent interaction called π-π stackingi.This interaction enables the grafting of the long biopolymers on graphene. The figure present an atomic force microscope (tapping mode) image of several molecules of single stranded DNA (extracted from Lambda Bacteriophage virus) bound to the surface of graphene.

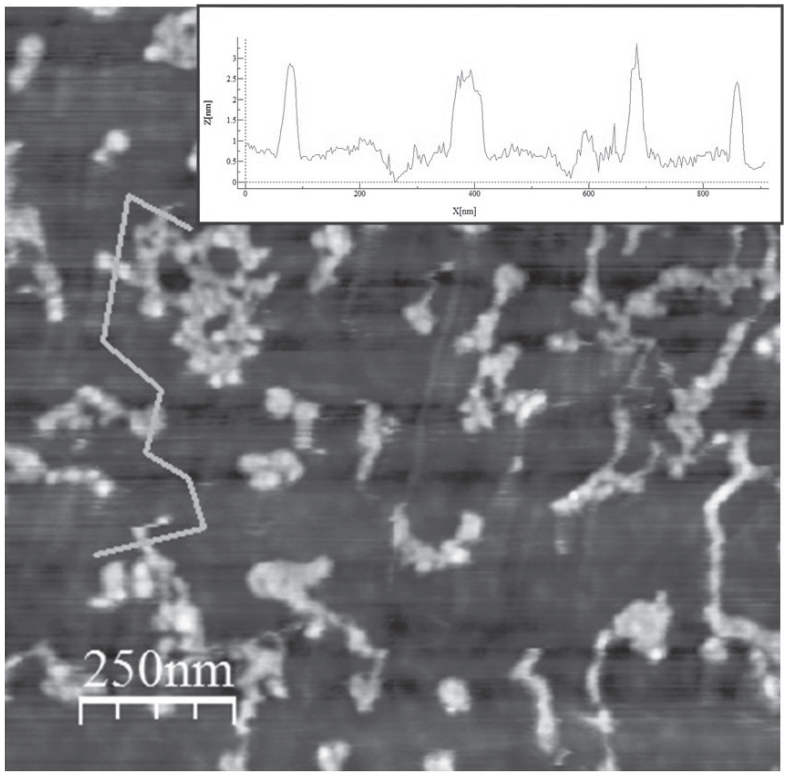

2 µm square AFM image of the surface exfoliated graphene with adsorbed single stranded DNA. The blue line marks the path of a height profile (inset) that shows the 2 nm high features as the scan traverses strands of DNA.

T. Alva, H. Craighead, Cornell University
Work performed at Cornell NanoScale Facility

Microfluidic Integration of Nanomechanical Resonators for Protein Analysis in Serum

This work describes a technique for reversibly encapsulating nanomechanical resonant sensors within microfluidic channels that are reusable and easy to fabricate. We demonstrate the feasibility and sensitivity of our microfluidic system by detecting prostate specific antigen (PSA) at 1–100 fM concentrations in serum, using a nanoparticle-based mass-labeling sandwich assay. By comparing these results to our previous data for PSA detection, we observe enhanced assay sensitivity in a significantly reduced time with the microfluidic assay. In addition, we show that a binary mixture of the proteins vascular endothelial growth factor (VEGF) and interleukin-8 (IL-8) can be detected in serum using a single microfluidic channel. This work lays the groundwork for future applications of these nanomechanical resonant devices for highly sensitive, multiplexed protein analysis using microfluidics.

P.S. Waggoner, C.P. Tan, H.G. Craighead, Cornell University
Work performed at Cornell NanoScale Facility

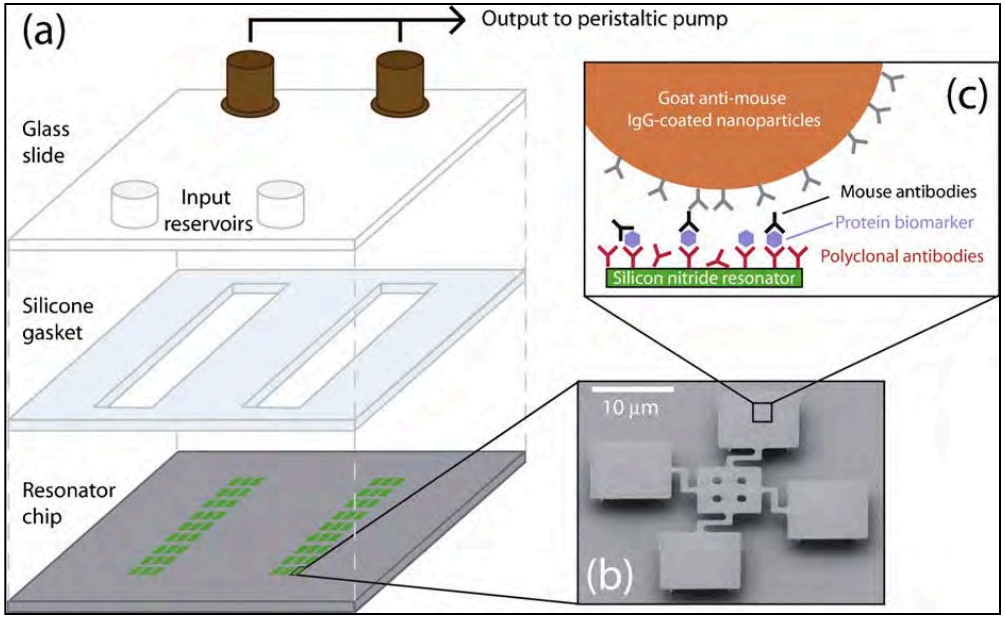

Schematic of microfluidic-resonator device architecture showing (a) the overall design, (b) individual resonators from on-chip arrays and (c) a depiction of the specific surface chemistry used for biosensing.

MEMS-based Piezoelectric Vibrational Energy Harvester

MicroGen Systems is developing a MEMS based energy harvesting system that can replace the need for batteries for low power applications. The power source consists of a tiny sheet of a piezoelectric material that generates electricity when it is flexed, mounted on a proprietary shock-resistant base. Vibration, such as from a spinning tire, causes the tiny flap to swing back and forth, generating current that charges an adjacent thin-film battery. The prototype, about the size of a dime or less, puts out up to 200 microwatts. As circuits become smaller and need less power the device can shrink with them.The generator can be mass produced on silicon wafers by the same processes used to make circuit chips. Typical frequencies range between 50 and 250 Hz, and *G*-levels are 0.5 ± 0.25 *g* (*g* = 9.8 m/s^2) or lower. Recent results for the device are 75 Hz, open-circuit voltage OCV = 1.5 Volts, and loaded power *P* = 200 mWatts at *G* = 1.0 *g* and *P* = 50 mWatts at G = 0.5 g. A world record! . A primary application will be to replace batteries in wireless sensors.

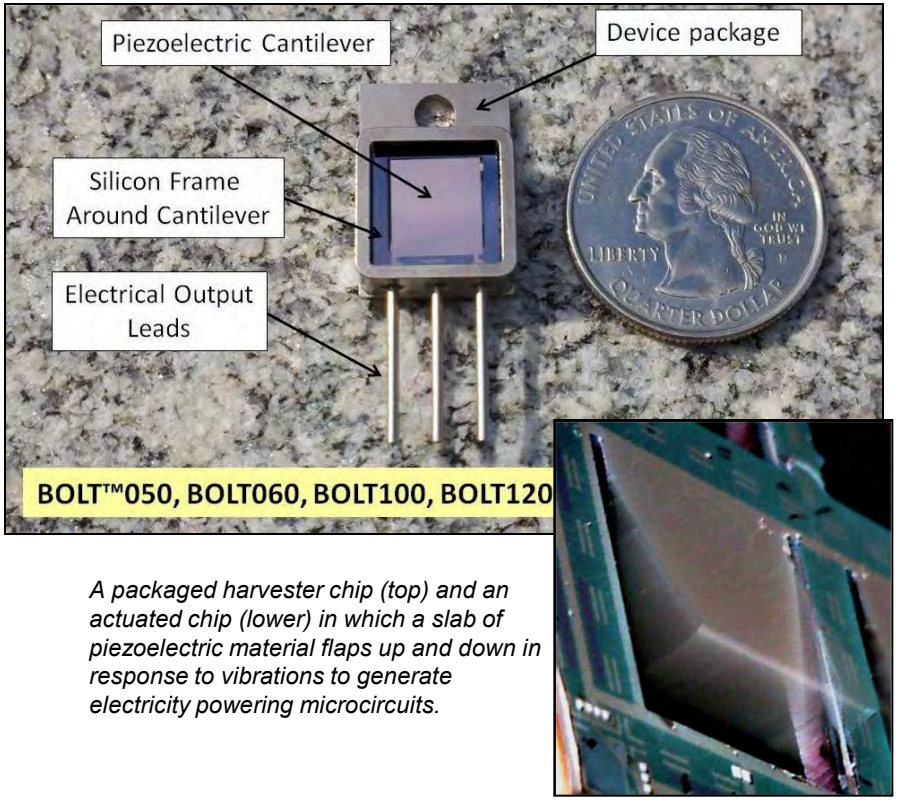

A packaged harvester chip (top) and an actuated chip (lower) in which a slab of piezoelectric material flaps up and down in response to vibrations to generate electricity powering microcircuits.

R. Andosca, MicroGen Systems LLC
Work performed at Cornell NanoScale Facility

Ultra-Sensitive Biodetection Using Photonic Crystal Nanocavities

The Fauchet group has developed a novel photonic crystal design where nanocavities are coupled to a two-dimensional photonic crystal waveguide for sensing applications [1,2]. This design allows light to be transmitted through the waveguide except at frequencies that correspond to the resonant mode of the nanocavity where a sharp transmission dip is observed. By tuning the nanocavity radius and placing the photonic crystal structures in series, multiple transmission dips can be obtained in the output spectrum, as each nanocavity possesses a distinct resonant wavelength. We have demonstrated very sensitive error-corrected detection of protein molecules with this new design. This design also opens up opportunities for multiplexed biosensing of nanometer sized particles and biomolecules on a single platform, provided the nanocavity dimensions are appropriate. The group has designed a two-dimensional W1 photonic crystal waveguide structure by removing a single array of central air holes. A large nanocavity in the waveguide is formed by removing three holes from the first and second rows adjacent to the waveguide, and by creating a defect hole with double the radius of the surrounding air holes. The lattice constant 'a' is chosen to be ~ 400 nm for operation near wavelength of 1500 nm.

P. Fauchet group, U. Rochester
Work performed at Cornell NanoScale Facility

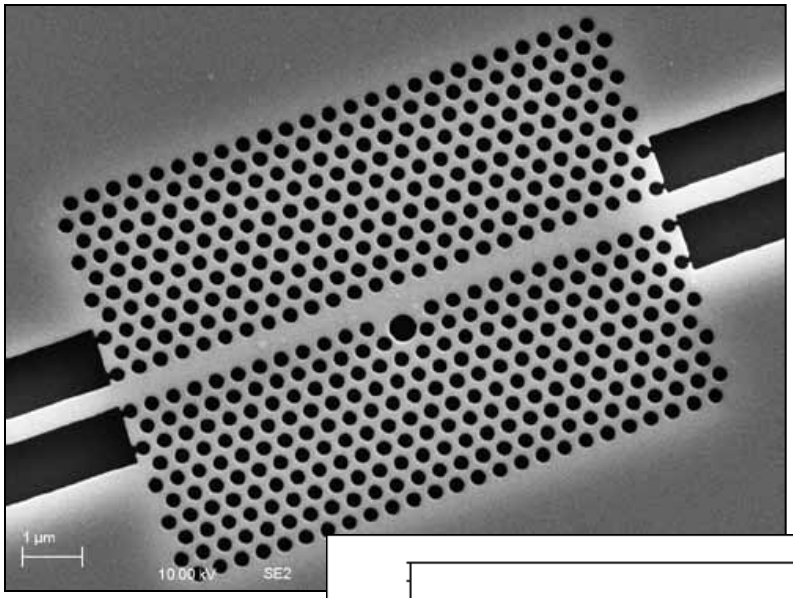

SEM image of a nanocavity coupled photonic crystal waveguide device.

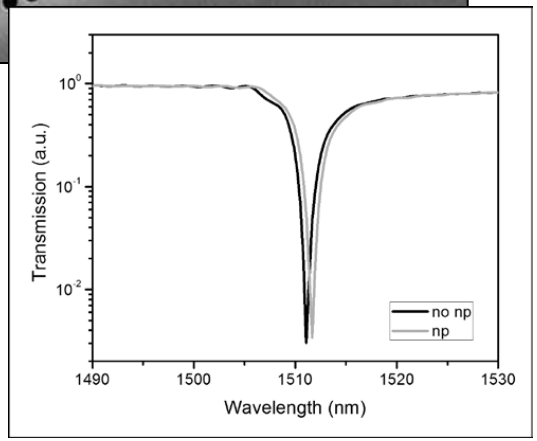

Computed transmission spectra of the nanocavity in the presence and absence of a single nanoparticle

DNA Methylation Profiling in Nanochannels

Epigenetic regulation is the inheritable modification of gene activity without influencing the underlying DNA sequence. DNA 5-cytosine methylation is one of the most widely studied mechanisms influencing epigenetic gene regulation and is generally thought to suppress gene expression. One of the effects of DNA methylation is to physically impede the binding of transcription factors to their recognition sites, while the other is to bind proteins containing methyl-CpG-binding domains (MBDs), which recruit additional proteins involved in the modification of chromatin (where CpG is cytosine and guanine separated by only one phosphate) In this work, methylation patterns are detected through binding of a fluorophore-tagged methyl-CpG-binding domain protein fragment to the interrogated dsDNA segment, as shown in the top figure . The binding pattern along the DNA is detected by fluorescence microscopy. In order to achieve single-gene relevant resolution, DNA is stretched by confinement to a quasi one-dimensional nanochannel (lower figure) The technique is, thus, conceptually similar to fluorescence in-situ hybridization on molecules that were enlongated molecules, which are arrested in their extended configuration through a technique such as molecular combing.

Shuang Fang Lim, Alena Karpusenko, John J. Sakon, Joseph A. Hook, Tyra A. Lamar, and Robert Riehn, North Carolina State University
Work performed at Cornell NanoScale Facility

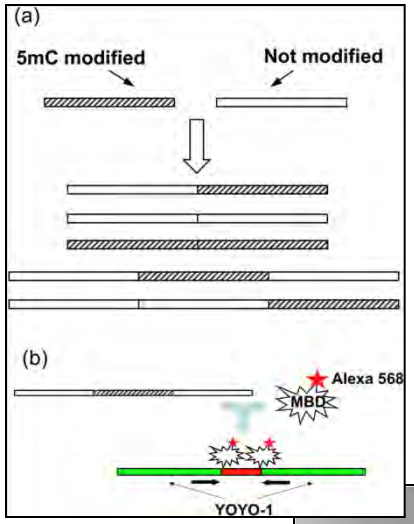

(a) Schematic of possible outcomes of DNA concatemer formation with 5-cytosine methylated (5mC) and nonmethylated segments.
(b) Schematic of Alexa568-MBD to DNA concatemer. The entire molecule is stained using the green stain YOYO-1 and Alexa568-MBD binds to methylated stretches.

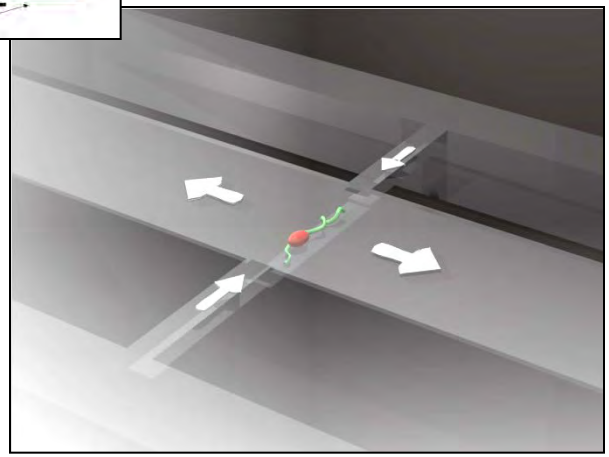

Schematic of a device with two microchannel feeds (top and bottom) that are bridged by a nanochannel (inflowing arrows) containing an Alexa568-MBD labeled DNA concatemer. A shallow central shunt channel (outflowing arrows) allows the use of pressure-driven flow

BIOMICROFLUIDICS 5, 034106 (2011)

Suspended Carbon Nanotube Devices for Single Molecule Sensing

The two-terminal resistance of a carbon nanotube (CNT) device is sensitive to the binding of biomolecules onto the CNT surface. Several groups have demonstrated this effect using CNTs lying on substrates, however, there are compelling reasons to extend these experiments to suspended CNT devices. Suspended CNTs are further away from charge traps in insulating substrates which introduce noise and limit the sensitivity of CNT-based electronic sensors. Suspended CNT devices also allow measurements of the interactions between the biomolecules and CNTs without interference from the substrate. Preliminary electrical data of our suspended CNT devices shows significant improvements in device sensitivity. The group has observed higher transconductance than standard CNT devices.

Ethan D. Minot, Joshua Kevek, Tal Sharf
Oregon State University
Work performed at Cornell NanoScale Facility

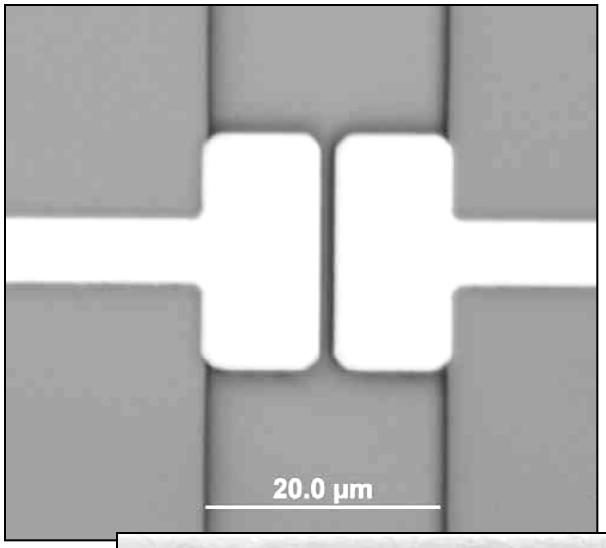

Optical image of a device before CNT bridging the gap between the electrodes.

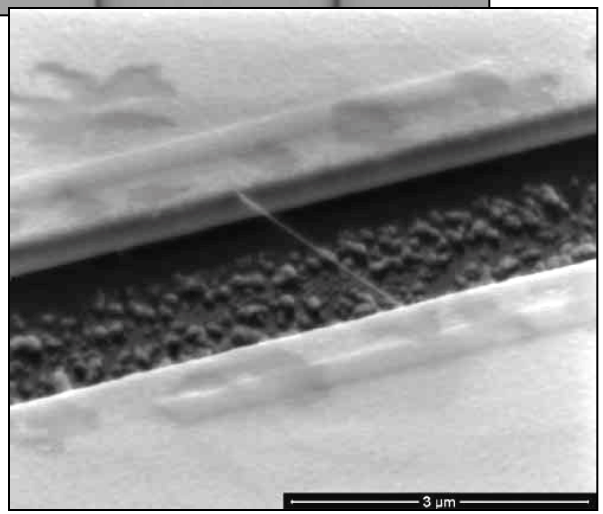

Scanning electron microscope image of a suspended SWNT detector

Zero Mode Waveguides for Single-Molecule Real-Time Detection

Metallic subwavelength apertures can be used in epi-illumination fluorescence to achieve focal volume confinement. Because of the near field components inherent to small metallic structures, observation volumes are formed that are much smaller than the conventional diffraction limited volume attainable by other methods. Using an electron beam lithography process, uniform arrays of such apertures can be manufactured efficiently in large numbers with diameters in the range of 60–100 nm. The apertures were characterized by scanning electron microscopy, optical microscopy, focused ion beam cross sections/transmission electron microscopy, and fluorescence correlation spectroscopy measurements, which confirmed their geometry and optical confinement. Process throughput can be further increased using deep ultraviolet photolithography to replace electron beam lithography. This enables the production of aperture arrays in a high volume manufacturing environment.

Mathieu Foquet, Pejman Monajemi, Drew Martinez, Omar Negrete, Pacific BioSciences
Work performed at Cornell NanoScale Facility

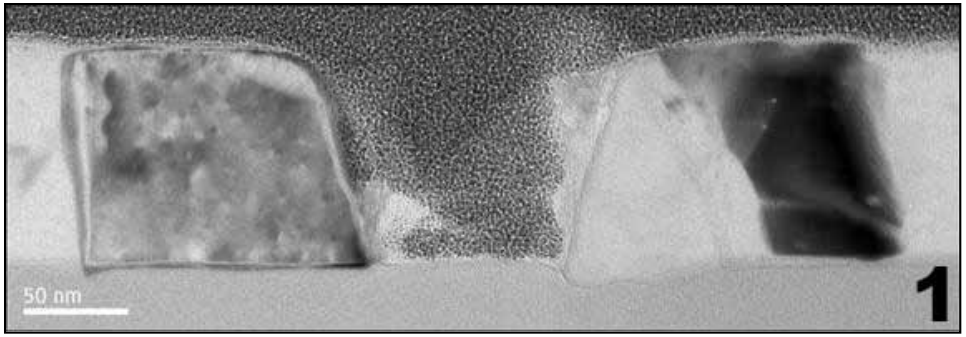

Transmission electron microscopy image of a cross section of an ebeam produced Zmw in aluminum

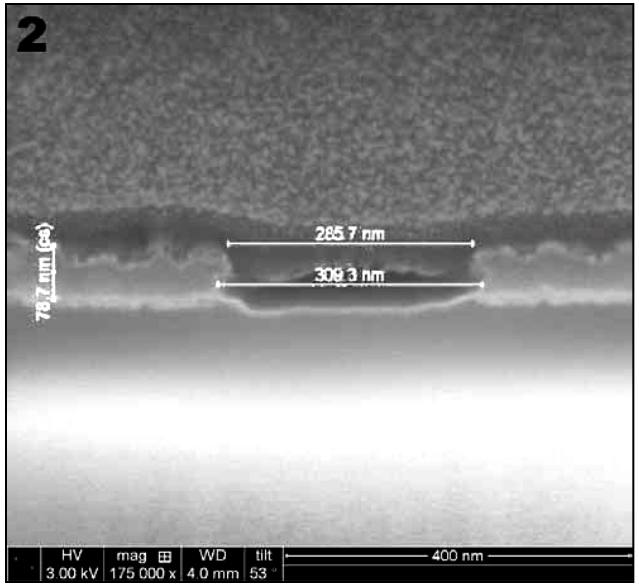

scanning electron microscopy image of a cross section of an optically patterened Zmw in aluminum

Fabrication of Flexible Microelectrodes for Chronic Implantation

Conventional silicon-based probes with multiple recording sites make it possible to collect neural signals at the sub-millimeter scale from small volumes of tissue. However, the rigid nature of these probes creates a tissue scar that, with time, impairs the quality of the recordings. Therefore, a great deal of research in neural engineering deals with the development of flexible probes to decrease the mismatch between the mechanical properties of the implanted probes and biological tissue. This work is to fabricate probes with long-term implantation capacity, high quality signal recording, and facile packaging and their *in vivo evaluation in recording neural activity in the rat brain.* The fabrication of probes involved the deposition and patterning of alternating layers of polyimide, platinum (Pt) and SU-8. The combination of polyimide with SU-8 improve the stiffness of the probes, making easier their manipulation during the implantation into the brain, as well as facilitating their interconnection to external electronics.

George G. Malliaras, Esma Ismailova, Dion Khodagholy, Ecole Nationale Supérieure des Mines de Saint Etienne, France
Work performed at Cornell NanoScale Facility

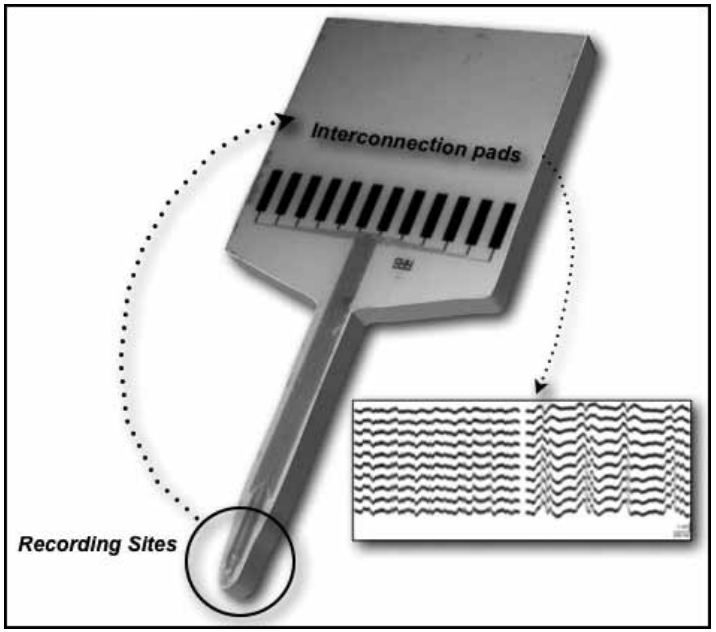

Layout of the polyimide probe. The insets show the cortical recordings: a) of an anesthetized rat; b) after bicuculline adding.

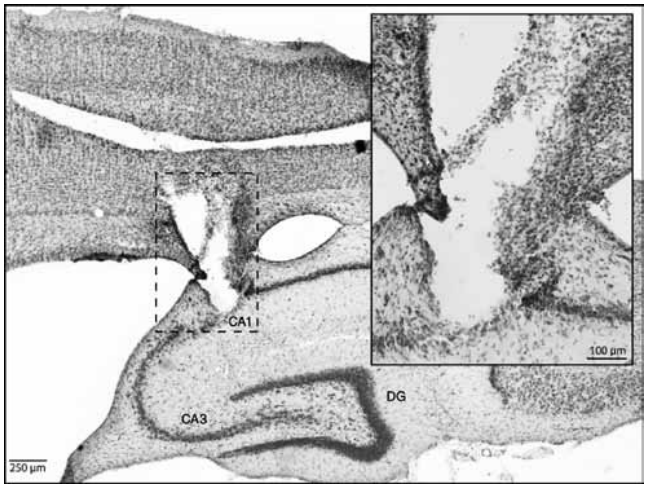

a brain slice around the placement of the probe. The main frame shows the final depth reached by the implanted microelectrode (dashed box), corresponding to the CA1 region of the dorsal hippocampus. The inset shows the area of the dashed box in more detail.

Controlled Storage of Light in Silicon Cavities

Delay elements play an important role in quantum computing and optical signal processing which calls for the need of efficient controlled delay elements with large characteristic storage time. This work proposes a novel solution to this problem by separating the primary functionalities (capture, storage and release of the light pulse) of the light storage system into separate cavities. By doing so it ensures that the light only minimally interacts with free carriers. To date, the group experimentally demonstrated delay that can be continuously varied over ~300ps (with an intrinsic exponential decay time of ~160ps). The delay achieved is four times larger than previously demonstrated active optical delays. The technique is only limited by the quality of the cavities used and can be easily extended to nanosecond delays with lower-loss cavities which inherently have a longer photon life time. It is capable of arbitrarily storing and releasing a pulse of light through dynamic tuning of a system of microcavities. The inherent storage time is more than 32 times the duration of the stored pulse.

Ali W. Elshaari, Abdelsalam Aboketaf, and Stefan F. Preble, Rochester Institute of Technology*
Work performed at Cornell NanoScale Facility

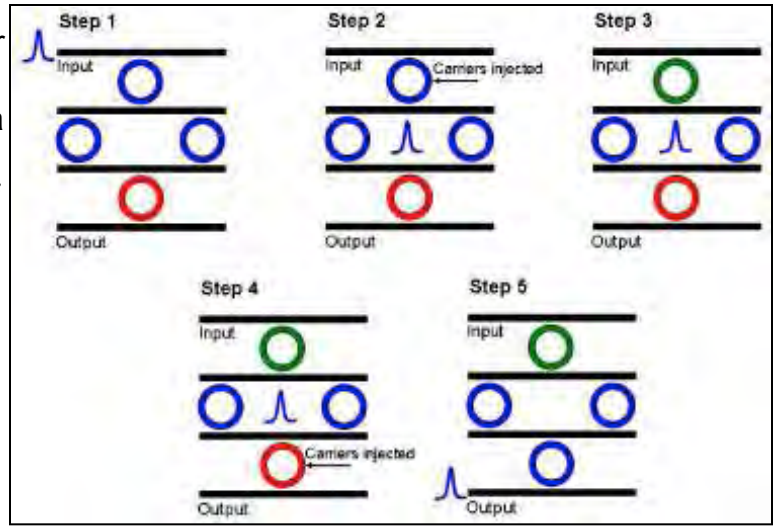

Schematic the system and its operation principle, (Step 1) shows the acceptance state of the system. Bits are stored as shown in (Steps 2 and 3) then released in (Steps 4 and 5)

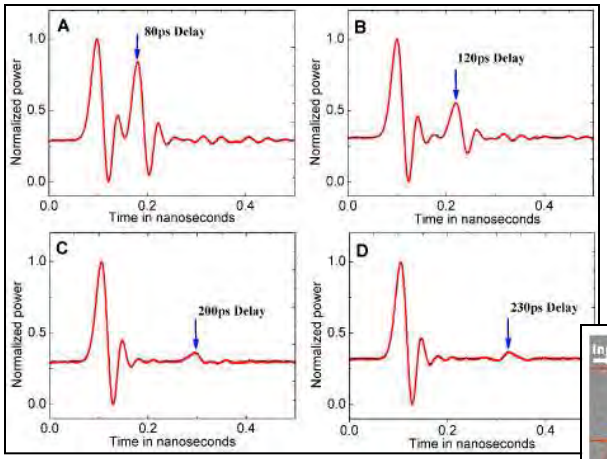

Different delays are measured through changing the time between the store and the release top pumping pulses..

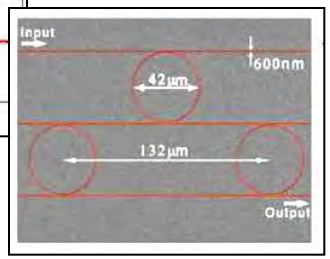

Softened Elastic Response and Unzipping in Chemical Vapor Deposited Graphene Membranes

The tensile behavior of graphene sheets was modeled on the CNF cluster using the molecular dynamics code LAMMPS. It was found that grain boundaries, in general, reduce the strength of graphene sheets and that the presence of subnanometer voids near the grain boundaries can reduce the sheet strength even further. This result is consistent with the mechanical properties of graphene sheets observed in experiments at Cornell using AFM indentation.

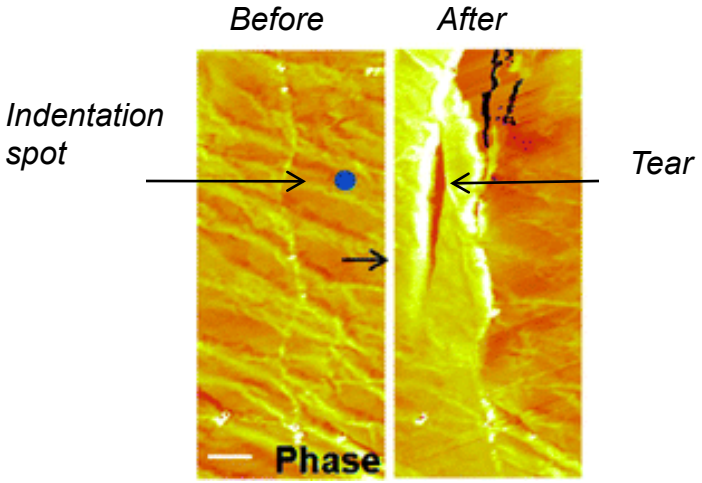

Phase Image of AFM indentation at blue spot. Graphene tears along grain boundary.

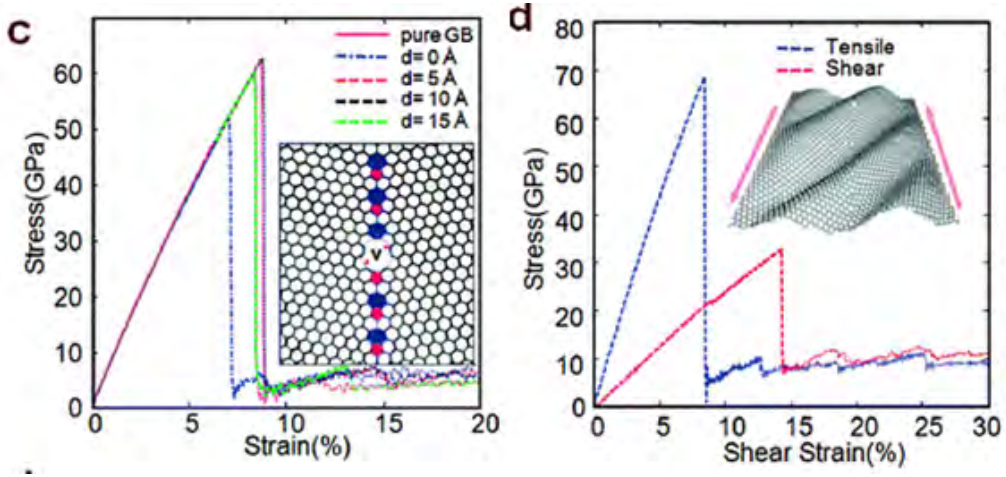

Strength of graphene sheets for (c) grain boundary with void and (d) decreased breaking strength due to shearing in presence of grain boundary.

Work performed on the computational resources of the Cornell Nanoscale Facility
Houlong Zhuang, Arunima Singh ,Richard Hennig (Material Science, Cornell)

*C. S. Ruiz-Vargas et al., Nano Lett., **11**, 2259 (2011).*

Electrochemical and Computational Studies on the Electrocatalytic Effect of Conducting Polymers toward the Redox Reactions of Thiadiazole-Based Thiolate Compounds

Organosulfur compounds could serve as cathodes in lithium-ion rechargable batteries. They suffer, however, from slow charging and recharging. In this paper, the authors examined different conducting polymers that could accelerate the charge kinetics of the organosulfur compounds and make them commercially viable electrode materials.

In order to accelerating charging, they found that the polymer window of conductivity needed to overlapped with the formal potential of the organosulfur compound. Density functional calculations done at the CNF showed that the polymer HOMO (highest occupied molecular orbital) energy level could be used to predict the ordering of the oxidation potentials of different polymers. In addition, visualization of the HOMO level indicates that electrocatalytic activity increases as the HOMO shifts away from the Th sulfur.

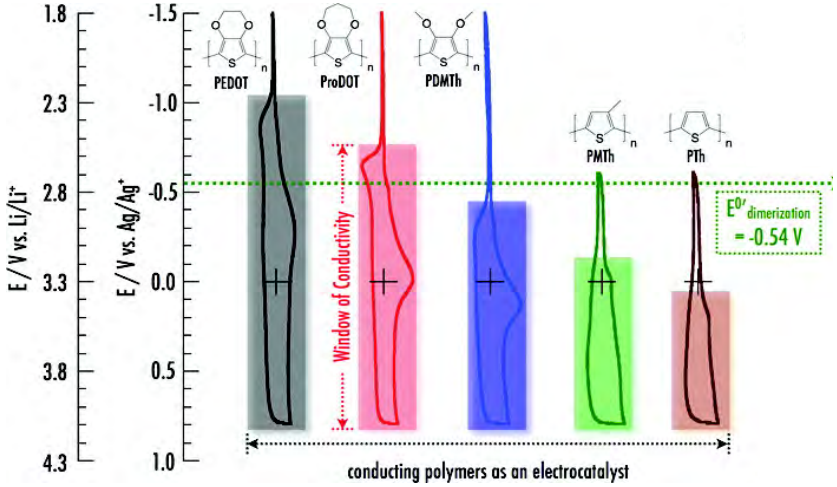

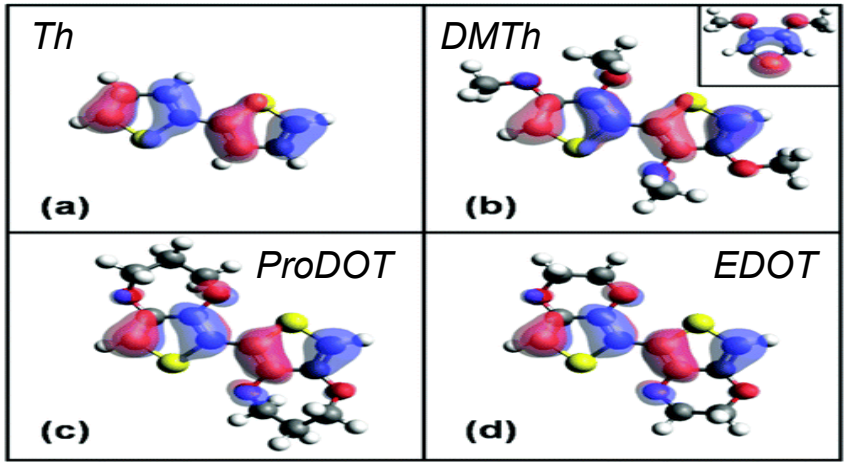

Work performed in part on the Computational Cluster at the Cornell Nanoscale Facillity

Gabriel G. Rodríguez-Calero; ***Michael A. Lowe****;;*
Héctor D. Abruña, (Chemistry, Cornell University)
Yasuyuki Kiya *(Subaru Technical Research Center, Japan)*

Gabriel G. Rodríguez-Calero; ***Michael A. Lowe****;* ***Yasuyuki Kiya****;*
Héctor D. Abruña;
J. Phys. Chem. C ***2010,*** *114, 6169-6176*

New Type of Magnetic Tunnel Junction Based on Spin Filtering Through a Reduced Symmetry Oxide: FeCo|$Mg_3B_2O_6$|FeCo

Magnetic tunnel junctions with high-tunneling magnetoresistance values such as Fe | MgO | Fe capitalize on spin filtering in the oxide region based on the band symmetry of incident electrons. However, these structures require magnetic leads and oxide regions of the same cubic symmetry class.

A new magnetic tunnel junction (FeCo | $Mg_3B_2O_6$ | FeCo) is presented that uses a reduced symmetry oxide region (orthorhombic) to provide spin filtering between the two cubic magnetic leads. Analysis of the complex band structure (for real and imaginary k) of Kotoite ($Mg_3B_2O_6$) based on density functional calculations shows that significant spin filtering could occur in this system. This new type of magnetic tunnel junction may have been fabricated already and can explain recent experimental studies at Cornell of rf-sputtered FeCoB | MgO | FeCoB junctions where there is significant B diffusion into the MgO region.

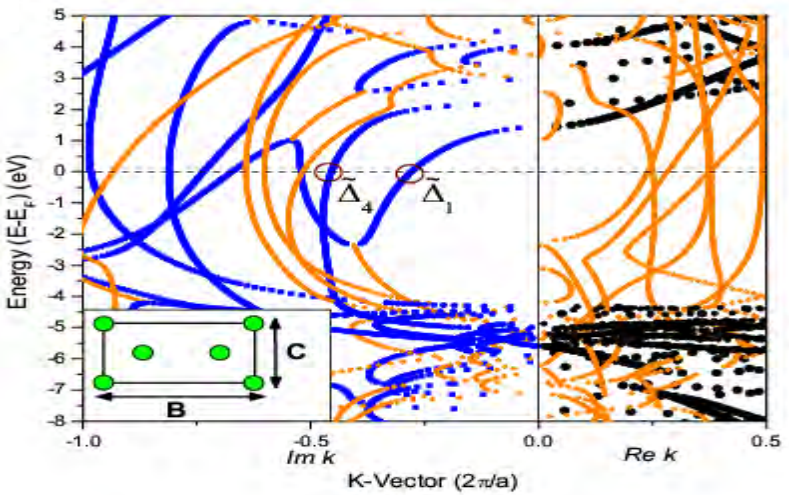

Complex Band Structure (real and I maginary k) for Kotoite

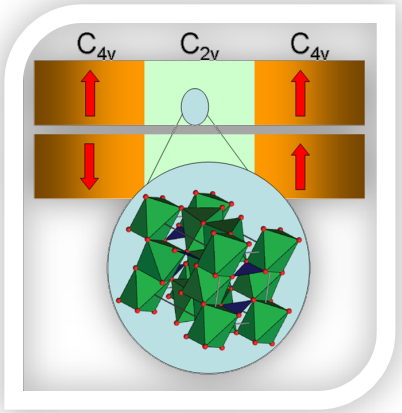

Schematic of FeCo | $Mg_3B_2O_6$ | FeCo tunnel junction showing crystal symmetry

Work performed using the computational resources of the Cornell Nanoscale Facility by Derek Stewart, Cornell University

Derek A. Stewart, Nano Letters, 10, 263 (2010)

Photogenerated Exciton Dissociation in Highly Coupled Lead Salt Nanocrystal Assemblies

Nanocrystals hold great promise for photovoltaic devices. However, much is still unknown about the coupling between individual nanocrystals. This work examines charge transfer and exciton dissociation in lead salt nanocrystals with different linker molecules under illumination. As part of this work, ab-intio calculations were done to determine the HOMO-LUMO energy levels of different length nBDT bi-linker molecules connecting lead salt nanocrystals and how this affected the transfer rate between nanocrystals. Evidence was found for two different types of transfer mechanisms.

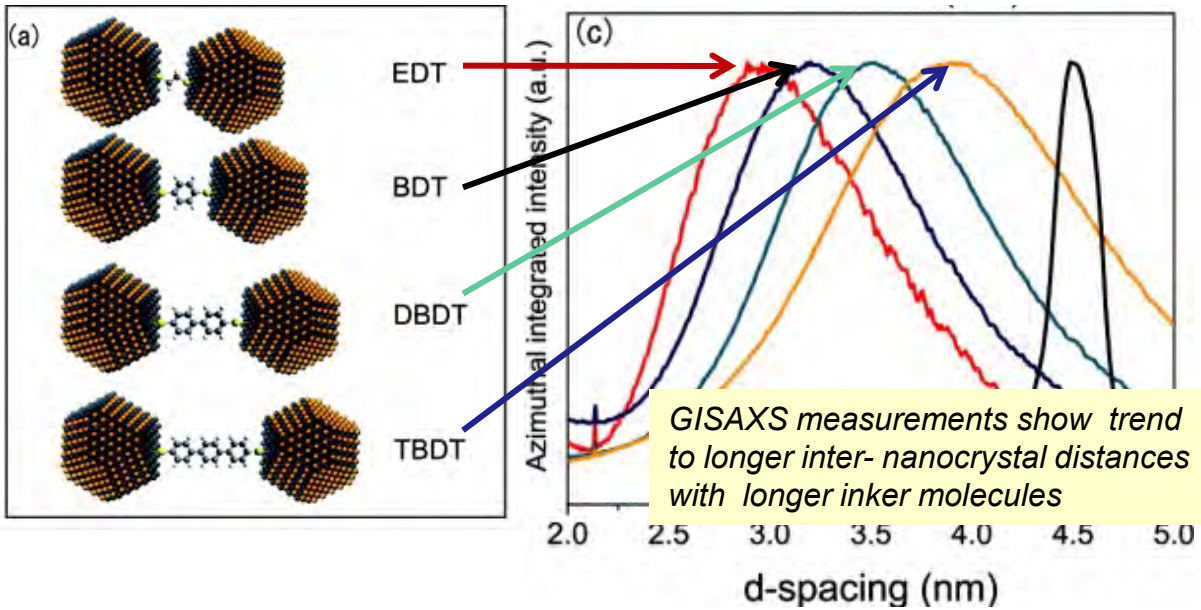

GISAXS measurements show trend to longer inter- nanocrystal distances with longer inker molecules

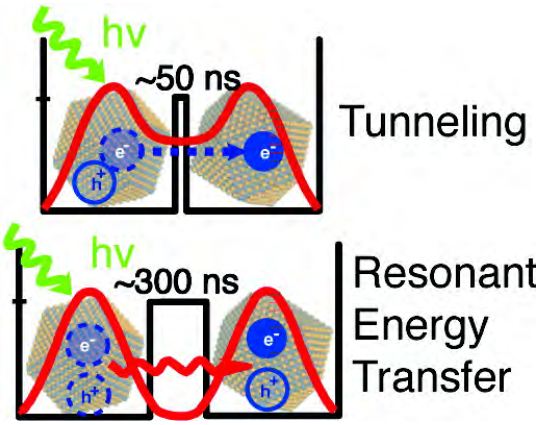

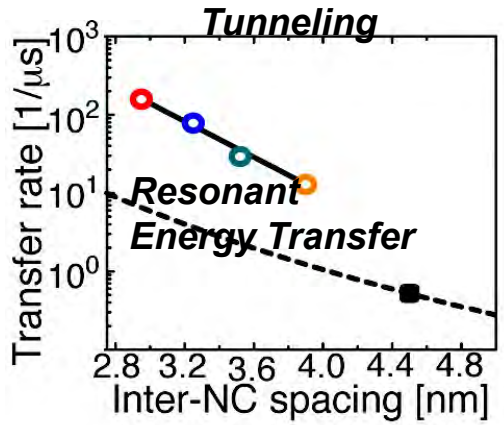

Work performed on the computational resources at the Cornell Nanoscale Facility: Byung-Ryool Hyun, Adam Bartnik,Tobias Hanrath, Frank Wise (Cornell). The devices used in the experimental part of this work were also fabricated in the Cornell Nanoscale Facility.

*J. J. Choi, J. Luria, **B.-R. Hyun**, **A. C. Bartnik**, L. Sun, Y.-F. Lim,, J. A. Marohn, F. W. Wise, and T. Hanrath, Nano Letters, 10, 1805 (2010)*

NNIN Site at Stanford University

Stanford Nanofabrication Facility

MEMS Microdisplay

Alces' MEMS microdisplay is the cornerstone of a next-generation laser display system whose purpose is to expand the possibilities of displays and projectors in professional, military, and consumer applications. Using CMOS-compatible fabrication processes, MEMS microdisplays are fabricated at SNF's facilities for use in Alces' display systems. The MEMS "pixels" are engineered from a bilayer of silicon nitride and aluminum suspended across a sacrificial layer of amorphous silicon over a conductive silicon substrate. After releasing in XeF_2, the MEMS ribbons are electrostatically controlled by applying a voltage between the ribbon and substrate to displace the ribbon downward and adjust the brightness of the pixel.

Dave Bloom, Matt Leone
Alces Technology Jackson, WY

Work performed at Stanford Nanofabrication Facility

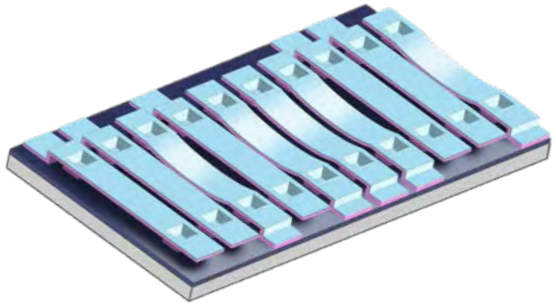

Alces' MEMS microdisplay is composed of a linear-array of electrostatically addressable and reflective ribbons

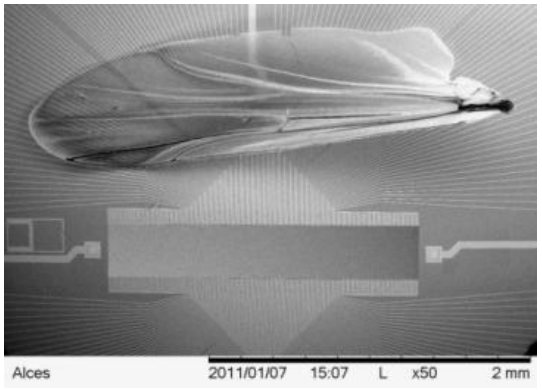

MEMS prototypes are fabricated with a simple 4-mask process MEMS, and with short-fabrication cycles feedback on design changes is quickly generated

Packaged MEMS microdisplays are joined with custom electronics and laser illumination to create a high-performance laser projection display system

ALD-Metal Bolometer and Capacitive Pressure Sensors

BOSCH
Invented for life

A bolometer is a thermal detector that makes use of a temperature-dependent resistor. The purpose of this work is to create an uncooled bolometer with improved performance via the use of a freestanding, several nanometer thick platinum layer deposited using atomic layer deposition (ALD). The structures were fabricated using a combination of the Stanford Nanofabrication Facility and other labs.

In addition to completely new devices, the SNF is also being used to perform research on well established MEMS devices. To leverage their relatively low temperature sensitivity, a new type of capacitive pressure sensor is being investigated that makes use of an electrically isolated electrode embedded in the membrane layer. Such a device allows an increased fractional capacitance change and reduced sensitivity to package stress.

Various researchers at Robert Bosch LLC Research and Technology Center, Palo Alto, CA in collaboration with students, faculty, and staff at Stanford University

Work performed at the Stanford Nanofabrication Facility

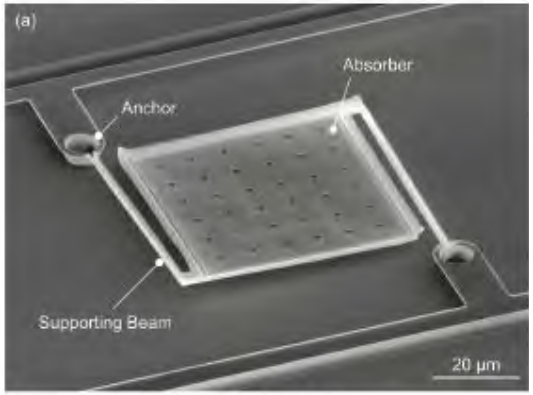

An uncooled ALD-metal bolometer

The bolometer anchor and stiffening trench

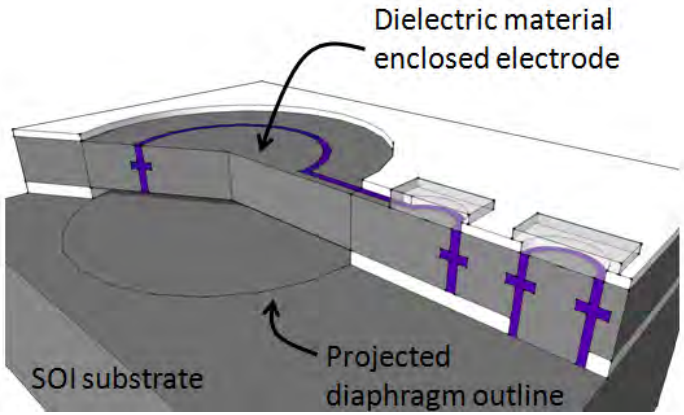

A capacitive pressure sensor with an electrically isolated electrode incorporated into the released membrane.

Microstructure Drug Delivery

Corium's proprietary MicroCor® Transdermal Drug Delivery System (TDS) uses biodegradable microstructures to efficiently deliver peptides, proteins, vaccines and other macromolecules across the skin in a user friendly manner.

The work at SNF is focused on designing and understanding the impact of different microstructure array features on overall device performance. The image on the right shows good skin penetration profile using one of the several designs being evaluated.

MicroCor Transdermal Drug Delivery System

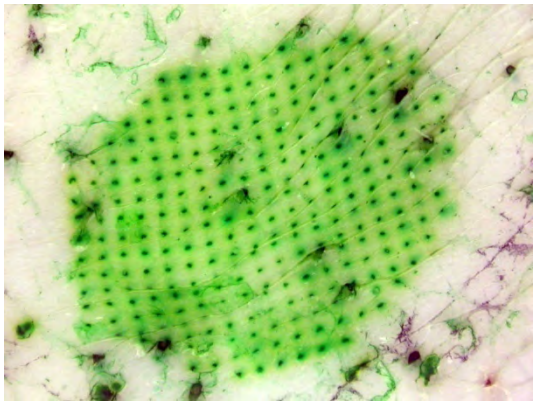

Skin showing good penetration by MSA

Ashutosh Shastry, Corium International, Inc.
Work performed at the Stanford Nanofab Facility

Si Nanowire Arrays as Silicon Photomultipliers (SiPMs) for Medical Imaging

The purpose of this project is to combine recent developments in nanomaterials with the concept of SiPMs to develop cost effective, large area photodetectors for applications in medical imaging and low light sensing applications. The SNF-fabricated components of this system are the silicon nanowires grown inside a template made up of an array of insulating nanotubes on a quartz substrate generating a close-packed array of vertically-oriented nanowires. A gold layer positioned at the bottom of each nanotube acts as the catalyst for silicon growth. By doping the silicon as it is grown, each nanowire becomes a p-i-n photodiode. A resistive layer provides the necessary quenching resistance for each photodiode, and pixels are defined by ganging the outputs of a region of nanowires together.

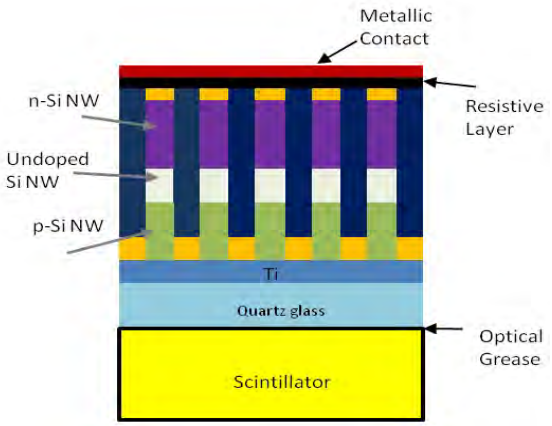

Final detector assembly; Si nanowires are grown with and without doping to form p-i-n photodiodes inside the Al_2O_3 nanotubes. Following the growth, a resistive layer and metallic contact are placed on top of the nanowire array. A scintillator is coupled to the opposite side of the quartz substrate.

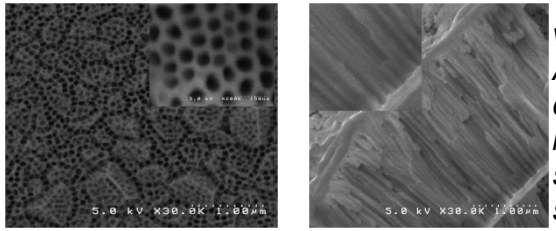

Top and cross sectional view of the nanotubular Al_2O_3 template. Pore diameter: 40-60 nm, pore length: 1.5 μm. Inset shows magnified cross sectional image of the template.

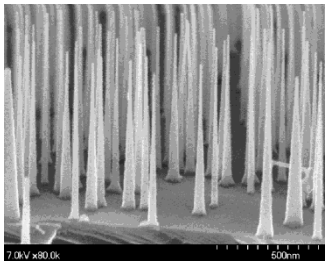

Si nanowires grown with uniform length on a patterned gold substrate. Nanowire diameters are 50-70 nm.

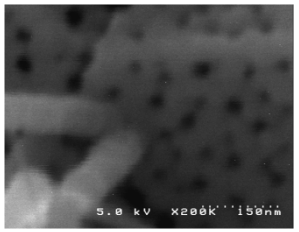

Si nanowire grown inside nanotubular Al_2O_3 template. The nanowire has grown out of the template due to longer growth time.

Thulasi Gandhi, Neal E. Hartsough, Jan S. Iwanczyk and William C. Barber, DxRay, Inc.
Work performed at Stanford Nanofabrication Facility

OndaVia, Inc.

OndaVia develops microfluidics-based technologies to provide sophisticated analysis of trace contaminants in water.

Our portable Raman spectroscopy-based instrument couples with our single use eSERS™ (Embedded Surface Enhanced Raman Spectroscopy) cartridges for field-based, rapid and sensitive analyses. We can measure a wide range of organics, inorganics, endocrine disrupting compounds, pharmaceutical and personal care products at appropriate low levels of detection.

Our eSERS cartridge relies on a patent-pending design that permits the strategic placement of Raman-enhancing nanoparticles. During use, a single drop of sample is placed onto the cartridge, and the cartridge is inserted into the Raman instrument . In a matter of seconds, the instrument analyzes the sample and presents the results to the user.

First Generation Raman Instrument

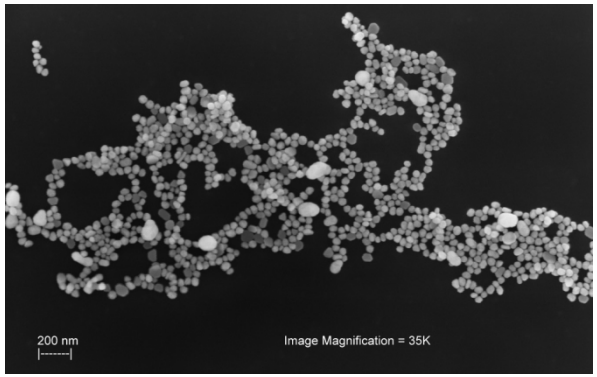

Nanoparticle Cluster (hot spot) imaged with an SEM

Perchlorate Cartridge

OndaVia, Inc.
Work performed at Stanford Nanofabrication Facility

Low Temperature Junction-less Transistor suitable for Monolithic 3DIC

The junction-less transistor (JLT), or gated resistor, is one transistor type that potentially could be easily constructed with a layer transfer Monolithic 3D flow -- Layers of doping activated at high temperature (~900°C), then all subsequent processing (post-layer transfer) is performed at less than 400°C: TEL plasma gate oxide, Al or Pt gates, plasma etching, etc.

Scout lots utilizing poly-crystalline silicon for the channel material helped develop metrology and processing techniques that resulted in successful transistor formation (example Id-Vd curve on right), but very low Ion due to very high contact resistance & a polycrystalline channel.

Cored SOI wafers were next utilized to provide a mono-crystalline & thinner silicon channel (10nm) to allow higher channel doping & more effective gate control, and thick (70nm) source/drains for better contact resistance. Unfortunately, this was scrapped in-line with no result.

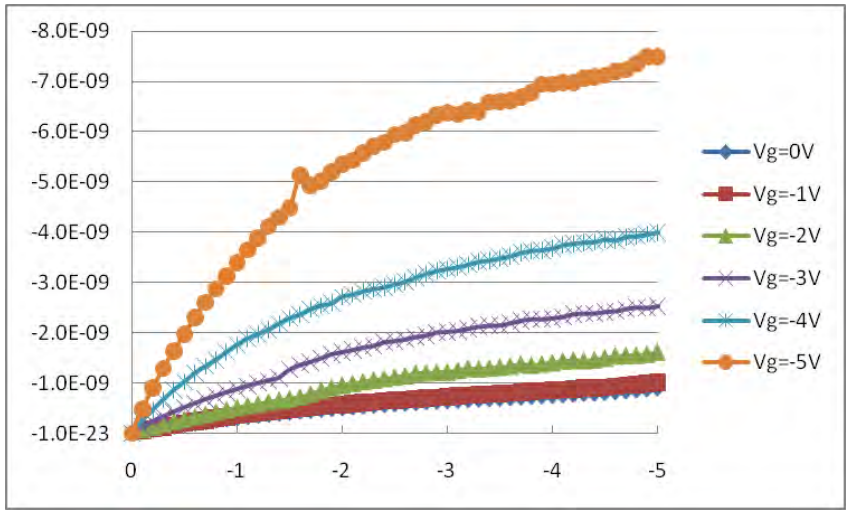

I_d-V_d curve family at various Vg of a low temperature polysilicon channel pJLT, aluminum gate. W/L = 100/0.45um, channel thickness 20nm, 5nm gox, 5e18 channel doping.

Brian Cronquist, Deepak Sekar, Paul Lim, Zvi Or-Bach
NuPGA/Monolithic 3D Inc.
Work performed at Stanford Nanofabrication Facility

Concentrating and Detecting Waterborne Pathogens for Resource-limited Settings

To address the need for fast, affordable, and accurate diagnostics for waterborne pathogens, we develop a novel method for detecting pathogens in water sources using a fully integrated microfluidic device that concentrates and electrochemically detects the DNA of bacterial cells.

Fluidic channels for concentrators and detectors were fabricated by standard photolithography and dry etching. The detectors incorporate two gold working electrodes, a platinum counter electrode, and a platinum reference electrode fabricated by standard photolithography. The probe undergoes a redox reaction with the gold to provide a specific current depending on the target DNA concentrations.

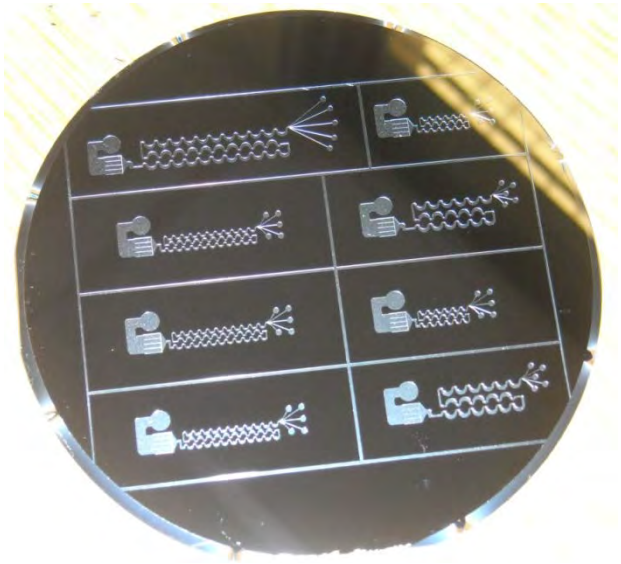

Concentrators implementing asymmetrically curved channels

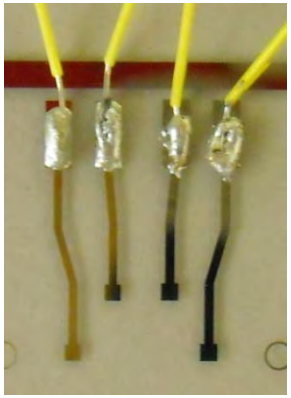

DNA detection chamber incorporating gold working electrodes, platinum counter and reference electrodes.

Sarah Ghanbari and Unyoung Kim,
Santa Clara University

Work performed at Stanford Nanofabrication Facility

Graphene Nanopores on CMOS

The purpose of the Graphene Nanopore on CMOS project is to develop a universal small molecule detector, capable of even sequencing DNA, that is high speed and highly sensitive. The SNF-fabricated components of this system have been the growth of a wafer with layers that mimics an ON-SEMI fabricated device, the large area fabrication of nanopores on these wafers, and development of a process for large area graphene transfer on thin (40nm) TEOS oxide membranes. The ON-SEMI specified wafers serve as wafers for process development of nanopores. The nanopores are patterned on a on a thin oxide membrane using eBeam lithography and RIE. Graphene nanopores are fabricated by first transfering the graphene on the membrane, then patterned, and etched

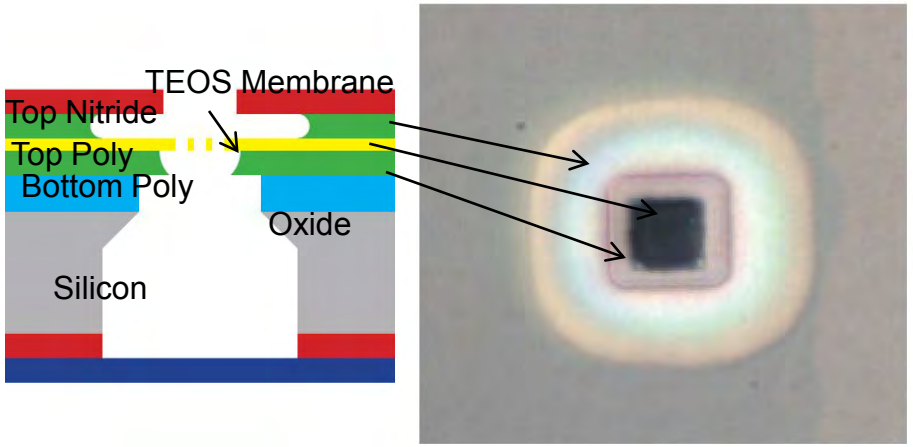

Cross section picture and top-view micrograph of a nanopore device.

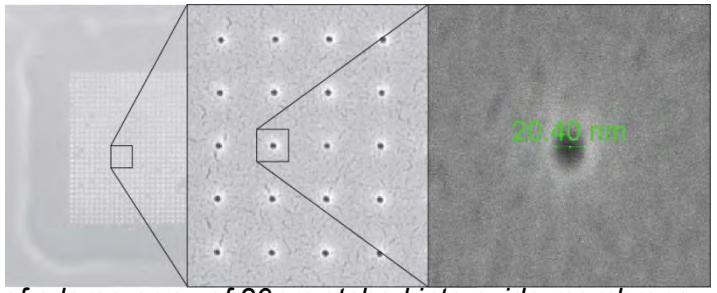

SEM of a large array of 20nm etched into oxide membrane

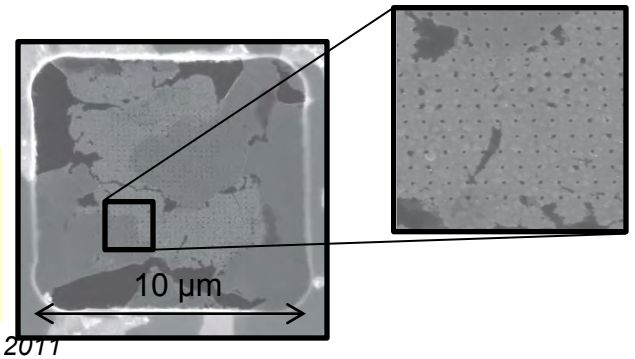

SEM of a large array of 20nm etched into a large graphene sheet on an oxide membrane

Kaveh Milaninia, Ashfaque Uddin, and Luke Theogarajan, University of California, Santa Barbara

Work performed at Stanford Nanofabrication Facility

Nanotechnology-Enabled Artificial Kidney

We are actively developing an implantable renal replacement device that will provide therapeutic benefits on the order of kidney transplants to the 500,000+ End Stage Renal Disease patients in the US. Our key component is a silicon nanoporous membrane (SNM) fabricated with highly uniform sub-10 nm pores, which enables our device to provide therapeutic benefit in a compact form factor that is suitable for implantation. Our SNMs are currently fabricated at the SNF, specifically utilizing the ASML PAS 5500 UV Stepper and STS DRIE tools, and are being used in ongoing animal studies.

Shuvo Roy, Rishi Kant, Ken Goldman, William Fissell, and Aaron Fleischman; UCSF, H-Cubed Inc, and Cleveland Clinic.

Work performed at Stanford Nanofabrication Facility (SNF)

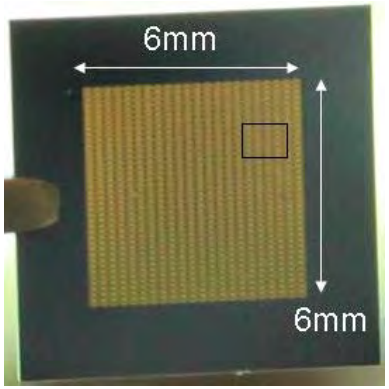

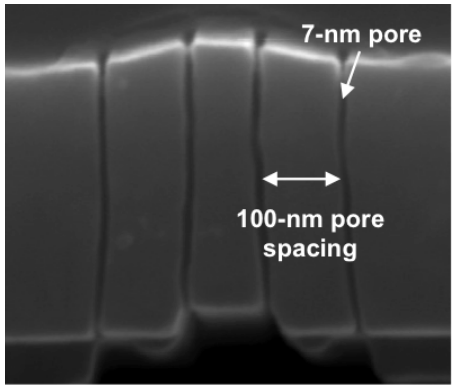

(Left) Photograph of a SNM chip and (Right) SEM of membrane cross-section with 7 nm-wide slit pores spaced 100nm apart fabricated on a 0.4 μm-thick polysilicon layer.

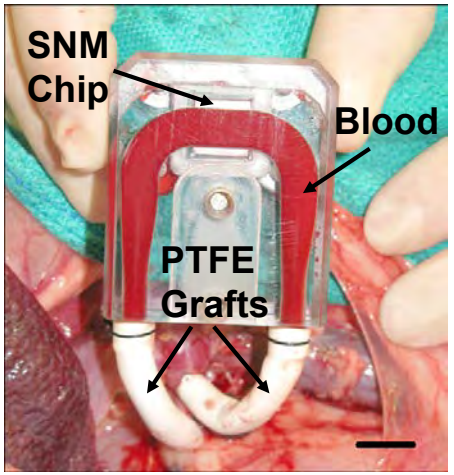

Photograph of a membrane chip mounted in a polycarbonate cartridge that is surgically implanted in a mini-pig for hemofiltration.

Lateral NEM Switch Technology for Robust, Low-Power Digital Systems

Nanoelectromechanical switches are designed for robust, low-power computation in complement with standard CMOS devices. High efficiency is achieved by using the stored energy of the device to switch. The devices fabricated at the Stanford Nanofabrication Facility (SNF) include single relays and chained relays in logic gates, as well as CMOS logic to prove procedural and functional compatibility. Polysilicon features are coated with HfO_2 then Pt or Tin using an ALD process. The beam is then released in HF followed by CPD.

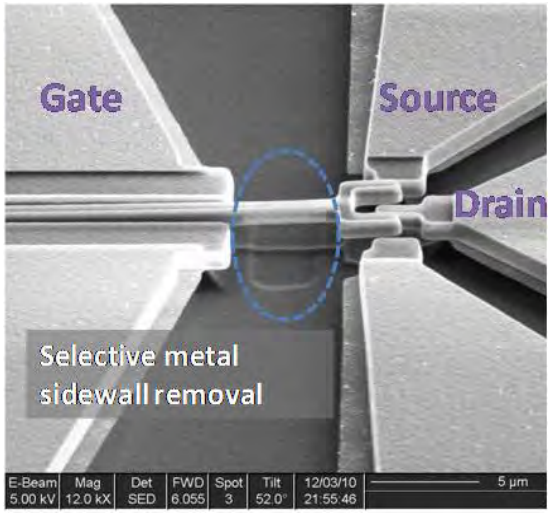

A 6 terminal logic element with sidewall isolation.

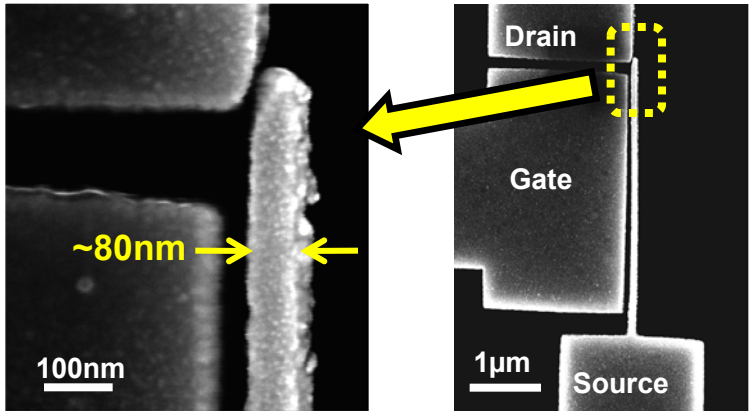

A 3 terminal device making contact.

R. Parsa, S. Chong, C. Chen, K. Yoo, W. S. Lee, X. Shen, D. Lee, J Provine, S. Mitra, R. T. Howe, and H.-S. Philip Wong

Collaborators include SEMATECH, Altera and IME-Singapore.

Work performed at Stanford Nanofabrication Facility

High-Yield Nanoscale Molecular Junctions

The purpose of the Molecular Junctions Project is to develop a high-yield, low variability device structure to enable comparable measurements across a range of organic self-assembled monolayers. The devices incorporate a silicon nitride dielectric layer, which is deposited and etched using the STS Plasma Enhanced Chemical Vapor Deposition and MRS Reactive Ion Etch tools in the SNF.

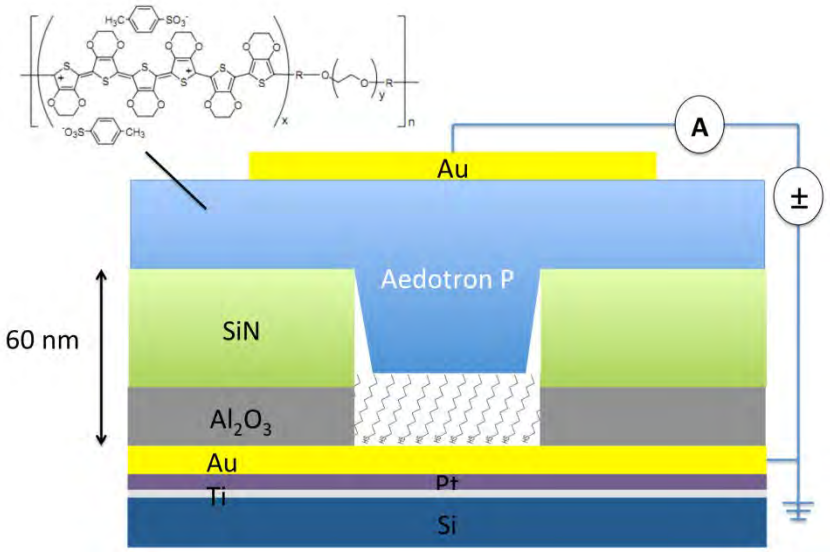

Schematic of a molecular junction

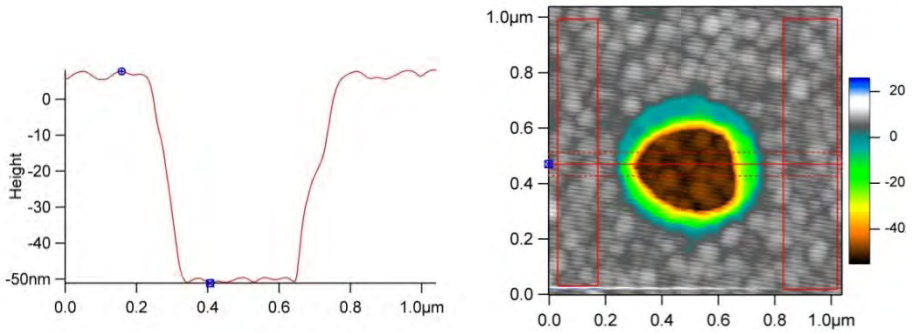

Atomic force microscope image of a 330 nanometer diameter molecular junction before top contact deposition

Scanning electron microscope image of a 330 nanometer diameter junction

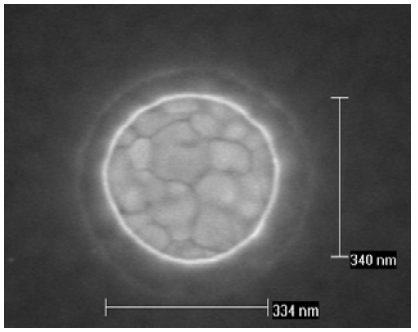

Alex Neuhausen, Ali Hosseini, Joseph Sulpizio, Chris Chidsey and David Goldhaber-Gordon, Stanford

Work performed at Stanford Nanofabrication Facility

Volumetric Intracardiac Ultrasound Imaging

The purpose of this project is to develop an intracardiac echocardiography (ICE) catheter for real-time, forward-looking, volumetric imaging. The heart of the catheter is a ring-shaped 2-D capacitive micromachined ultrasonic transducer (CMUT) array, which generates and senses ultrasound waves for imaging. The Ring CMUT array was fabricated using bulk and surface micromaching techniques, employing a wide range of equipments, such as, plasma etchers, oxidation furnace, and LPCVD deposition tools.

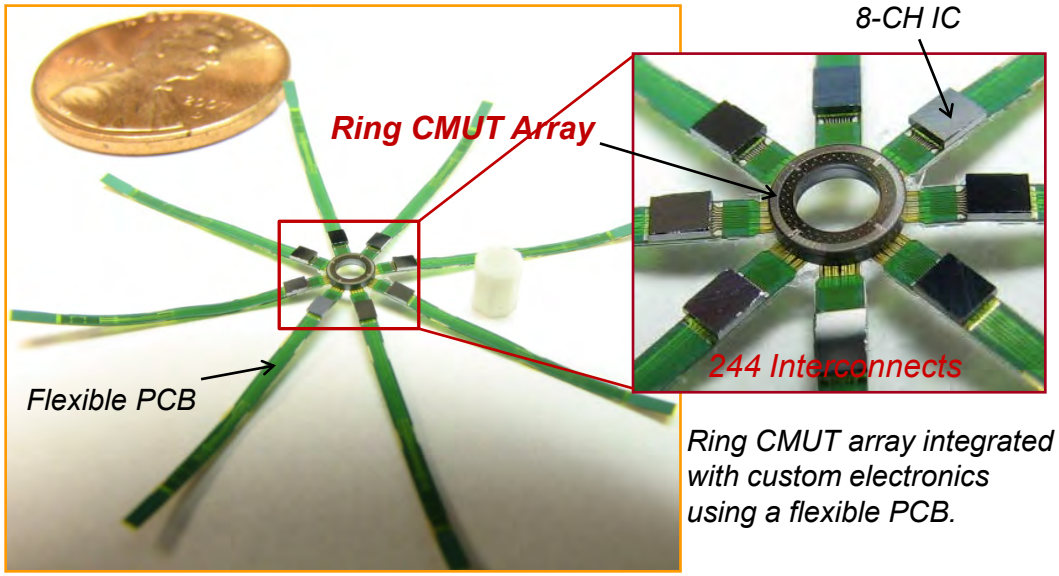

Ring CMUT array integrated with custom electronics using a flexible PCB.

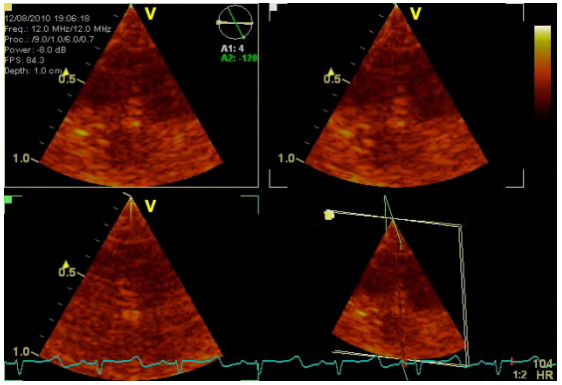

In vivo heart images of a porcine animal model acquired with a Ring CMUT ICE catheter.

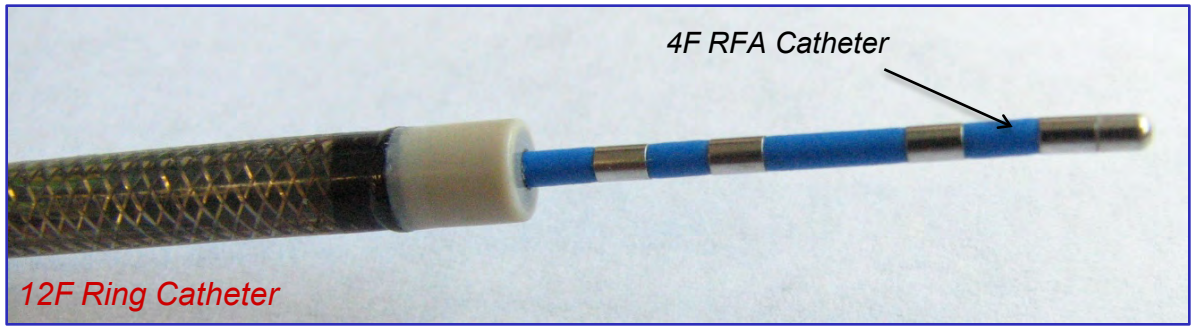

Photograph of a finalized 12F Ring CMUT ICE catheter, showing an external 4F RFA catheter introduced through its inner lumen.

Butrus T. Khuri-Yakub, Stanford University

Work performed at Stanford Nanofabrication Facility

Microfluidic Impedance Spectroscopy

Impedance spectroscopy is a powerful technique to analyze and characterize particles flowing in a stream.

A limitation of impedance spectroscopy is the low impedance signals produced by small particles. A technique of dielectric sheathing with two-phase flow was developed to increase the signal-to-noise ratio (SNR). Besides signal improvements, such approach would also allow smaller particles to be measured, over an extended frequency range.

A microfluidic impedance flow spectrometer based on dielectric hydrodynamic focusing (sheathing) was fabricated using laser-ablated 50 µm thick double-sided adhesives bonded to glass wafers with sputtered platinum microelectrodes. SNR improvements of up to 23 dB have been measured using this two-phase, dielectric sheathing approach.

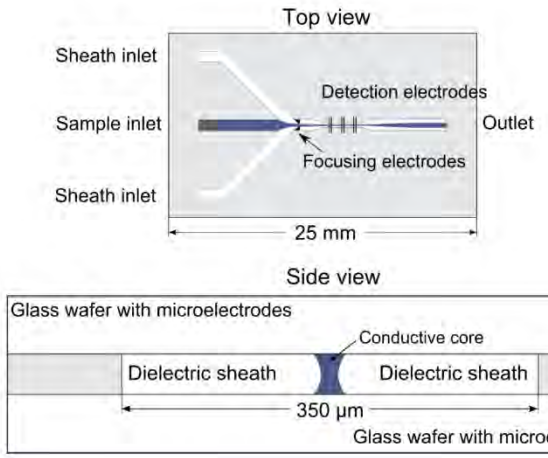

Schematics of a microfluidic channel for dielectric sheathing. Top: top view (including electrodes). Bottom: cross-sectional view.

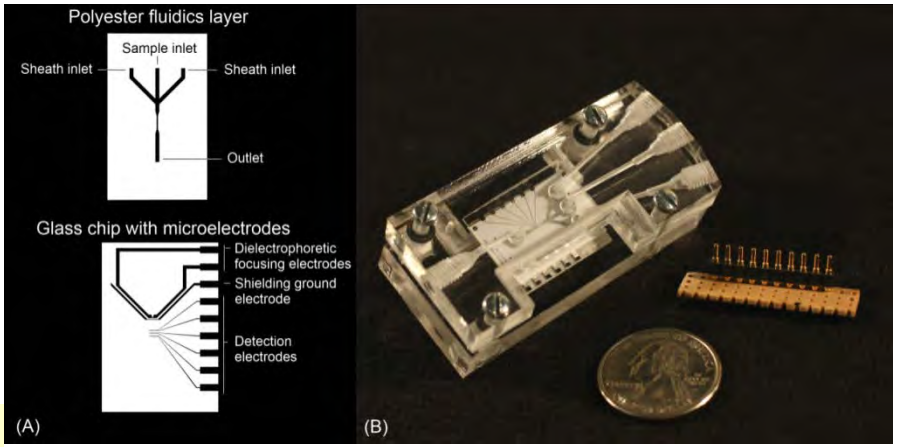

Pictures of fluidics layer, assembled glass chip, and complete fluidic cartridge.

M. Evander, L. Giovangrandi, A.J. Ricco, and G.T.A. Kovacs

Work performed at Stanford Nanofabrication Facility.

Ge/SiGe Quantum Well Waveguide Modulator

Electrical interconnects– the metal wires that carry data on distance scales ranging from on-chip to between backplanes of large datacom servers– are increasingly facing both density and energy limitations. Optical interconnects offer a possible solution, but many material and design challenges must first be overcome.

Optical modulators are a key component of future optical interconnect systems. Ge/SiGe quantum wells (QWs) are a Si-compatable material system with an extremely strong electroabsorption mechanism. By epitaxially growing these QWs in selective areas on a wafer, we are able to integrate them with low-loss Si waveguides, thus enabling high-speed, high contrast ratio QW waveguide modulators.

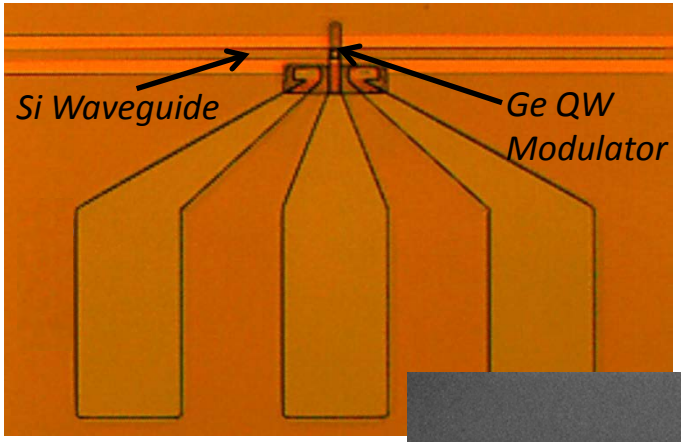

A Ge quantum well modulator integrated with a Si waveguide.

SEM image of the epitaxially-grown Ge/SiGe QWs grown in selective-areas on an SOI wafer.

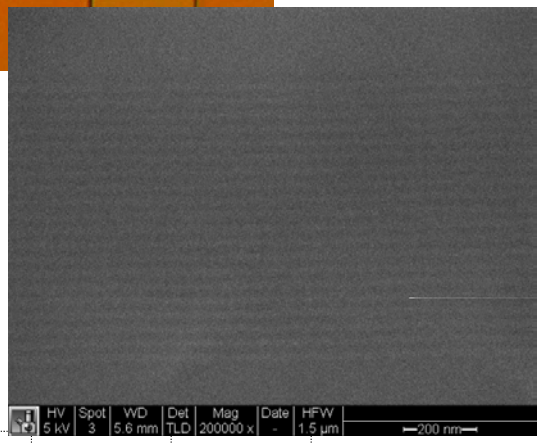

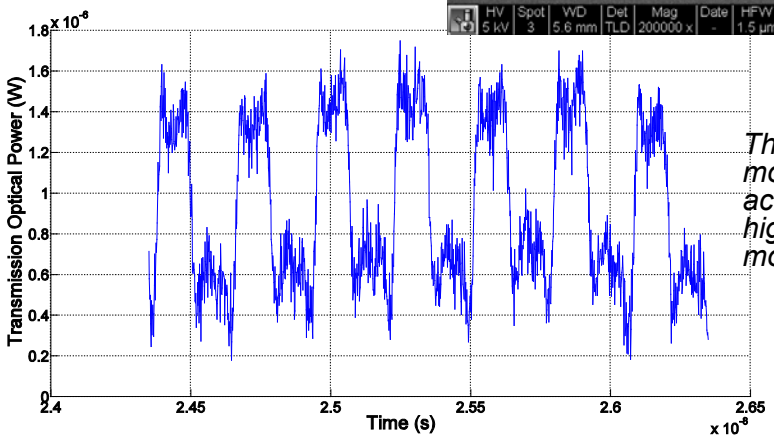

These GE QW modulators have achieved 3.5 GHz high-speed optical modulation.

Stephanie Claussen, Shen Ren, Ed Fei, Yiwen Rong, James Harris, and David Miller, Stanford
Work performed at the Stanford Nanofabrication Facility

NNIN

Nanometer scale two conductor waveguides for on chip optical interconnects

One of the key challenges to address in the implementation of on-chip optical interconnects is the issue of size mismatch between optical components like dielectric waveguides (μm) and transistors (nm). Two conductor waveguides with nm scale cross section present us with one solution for dense integration of on chip optical interconnects.

Present work has been aimed at fabrication and characterization of these waveguide structures. Figure 1 shows an SEM image of the fabricated structure along with the stub coupler for exciting the waveguide mode. Figure 2 shows a 2D photocurrent map of the device taken with orthogonal polarizations showing preferential excitation of the waveguide mode.

Dany Ly-Gagnon, Krishna Balram, Justin White, Pierre Wahl, Mark Brongersma and David A.B. Miller
Work performed at Stanford Nanofabrication Facility

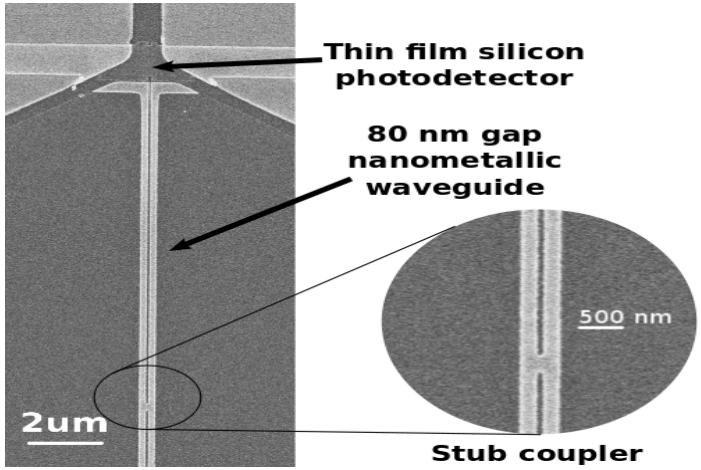

Fig.1 SEM image of fabricated device

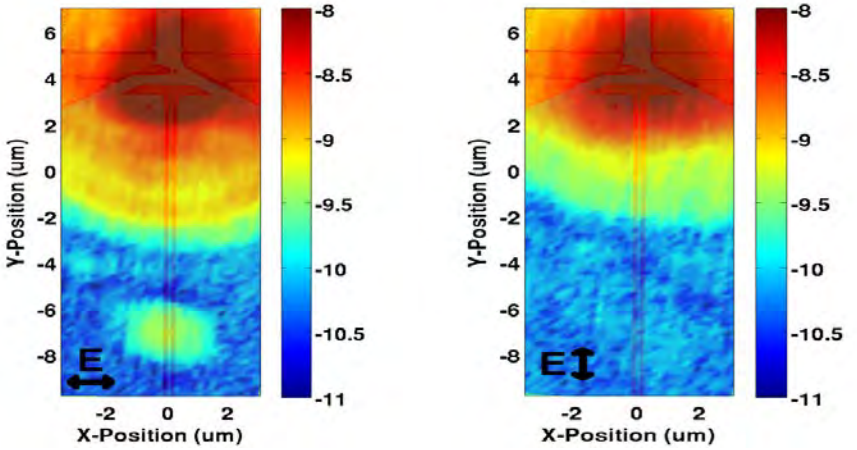

Fig.2 2D Photocurrent Map

Anti-Brownian ELectrokinetic Trap

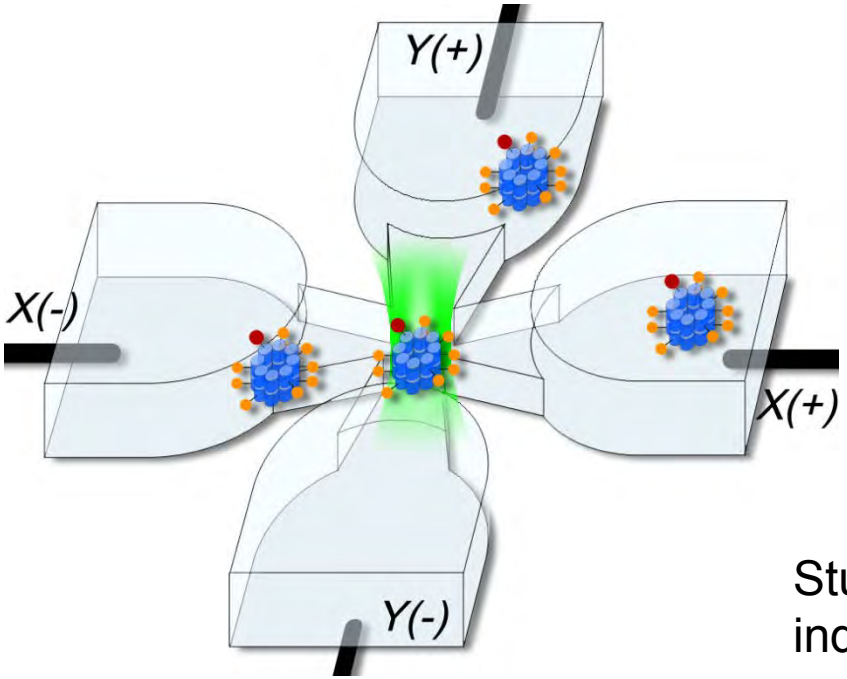

- **Optical detection + real time feedback forces via microfluidic channels**
- **Trap sub-10nm fluorescent particles (e.g. single biological proteins) in aqueous solution.**
- **Single molecule measurements reveal heterogeneity that is not accessible from ensemble-averaged experiments**

Study cooperativity in individual multi-subunit enzymes (chaperonin TRiC).

Y. Jiang et al, PNAS (2011, in press)

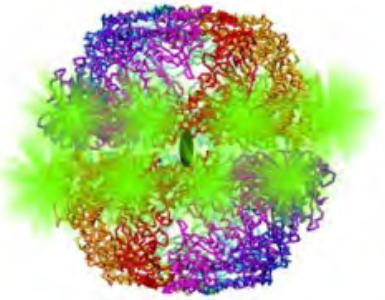

Study photophysics of single photosynthetic antenna proteins (allophycocyanin).

R. Goldsmith and W. E. Moerner, *Nat. Chem.* **2**, 179 (2010)

Moerner Research Highlights 2011

Self-Sensing, Coaxial-Tip Scanning Probes

A wealth of scanning probe techniques exists to image local electrical properties. The lateral resolution of these techniques is limited by stray capacitance between the probe and the sample. We have developed cantilever probes that feature a coaxial tip, shielding electric fields up to the tip apex, resulting in 2x improvement in lateral resolution over commercial metal-coated probes. Our probes also integrate a piezoresistor, enabling electrical measurement of cantilever deflection, and thus sample topography, without the conventional laser system which can perturb photosensitive samples.

The scanning probes are fabricated from silicon-on-insulator wafers through a combination of oxidation, diffusion, metalization and etching steps, performed in the SNF.

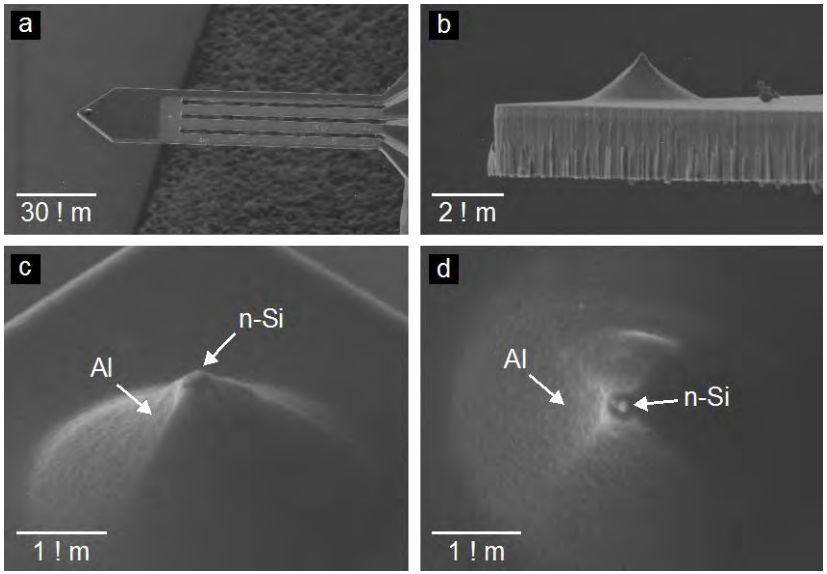

Scanning electron microscope images of (a) a representative scanning probe, (b) an unopened tip, and (c,d) a coaxial tip opened with focused ion beam milling shown at 52° and 0° tilt respectively. The diameter of the shield opening is 310 nm.

Nahid Harjee, Alexandre Haemmerli and Beth Pruitt, Stanford University

Work performed at Stanford Nanofabrication Facility

High Mobility III-V PMOS

Transistors based in III-V semiconductors have been used for a variety of analog and high frequency applications driven by the high electron mobilitiy. On the other hand the hole mobility in III-Vs has always lagged compared to Si and Ge. Our goal is to develop complimentary technology in the same III-V channel material. InGaSb is an attractive candidate for high performance III-V pMOSFETs due to its high bulk hole and electron mobility.

We have fabricated and studied InGaSb pMOSFETs with ALD Al_2O_3 dielectric and metal gate self-aligned source/drain formed by ion implantation. Parameters such as strain, valence band offset, effective mass and splitting between the light and heavy hole bands and dominant scattering mechanism which are important for optimizing hole transport are modeled and measured quantitatively using various experimental techniques. A record peak hole mobility of 960cm^2/Vs is demonstrated and the high hole mobility is maintained even at high sheet charge.

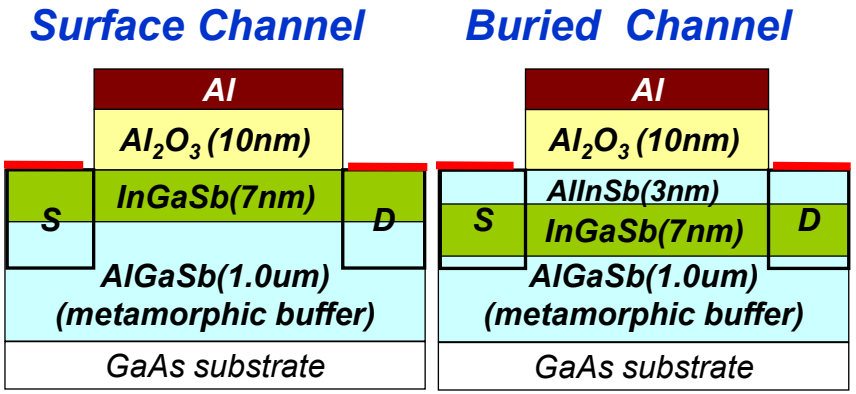

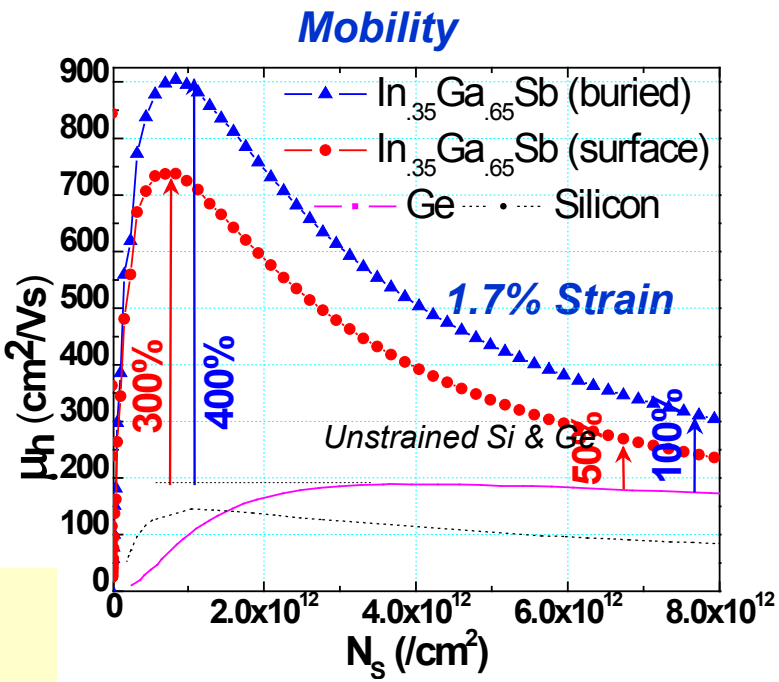

A. Nainani (K. Saraswat Group), in collaboration with NRL

Devices fabricated at Stanford Nanofabrication Facility

Electrically Pumped Photonic Crystal Laser

The purpose of electrically pumped photonic crystal laser project is to develop a very low power source for use in optical interconnect applications. In this project, a laser with a world record low threshold was demonstrated by taking advantage of unique photonic crystal properties. The Stanford Nanofabrication Facility (SNF) was used for the majority of the fabrication of the device with only a few implantation steps performed externally. Multiple rounds of electron beam and standard lithography are used along with dry etching, MOCVD, metallization, and oxidation steps. The final device consisted of a thin GaAs membrane with a conducting current path into the cavity region that was formed out of the ion implantation procedure. Some additional metallization was performed at facilities in UC Berkeley.

Bryan Ellis, Gary Shambat, Jan Petykiewicz, and Marie Mayer, and Jelena Vuckovic,
Stanford University and UC Berkeley

Work performed at Stanford Nanofabrication Facility and Berkeley Marvell Nanofabrication Laboratory.

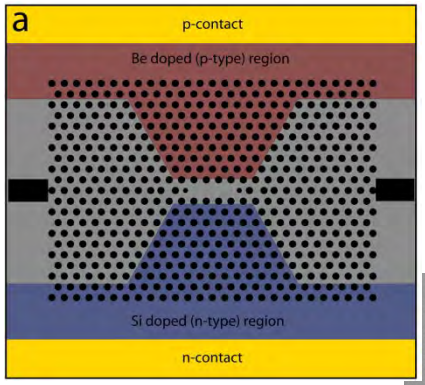

Layout of the photonic crystal laser design. A lateral p-i-n junction is formed in quantum dot containing GaAs.

Tilted angle SEM of a fabricated photonic crystal laser structure

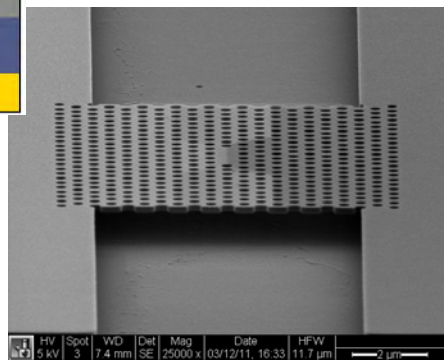

Experimental laser data: as the device is forward biased a clear lasing threshold is observed (left) and an IR speckle pattern is seen from the output emission (right)

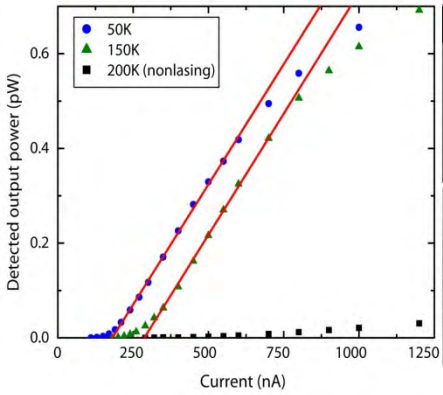

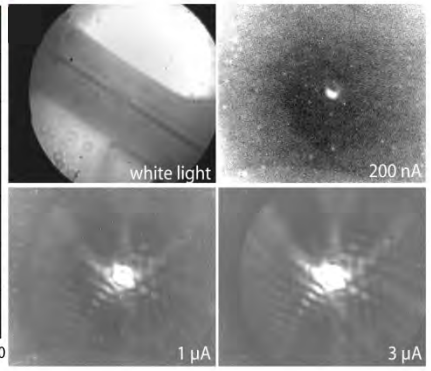

3D - FPGA

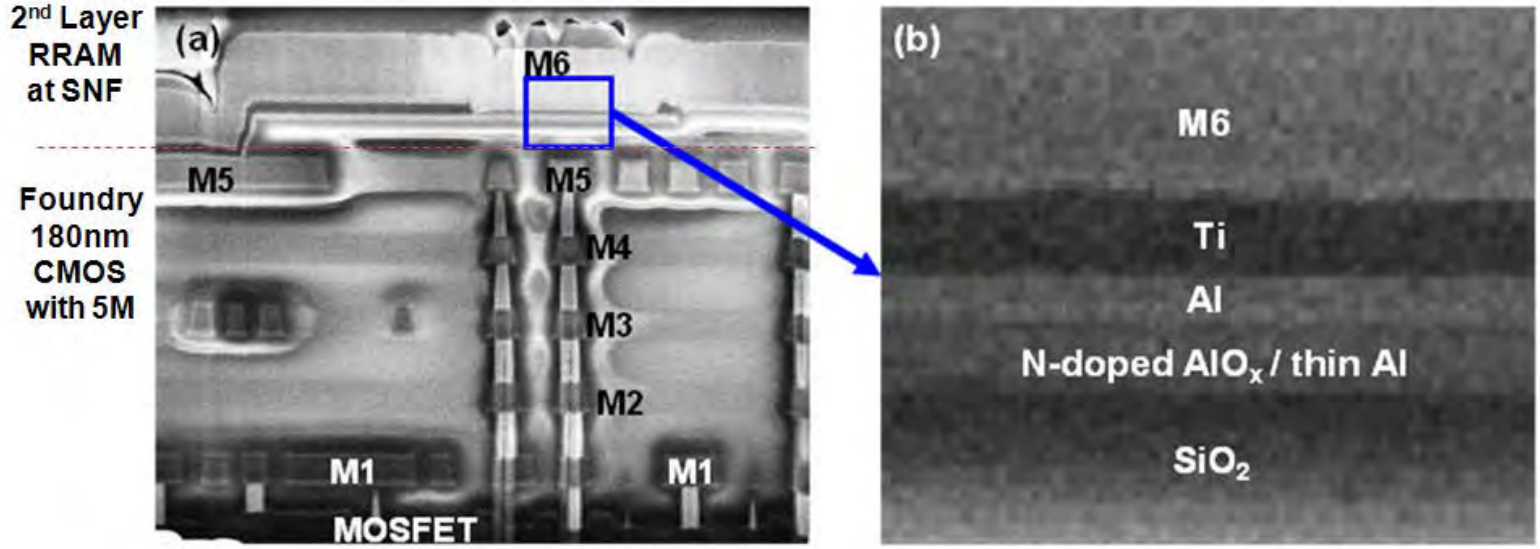

Cross-sectional View of 3D-FPGA

Expanded View of RRAM

The 3-Dimensional Field-Programmable Gate Array is composed of (1) a 180nm CMOS wafer with 5 metal layers fabricated at foundry, and (2) resistive random-access-memory and metal-6 fabricated at Stanford Nanofabrication Facility. By stacking the configuration memory on CMOS, the chip area is reduced by 40%.

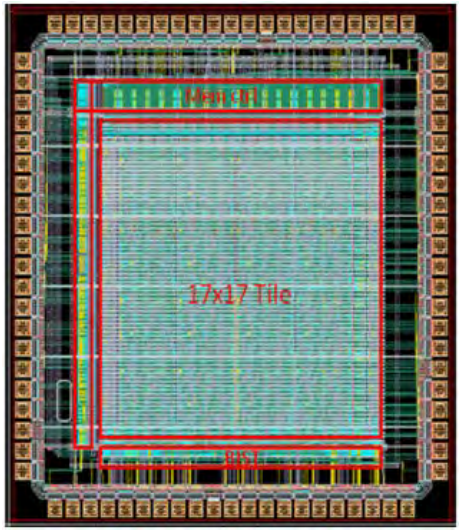

Top View of 3D-FPGA

Simon Wong, Stanford University

Work performed at Stanford Nanofabrication Facility

High-Throughput Selective Single-Cell Capture

Our lab has produced several high-throughput methods for capturing large, statistically significant numbers of single-cells in a selective manner based on size and morphology which have minimal to no impact on cell viability.

Using the photolithography equipment at the Stanford Nanofabrication Facility, our lab created master molds for PDMS microchips that incorporated two types of filters composed of pores with controllable diameters. One filter is a chemically etched rigid PET membrane of randomly patterned conical nanopores. The other is a PDMS filter that can be specifically patterned from a master mold, also made in the SNF. Both give the user selective control over cell capture, which we have used for observation and sample purification purposes.

Romana Schirhagl, Eric Hall, Peng Guo, &
Richard Zare, Stanford University

Work performed at Stanford Nanofabrication Facility

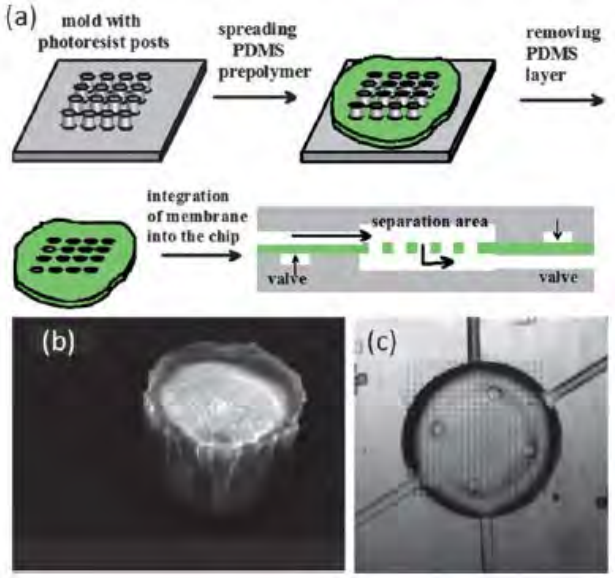

Fabrication of a PDMS membrane (a) with pores that can be controlled by size of SU-8 mold post diameters (b) and integrated into a PDMS microfluidic chip (c).

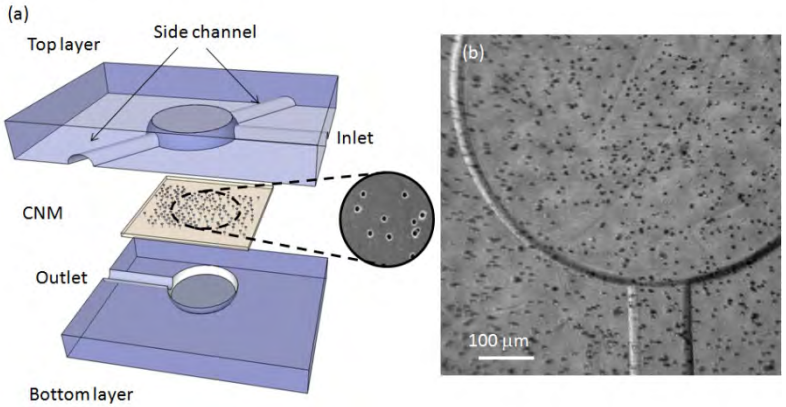

Integration of a rigid PET nanoporous membrane into a microfluidic device (a) capable of capturing large numbers of single cells, one per pore (b).

Passivation Studies for Efficient Si Wire Radial Junction Solar Cells

Vertically aligned Si wire radial junction solar cells have been highlighted due to their efficient charge-carrier collection and enhanced light absorption. Nevertheless, they still face critical challenges such as large junction and surface recombination losses due to their inherent large junction and surface areas. The purpose of this study is to develop effective junction and surface passivation strategies to improve their efficiencies. In this study, we dry-etched Si wafers to form Si microwire vertical arrays, in order to focus on the passivation studies only. Thin-poly Si, which is used for junction passivation and junction formation, was deposited by using conventional CVD. The outermost a-SiN:H shell was formed by using PECVD for surface passivation. Remarkably, our junction and surface passivation strategies effectively increase the efficiency from 7.2% to 11.0%.

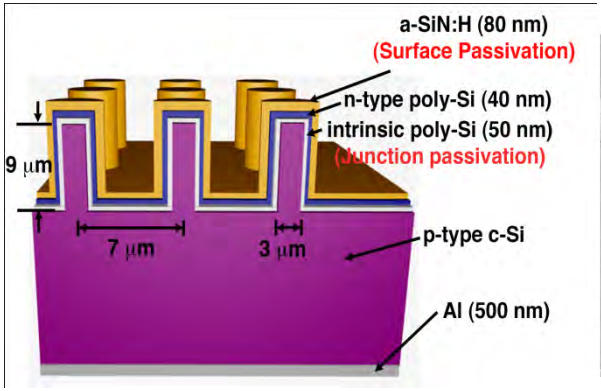

Schematic of effective junction and surface passivation strategies for Si wire radial junction vertical array solar cells

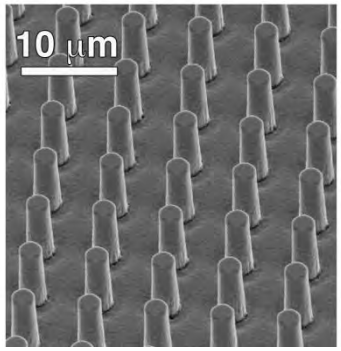

SEM image of Si wire radial junction vertical array solar cells

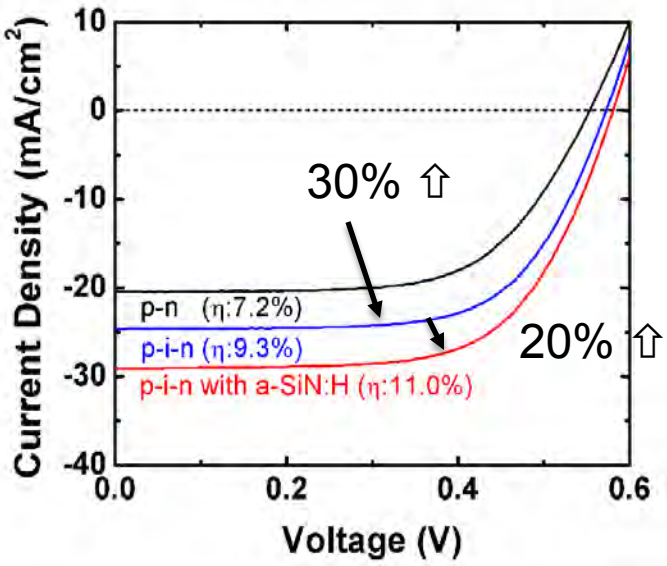

Light J-V curves of three different representative solar cells showing effective junction and surface passivation

Xiaolin Zheng, Mechanical Engineering, Stanford University

Work performed at Stanford Nanofabrication Facility

NNIN Site at Georgia Tech

Perspiration NanoPatch for Electronics Cooling

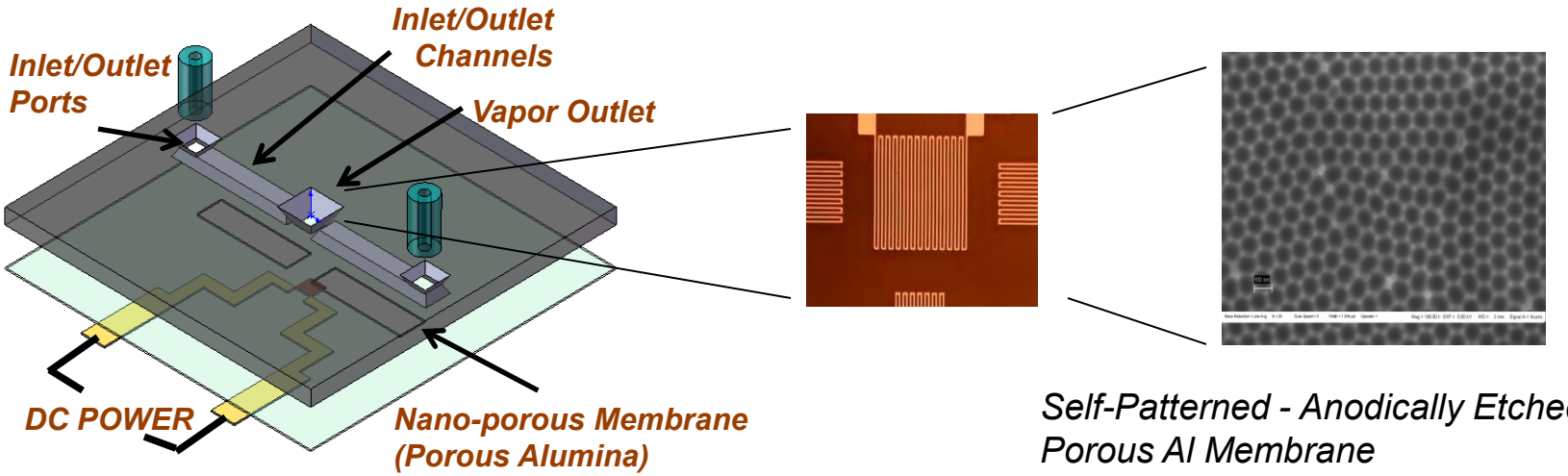

Self-Patterned - Anodically Etched Porous Al Membrane

Heat removal is a limiting factor in maximum power density in high performance IC's . The porous membrane fabricated here provides localized 2-phase cooling for hotspots. It dissipates extremely large heat fluxes and is compatible with CMOS fabrication. Heat removal exceeds 500 W/cm2 and Heat transfer coefficient exceeds 450,000 W/m2K !!!

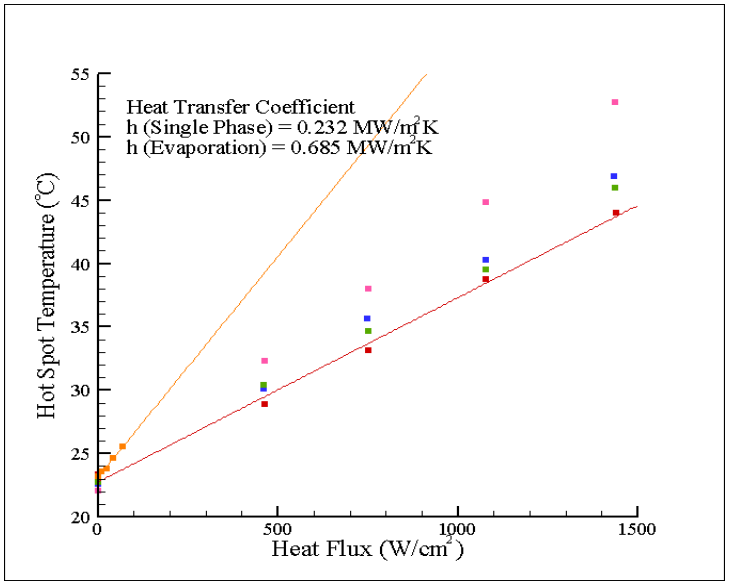

Student: Narayanan, S., PI's:Fedorov, A., and Joshi, Y.,- ME, Georgia Tech

Work performed at Georgia Tech

Nanoscale Geometry of the Adhesive Interface Regulates Integrin Recruitment and Adhesive Force

Bio-inspired surfaces, including micropatterned *substrates, are engineered to control cell adhesion in order to direct signaling and cell function.*

Biomolecular surfaces have been engineered to target specific adhesion receptors to modulate cell signaling and differentiation.

These biomolecular strategies are applicable to the development of 3D hybrid scaffolds for enhanced tissue reconstruction,"smart" biomaterials, and cell growth supports.

One cell / pattern

"Heat Map" Stacked Average

Integrin Binding

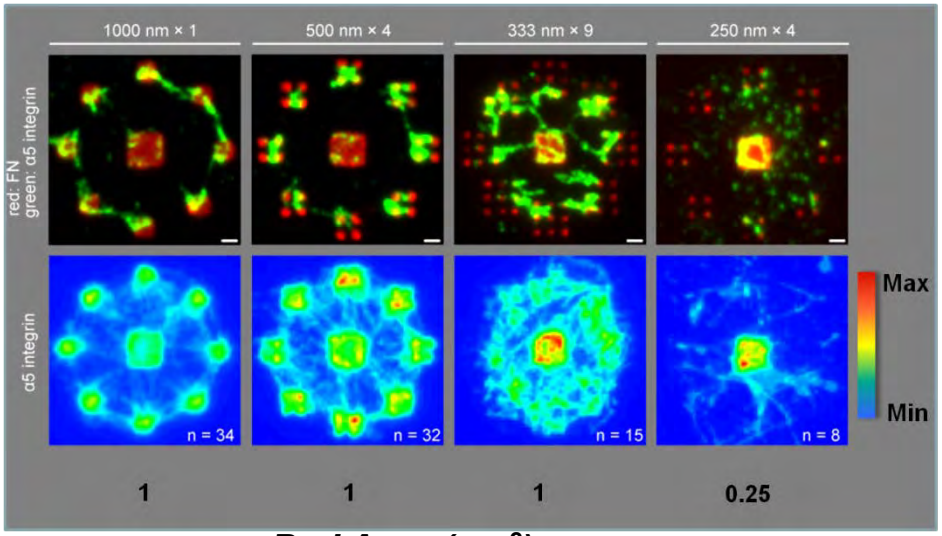

Pad Area (μm²)

Cell Adhesive Force

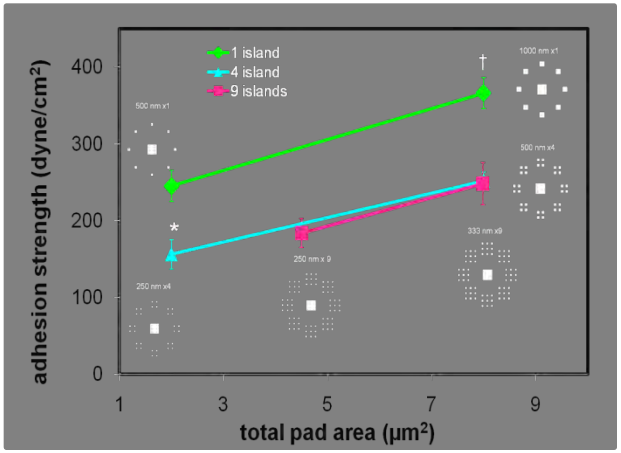

Student: Sean Coyer, PI: Andrés J. García- ME, Georgia Tech
Funded by NIH R01-GM065918

Work performed at Georgia Tech

Graphene p-n Junction

Nanoscale PN junction in Graphene

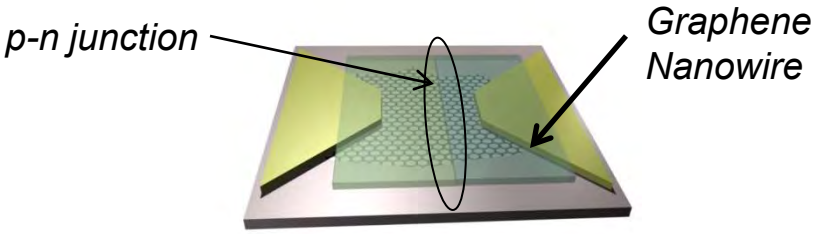

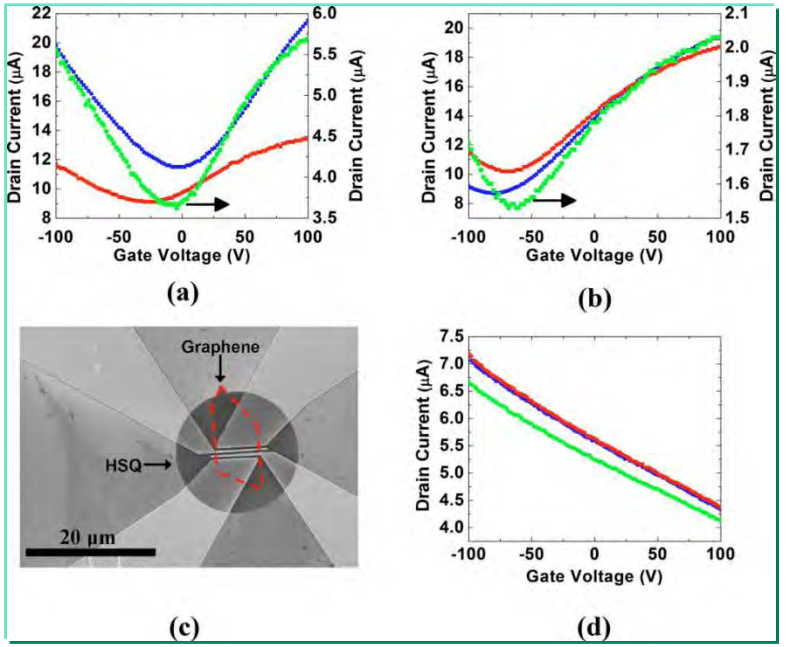

- *Graphene p-n junction formed in a single lithography step, using hydrogen silsesquioxane patterned on graphene*

- *Both electron and hole doping through control of the polymer cross-linking process.*

- *This dual-doping is attributed to the mismatch in bond strength of the Si–H and Si–O bonds in the film as well as out-gassing of hydrogen with increasing cross-linking.*

- *High spatial resolution, allowing for production of novel nano-scale devices using graphene; these novel devices will result in orders of magnitude savings in power while operating at a higher frequency than traditional Silicon CMOS devices*

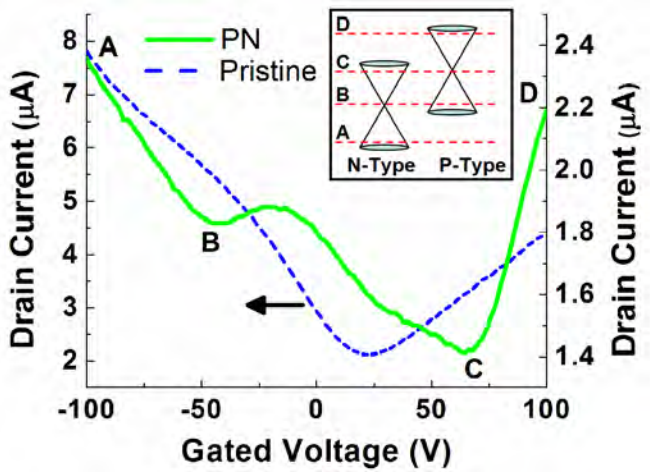

Student: K. Brenner, PI: R. Murali- Georgia Tech

Work performed at Georgia Tech

Studying the Properties of Assembled Nanoparticles of Different Shapes

Fundamental research of nanoparticles has been performed on arrays of nanorods, nanoprisms and nanorings, fabricated on the JEOL JBX-9300FS EBL system. The optical properties of the various systems were investigated spectroscopically. The plot shows the extinction spectra for **nanoprisms** at five different tip-to-tip interparticle separations . As the distance between the particles decreases, the peak redshifts

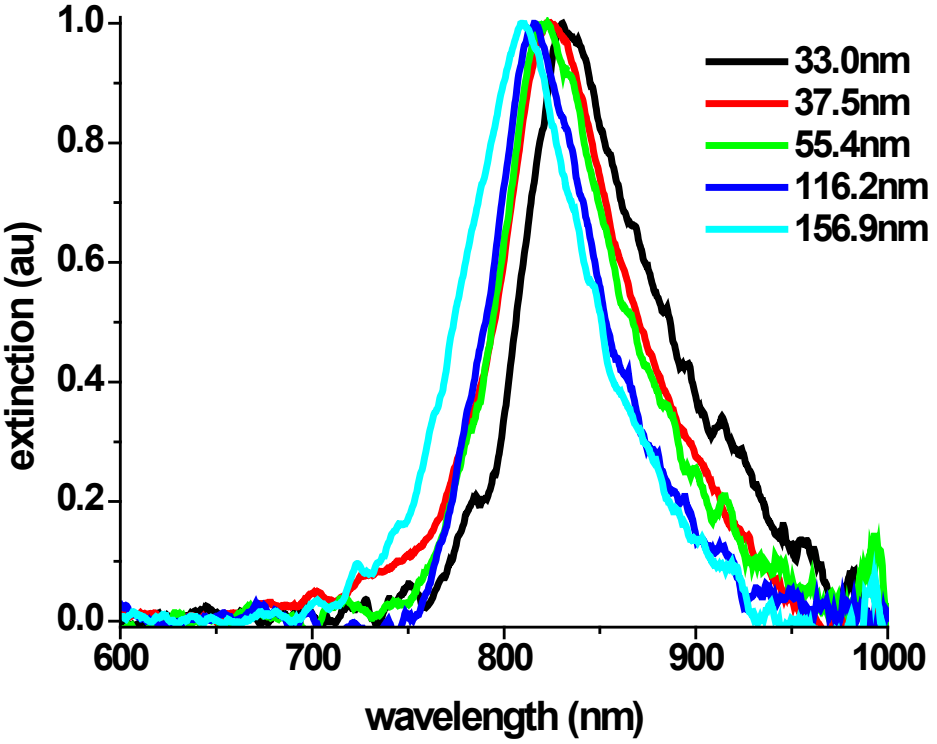

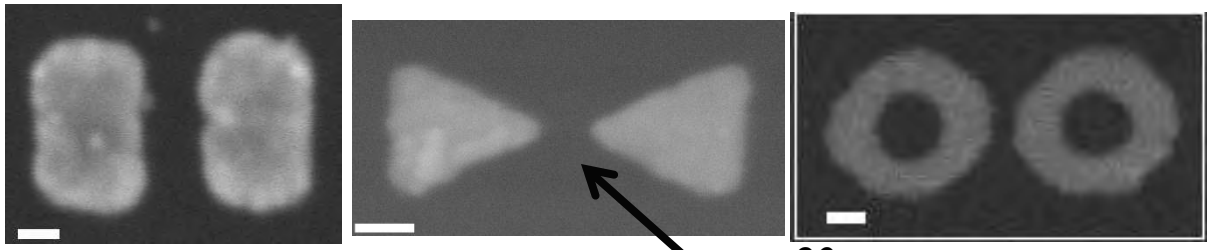

Student: Rachel Givens, PI: Mostafa El-Sayed-Chemistry, Georgia Tech

Work performed at Georgia Tech

Carbon Nanotube-Based Spindt Cathodes for Hall Effect Thrusters

Hall thrusters are appealing for a number of Earth-orbit space missions for their high specific impulse, high thrust efficiency, and high thrust density. Carbon Nanotube electrode arrays as Hall thrusters offer 10% fuel saving, a high level of redundancy and low power field emission extraction of electrons

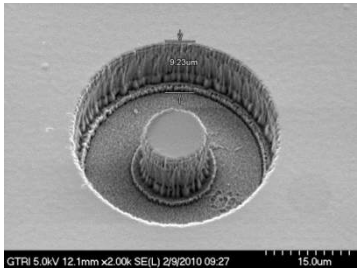

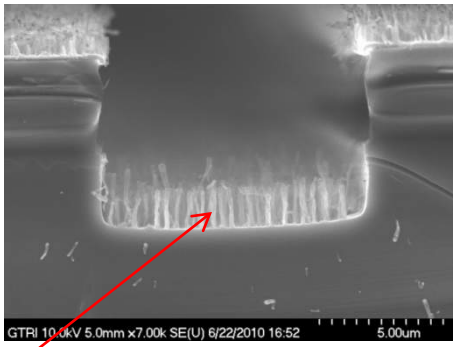

Carbon Nanotubes

Hall Thruster Under Test

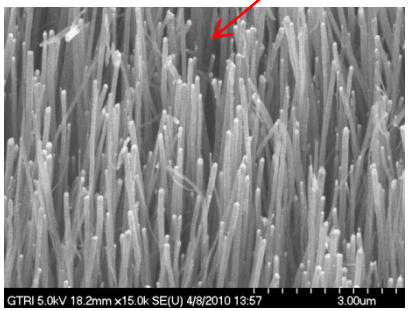

Dr J. Ready –GTRI, Georgia Tech
Prof. M. Walker - AE, Georgia Tech

Work performed at Georgia Tech

DARPA Funding:
- *HR0011-07-C-0056*
- *HR0011-09-C-0142*

Heterogeneous 3D Integration

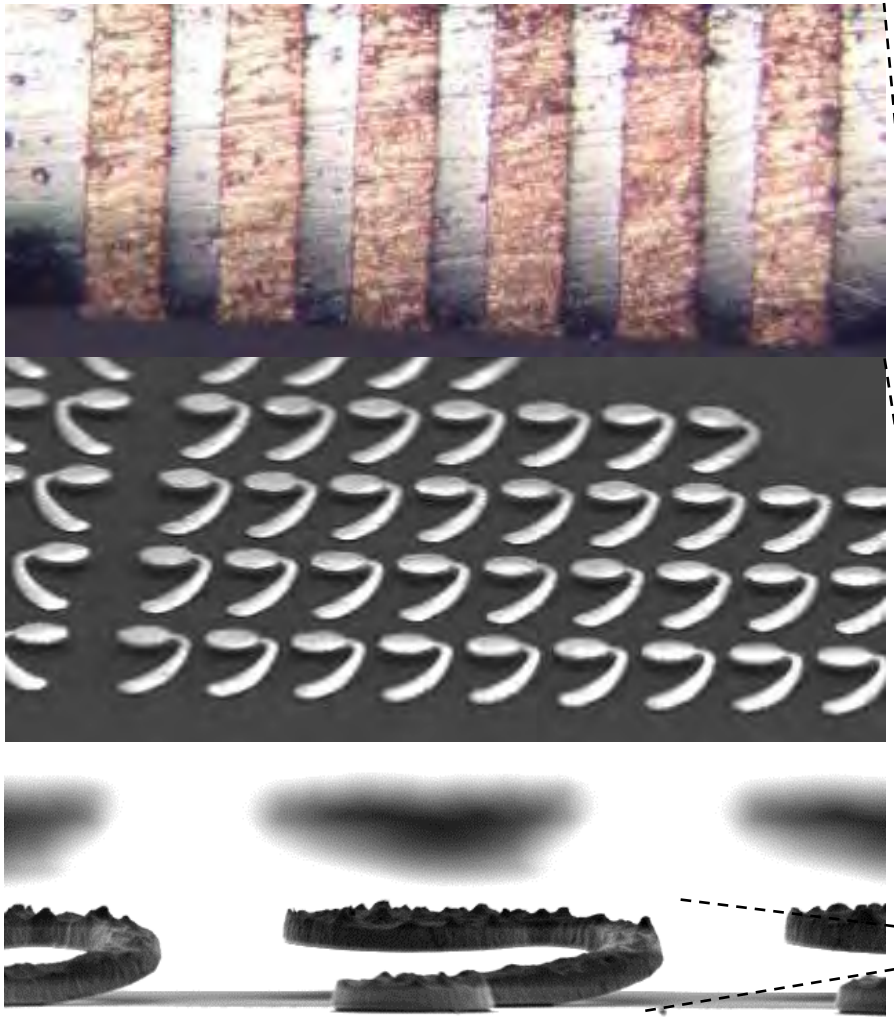

3D integration of arbitrary MEMS/sensors with a state-of-the-art CMOS

- *MEMS/Sensors are very sensitive to thermomechanical stress*
- *Flexible I/Os allow stress-free area-array vertical interconnections between dissimilar chips*
- *Fabrication and assembly of flexible I/O with 20um+ vertical range of motion have been demonstrated*
- *Flexible I/Os also enable temporary interconnections between chips; contaminated sensors can now be disposed while reusing the CMOS chip.*
- *Through-Silicon Via (TSV) allows sensors to be exposed to the environment.*
- *A new TSV process that can be fabricated in thick (500um) MEMS/sensor wafers have been demonstrated*

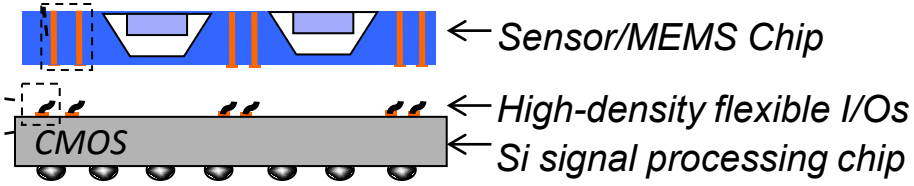

Student: H. S. Yang, PI: M. A. Bakir –ECE, Georgia Tech

Work performed at Georgia Tech

H. S. Yang et al., ECTC 2010, IITC 2010

Nanogenerators (NG)

Energy harvesting is critical to achieve independent and sustainable operations of nanodevices, aiming at building self-powered nanosystems.

Taking the forms of irregular air flow/vibration, ultrasonic waves, body movement, and hydraulic pressure, mechanical energy is ubiquitously available in our living environment.

The mechanical-electric energy conversion has been demonstrated using piezoelectric cantilever working at its resonating mode.

In the example to the right, the generated electric energy was effectively stored by utilizing capacitors, and it was successfully used to light up a commercial light-emitting diode (LED).

Lateral and packaged NG

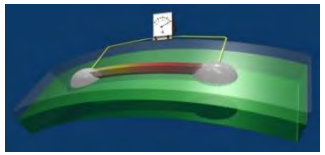

***Nature Nanotech.**, 4 (2009) 34*
***Nano Letters,** 9 (2009) 1201*

Powering nanodevices

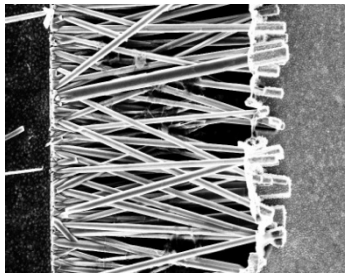

Lighting up a LED

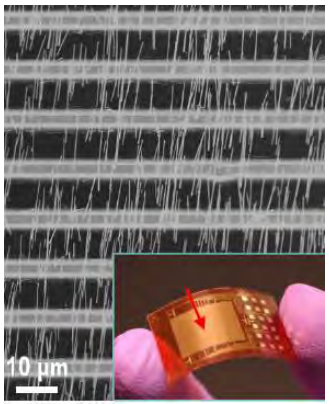

***Nano Letts.**, online*

In-vivo nanogenerator

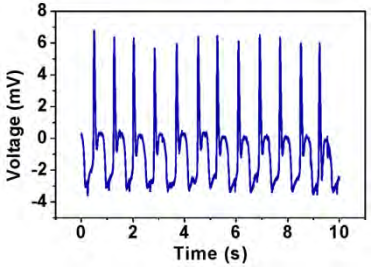

***Adv. Mater.** 22 (2010) 2534*

ZL Wang's group- MSE, Georgia Tech

Work performed at the Georgia Tech

Frequency Steerable Acoustic Transducer (FSAT)

A Frequency Steerable Acoustic Transducer (FSAT) is designed for directional sensing of guided waves. The considered FSAT is characterized by a spatial arrangement of the sensing material producing output signals whose dominant frequency component is uniquely associated with the direction of the incoming waves. The resulting FSAT can be employed both for directional sensing and generation of guided waves, without relying on phasing and control of a large number of channels.

The FSAT is realized by inkjet printing of the electrode patterns on a metallized polyvinylidene fluoride (PVDF) sheet using polymeric ink. The printed pattern is used as a mask for wet etching of the metallization and subsequently stripped away, leaving the desired electrode shape.

E. Baravelli, M. Senesi and M. Ruzzene,
School of Aerospace Engineering, Georgia Tech

Work performed at the Georgia Tech

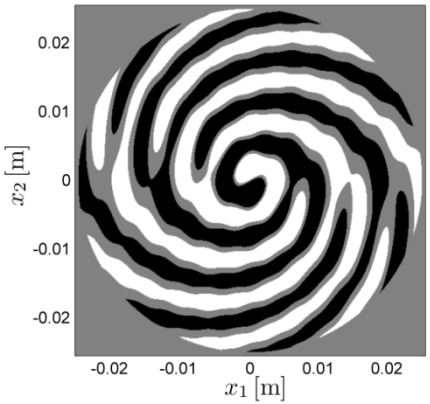

Spatial arrangement of the two FSAT electrodes (black and white areas)

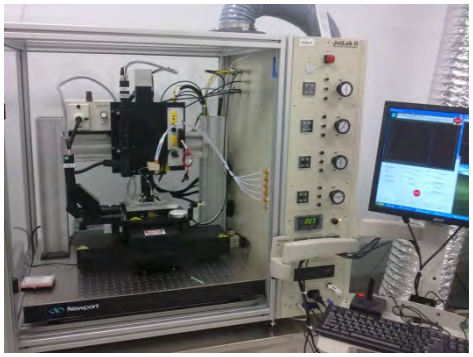

Inkjet printer

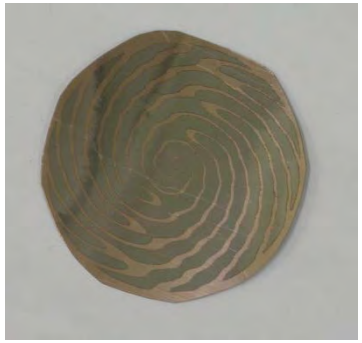

Inkjet-printed electrode patterns on a PVDF substrate

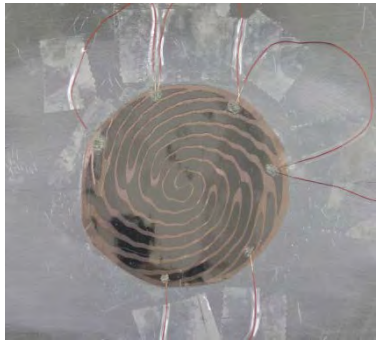

FSAT installation on an aluminum plate and connection of the electrodes

Hybrid Nanoplasmonic Photonic On-chip Sensors

Integrated nanoplasmonic photonic sensors are designed and implemented for on-chip sensing. The purpose of the novel integrated plasmonic photonic platform is to realize a lab-on-chip system for efficient light-matter interaction. This leads to a low-cost, highly sensitive, and portable sensing device for applications in point of care diagnostics in far reaching areas with limited resources, and also for chemical and environmental sensing. Different components of this sensing platform are fabricated using electron beam nanolithography, ICP etching, metal evaporation, and lift-off using the tools at GT-NRC. The device is fabricated on a Si wafer with layers of oxide, and nitride as the photonic component. The plasmonic component is implemented using gold nanoparticles.

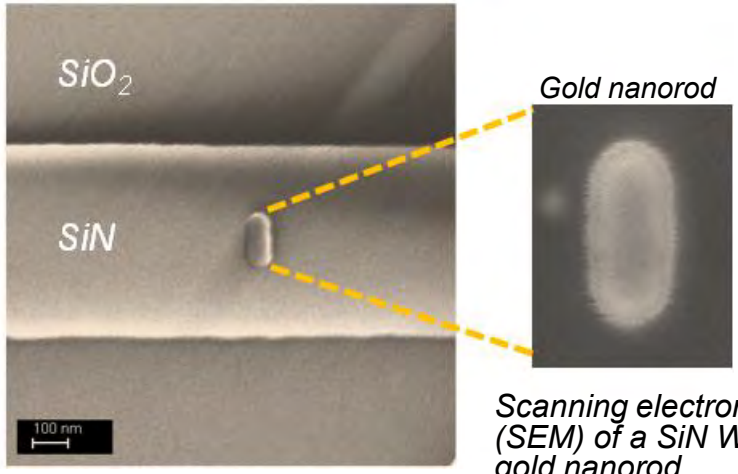

Scanning electron micrograph (SEM) of a SiN WG with a single gold nanorod

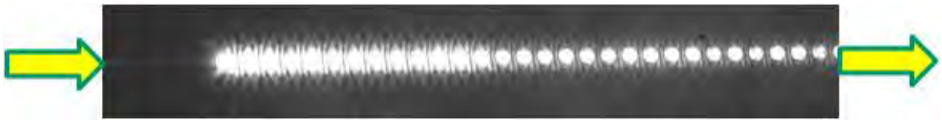

Top scattering darkfield image of an array of plasmonic gold nanorods excited on a waveguide at resonance. Each nanorod can probe a few target molecules.

Maysamreza Chamanzar and Ali Adibi, Georgia Institute of Technology

Fabrication performed at Georgia Tech

3D Nanofabrication using Metal-assisted Chemical Etching

The ability to fabricate 3D nanostructures with high feature fidelity, high aspect ratios and low cost is critically important to a number of fields including photonic devices, MEMS, nanofluidics and more. We developed a new technique that uses shaped metal catalysts in conjunction with Metal-assisted Chemical Etching (MaCE) of silicon to etch complex 3D micron and nanostructures in silicon in a simple, single lithography and single etch process.

In MaCE a metal catalyst serves to localize a galvanic redox reaction between an oxidizing agent and silicon where H_2O_2 is catalytically reduced on the metal, injection to holes (h^+) into the silicon. These holes enable the local oxidation *via* HF.

Examples include out-of-plane catalyst rotation to form curved, sub-surface 50 nm Si horns, coaxial spiraling stars and girds.

3D out-of plane rotation
Curved 50 nm sub-surface Si horn and vertically aligned thin metal films

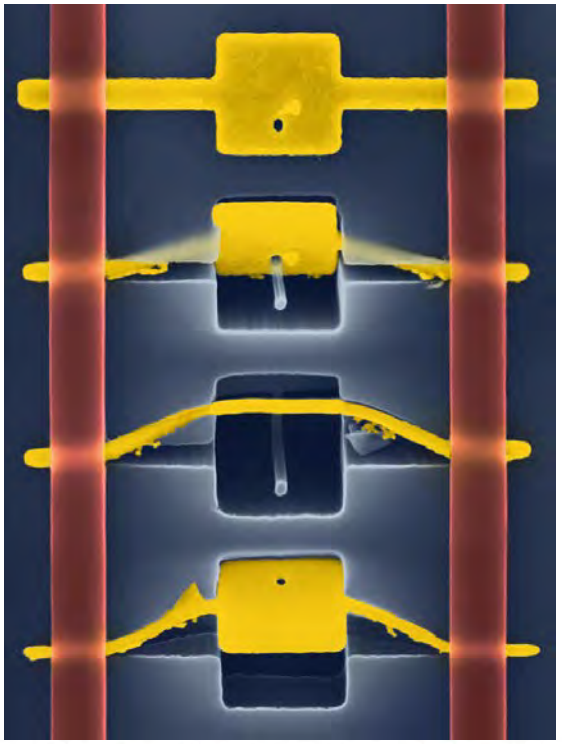

Coaxial Spiraling Star
Single etch 3D structures

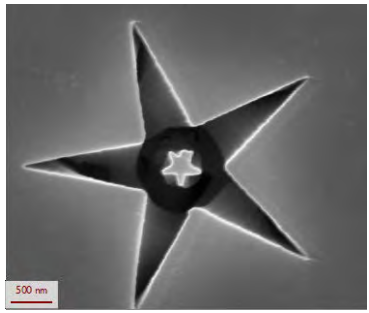

Spiraling Grids

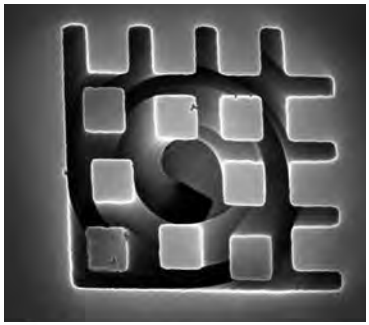

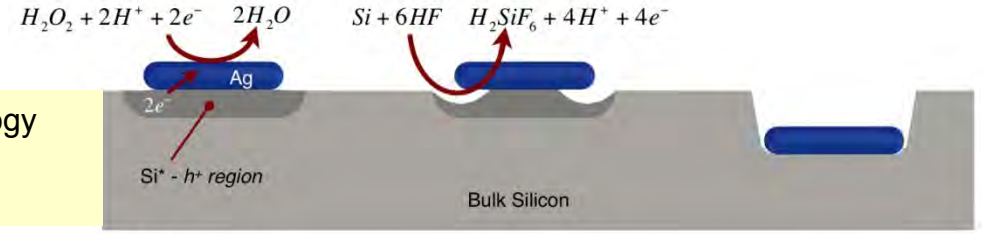

H_2O_2 is reduced on catalyst, injecting holes (h^+) into silicon

Si* is dissolved where exposed to HF

Catalyst travels into Silicon

Owen Hildreth and C. P. Wong, Georgia Institute of Technology

Work performed at the Georgia Tech

Biohazard Water Analyzer and Detector using Carbon Nanofiber Arrays

Biosensor chip

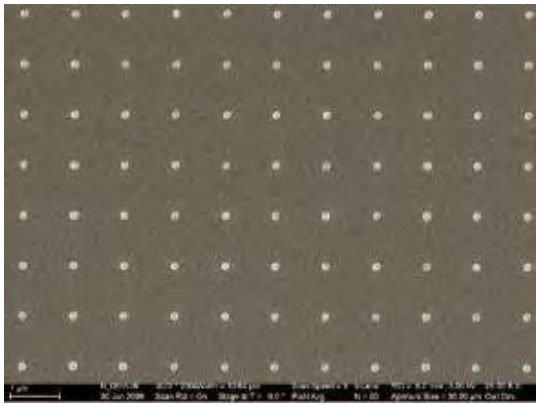

130 nanometer diameter Ni catalyst

resulting carbon nanofiber grown from Ni catalyst

Early Warning Biohazard Analyzer system

Early Warning is a developer of Biohazard Analyzers that directly measure the total and viable cell concentrations of individual species of bacteria, viruses and protozoa parasites.

NASA's biosensor works when a single strand of nucleic acid in a target solution comes into contact with a matching strand of nucleic acid attached to the end of an ultra-conductive carbon nanofiber. The matching strands form a double helix that generates an electrical signal which is used to determine the presence of specific microorganisms in the sample. Because of their tiny size, millions of carbon nanofibers can fit on a single biosensor chip allowing identification of very low cell counts. Early Warning has also developed its own intellectual property pertaining to electrochemical biosensing devices, detecting multiple organisms at the same time, detecting molecules over a wide range of concentrations, and mass fabrication methods.

Early Warning's Biohazard Water Analyzer is configured to detect the presence of both common and rare strains of pathogens associated with waterborne illnesses including E. coli indicator, E.coli O157:H7, Cryptosporidium, Giardia, and various waterborne bacteria and viruses. Water agencies, food & beverage companies, industrial plants, hospitals, airlines, and recreational water facilities could use the portable and wireless water analyzers without needing a laboratory or technicians.

Devin Brown, Georgia Tech, Bruce Gale, University of Utah
Alan Cassell, NASA Ames Research Center, Neil Gordon, Early Warning Inc.

Work performed at Georgia Tech

NNIN
www.nnin.org
Nanoscale Science Engineering & Technology

Mixed Dithiol Durene and Monothiol Phenylethanethiol Protected Au_{130} Nanoclusters

The project targets to elucidate the impacts of interfacial bond structures on the physiochemical properties of Au nanoparticles. The knowledge will advance the design and creation of functional nanomaterials for energy technology and biomedical applications.

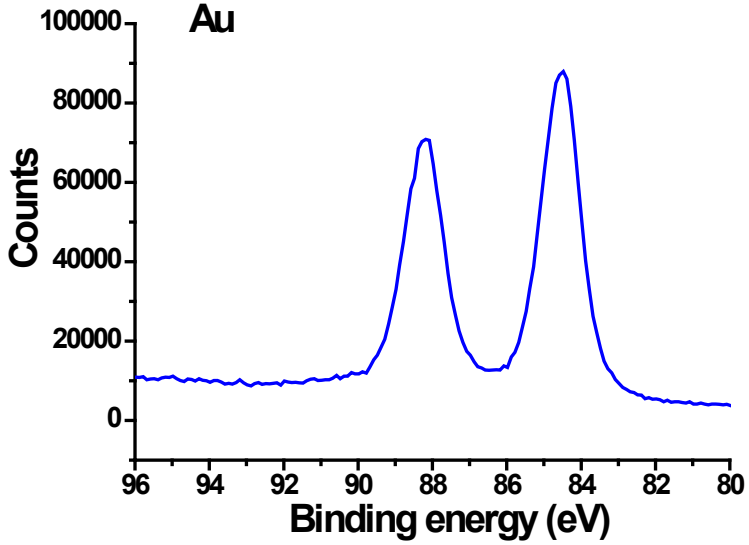

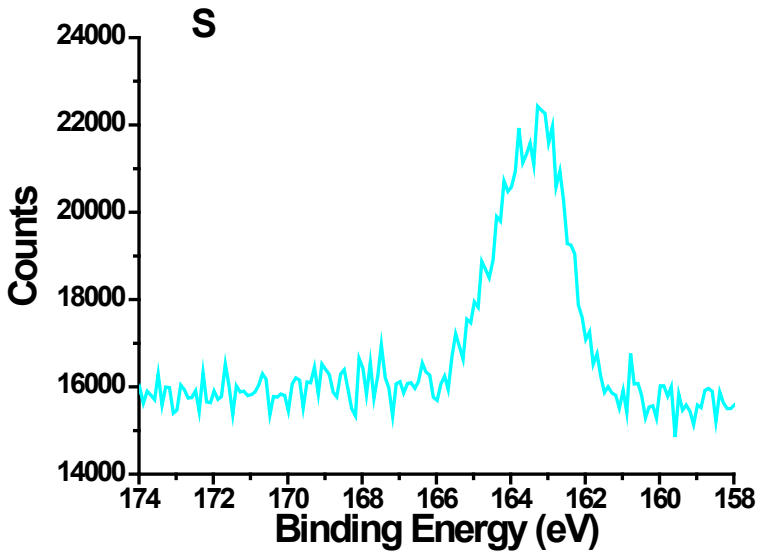

In addition to the well known quantum confinement, the energetics and structure of Au nanoclusters are tailored by designated dithiol ligands. As the size of nanomaterials decreases, the percentage of the surface atoms over those inner core atoms increases. Consequently, the impacts of core-ligand bonding on the overall properties intensify. Key knowledge of the interfacial bonding, the binding energy of Au and S, is quantified by XPS results.

*Zhenghua Tang, Donald A. Robinson, Nadia Bokossa, Bin Xu, Siming Wang, and Gangli Wang**
Department of Chemistry, Georgia State University, Atlanta, GA.

Work performed at Georgia Tech

In-Plane Cantilevers for Biochemical Sensing

The research focuses on the development of MEMS based sensors for biomedical and environmental applications. Currently, biochemical sample analysis is performed in a laboratory setting using large and expensive equipment. The aim of the work is the creation of an inexpensive sensing platform which can provide quantitative data quickly. Such a system could be used in: the field, at the point of care when there isn't time to send a sample to a lab, or for use as a low-cost diagnostic test, which unlike many currently available techniques could inexpensively provide a quantitative measurement of the concentration of a marker in a fluid.

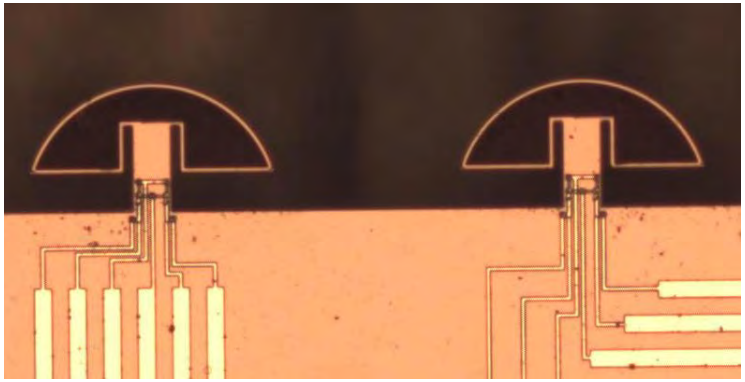

The system has the advantage of being fabricated in silicon so that the sensor and the integrated circuit to run it can be made using the same set of equipment, greatly reducing cost. The cantilevers studied here utilize the first in-plane flexural mode, in contrast to the commonly employed first out-of-plane flexural mode. In-plane mode operation gives advantages in terms of mass loading and resolution allowing for low detection limits in liquid-phase sensing applications. Initial biosensor testing experiments have been conducted by binding bovine serum albumin (BSA) to the cantilever surface and then detecting the presence of antibodies to BSA in PBS.

Luke A Beardslee, Oliver Brand, School of Electrical and Computer Engineering, Georgia Tech

Work performed at Georgia Tech

Biomimetic Angular Rotation Sensor for a Vestibular Prosthesis

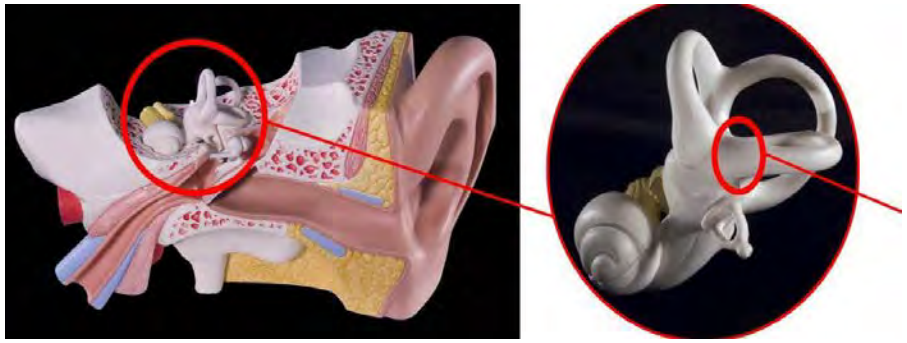

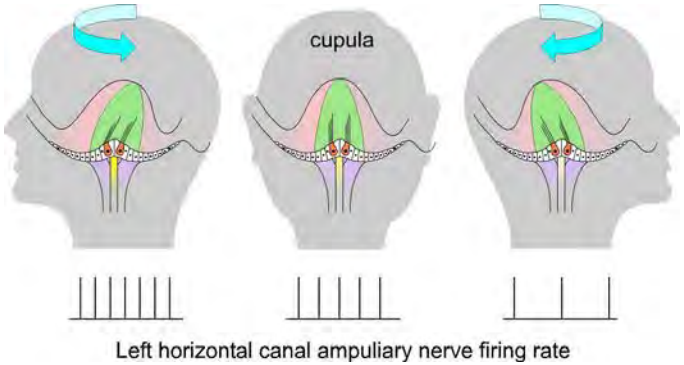

35.4% of US adults aged 40 years and older (69 million Americans) had a vestibular dysfunction (2001-2004). Falls are the leading cause of fatal and non-fatal injuries for persons age > 65 years. The inner ear's vestibular system provides cues about self motion that help stabilize vision during movement. These cues also enable us to orient ourselves with respect to our surroundings, which helps us to stand and walk. Current vestibular prostheses prototypes rely upon gyroscopes for capturing head motion. To provide a low-power alternative, an angular motion sensor similar to the natural human angular rotation sensor is being fabricated. Utilizing a spun-cast SU-8 based micromolding technique for etchless micropatterning, the device is fabricated using a PMMA. A top and bottom layer form a parallel plate capacitor serving as the sensor.

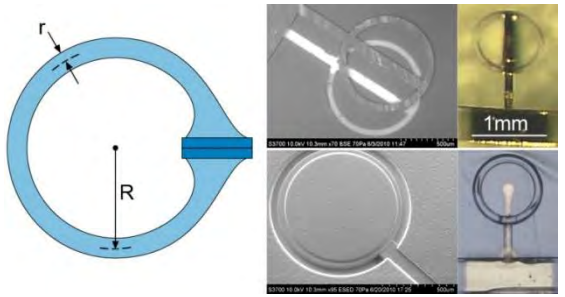

Figure. Left: Illustration of the MEMS-cupula and the SCC-torus. The sensor's axis of rotation is out of the page. The MEMS-cupula bisects the SCC-torus and deflects in response to angular acceleration induced fluid motion. The radius of curvature (R) and the lumen radius (r) are indicated. **Center**: Scanning electron micrographs of the SU-molds used to define the respective reference (top) and sense (bottom) electrodes of the MEMS-cupula. **Right**: Photographs of the fabricated MEMS-cupula electrodes. A released sense electrode (top) is shown. The bottom picture illustrates an unreleased reference electrode. The metallization on the bottom of each structure enables signal transfer. The total structure is formed by mating the reference with the sense electrode that has a "lip" and a groove for aligning and eventually sealing the two.

Students: M. McClain, H. Toreyin, J. Falcone, S. Datta Roy, PI: P. Bhatti –BioSystems Interface Lab, ECE, Georgia Tech

Multi-λ_s Light Source Based on Grating Coupled Laser Diodes with Wavelength Selective Elements

This work was focused on developing a multi-λ_s emitter for different applications such as WDM technique. The feasibility of the goal was shown. 2009-2010 involved a process requiring higher yields for a multi-dimension ARRAY assembly. Design of the multi-λ_s devices is based on GCSEL/DGR technology originally invented by the team (see image on the right). P-side grating couplers and N-side feedback grating monolithically integrated with the Broad Area laser diode were patterned using JEOL-9300FS electron beam lithography tool in GA tech facility. The table below shows the desired wavelengths matching grating period.

Wavelength of Interest	*Littrow Grating*
λ_{sw} *(nm)*	d_f *(nm)*
973.9	409.00
975.1	407.75
976.2	406.50
977.3	405.25

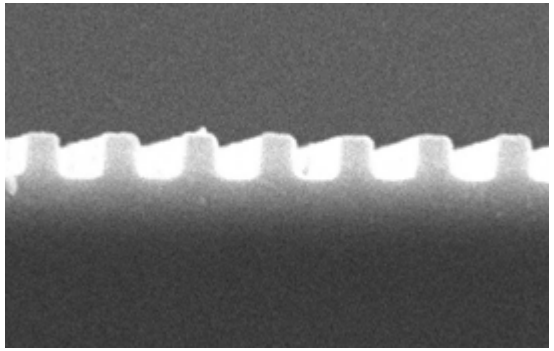

SEM image of one of one of the Littrow Gratings

Schematic of a WL GCSEL w/DGR

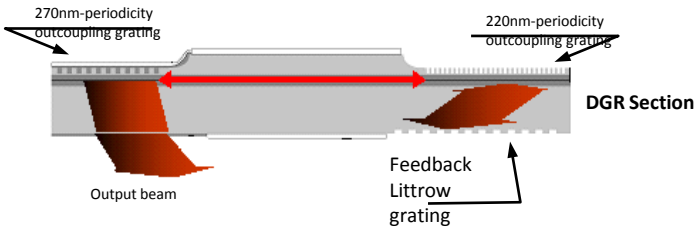

[1]O'Daniel et al. *Optics Lett.* **31**, 211 (2006)

Wafer inspection of the processed GCSEL/DGR emitters with active probing (wafer is n-side up).

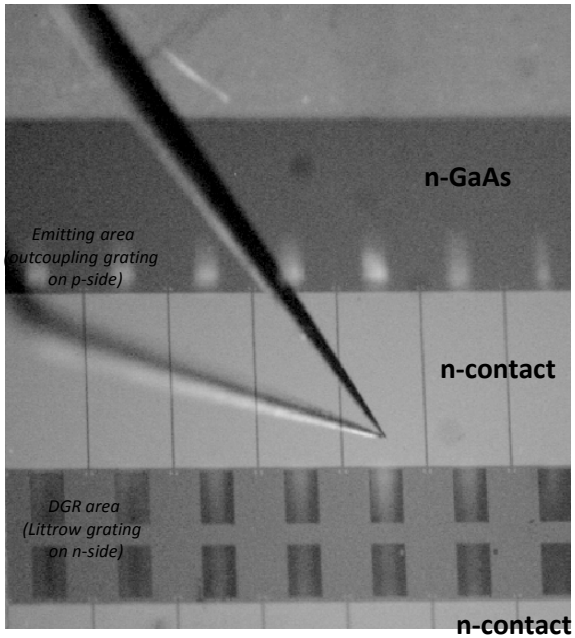

Viktor O. Smolski, Yigit O. Yilmaz, and Eric G. Johnson, University of North Carolina, Charlotte, NC.

Work performed at Georgia Tech

A Fully Electric Method for Detecting Mechanical Resonances in Cantilevered Carbon Nanotubes

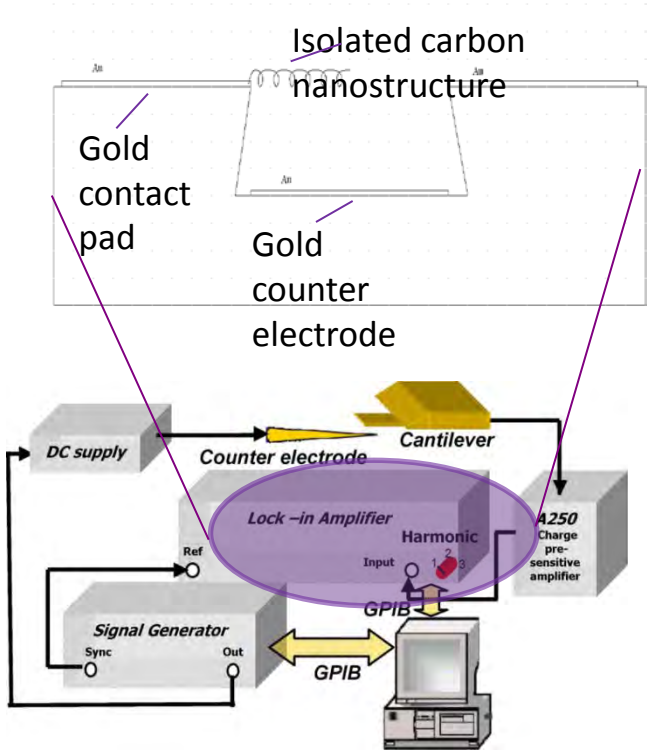

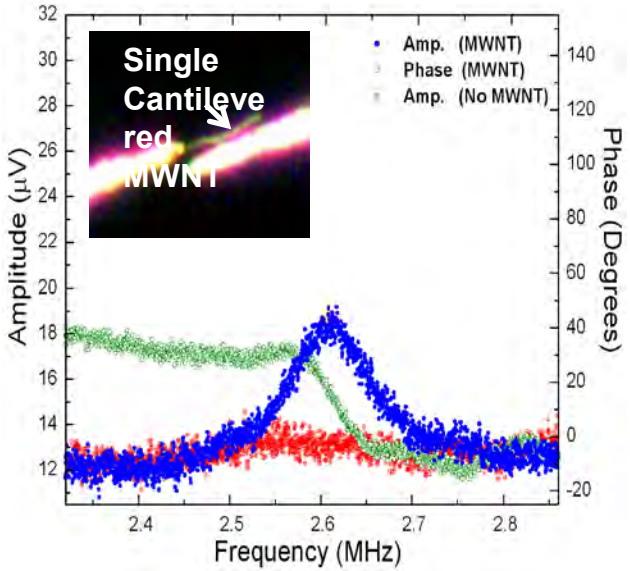

Apparao Rao, Doyl Dickel, and Malcolm Skove, School of Physics and Astronomy, Clemson University, SC. Work performed at Georgia Tech

Schematic of Clemson's HDR setup

Harmonic Detection of Resonance (HDR) is a technique developed at Clemson University which enables a fully electrical actuation and detection of the mechanical resonance of conducting, cantilevered structures. It has been shown to be extremely effective in the analysis of resonances in micro-cantilevers. We have also demonstrated that HDR is capable of detecting resonances in nanostructured cantilevers, in particular, a multi-walled carbon nanotubes (MWNT) attached to a tungsten probe tip. Our present setup uses two adjustable sharpened tungsten tips: one to attach the MWNT cantilever, and the second acts as the counter-electrode. In order to continue to progress HDR technology at the level of double walled (DWNT) and single walled carbon nanotubes (SWNT), we require fixed-position electrodes on which we can mount DWNTs, SWNTs or coiled carbon nanotubes. Our collaboration with Georgia Tech allows us to build these devices, moving our technology from the micron to the nanometer scale.

Development of Stroke Sensors

This work reports on a complementary use of surface of quartz crystal microbalance with frequency & dissipation monitoring (QCM) technologies to study interactions between a peptide antigen and polyclonal antibodies, in an experimental format suitable for diagnostic assays. In the chosen model, a synthetic NR2 peptide the fragment of NMDA neuroreceptors (a stroke associated antigen) was immobilized by an optimized chemical protocol applicable to QCM sensors. A preliminary study of the peptide immobilization was performed to optimize the signal-to-noise ratio using mixed self-assembled monolayers n a gold surface. Under our conditions, the antibody detection limit was determined to be 0.02nM in diluted human serum. This value is in agreement with the reported rank distribution of NR2 antibodies in non-stroke patient sera. Label-free and real-time technologies such as QCM could be precious tools in future diagnostic assays.

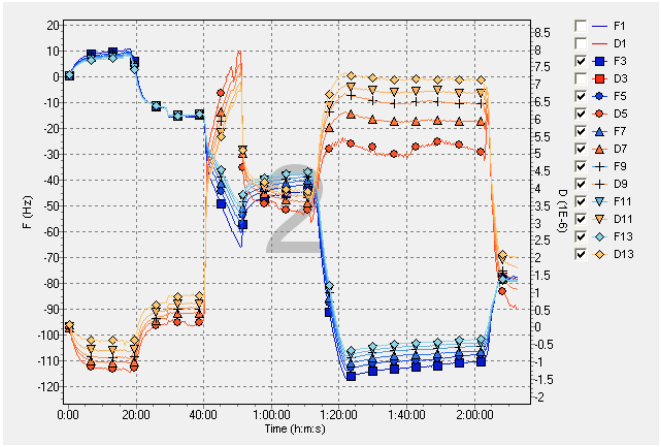

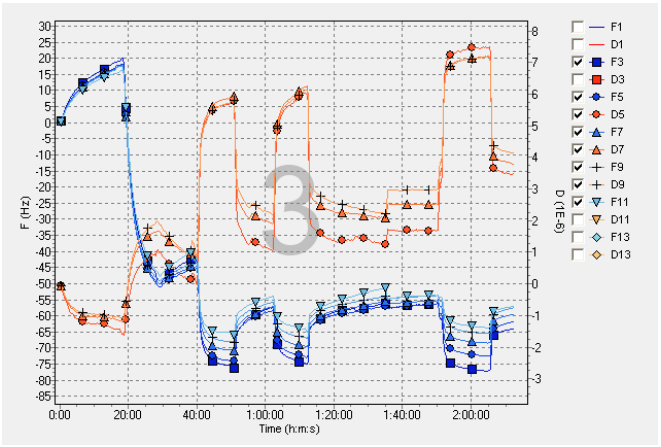

Svetlana A. Dambinova, DSc, PhD, Well Star College of Health & Human Services, Kennesaw State University, Kennesaw, GA
Galina A. Izykenova, PhD, Arthur Bagumyan, BS, CIS Biotech, Inc., Atlanta, GA
Work performed at Georgia Tech

*Work in progress, started from **Oct, 2010***

Characterization of Europium-Doped Silica Nanoparticles

Silica nanoparticles are synthesized using the Stöber (sol-gel) method, which uses a bulk ethanol solution in the presence of ammonium hydroxide, tetraethylorthosilica (TEOS). A europium complex (Eu-L) can be encapsulated within the silica nanoparticles (Eu-L-NP). The free Eu-L displays weak metal-based luminescence, while the nanoparticle encapsulated complex exhibits strong metal-based luminescence, at room temperature. Current work includes characterizing the luminescence properties of these materials and performing a full optimization study of their formation via electron microscopy.

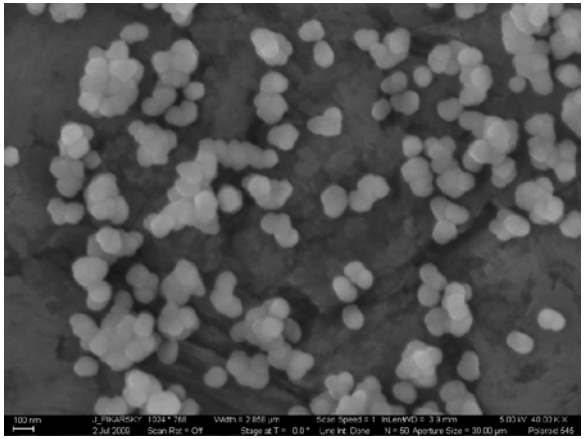

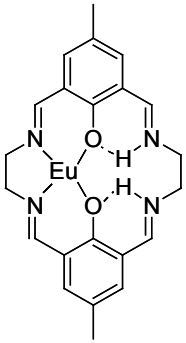

Eu-L

NP

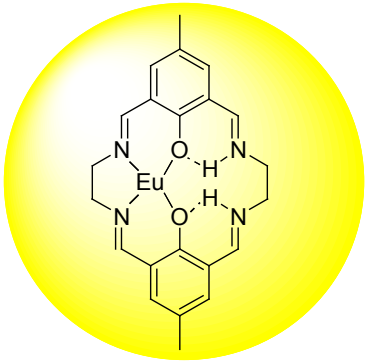

Eu-L-NP

Joshua Smith, Armstrong Atlantic State University
Work performed at Georgia Tech

Inkjet Printing of Transdermal Patches

Transdermal drug delivery can be achieved through microneedle skin perforation, followed by application of a flexible drug-containing patch. Inkjet printing technology provides a novel method for patch preparation. The drug or formulation is applied in a uniform thin layer on a polymer backing membrane and allowed to dry. This method can be adapted for protein therapeutics as well as vaccines.

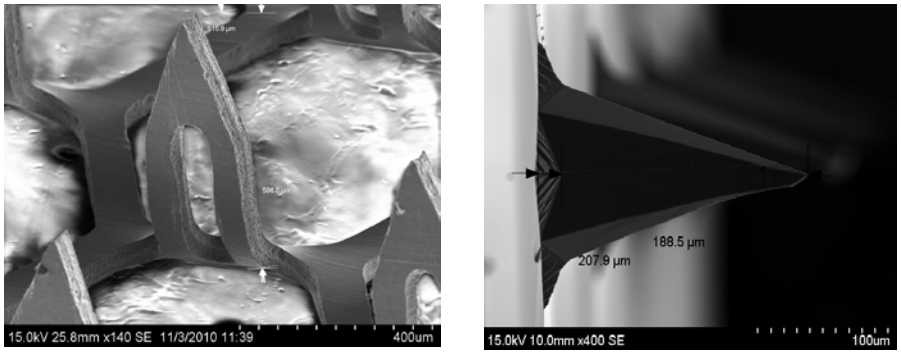

Two types of microneedles used for transdermal drug delivery.

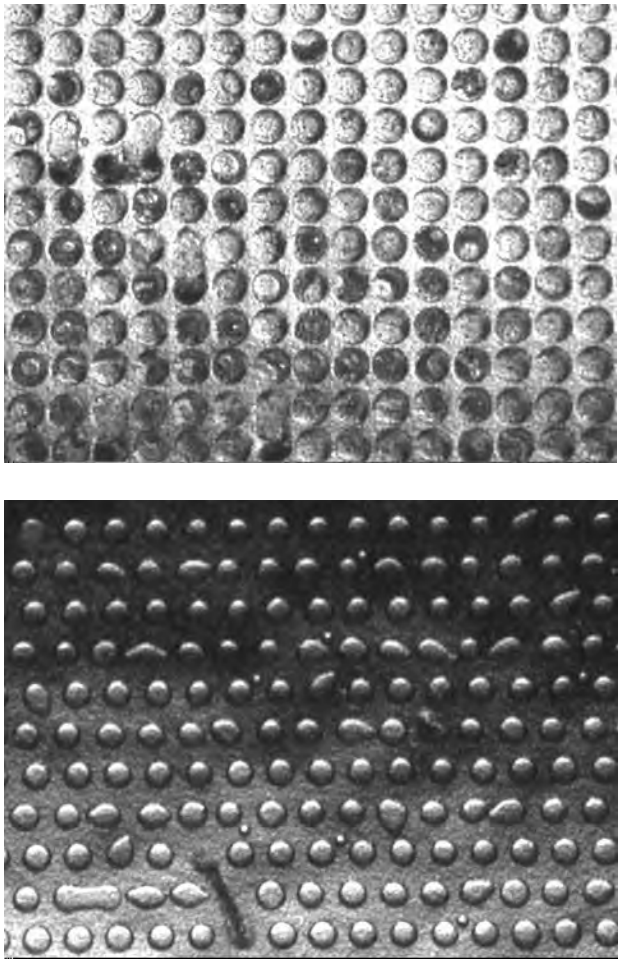

Printed protein formulation patches using burst effect (top) and print on fly mode (bottom)

Sonal Saluja, Vijay Kumar, and Ajay Banga, Mercer University
Work performed at Georgia Tech

Design of Gold Nanoparticle-Apo-Tf-Ruthenium Organometallic Conjugates for Drug Delivery

Metal based anticancer drug such as cisplatin and $[Ru^{II}(\eta 6\text{-p-cymene})(en)Cl]PF_6$ have severe side effects as they tend to bind proteins present in blood plasma. A drug delivery system consisting of a gold nanoparticle (AuNP) conjugate of protein bound metal complex, which can be released due to intercellular pH change, may reduce some of the side effects. A ruthenium organmetallic, $[Ru^{II}(\eta 6\text{-p-cymene})(en)Cl]PF_6$ has been shown to bind apo-Tf forming an adduct and further study is in progress to explore the binding of this adduct to the AuNP surface.

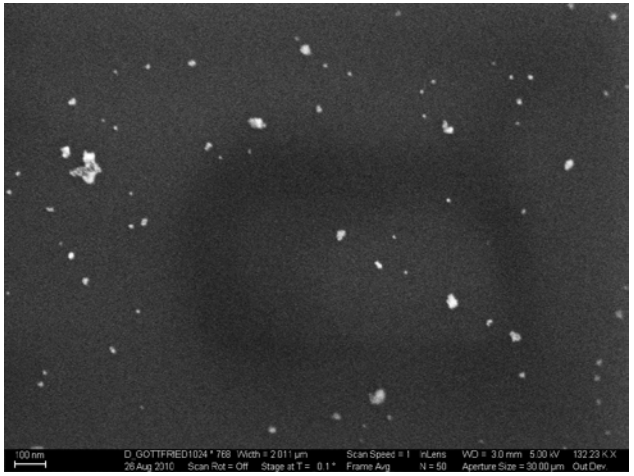

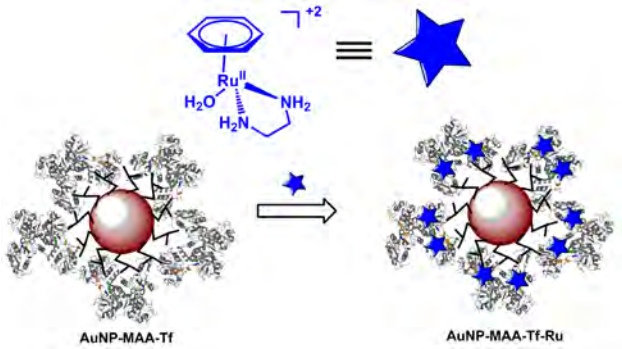

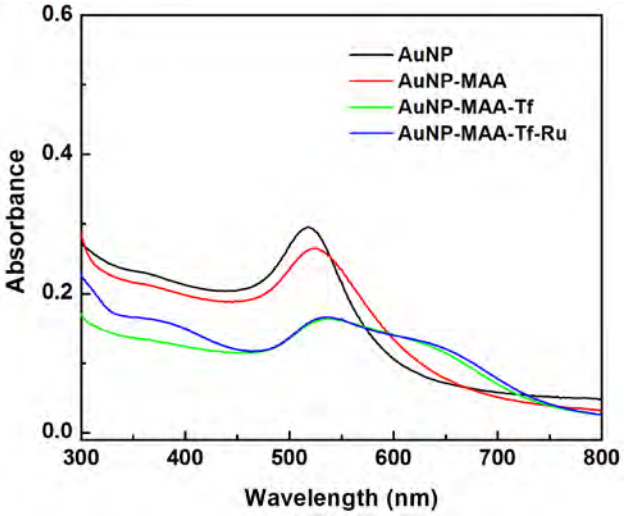

Bharat Baruah, Kennesaw State University
Work performed at Georgia Tech

Self-Sustained Micromechanical Oscillators and Nanobalances

Under appropriate conditions, thermally actuated micromechanical resonant structures are capable of self-sustained oscillation without the need for supporting electronic circuitry. This is enabled by interactions between thermal actuation and the piezoresistive effect in such structures leading to an internal positive feedback mechanism. Single crystalline silicon extensional mode dual plate resonators with frequencies in the few MHz range have been fabricated to demonstrate this concept. Such devices can initiate self-sustained oscillation under both vacuum and atmospheric pressure by passing only a DC bias current through them. Other than being single-device fully-micromechanical frequency references, such devices present the technological basis for implementation of highly sensitive nanobalances for sensory applications. In this example, a self-oscillating silicon structure has been utilized as an air-borne particulate counter capable of simultaneous mass measurement of individual particles without the need for supporting analog circuitry. Mass sensitivity of the sensors were measured using artificially generated aerosol particles to be in the 10-30 Hz/pg range allowing detection and mass measurement of individual particles with submicron diameters.

SEM view and output voltage of a self-oscillating 4.6MHz 3μm thick thermal-piezoresistive resonator. Only a DC bias current of 1.4mA is being applied to the resonator (no amplifier).

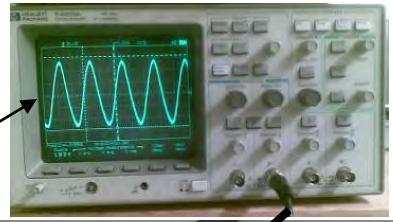

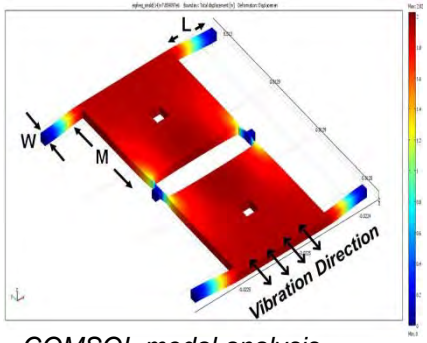

COMSOL modal analysis, showing the in-plane resonance mode shape of interest for the 4.6MHz dual-plate oscillator.

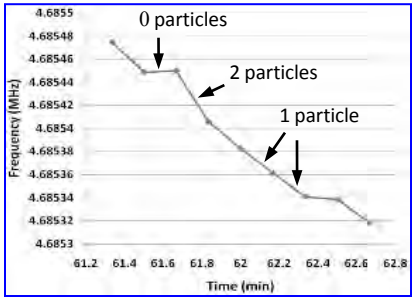

Measured oscillator frequency shift due to mass loading.

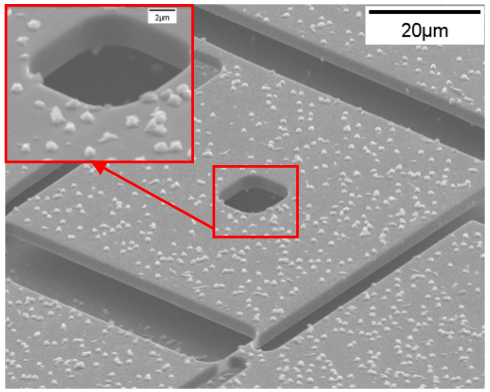

SEM view of the same micromechanical oscillator after exposure to artificially generated air-borne particles.

Siavash Pourkamali, University of Denver
Fabrication performed at Georgia Tech

Bit-patterned perpendicular magnetic media

The project targets to employ E-beam lithography to pattern perpendicular anisotropy $Co_{80}Pt_{20}$ films into nanopillar arrays as bit-patterned perpendicular magnetic media for next-generation recording media with ultra-high data storage capacity. The magnetic $Co_{80}Pt_{20}$ thin films were deposited by sputtering, and negative resist HSQ was spin-coated on the top of $Co_{80}Pt_{20}$ films for electron-beam lithography. The SEM images reveal that as density increase the nanopillar diameters get larger. These nanopillar arrays act as masks for ion miller etching. After etching, the magnetic properties of $Co_{80}Pt_{20}$ nanopillar arrays were characterized by alternating gradient field magnetometer (AGM) and magneto-optical Kerr effect magnetometer (MOKE). Furthermore, magnetic force microscopy (MFM) was used to study the domain structure. Our results show that E-beam lithography provides a promising way to pattern perpendicular magnetic media.

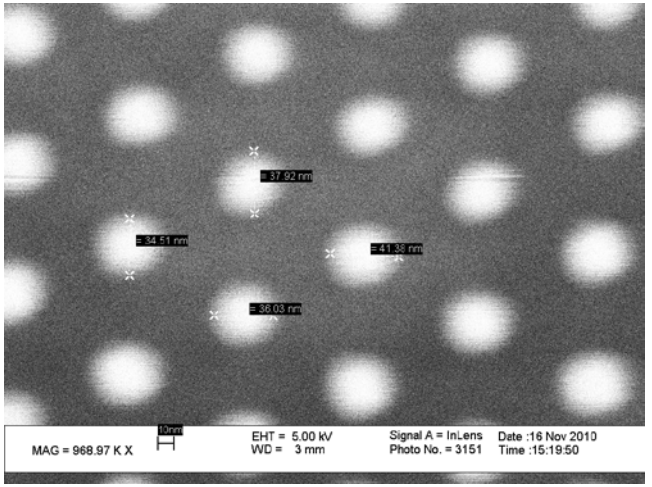

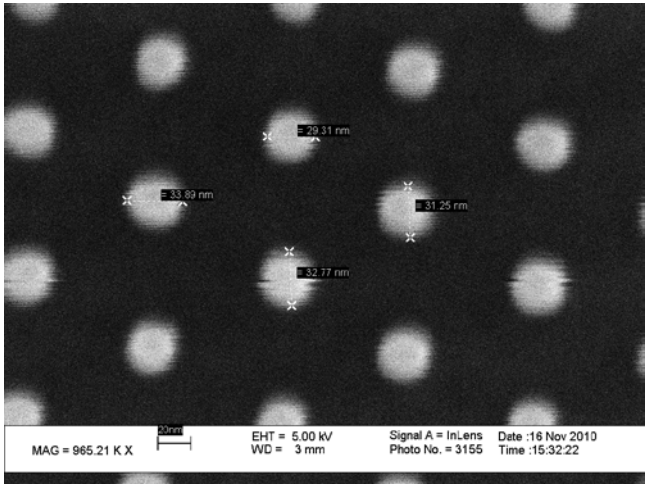

Zhenzhong Sun, Su Gupta and Dawen Li, MINT Center, The University of Alabama, Tuscaloosa, AL

Work performed at Georgia Tech

NNIN Site at the University of Michigan

Lurie Nanofabrication Facility

High Efficiency Color Filters

A sub-wavelength grating structure fabricated on dielectric layers was used to create a thin film color filter targeting very high transmission efficiency. The grating is used to couple light of a specific frequency band into the dielectric waveguide layers to allow transmission while reflecting other portions of the spectrum. A specific color band can be achieved by changing the period of the grating and bandwidth can be controlled by the dielectric layers.

This structure was created using nanoimprint lithography for large area applications with gratings of 280 nm and 420 nm used to demonstrate blue and red color filters, respectively. A fabricated 420 nm period grating along with a comparison of data and simulation for a red color filter achieving ~90% transmission is shown to the right. With such high efficiency and control, this structure could challenge current color filter technology in various fields.

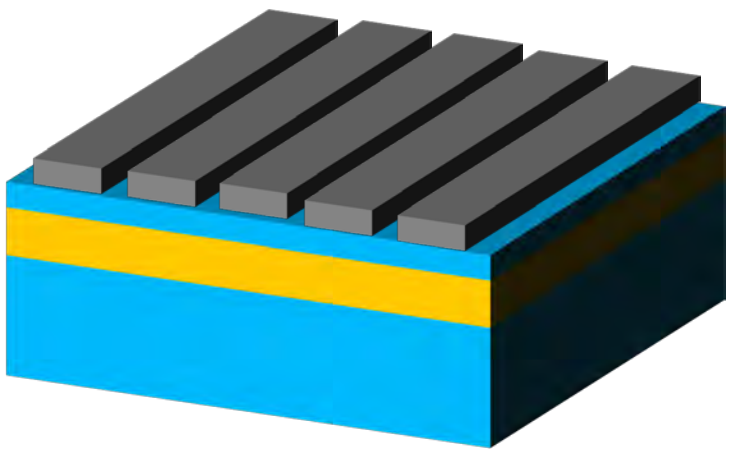

Color filter structure consisting of a sub-wavelength metal grating patterned on dielectric layers.

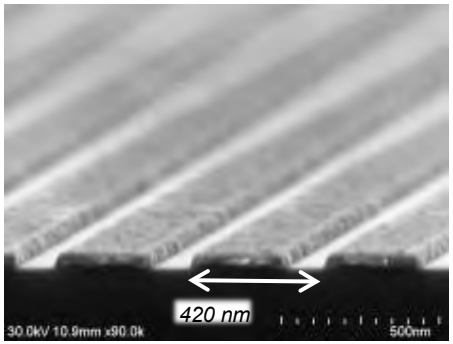

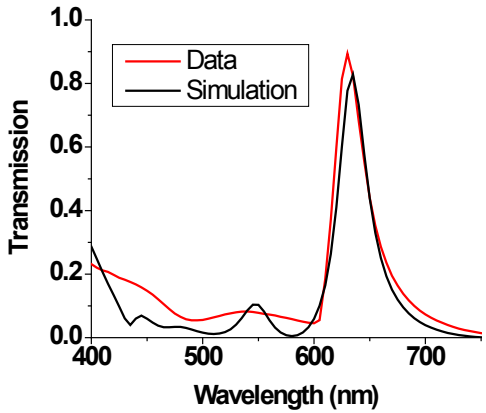

SEM image of 420 nm period grating used for red filter (left) and plot showing data and simulation TM transmission values for the fabricated color filter (right).

Kaplan, T. Xu, Y.K. Wu, and L.J. Guo, University of Michigan

Work performed at U Michigan Lurie Nanofabrication Facility

Photonic Crystal Microdisk Lasers

A photonic crystal PC microdisk laser cavity was introduced and demonstrated. The microlaser utilizes lossless surface modes within the PC forbidden band for vertical confinement and whispering gallery modes for lateral confinement. Analysis showed that this type of cavity mode has a smaller mode volume and a larger confinement factor than other resonant modes in the microdisk stacks. Initial experiments demonstrated lasing of optically pumped wavelength-size microdisks with four period GaAs/AlGaAs PCs and InGaAs quantum dots as gain media.

Y.H. Chen, Y.K. Wu and L.J. Guo, University of Michigan

Work performed at U Michigan Lurie Nanofabrication Facility

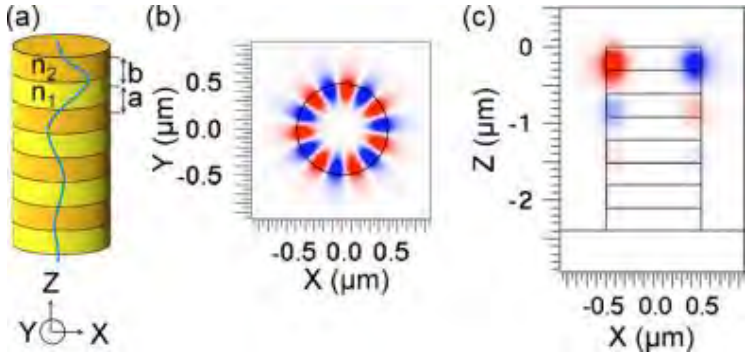

PC microdisk cavity supporting surface mode guided WGM

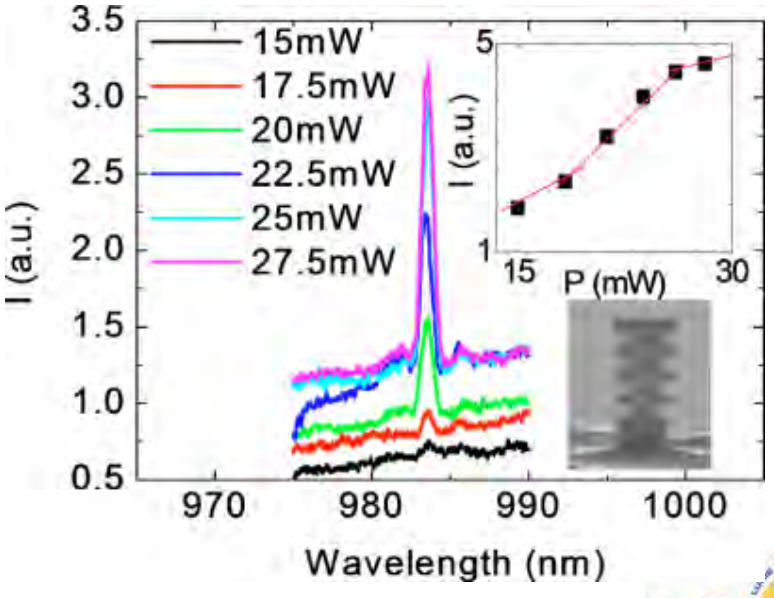

Evolution of lasing peaks from PC microdisk

Endoscopic Dual-Axes Confocal Microscopy

Microactuators are being developed for the purpose of dual-axes confocal microscopy from an endoscope-compatible instrument. The primary micro-actuators under development are thin-film lead-zirconate-titanate (PZT) vertical translational actuators, with stroke length > 200 microns. These actuators will enable cross-sectional, dual-axes confocal imaging of in-vivo tissue from an instrument <5 mm in diameter, with imaging depths potentially as large as 500 microns. Also under development are a variety of electrostatic scanning micro-mirrors for lateral imaging based on principles of parametric resonance.

K. Oldham, University of Michigan

Work partially performed at U Michigan Lurie Nanofabrication Laboratory

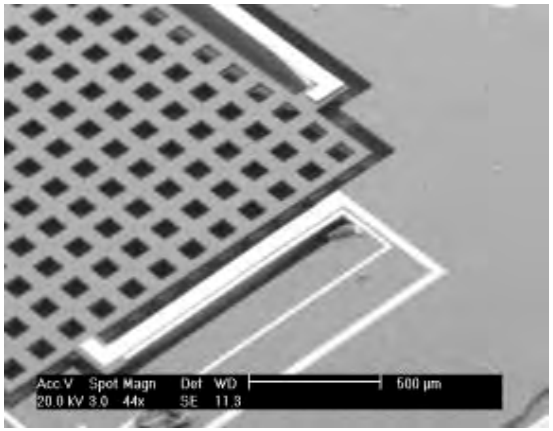

Vertical piezoelectric microactuator with integrated position sensing for into-tissue scanning (micro-mirror to be installed on central platform).

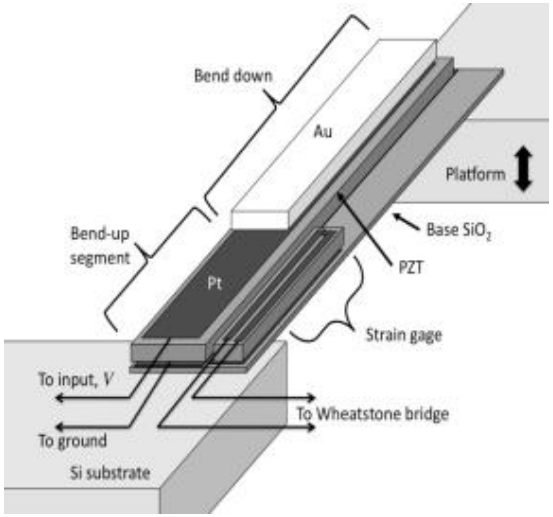

Schematic view of thin-film piezoelectric actuator structure.

3-D Characterization of Ostracod Fossil Surface Morphology

Quantitative morphological analysis of ostracod whole surface features can reveal important information about ontogeny, sexual dimorphism or as paleoindicators of seawater salinity concentrations as well as climate temperature variations. 3D digitization and surface metrology are used with respect to microfabrication concepts. Using laser confocal microscopic methods and metrological statistical analyses to perform 3D analyses of fossil specimens we are able to quantify ostracod surface morphology as a measure of ontogenetic change and make inferences about paleoclimate change.

J.L. Pappas and D.J. Miller, Museum of Paleontology, University of Michigan

Work performed at U Michigan Lurie Nanofabrication Facility

Ctenoloculina acanthina

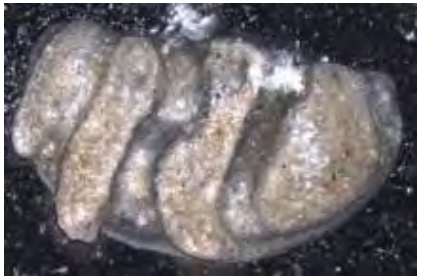

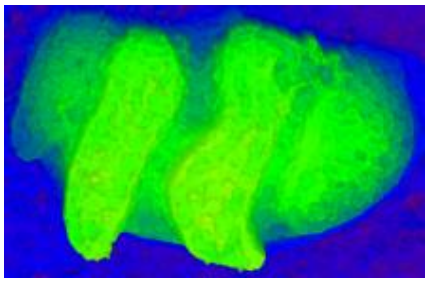

Analysis parameter			
Sq	7.820 [µm]	Ssk	0.377
Sku	11.683	Sp	101.770 [µm]
Sv	70.080 [µm]	Sz	171.850 [µm]
Sa	5.341 [µm]	Sk	13.989 [µm]

Ctenoloculina cicatricosa

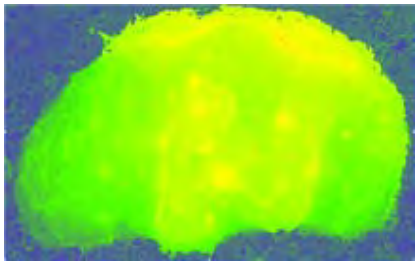

Analysis parameter			
Sq	18.458 [µm]	Ssk	1.139
Sku	27.773	Sp	359.778 [µm]
Sv	219.601 [µm]	Sz	579.379 [µm]
Sa	12.126 [µm]	Sk	32.269 [µm]

From metrological analysis, e.g., a male C. acanthina has a smoother surface morphology (Sa=5.341) than a female C. cicatricosa (Sa=12.126).

Silicon Nanostructures for High Efficiency Thermoelectrics

In this work we have used an organic block copolymer template in conjugation with standard photolithography techniques to fabricate regular nanoscopic patterns in silicon, ~5−50 nm in diameter, over arbitrarily large areas.

Silicon has been previously proposed as a viable thermoelectric material. However, the relatively high thermal conductivity of bulk silicon leads to extremely low efficiency for thermoelectric devices based on bulk silicon.

The nanoscopic features generated using the above methodology are expected to severely curtail heat transport, as the nanoscopic features serve as scattering sites for phonons. However, these nanoscopic features do not significantly affect electron transport, allowing for the synthesis of high efficiency thermoelectric devices based on nanostructured silicon.

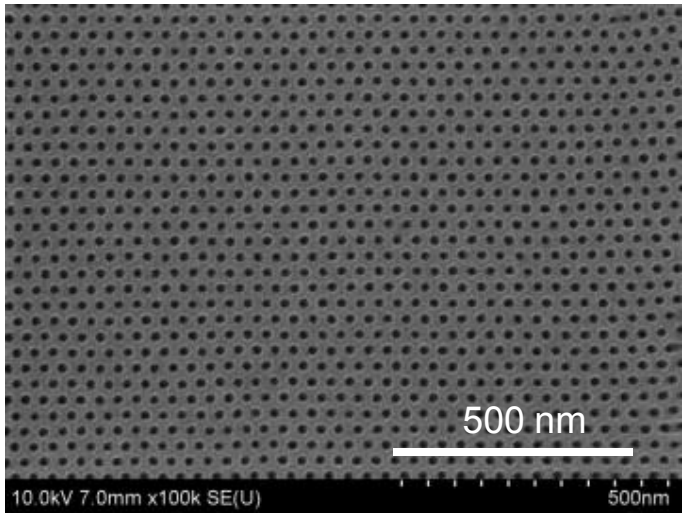

Nanoporous Silicon

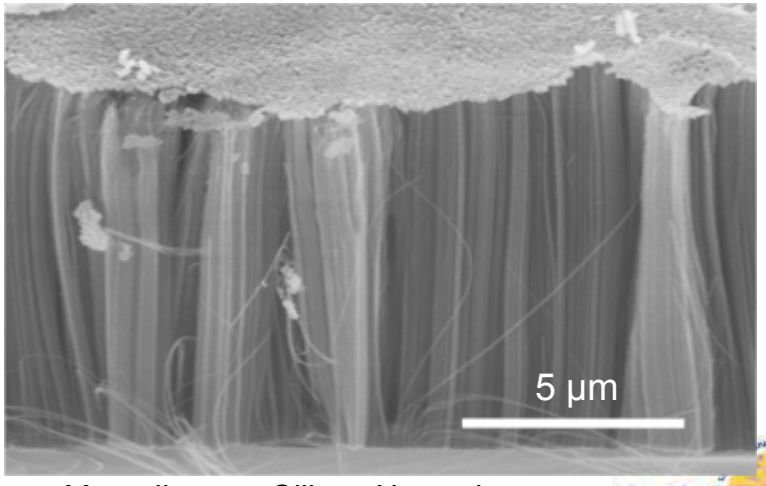

Monodisperse Silicon Nanowires

A.Boukai and A. Tuteja, University of Michigan

Work performed at U Michigan Lurie Nanofabrication Facility

MRI Perfusion Phantom Project

The goal of this project is to design a phantom with the capability to mimic hemodynamics in microvasculature. The phantom needs to provide a large network of microchannels, similar to capillary beds in vascular system. Simulating many of the parameters affecting perfusion, such as dispersion, require large number of flow pathways in microscopic scale. Microfabrication and particularly SU-8 lithography followed by PDMS molding is a great candidate technique for the perfusion phantom because it is accurate, fast and inexpensive. In addition, PDMS is a MRI friendly material.

The microfabricated phantom was used to simulate the blood perfusion in tissues.

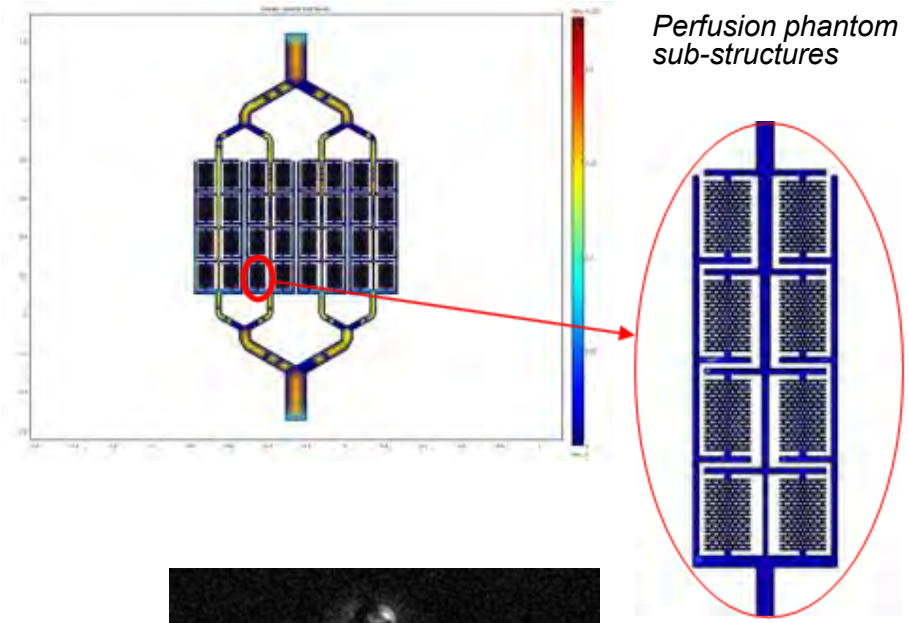

Perfusion phantom sub-structures

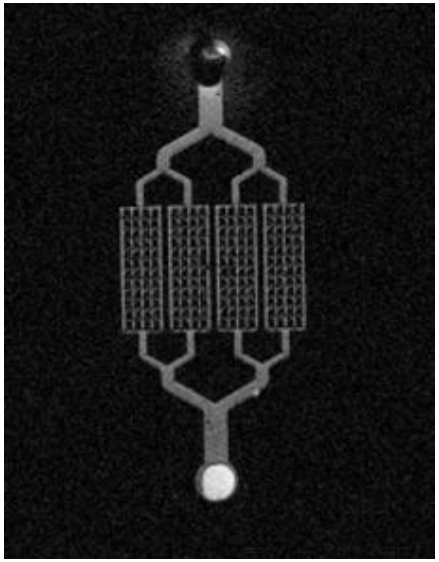

High resolution MRI of the microfabricated phantom by Dr. Swanson

B. Ebrahimi, S.D. Swanson, T.E. Chupp, University of Michigan

Work performed at U Michigan Lurie Nanofabrication Facility

Integration of Piezoelectric Materials into MEMS

Bulk piezoelectric ceramics, unlike deposited piezoelectric thin films (such as sputtered AlN or sol-gel PZT), provide greater electro-mechanical force, structural strength, and charge capacity, which are highly desirable in many MEMS applications including high-force actuators, harsh-environmental sensors, and micro-power scavengers. We have developed a new CMOS-compatible wafer-level process to obtain thin films of bulk piezoelectric materials on silicon. The process involves low-temperature aligned solder bonding of commercially available bulk piezoelectric substrates on silicon, and mechanical thinning to obtain the desired PZT thickness (5-100 μm).

E.E. Aktakka, R.L. Peterson, and K. Najafi,
University of Michigan

Work performed at the U Michigan Lurie Nanofabrication Facility

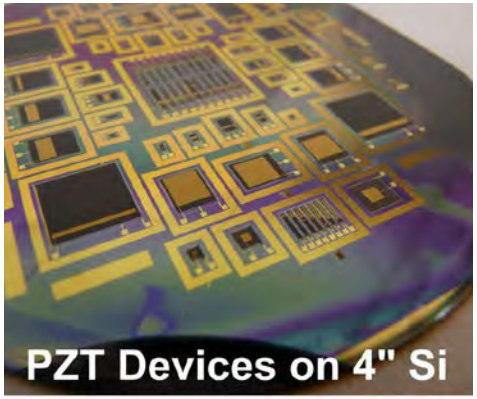

Fabricated PZT cantilever beam and diaphragm actuators, and vibration energy harvesters on a 4" silicon wafer.

SEM image of a thinned-PZT and Si unimorph cantilever beam cross-section.

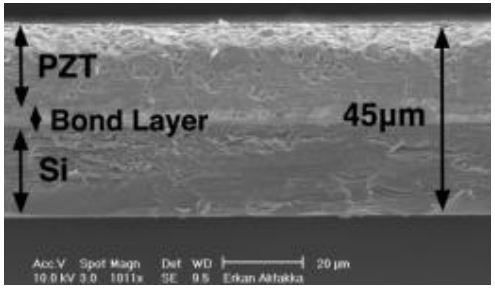

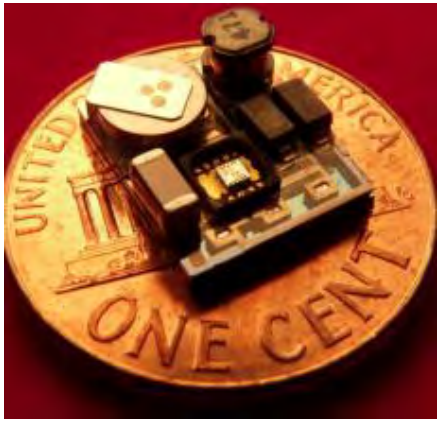

A packaged thinned-PZT vibration energy harvester integrated with its power management IC and surface mount circuit components.

Micromachined Cylindrical Rate-Integrating Gyroscope (CING)

The purpose of this research is to develop a batch-manufacture-able high-performance rate-integrating gyroscope using conventional MEMS fabrication processes.
Novel sensor architecture for the rate-integrating gyroscope has been developed. The sensor has been fabricated using the silicon-on-glass (SOG) process. The process involves high-aspect ratio DRIE of highly-p-doped (111) Si wafer, recess definition on a borosilicate glass wafer, anodic bonding, and releasing of the structure using the DRIE. The developed sensor measures size of 6mm x 6mm x 0.3mm, and operates at a frequency of ~17kHz, with a Q of 20,000~70,000.

J.Y. Cho, R.L. Peterson and K. Najafi,
University of Michigan

Work performed at the U Michigan Lurie Nanofabrication Facility

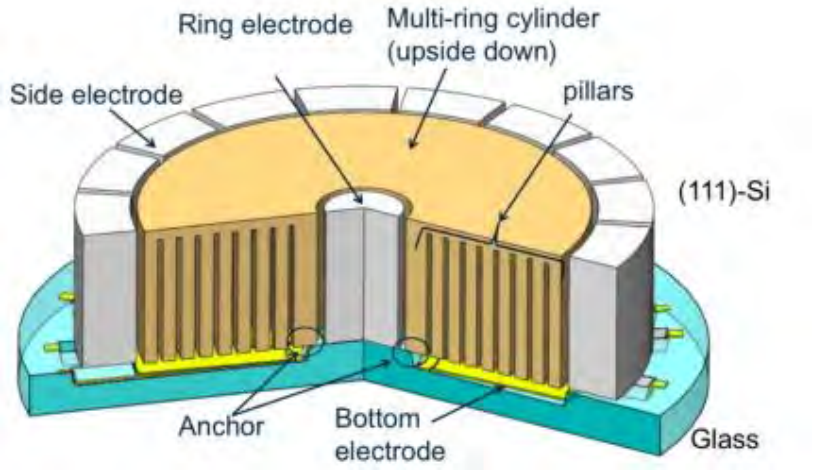

Architecture of the CING

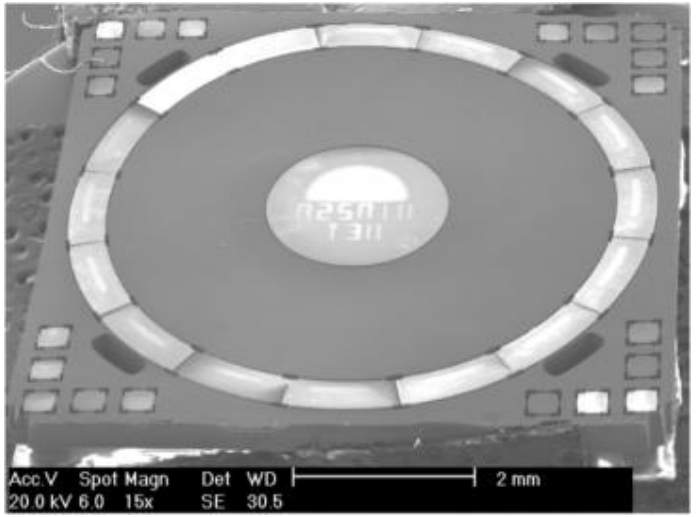

SEM picture of the CING fabricated with the silicon-on-glass (SOG) process

Self-Switching Microfluidic Circuits

Networks of normally closed elastomeric valves are designed such that they provide auto-regulation of flow. In this concept, there are no interconnects for control flow; the only input is the direct infusion of the reagents at a constant flow rate. An interconnected network of fluidic capacitors that provide time delays, valves that open and close at defined threshold pressures, and channels that serve as resistors convert the constant input flow to discrete control signals that direct fluid to different parts of the device at defined times. This concept is reminiscent of electronic devices that continually operate based on the instructions encoded by the embedded integrated electronic circuit as long as power (i.e. direct current from a battery) is supplied.

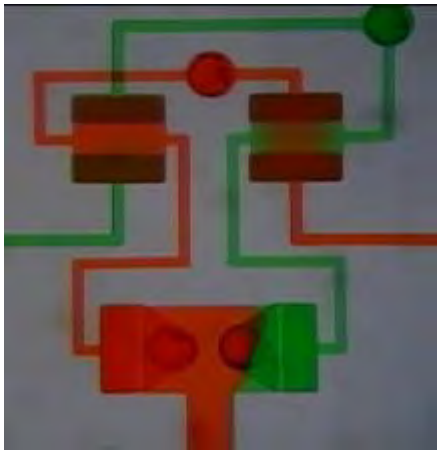

Microfluidic oscillator made by two switch valves that interact with each other

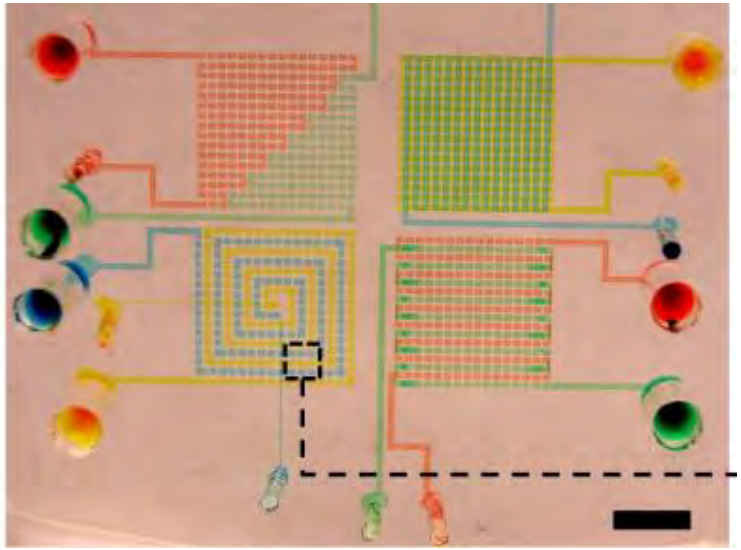

Fabrication of a device with over 1000 normally-closed valves

S. Takayama, University of Michigan

Work partially performed at U Michigan Lurie Nanofabrication Facility

CD4+ T-cell Counting Biochip for Monitoring HIV/AIDS in Resource Limited Settings

The purpose of this project is to develop an inexpensive lab-on-a-chip device for the point-of-care (POC) monitoring of HIV/AIDS in the resource limited settings of the world. We are developing a biochip (microfluidic device) which can perform CD4+ T-cell counting for HIV/AIDS monitoring. We have developed a cell trapping biochip with a novel 3D trapping architecture for capturing human white blood cells (WBCs). This biochip enables to obtain a high (> 90%) trapping efficiency of WBCs.

We envision integration of the above biochip with an on-chip microscopy technique, hence eliminating the need for bulky and expensive external microscopy setup. Towards this end, we have developed a high numerical aperture (NA) doublet microlens array for on-chip imaging of micron sized objects. These microlenses are capable of direct image formation on an inexpensive imaging sensor without the use of any intermediate optics.

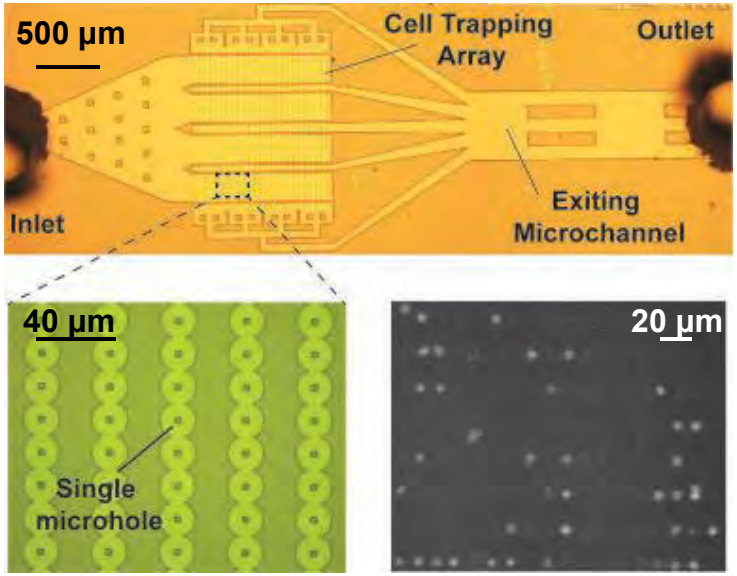

Microfluidic biochip for trapping WBCs. Fluorescent image shows WBCs trapped in the device.

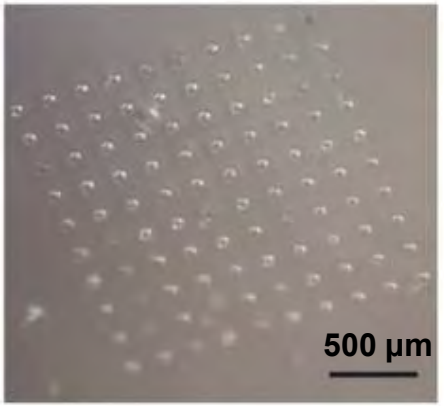

Scale bar 20 µm

Doublet microlens array for imaging µm size objects. Micron-sized patterns imaged directly on a CCD sensor.

A. Tripathi and N. Chronis, University of Michigan,
B. Work performed at U Michigan Lurie Nanofabrication Facility

Worm Sorter Project

The Worm Sorter is a microfluidic device designed to sort living *C. elegans*, nematodes around 1 mm in length. Animals expressing fluorescent protein sensors can be imaged and sorted one at a time in the device.

In the LNF, the moulds for the control channels and flow channels of the device are fabricated using photoresistive material on silicon wafers. PDMS layers are then poured onto these moulds, cured, and bonded together using oxygen plasma.

Valves in the finished device can be opened and closed by external pressure to maneuver and hold each worm in position for imaging.

M. Kim, N. Niemuth, and U. Jakob, University of Michigan

Work performed at the U Michigan Lurie Nanofabrication Facility

A micofluidic device for sorting live C. elegans.

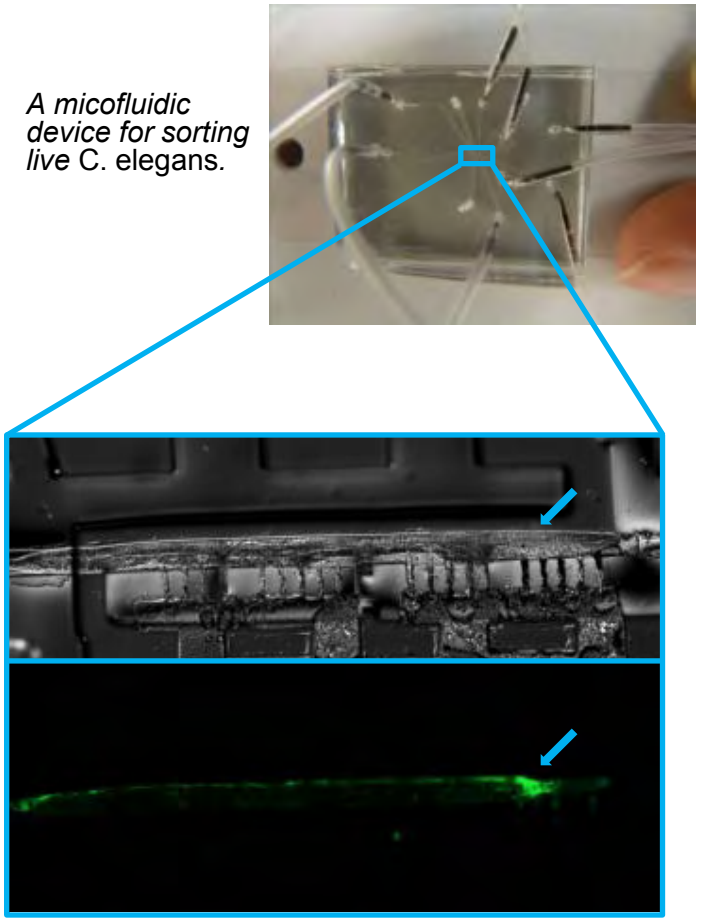

Using the Worm Sorter, DIC (top) and fluorescence (bottom) images were taken of a nematode expressing a fluorescent protein sensor in its neurons. Arrows indicate the nerve ring in the head of the worm.

Wafer Scale Growth of Homogeneous Bilayer Graphene film by Chemical Vapor Deposition

Pristine single and few-layer graphene are intrinsically semimetals and introducing energy bandgap requires patterning nanometer width graphene ribbons, or utilizing special substrates. The recent discovery of electric field induced bandgap opening in bilayer graphene opens a new door for making semiconducting graphene and makes bilayer graphene particularly attractive for graphene based electronics. Despite intensive research, synthesizing homogeneous bilayer graphene in large size has proven extremely difficult and most bilayer graphene samples are fabricated by mechanical exfoliation, limiting their sizes at micrometer scale.

We have demonstrated homogeneous bilayer graphene films over at least 2”x2” area, synthesized by chemical vapor deposition (CVD) on thin Cu foil and transferred to arbitrary substrates. The size of our bilayer graphene film is only limited by the synthesis apparatus and can be readily scaled up, thus enabling wafer scale graphene electronics and photonics. The bilayer nature of graphene film has been verified by Raman spectroscopy, AFM and TEM. Spatially resolved Raman spectroscopy has confirmed a bilayer coverage of over 99%. Electrical transport measurements on dual-gate bilayer graphene transistors have shown bandgap opening in 98% of the devices.

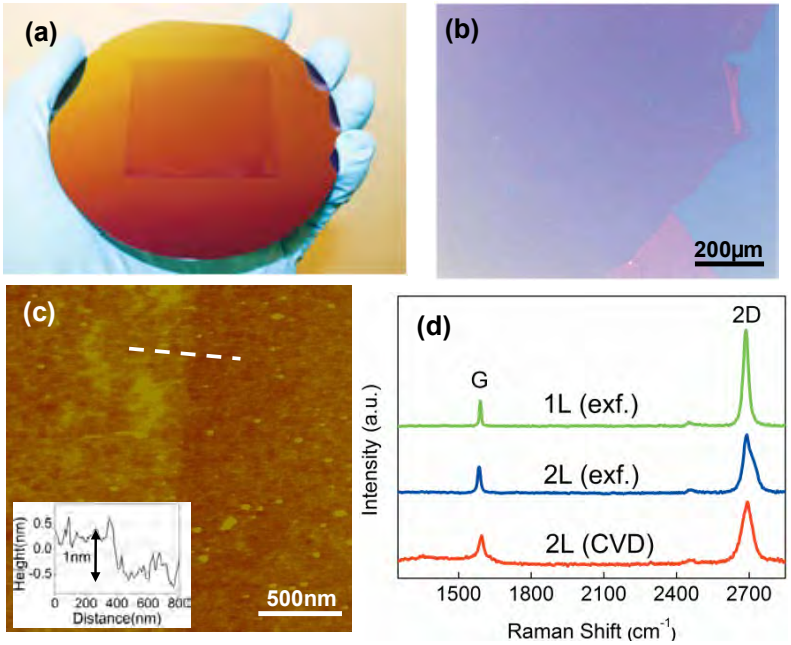

Photograph of 2inch x 2inch bilayer graphene sample and optical microscope image, AFM image and Raman spectrum result.

S. Lee, K. Lee and Z. Zhong, University of Michigan

Work performed at U Michigan Lurie Nanofabrication Facility

Capacitive Spring Softening in Single-Walled Carbon Nanotube Nanoelectromechanical Resonators

Gate induced frequency tuning of nanoelectromechanical (NEM) resonators is known to be governed by two mechanisms: the elastic hardening effect which increases the resonance frequencies, and the capacitive softening effect which decreases the resonance frequencies.

In this project, we report the capacitive spring softening effect observed in single-walled carbon nanotube NEM resonators. The nanotube resonators have dual-gate configuration. Downward resonance frequency shifting is observed with increasing end-gate voltage, which can be attributed to the capacitive softening of spring constant. Furthermore, in-plane vibrational modes exhibit much stronger spring softening effect than out-of-plan modes. Our dual-gate design should enable the differentiation between these two types of vibrational modes, and open up new possibility for nonlinear operation of nanotube resonators.

C.C Wu and Z. Zhong, University of Michigan

Work performed at the U Michigan Lurie Nanofabrication Facility

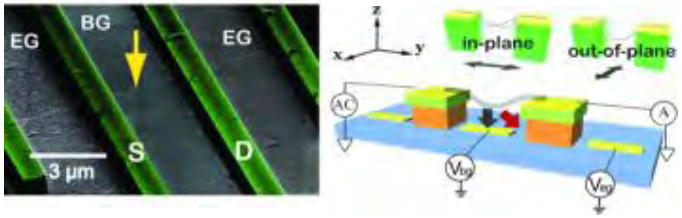

Device geometry of dual-gate SWNT resonators and qualitative sketch of how electrostatic force interacting with CNT when V_{bg} or V_{eg} is applied

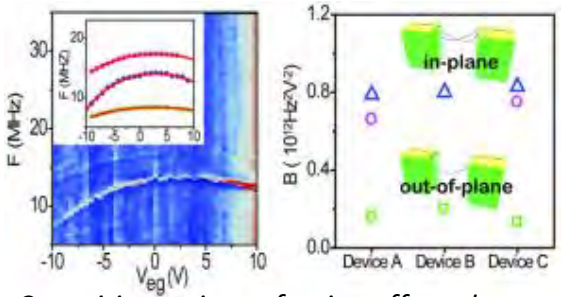

Capacitive spring softening effect observed on different vibrational modes.

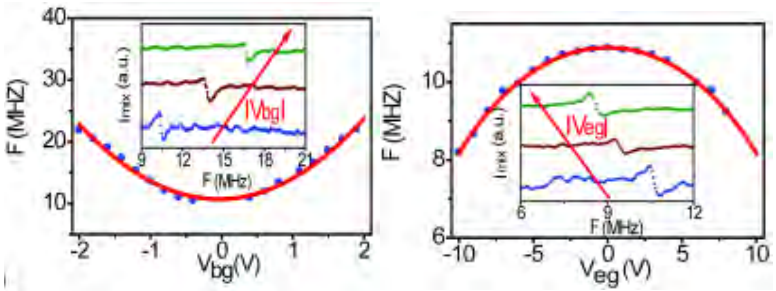

Resonance characteristics of a dual-gate SWNT resonator

Zero-Mode Waveguides Single Molecular Imaging

Zero-mode waveguides (ZMWs) are nanoscale metallic optical waveguides exhibiting no propagating modes. As light incidents at the ZMW, the optical intensity exponentially decays, resulting in a zeptoliter excitation volume confined at the entrance of the waveguide. Therefore, ZMWs are suitable for single-molecular sensing at a physiologically relevant concentration, typically on the order of micromolar or more.

This project aims to develop a low-cost solution for real-time single-molecular imaging based on a large array of ZMWs. Our approach combines industrially mature microlithography and novel electrodeposition pattern shrinking process. Fluorescent spectroscopy experiments have successfully showed the viability for single molecular sensing.

C.H. Teng, T. Lionberg, E. Meyhofer, and P.C. Ku, University of Michigan

Work performed at U Michigan Lurie Nanofabrication Facility

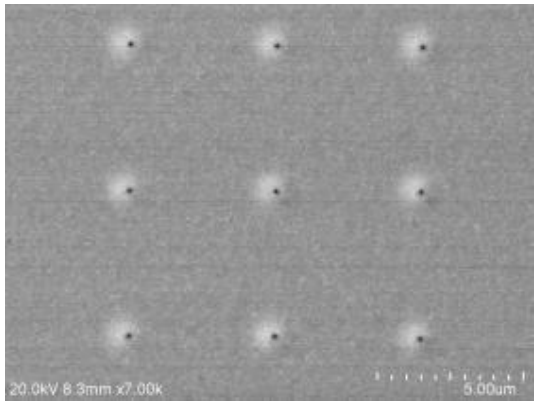

Gold nanoaperture array made by photolithography and electrodeposition nanopatterning technique.

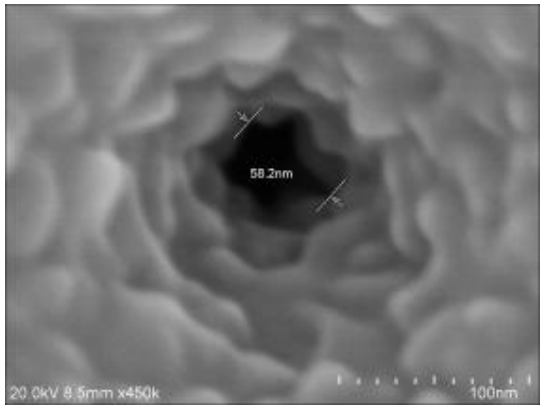

Nanoscale aperture enables single-molecular sensing at micromolar concentration.

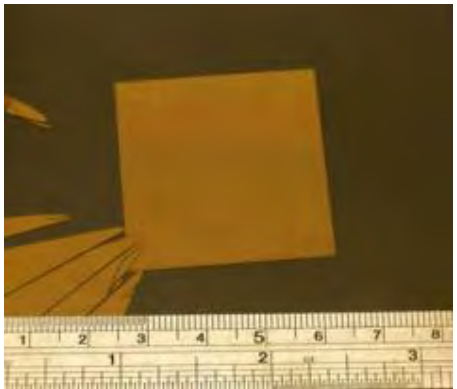

Image of LNF fabricated sample showing the capability of large area fabrication.

Site-Controlled III-Nitride Quantum Dots

III-nitride semiconductor quantum dots (QDs) exhibit large exciton binding energy (≥ 26 meV) and are ideal candidates to exploit various quantum optical phenomena at high temperatures including single-photon emission, strong-coupling, indistinguishable photon generation and one-atom lasing. The practical use of the III-nitride QDs as quantum light sources often requires the addressability of a single QD e.g. strong-coupling requires the precise placement of a single QD at the anti-node of an optical cavity. To date, most of the III-nitride QDs are fabricated by the self-assembled growth which does not establish site- and dimension-control, making them difficult to be utilized on the device level. Here we demonstrate a simple top-down etching method to produce site-controlled InGaN quantum dots exhibiting high uniformity and distinct, strong room-temperature (RT) single-dot luminescence. The results can provide a new opportunity for the realization of scalable room-temperature semiconductor quantum light sources.

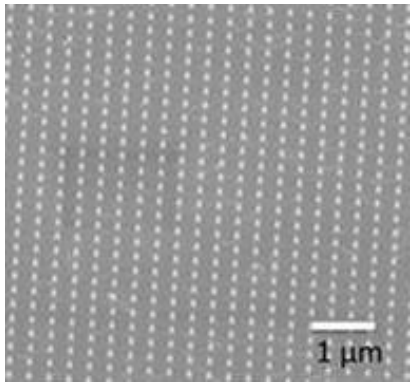

An array of uniform InGaN quantum disks

Single-disk room-temperature luminescence captured by CCD camera

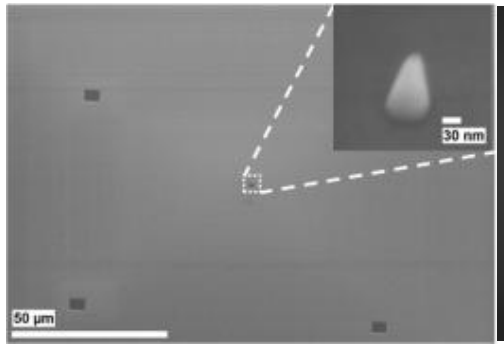

A stand-alone17-nm-diameter quantum disk embedded in the nanopillar, ready for single-dot optical characterization

Strong room-temperature luminescence observed even for a single quantum disk

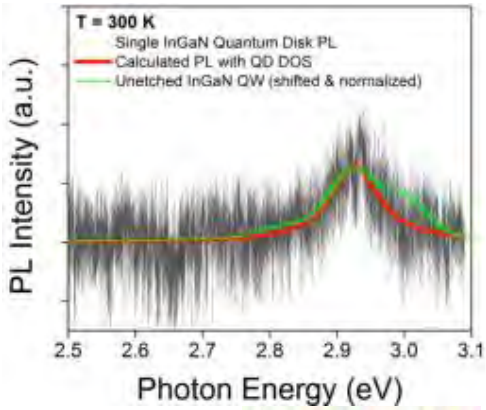

L.K. Lee, L. Zhang, H. Deng, and P.C. Ku, University of Michigan
Work performed at U Michigan Lurie Nanofabrication Facilities

Chemical Sensors for Extreme Environments

The lack of performing and reliable chemical sensors currently limits the quantitative studies of hydrothermal system at mid-ocean ridge. We propose here to improve the measurement of chemical components associated with hydrothermal vent fluids using high performance miniaturized sensor assembly and by ultimately developing on-board signal processing.

We have now fabricated major components including YSZ diaphragms with deposited metal electrodes, Macor® ceramic backing, and sensing electrode made from Hg/HgO paste. The integration process using microfabrication-based techniques is in progress.

Y. Gianchandani and T. Li, U. Michigan and B. Seyfried and K. Ding, U. Minnesota

Work performed at U Michigan Lurie Nanofabrication Facility

Effect of Length and Contact Chemistry on the Electronic Structure and Thermoelectric Properties of Molecular Junctions

Picowatt-resolution calorimetry is necessary for fundamental studies of nanoscale energy transport. Here, we report a microfabricated device capable of <4 pW resolution—an order of magnitude improvement over state-of-the-art room temperature calorimeters. This is achieved by the incorporation of two important features. First, the active area of the device is thermally isolated by thin and long beams with a total thermal conductance (G) of 600 nW/K. Further, a bimaterial cantilever thermometer capable of a temperature resolution (ΔT_{res}) of 4 μK is integrated into the microdevice. The small thermal conductance and excellent temperature resolution enable measurements of heat currents ($q=G \times \Delta T_{res}$) with a resolution <4 pW.

S. Sadat et al. Appl. Phys. Lett., 2011

S. Sadat, Y.J. Chua, W. Lee, Y. Ganjeh, K. Kurabayashi, E. Meyhofer and P. Reddy, University of Michigan
Work performed at the U Michigan Lurie Nanofabrication Facility

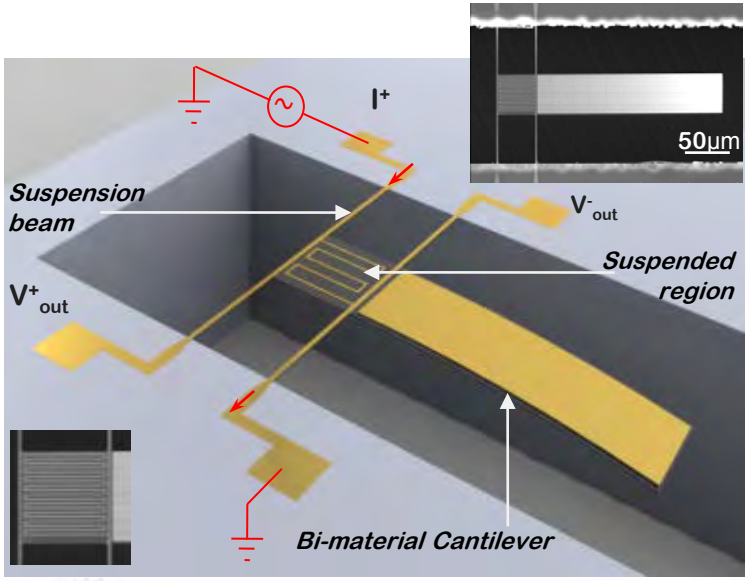

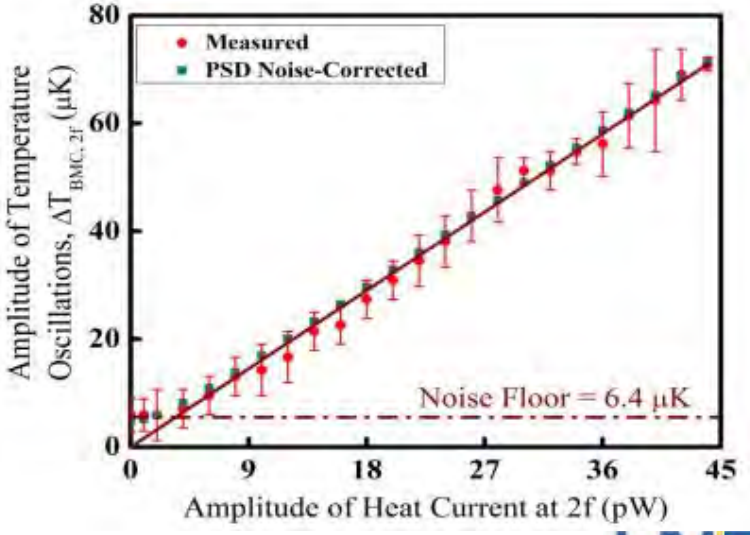

A Temperature Invariant Tunable Front-end Filter for UHF Tactical Radio

The goal of this project is to implement a reconfigurable front-end filter that can be tuned from 1 GHz to 500 MHz providing better performance than CMOS technology and smaller foot-print than PCB counterparts.
In the fabrication process, three metal and two sacrificial layers are utilized allowing simultaneous implementation of tunable capacitors, MIM capacitors, and high-*Q* inductors. The filter is implemented using an inductively coupled third-order coupled resonator configuration. Each LC tank is composed of four tunable capacitors. Each capacitor is electrostatically actuated with a tuning ratio of more than 5 to 1. Tunable capacitors are designed to be robust against temperature and stress variations; hence the tunable filter can function in various environmental conditions. The measured tuning speed of the integrated filter is better than 100 μs and the IIP3 is better than 20 dBm. The size of the fabricated filter is less than 1.5 cm × 1.0 cm.

Y. Shim and M. Rais-Zadeh, University of Michigan
Work performed at U Michigan Lurie Nanofabrication Facility

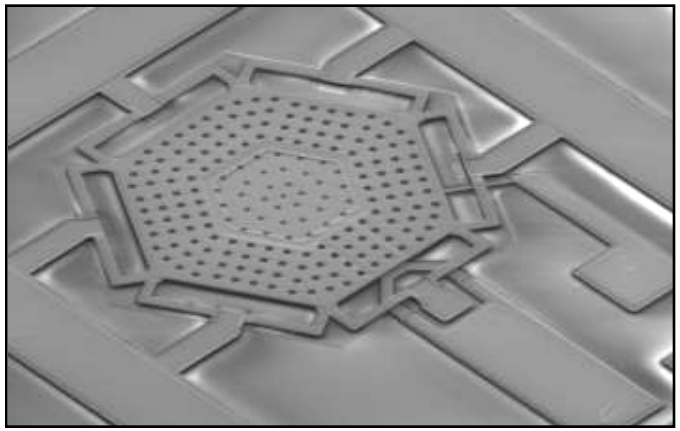

An RF tunable capacitor with a dual-gap configuration, having a tuning range of more than five and quality factor of more than 100 at 1 GHz at all tuned states.

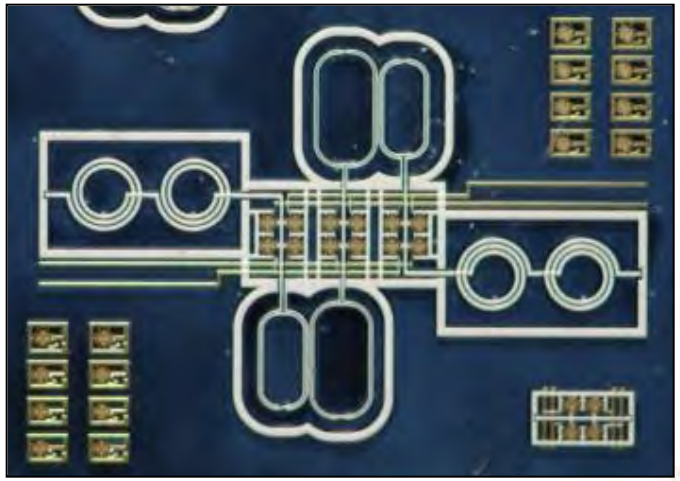

An integrated tunable bandpass filter which covers 500 MHz to 1 GHz with 10 to 14% bandwidth and less than 4 dB insertion loss.

Low-Power Electromechanical Sensor Array for IR Detection

This project aims at developing a platform technology for low-noise electromechanical sensor array used for infrared (IR) detection. The proposed architecture consists of a parallel array of high-*Q* gallium nitride (GaN) micromechanical resonators to sense the frequency change induced by incident IR radiation.

To model the change in resonant frequency, FEM simulation models are used to simulate the piezoelectric and pyroelectric properties of GaN, and help in optimizing the design for highest sensitivity.

Modeling the resonator as an equivalent electrical circuit using the modified Butterworth-van Dyke (mBVD) model is also used to gain insights into the device performance.

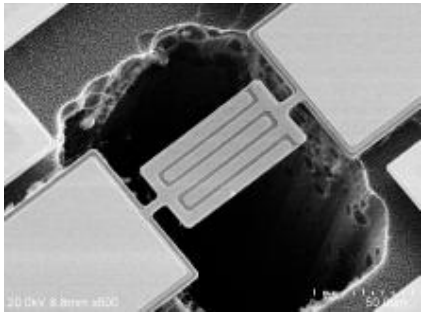

SEM image of fabricated GaN contour mode resonator nominally working at 167 MHz

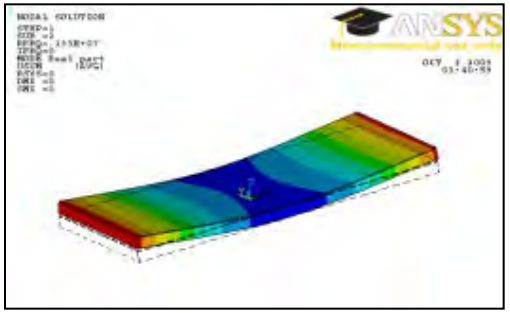

ANSYS simulation of flexural mode resonance of a free-free resonator

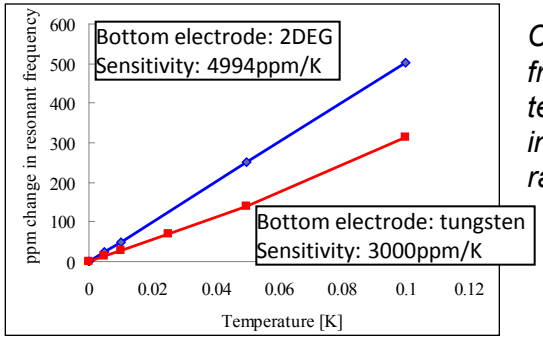

Change in resonance frequency vs. temperature change induced by IR radiation.

V. Gokhale and M. Rais-Zadeh, University of Michigan
Work done at U Michigan Lurie Nanofabrication Facility and with NNIN/C@Michigan

Sensitive Detection of CTCs by Graphene Oxide

Technological obstacles in isolation and capture of circulating tumor cells (CTCs) from blood continue to stymie the progress in quantifying CTCs for early diagnosis and effective monitoring of therapeutic response in patients. Self-assembly of functionalized graphene oxide (GO) is a promising nanomaterial for capture of tumor cells. The integrated nano microfluidic device with functionalized GO/gold can be used as bioengineering tools to CTCs using breast cancer cell line.

H.J. Yoon, K. Lee, Z. Zhang, T. Pham, S. Nagrath, University of Michigan

Work performed at U Michigan Lurie Nanofabrication Facility

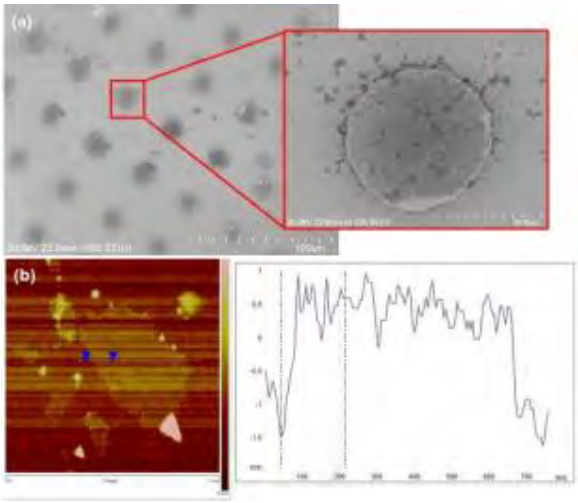

Self-assembled graphene oxide

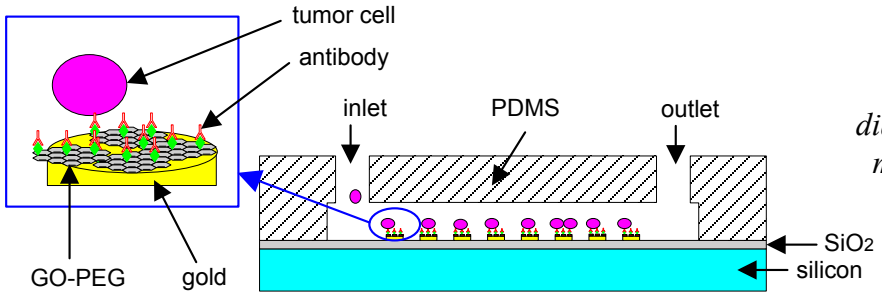

Schematic diagram of the microfluidic device

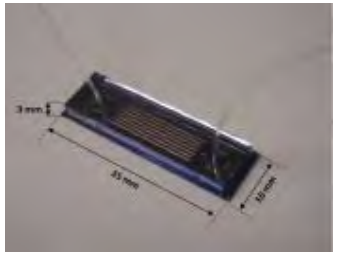

Photograph of the fabricated device

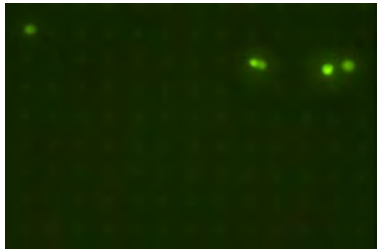

Captured MCF-7 cells

3D Microfabrication Using Carbon Nanotubes

Lithographically defined patterns of vertically aligned carbon nanotubes (CNTs) are transformed into three-dimensional (3D) geometries by self-directed capillary action initiated by liquid condensation. In addition to their novel geometries, the properties of densely packed CNT microstructures make them attractive as a new microfabrication material. Building from our demonstration of capillary forming to create diverse 3DCNT microstructures in 2010, we have: (1) used CNT/polymer nanocomposite microstructures as masters for replica molding of polymer microstructures; (2) demonstrated that capillary buckling of vertical CNTs enables programmable fabrication of multi-directional horizontal CNT (HA-CNT) networks; and (3) created a fabrication method for corrugated CNT microarchitectures, which have geometrically tunable mechanical properties. This work may find future applications in cost-effective fabrication of biomimetic surfaces, metamaterials, multi-scale circuits, and novel sensors and actuators.

A.J. Hart, University of Michigan, Work performed at
U Michigan Lurie Nanofabrication Facility

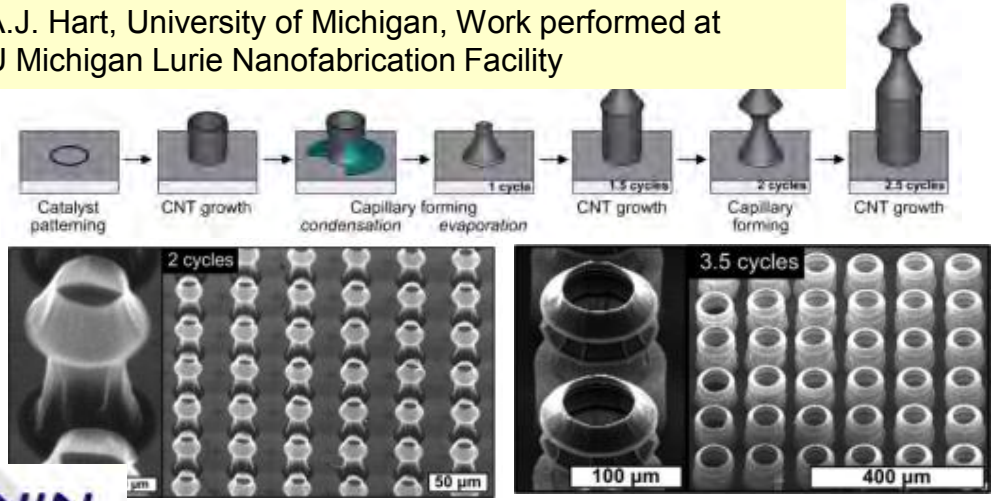

Corrugated CNT microsprings (ACS Nano 2011)

CNT-based replica molding (Lab on a Chip 2011)

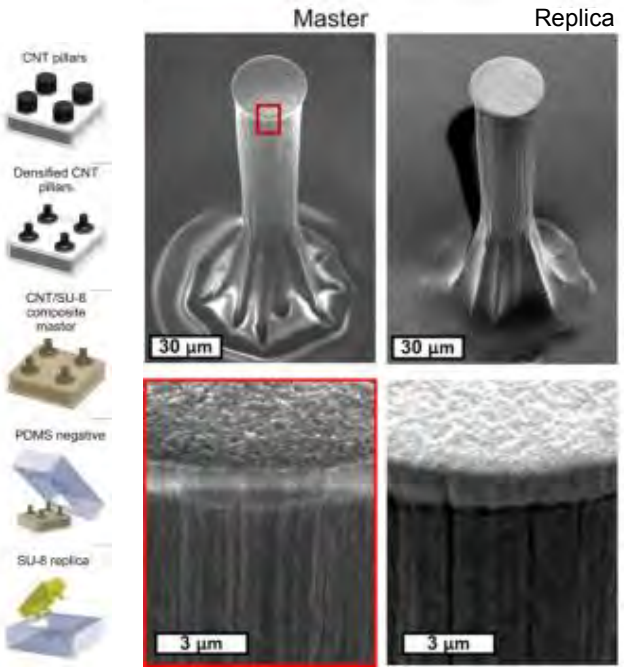

HA-CNT patches and networks (Langmuir 2011)

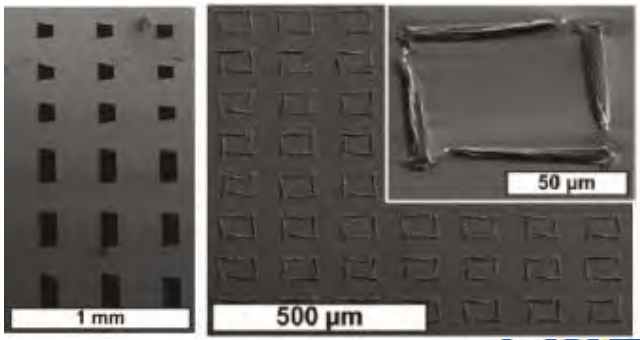

Piezoresponse Force Microscopy of $In_{0.2}Ga_{0.8}N$ Quantum Dots

InGaN quantum dot (QD) materials are currently being investigated for light emitting diodes. However, due to a large lattice mismatch between InN and GaN, the piezoelectric field in InGaN will have a significant impact on the optoelectronic properties. Piezoresponse force microscopy (PFM), which is an extension of the atomic force microscope , allows direct nanoscale measurement of the piezoresponse of InGaN QDs. With this method, it is possible to investigate the correlation between the strain in the QD versus the QD shape and also extract piezoelectric coefficients for the direct calculation of the piezoelectric field.

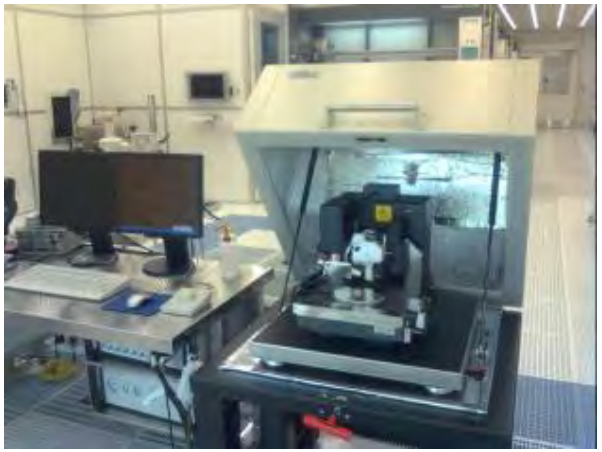

(a)

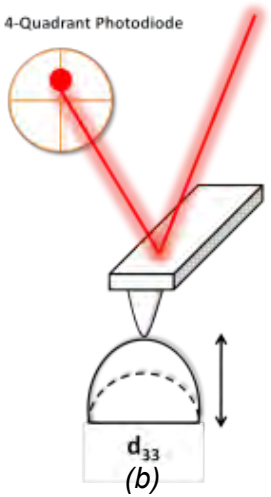

(b)

(a) Atomic force microscope used for measurements (b) Diagram of an ideal vertical PFM response on a QD

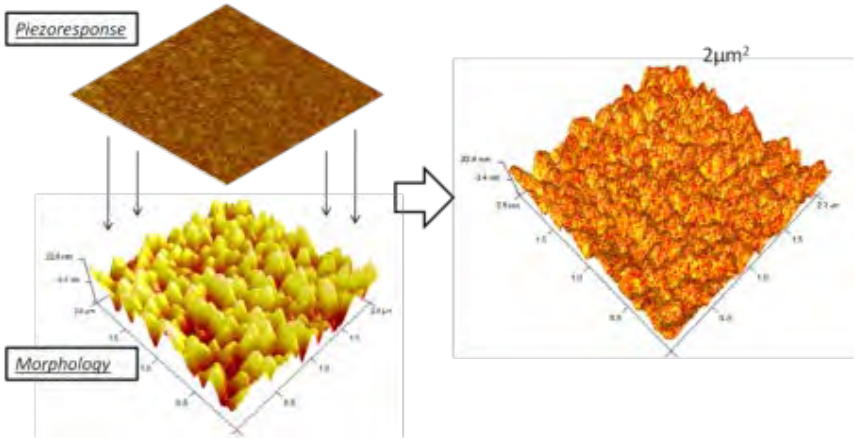

Piezoresponse data overlay on the height data of a 2 μm² area for correlation study

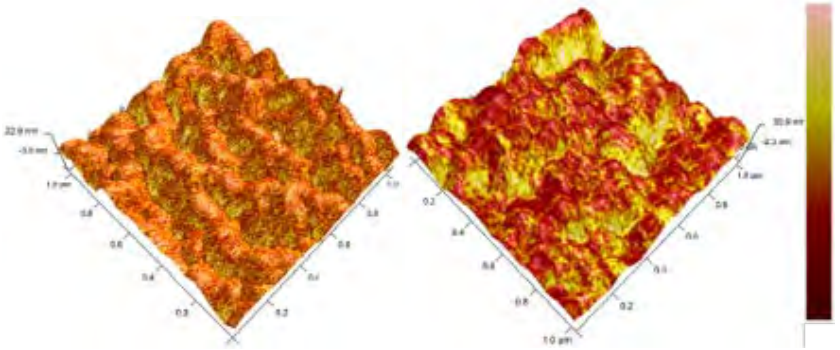

(a) (b)

(a) Vertical and (b) lateral piezoresponse QD correlation of a 1 μm²

A. Bayraktaroglu, M. Zhang, A. Banerjee, P. Herrera-Fierro, P. Bhattacharya, and J. Phillips, University of Michigan
Work performed at U Michigan Lurie Nanofabrication Facility

Intrinsically Switchable & DC Voltage Dependent Acoustic Wave Resonators Based on Ferroelectric BST

The purpose of this work is to design intrinsically switchable & dc voltage dependent acoustic wave resonators and filters. By doing that, it is possible to remove RF switches in a filter bank or in a resonator bank, to minimize additional losses, area and complexity in the design. The electrostriction property of BST is exploited for intrinsic switchability. We are currently designing, fabricating and characterizing BST-on-silicon composite thin film bulk acoustic wave resonators (FBAR). The low acoustic loss of silicon and electrostrictive property of BST is combined to obtain high quality factor (Q), intrinsically switchable resonators.

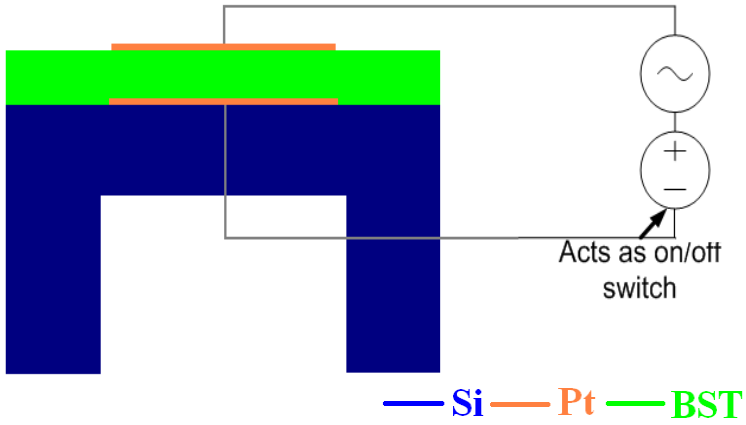

Schematic of the composite FBAR

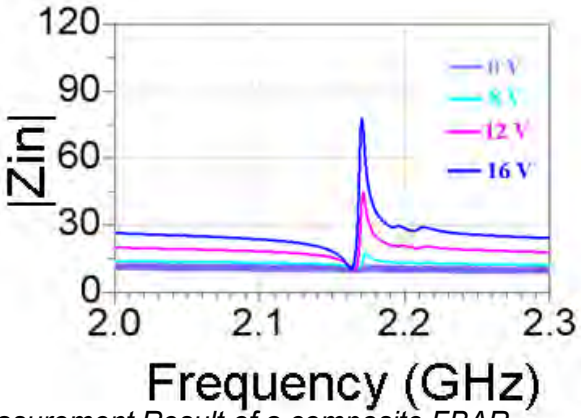

Measurement Result of a composite FBAR

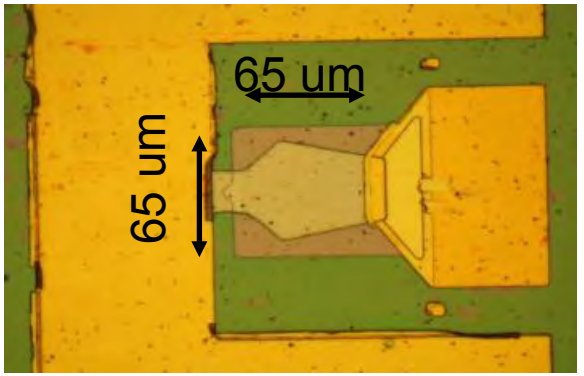

Microscope photo of a Composite FBAR

S. Sis, V. Lee and A. Mortazawi University of Michigan
Work performed at U Michigan Lurie Nanofabrication Facility

High-throughput Microfluidic Chip for Photodynamic Therapy (PDT) Screening

In this project we are developing a microfluidic chip that can provide the control of all these three crucial parameters in photodynamic therapy including the concentration of photosensitizers, oxygen levels and activating light intensity. By using the microfluidic gradient-generating networks, we can simultaneously provide nine different concentrations of photosensitizer. Also by imposing an extra gas layer in the top channel, we can provide different oxygen levels for each flow layer through molecular diffusion across the thin PDMS membrane which separates the two layers. Also exposure dose can be controlled by an LED light source. Methyleneblue (MB), which has been used for a variety of applications as photosensitizer, and rat C6 glioma tumor cells are adopted for PDT efficiency test. We observed distinctive viability for various Methyleneblue concentrations, oxygen levels and exposure doses. From this, we could determine the minimum (threshold) level of these parameters required for reaching certain effectiveness.

X. Lou, G. Kim, Y.-E. L. Koo, R. Kopelman, E. Yoon,
University of Michigan
Work performed at U Michigan Lurie Nanofabrication Facility

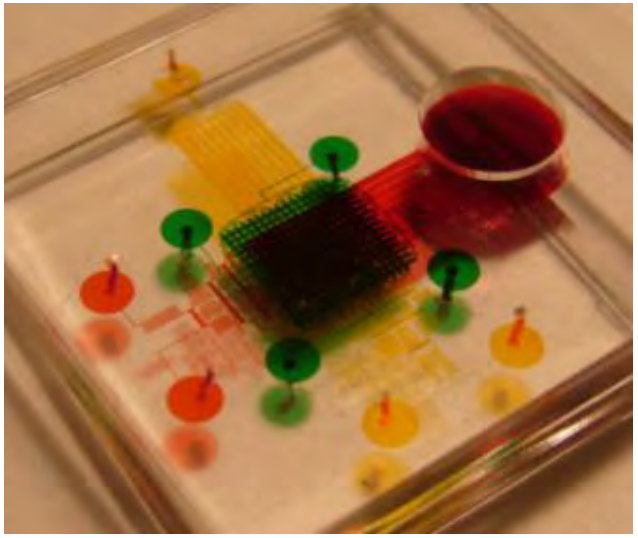

Figure 1. Photograph of fabricated PDT with food color filling.

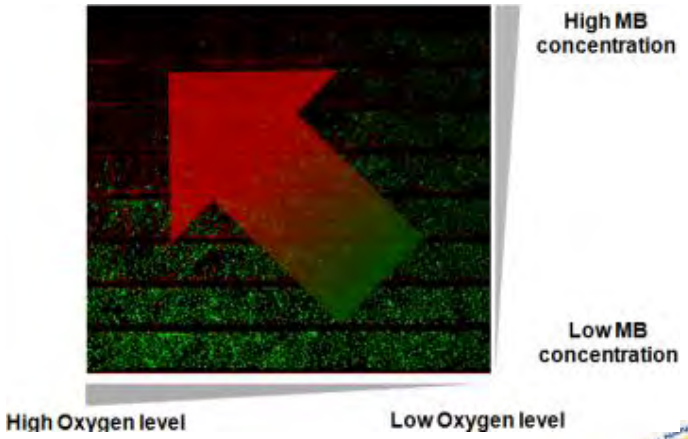

Figure 2. Typical result of C6 cell in chip viability after PDT treatment

Integration of Neural Probes with Waveguides for Optical Stimulation

The purpose of this project is to develop a neural probe capable of simultaneous optical stimulation of neurons and electrical recording of the neural signals. Genetically modified neurons expressing light sensitive ion channels can be selectively stimulated by a light source. Corresponding neural signals triggered by the stimulation can then be recorded by the electrodes. The probe will allow the neural scientists to begin defining specific functions and connectivity of the complex neural circuitry of the central nervous system.

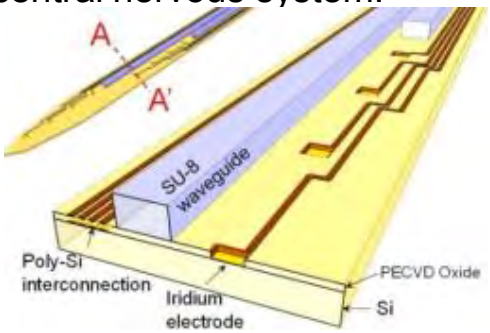

Schematic diagram of the proposed neural probe integrated with waveguides and cross-sectional view of the probe shank in direction of AA'

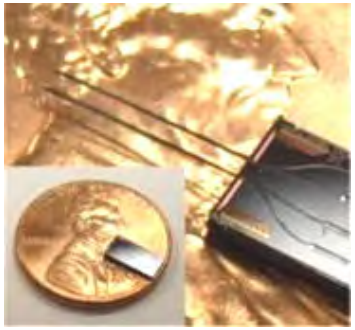

Fabricated neural probe with double waveguides on each shank on a U.S. penny

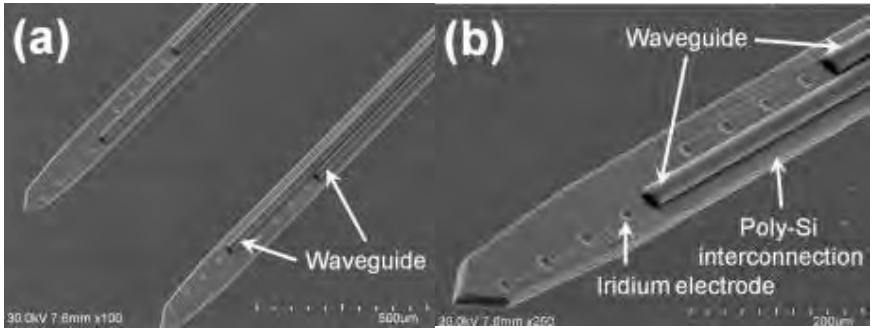

SEM images of the fabricated neural probe integrated with double-waveguides on a shank: (a) Top view of dual shank showing double waveguides on each shank

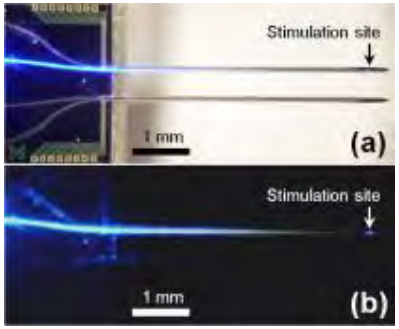

Light transmission through one of the waveguides to the end of the waveguide: (a) a bright field microscope image; and (b) a dark field microscope image.

M. Im, F. Wu, and E. Yoon, University of Michigan
Work performed at U Michigan Lurie Nanofabrication Facility

Thiolated Gold Nanoparticle Chemiresistors

The project addresses challenges of miniaturizing vapor sensors employing monolayer protected gold thiolated nanoparticles as interface layers on transducers formed from simple interdigitated electrodes for integration into a micro-gas chromatography system (μGC). Electrodes are fabricated via electron beam lithography. Nanoparticle deposition is done with a micro-dispensing system and can be further patterned via electron beam induced crosslinking to form tightly spaced (~4 μm spacing) sensors. For integration into a μGC system, electrode arrays can be fabricated with capillary inlets/outlets etched into the silicon chip. To minimize the chamber area and improve the sensor's performance, the arrays can be capped with a glass lid with a small etched recess.

E. Covington and Ç. Kurdak, University of Michigan
Work performed at U Michigan Lurie Nanofabrication Facility

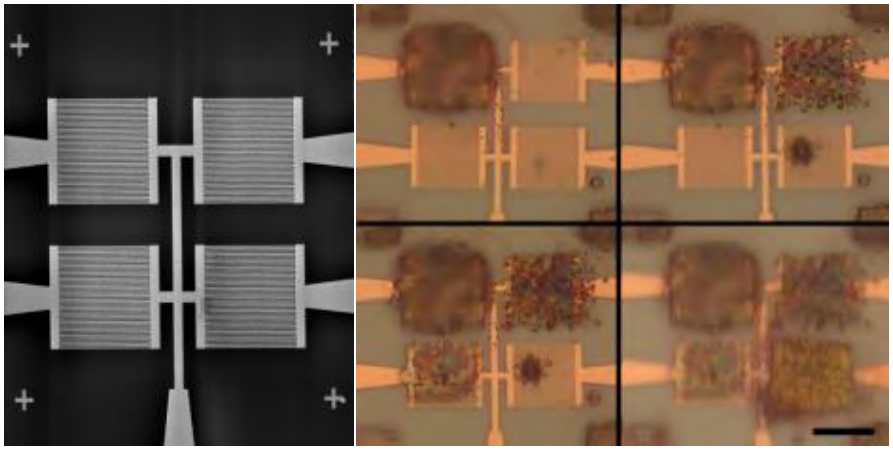

(left) SEM image of a "nanoarray" comprised of 4 sets of interdigitated electrodes with 100 nm width and spacing. (right) A nanoarray patterned with four different nanoparticle films using electron beam induced crosslinking. Scale bar is 10 μm.

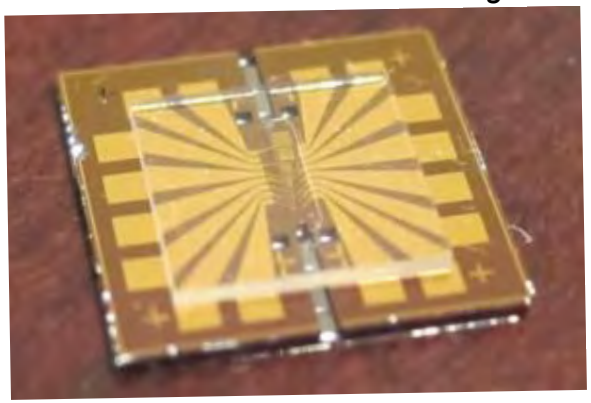

An eight sensor array on Si with 380 μm etched grooves for capillary inlet and outlets. The array is covered with a glass lid with a 100 μm recess for vapor testing.

Printing Antennas onto Contoured Substrates

The purpose of the direct transfer patterning process to fabricate 3-D antennas. We have developed a process involving a patterned PDMS stamp to transfer its pattern onto an arbitrarily contoured substrate. Using this process, we can fabricate 3-D antennas that were previously considered too difficult to fabricate. Thus far we have focused on fabricating electrically small antennas. We have fabricated some of the best performing small antennas to date: We have achieved efficiencies of 70% with quality factors of 1.8 times the physical limit.

C. Pfeiffer, X. Xu, S. Forrest, and A. Grbic,
University of Michigan
Work performed at the U Michigan Lurie Nanofabrication Facility

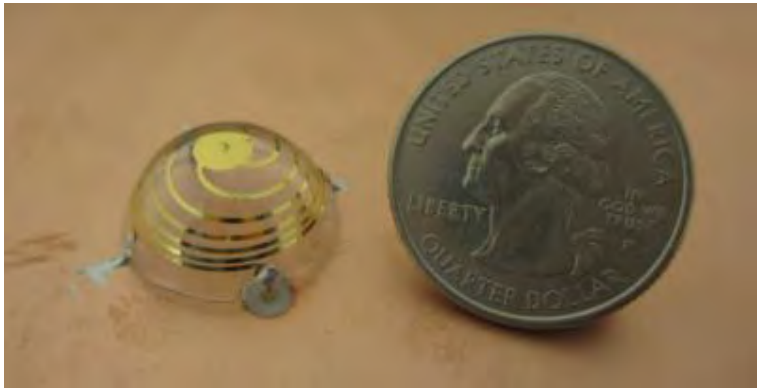

Printed spherical helix antenna that is 1/15 times the wavelength. This is about a quarter of the size of conventional small antennas.

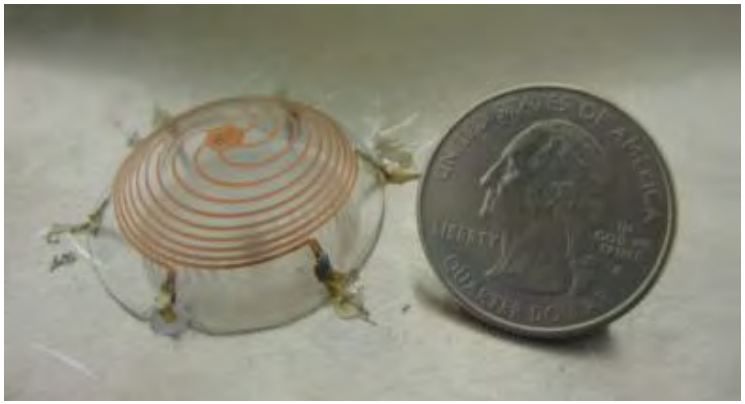

Another spherical helix antenna printed onto the upper half of a hemisphere.

Fast Force Probes for Mechanobiology

We aim to develop a new tool for the study of mechanobiology at the microsecond time scale. The first major application of the force probe will be the cochlear hair cell, the sensory neuron in your inner ear that allows you to hear. Existing tools are not simultaneously fast, sensitive, and compliant enough to investigate cochlear hair cell function in mammals.

The devices are fabricated from silicon on insulator wafers and utilize a piezoresistive force sensor. The backside DRIE step, which releases the cantilevers from the wafer, is performed at the LNF.

Force probe mounted on a printed circuit board

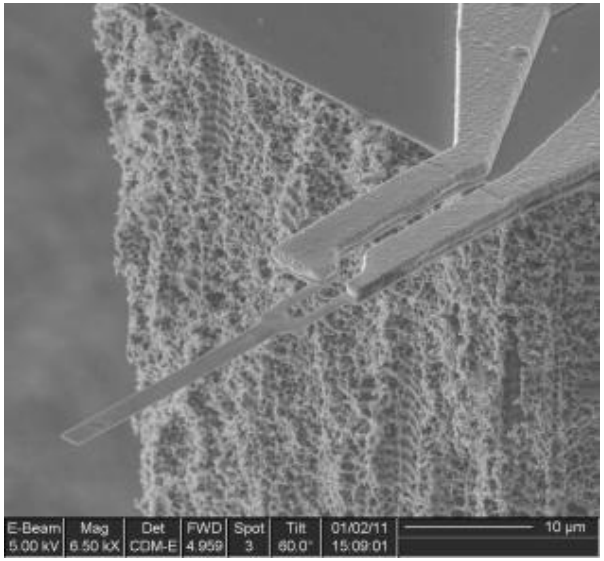

Electron micrograph of the force probe tip. Force is transduced by a doped silicon piezoresistor.

J. Doll and B. Pruitt, Stanford University

Work partially performed at the U Michigan Lurie Nanofabrication Facility.

Post-CMOS Parylene Packaging for On-chip Biosensor Arrays

The opportunity to integrate microfluidic devices with CMOS instrumentation is attractive to many biological and biomedical sensor applications. However, the packaging of CMOS circuitry for use within a liquid environment remains as an open challenge. The purpose of this project is to develop a unique packaging scheme that is suitable for CMOS circuit chip to operate in liquid environment with integrated on-chip biosensor arrays. Parylene is chosen as the packaging material by its excellent biocompatibility and chemical inertness.

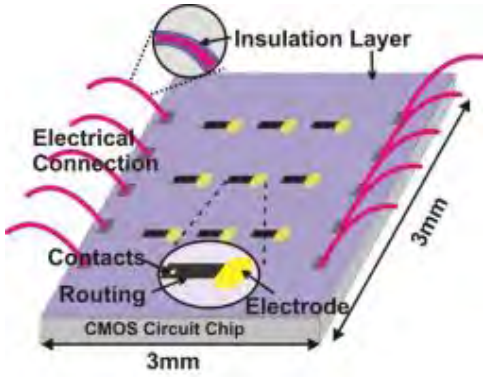

Conceptual illustration of a CMOS circuit chip with on chip electrode array and insulation of chip surface and bonding wires.

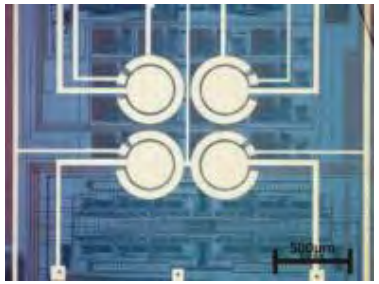

2 ×2 electrode array fabricated on a CMOS chip with working, counter and reference electrodes.

Die photo after packaging of 3 ×3mm2 CMOS potentiostat chip with post-CMOS electrode array.

L. Li and A. Mason, Michigan State University
Work performed at U Michigan Lurie Nanofabrication Facility

Micromachined Transducer Arrays for 3D Imaging

Sonetics Ultrasound, Inc. is developing large-scale MEMS transducer arrays intended for real-time 3D ultrasound imaging. Sonetics' patent-pending technology uses standard integrated circuit fabrication steps to build thousands of micromachined electrostatic membrane transducers on a chip. These transducers produce short pulses of acoustic energy and detect echoes returning from features in tissue. When combined with low-noise front-end circuits and sophisticated signal processing hardware, high-quality 3D medical images can be acquired. Because the arrays are batch fabricated on silicon wafers, they promise to provide significant cost-savings and performance improvements over traditional manually-assembled piezoelectric transducer technology. The transducer array fabrication sequence relies on standard CMOS processes plus specialized metal etching and deposition of thin films such as PECVD dielectrics and parylene.

D. Lemmerhirt and C. Rich Sonetics Ultrasound, Inc.
Work performed at U Michigan Lurie Nanofabrication Facility

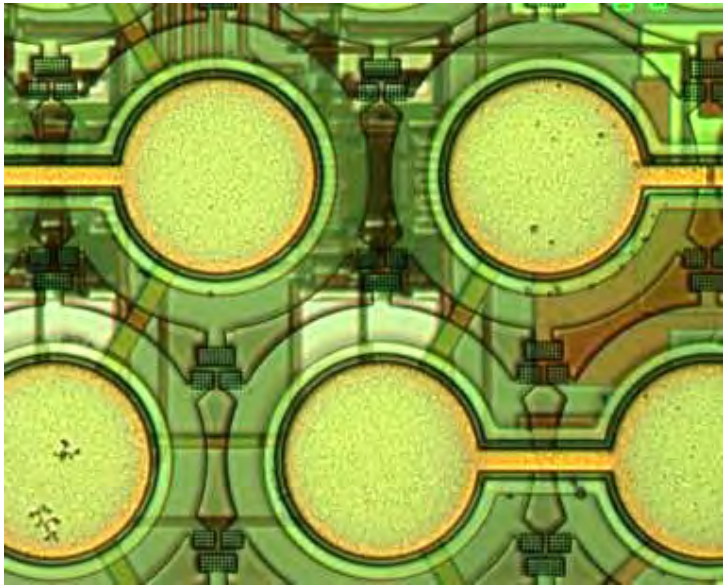

MEMS ultrasound transducer elements with CMOS circuits integrated beneath.

(Left) Handheld imaging probe based on the MEMS ultrasound chip. (Right) MEMS array chip mounted on a flex circuit for probe integration.

NNIN
www.nnin.org
Nanoscale Science Engineering & Technology

LNF
UNIVERSITY OF MICHIGAN

Evigia Systems Sensors

Evigia is currently developing a variety of energy-efficient sensors and sensing systems for integration with radio-frequency identification tags (RFID). Evigia's core technology is on post-CMOS proprietary integration of MEMS/NEMS sensors and circuits and packaging at wafer-level, and ultra low-power circuits and ultra low-power sensors. LNF is essential for Evigia to produce prototypes and to perform R&D activities prior to technology transfer to standard commercial MEMS manufacturing facility for production ramp.

One of the devices fabricated at LNF is an ultra-thin MEMS capacitive pressure sensor with high pressure sensitivity of better than 150aF/Pa, and small die size of 1.0mm × 1.0mm × 60μm, shown here. It is able to detect ambient pressure change with a resolution of 0.025% in a pressure range +/-3.5KPa.

G. Meng, W. Zhu, Y. Zhang, Evigia Systems, Inc.
Work performed at U Michigan Lurie Nanofabrication Facility

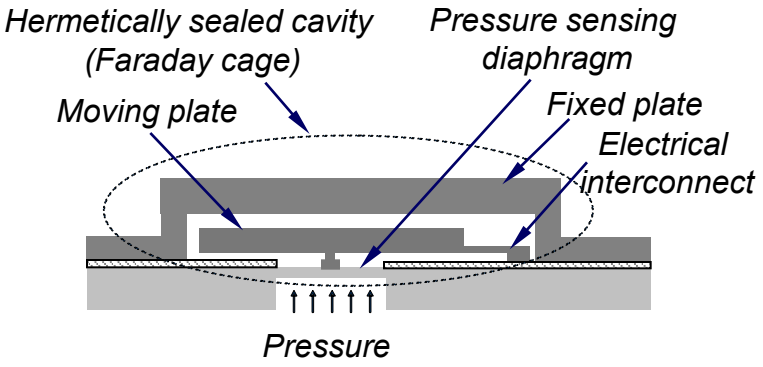

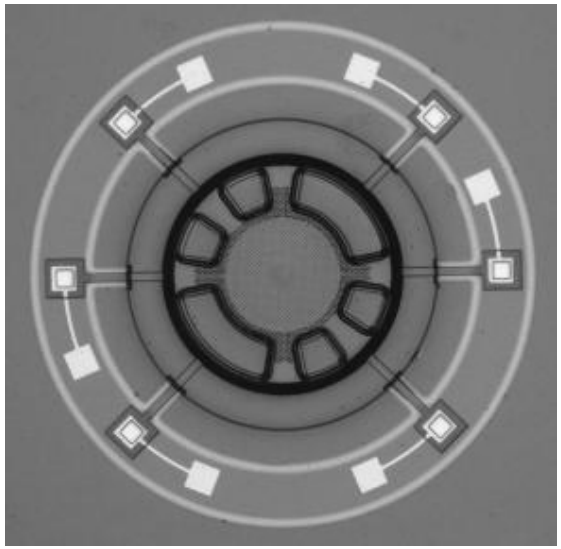

High-Sensitive Ultra-Thin MEMS Capacitive Pressure Sensor

Passive and Remote Magnetic Microsensor with Thin-film Giant Magnetoimpedance Element and Surface Acoustic Wave Transponder

This passive wireless magnetic sensor can be used in many magnetic sensing applications especially for the implanted devices, in harsh environments and on rotating or moving parts.
The Giant Magneto Impedance (GMI) Sensor acts as an impedance load for the Surface Acoustic Wave (SAW) device, which serves as a transponder. When the two-port SAW is wirelessly interrogated, one of its interdigital transducers(IDT) acts as reference reflection compared to the reflection of the IDT with the GMI sensor load.

H. Al Rowais, B. Li, C. Liang, J. Kosel, King Abdullah University of Science and Technology (KAUST) and S. Green, Y. Gianchandani, University of Michigan.

Work performed at U Michigan Lurie Nanofabrication Facility

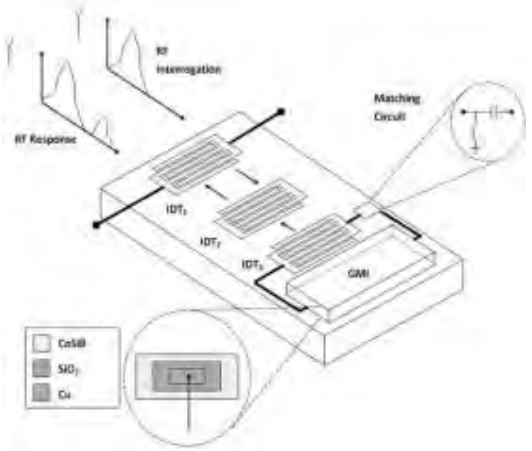

Schematic of the principle of operation of the wireless sensor device.

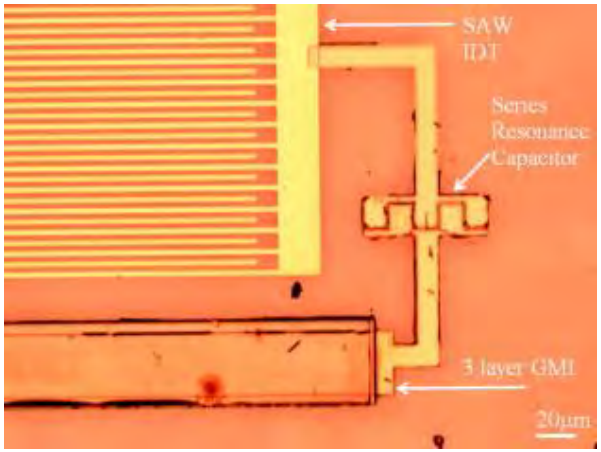

Optical microscopic picture of the IDT of the SAW transponder, the GMI sensor element and the comb capacitor.

IPMC-based Artificial Lateral Line System

This project aims to develop an artificial lateral line system consisting of arrays of IPMC (Ionic Polymer-Metal Composite) cilia, which are micro flow sensors created by micro-fabrication processes. This lateral line system requires IPMC hairs to project out of the substrate to effectively interact with flows, which is challenging to realize with traditional planar MEMS processes. Si wafers serve as substrate for these freestanding IPMC hairs during processing. Another challenge is that it is difficult at micro scale to chemically deposit metal only on two surfaces of a polymer membrane

.

Characterized by intimate interplay between biology and engineering, this interdisciplinary project is expected to develop the fundamental understanding of IPMC material dynamics and their interactions with flow.

H. Lei and X. Tan, Michigan State University

Work partially performed at U Michigan Lurie Nanofabrication Facility

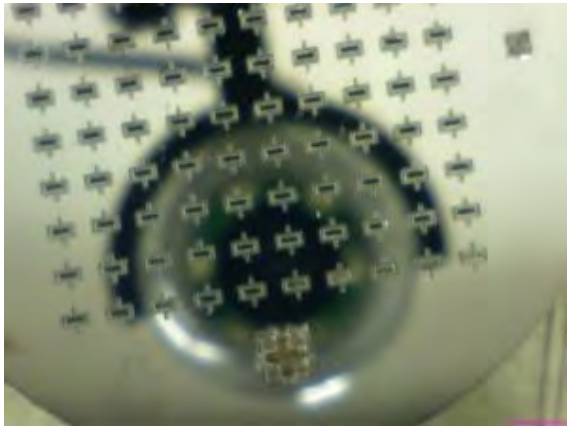

SU-8 patterning on etched through Si wafer

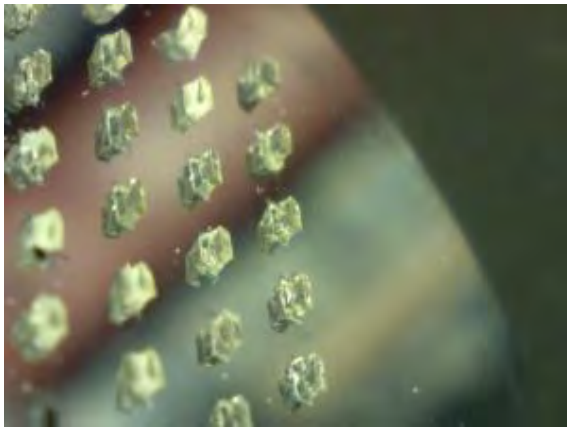

Nafion molding

Localized Surface Plasmon Resonance Sensor Chip

This project is aimed at developing novel Localized Surface Plasmon Resonance (LSPR) sensors. The sensor chips are prepared by Physical Vapor Deposition (PVD) using a thin layer of gold onto pre-treated glass slides. The deposition process is performed at the LNF. After deposition, with proper custom-developed surface modification, this sensor has the potential to serve as a reliable, portable and sensitive biosensor platform.

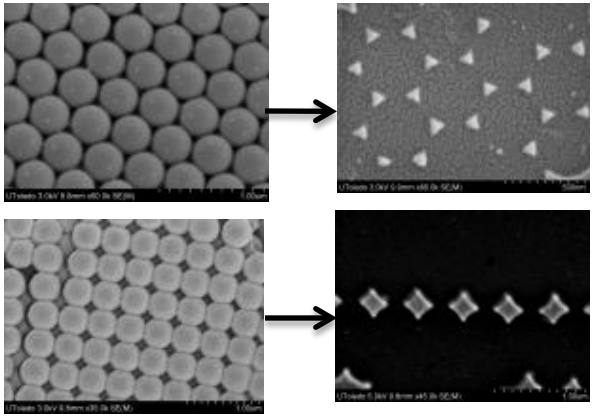

Uniform nano gold array fabricated by PVD gold onto nano-polystyrene beads coated surface. SEM images captured by Hitachi S-4800 in University of Toledo, Center for Materials and Sensor Characterization; nano gold size: 20-30 nm

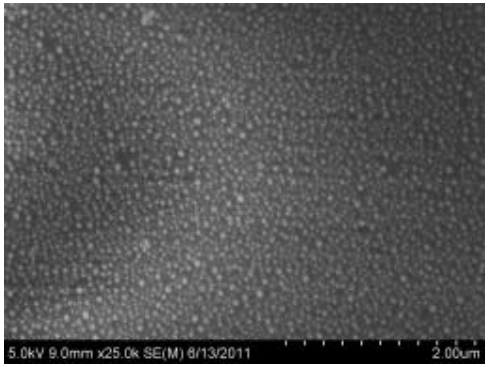

An uniform nano gold coated surface prepared by PVD and heat treatment; nano gold size 30-40 nm

R. Zheng, B. Clarke, N. Reaver and B.D. Cameron, University of Toledo

Work performed at U Michigan Lurie Nanofabrication Facility

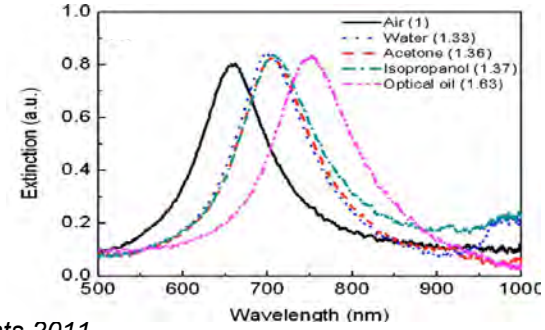

Preliminary sensor response

MEMS Deformable Mirrors for Focus Control Imaging Applications

We are currently exploring the feasibility of a surface micromachining process for deformable membrane mirrors with SU-8 2002 as the membrane material. Our initial process used PSG as a sacrificial layer and involved wet etching for release of the membranes, but delamination and stiction were issues

.

Dry etching of silicon with XeF_2 gas at the Lurie Nanofabrication Facility proved to be a simpler and better fabrication method for these mirrors. They were demonstrated in a 40x 0.4NA microscope for focus control. The mirrors show promise for improving focus control in imaging applications such as endoscopic microscopy and cell phone cameras.

Lukes et al, MOEMS and Miniaturized Systems IX, (2010)
Lukes et al, MOEMS and Miniaturized Systems X, (2011)

Picture by Kelly Gorham

MEMs deformable mirror mounted for easy implementation into focus control imaging applications.

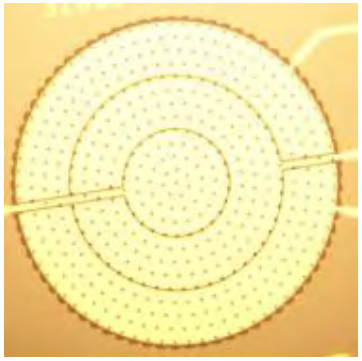

Topside view of a mirror released in XeF_2.

S.J. Lukes and D.L. Dickensheets, Montana State University

Work performed at U Michigan Lurie Nanofabrication Facility

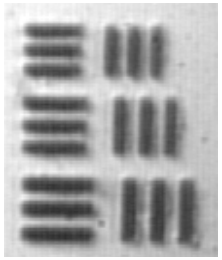

228 lp/mm USAF target resolved at a focal shift of 137 μm induced by electrostatic actuation of the mirror.

Optical Antenna Project

The purpose of the optical patch antenna project is to confine light at nano scale with probable application in single molecule studies. We have used the latest nano fabrication techniques to make these patch antennas on a silicon substrate.

Advanced deposition techniques like Atomic Layer Deposition allow us to precisely vary the dielectric gap thickness together with a robust control on the other experimental conditions and with experience. Periodic cylindrical metallic patches are patterned using electron beam lithography on the dielectric layer of Alumina. Several diameters of the metallic patches were fabricated to understand the effect of size on the efficiency of the metallic patches to trap light in the nano cavity formed in the dielectric layer between the patches and the underlying base metal layer.

A. Chakrabarty, F. Wang, B. Joshi, Q.H. Wei, Kent State University

Work performed at U Michigan Lurie Nanofabrication Facility

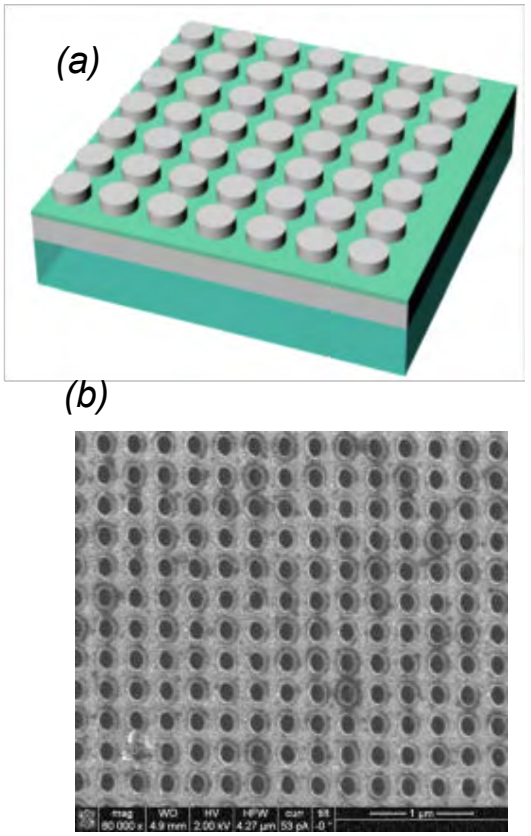

(a) Schematics of the proposed optical patch antenna. (b) Scanning electron micrograph of the top view of the fabricated patch antenna.

Understanding the Lubricant Degradation Cycle at the Nanoscale

This project aims to use atomistic computer simulations to better understand lubricant breakdown at the nanoscale. Quantum and classical algorithms will be combined to characterize/predict the reactivity of chemical species resulting from oil degradation processes (thermal cracking, oxidation, etc) and how their presence affects the oil's performance properties, i.e viscosity, thermal conductivity, etc.
The simulation results bring many commercial opportunities for designing MEMS devices capable of detecting/tracking oil breakdown.

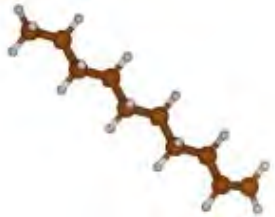

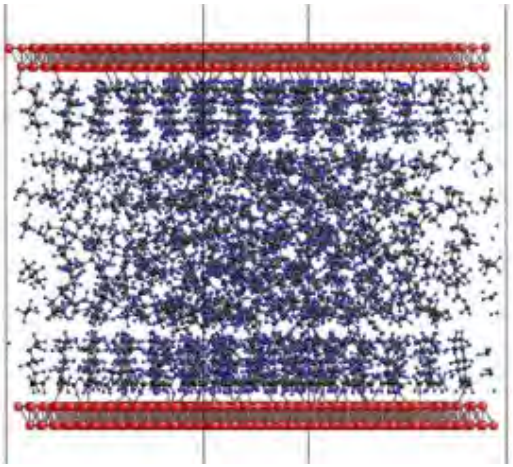

A model of oil-metal interactions at surfaces

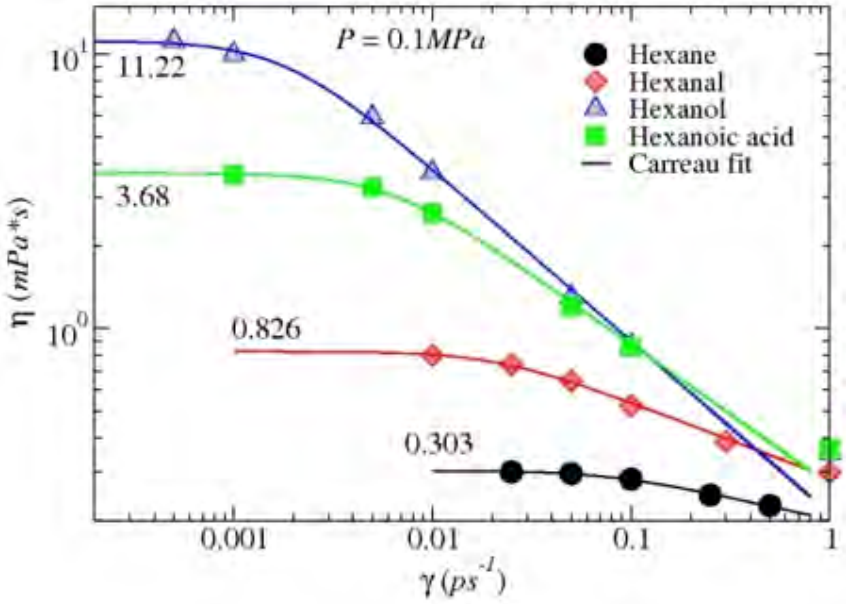

C. Campana and R. Miller, Carleton University, GASTOPS

Work performed at NNIN/C@Michigan

NNIN
www.nnin.org
Nanoscale Science Engineering & Technology
UNIVERSITY OF MICHIGAN

MEMS Capacitive Accelerometer

The purpose of the MEMS Capacitive Accelerometer project is to fabricate motion sensors capable of sensing roll, tilt, free fall, and accelerations in the x-, y-, and z-directions. This device will be fabricated using a Silicon On Glass (SOG) process developed at the University of Michigan LNF. The springs of each individual device allow the proof mass to deflect during acceleration events thus changing the capacitance values between sensing fins. The sensing fins will detect accelerations in the x- and y- directions while the z- direction will be sensed with the bottom electrode. Based on numerical simulations done at NNIN/C with Comsol Multiphysics, this device will be capable of sensing accelerations up to +/- 5 g and will have a capacitance range on the order of femtofarads.

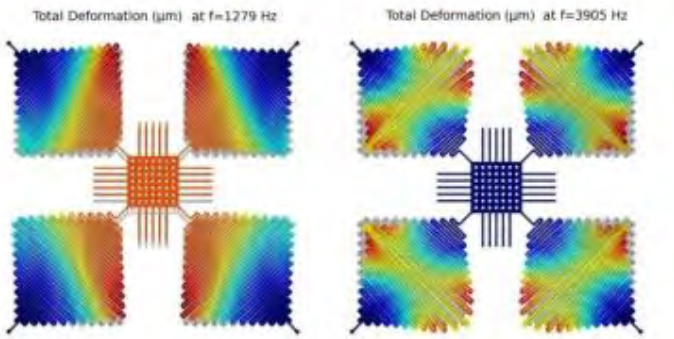

Total deformation of the proof-mass and serpentine springs at two different fundamental frequencies.

Top: Images of the completed 1.5 mm x 1.5 mm capacitive accelerometers.
Left: Finished wafer after the fabrication.

K. Petsch and T. Kaya, Central Michigan University

Work performed at U Michigan Lurie Nanofabrication Facility and NNIN/C@Michigan

ePack: Wafer-Level Packaging

ePack's expertise is hermetic and vacuum encapsulation of MEMS devices and protection against vibration and temperature fluctuation in the environment. ePack has served military, automotive, and industry customers since 2008.

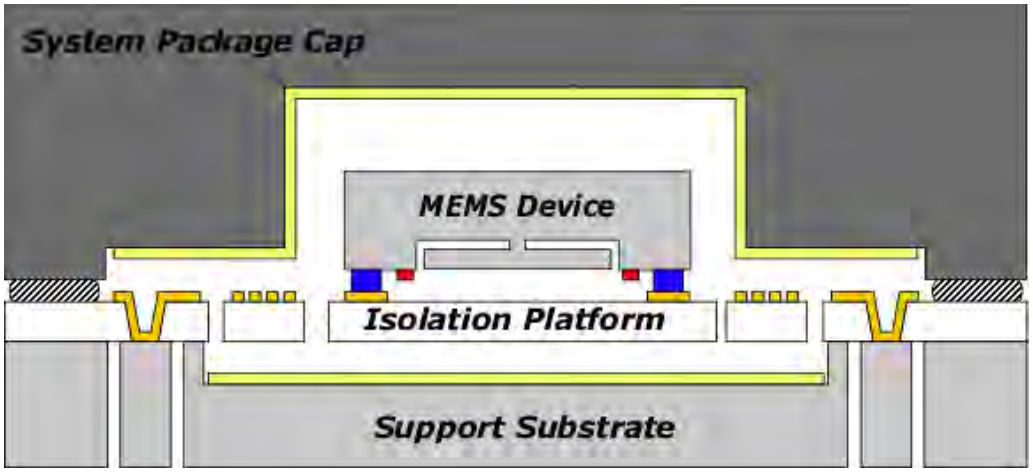

Environmental Resistant package (ERP) – for temperature, vibration and shock protection

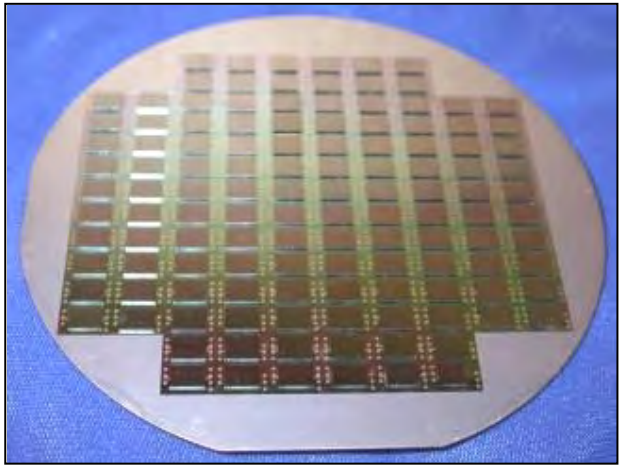

Standard MEMS Packages – for vacuum/ hermetic encapsulation

ePack, Inc
Work performed at U Michigan Lurie Nanofabrication Facility

NNIN Site at UCSB

Magnetoconductance Oscillations and Evidence for Fractional Quantum Hall States in Suspended Bilayer and Trilayer Graphene

"We report pronounced magnetoconductance oscillations observed on suspended bilayer and trilayer graphene devices with mobilities up to 270,000 cm^2/(V-s). For bilayer devices, we observe conductance minima at all integer filling factors between 0 and 8, as well as a small plateau at ν=1/3. For trilayer devices, we observe features at ν= 1, 2, 3, and 4, and at ν~0:5 that persist to 4.5 K at B = 8 T. All of these features persist for all accessible values of V_g and B, and could suggest the onset of symmetry breaking of the first few Landau levels and fractional quantum Hall states"

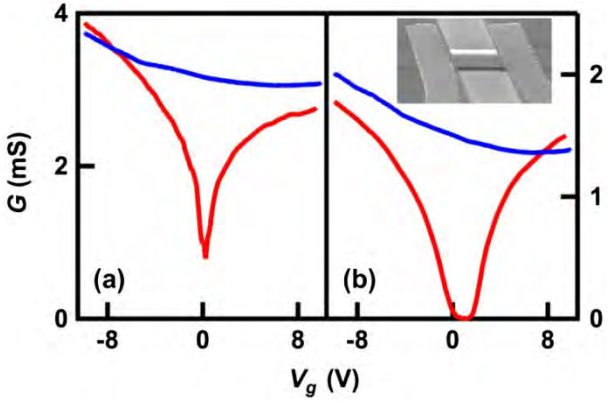

G(Vg) for (a) BLG and (b) TLG devices at T = 4:2 K. Upper and lower curves are taken before and after current annealing, respectively. Inset: SEM image of a suspended graphene device

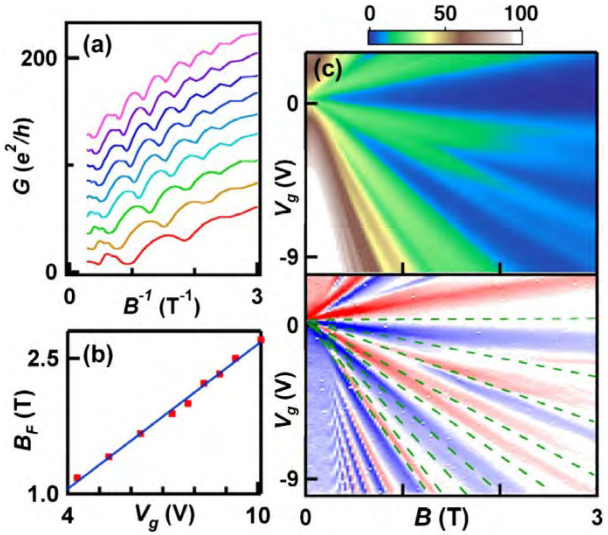

Data from a bilayer device BL1 at 300 mK. (a) G vs 1/B at V_g = 3, 4, 5, 6,7, 7.5, 8, 8.5, 9, and 9.8 V (bottom to top). The traces are offset for clarity. (b) B_F(Vg) and a linear fit to the data points. (c) G(Vg) at B = 3, 2, and 1.5 T (bottom to top). The traces are offset for clarity. The numbers indicate the |v| values that correspond to the local conductance minima.

Wenzhong Bao, et. al. , UC Riverside.
Work partially performed at UCSB

*Wenzhong Bao, et. al, PRL **105**, 246601 (2010)*

Supported by NSF and ONR

Anomalous Current-Voltage Characteristics in Suspended Carbon Nanotubes and Phonon Relaxation Dynamics

Description:
Suspended carbon nanotube field effect transistors show a sudden drop in current "kink" in the *I-V* characteristics when measured in gaseous environments. This kink does not appear in vacuum and changes in character and severity with the applied gate voltage.

Result:
The kink is found to be the threshold of the optical phonon emission which can only be observed in defect free suspended carbon nanotubes with non-equilibrium phonon population.

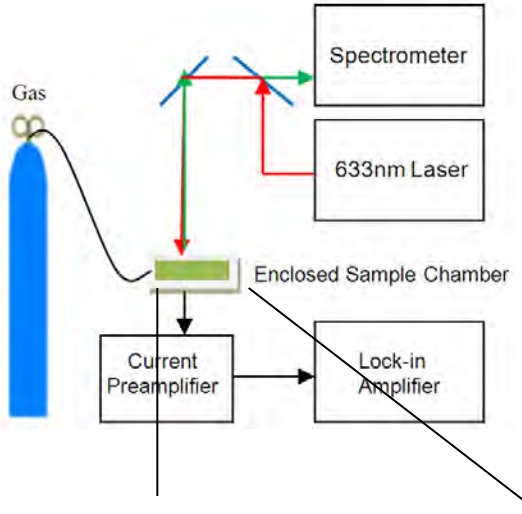

M. Amer, A. Bushmaker, S. Cronin,
Physics Dept. USC.
Work partially performed at UCSB

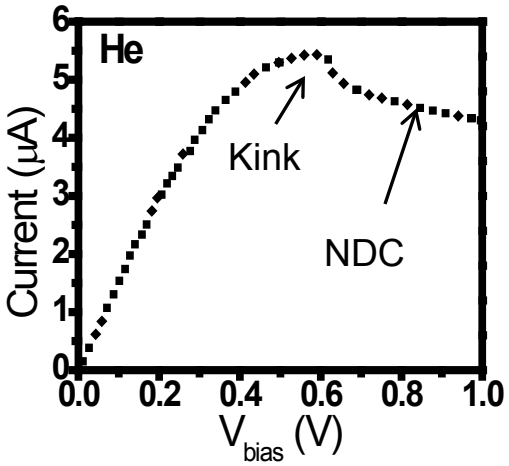

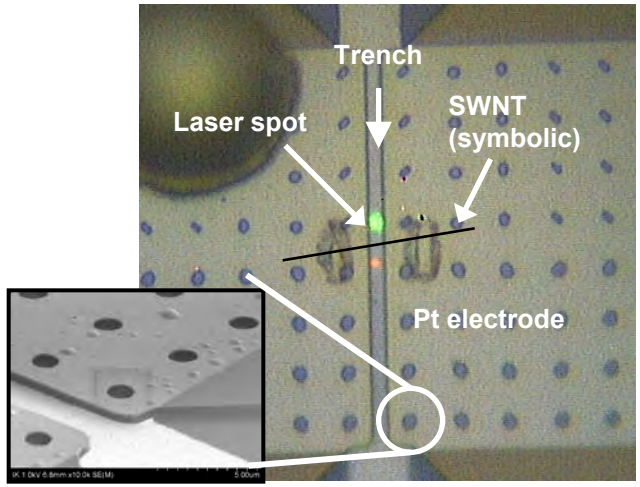

Funding Agencies:
ONR Award No. N000141010511
NSF award No. CBET-0854118
DOE Award No. DE-FG02-07ER46376

M.Amer, A, Bushmaker, S, Cronin, "Anomalous Current-Voltage Characteristics in Suspended Carbon Nanotubes and Phonon Relaxation Dynamics", *APS March meeting*, 2011.

Compact Chip-Scale Filter Based on Curved Waveguide Bragg Gratings

In this work, we demonstrated straight and curved filters based on waveguide Bragg gratings. Both filters had a total length of 920 μm, a stop band of 1.7 nm, and an extinction ratio larger than 23 dB. The curved structure occupied an area of 190 μm ×114 μm, attaining packing efficiency of $L/A^{1/2} \approx 6:2$. Nevertheless, it exhibited the same performance as its straight counterpart. The proposed approach opens a route to avoid the stitching errors present in the typical lithographic process of long structures. The developed analytical model aims to assist in the design of such structures in the future.

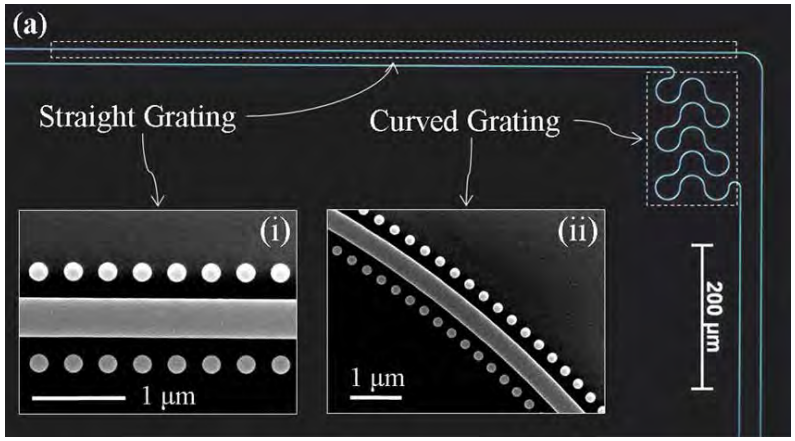

Dark-field micrograph of the fabricated structures: the marking shows the curved and the straight gratings of the same length. Insets (i) and (ii) show SEM micrographs of the straight and the curved gratings, respectively

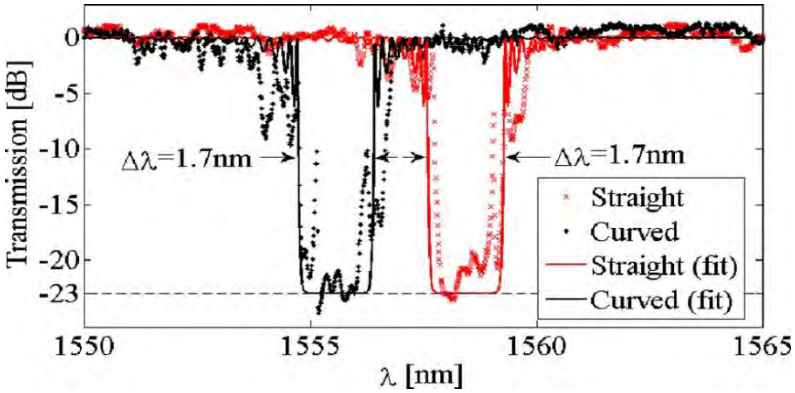

Measured transmission spectra for straight (red crosses) and curved (black dots) gratings

S. Zamek, et. al.
ECE Dept., UC San Diego

Work partially performed at UCSB

S. Zamek, et. al., "Compact chip-scale filter based on curved waveguide Bragg gratings" Optics Letters 35(20), 3477-3479 (2010)

DARPA, NSF, USAFOSR, USARO

Highest Electricity Conversion Efficiency Achieved by GaN FET & Diode

- *Most electricity is regulated before use.*
- *Efficiency is key in energy saving.*
- *GaN FET & diode by Transphorm Inc. achieve >99% efficiency in a 1:2 boost converter.*
- *GaN power devices reduce energy loss in Si devices by 45%.*
- *GaN solution drastically simplifies converter circuits: No gate resistor, no snuber, no insulating shim*

Work by Transphorm Inc., Goleta, California
Part of earlier power device development performed at UCSB NNIN Facility

A Total GaN Converter to boost voltage from 220V to 400V

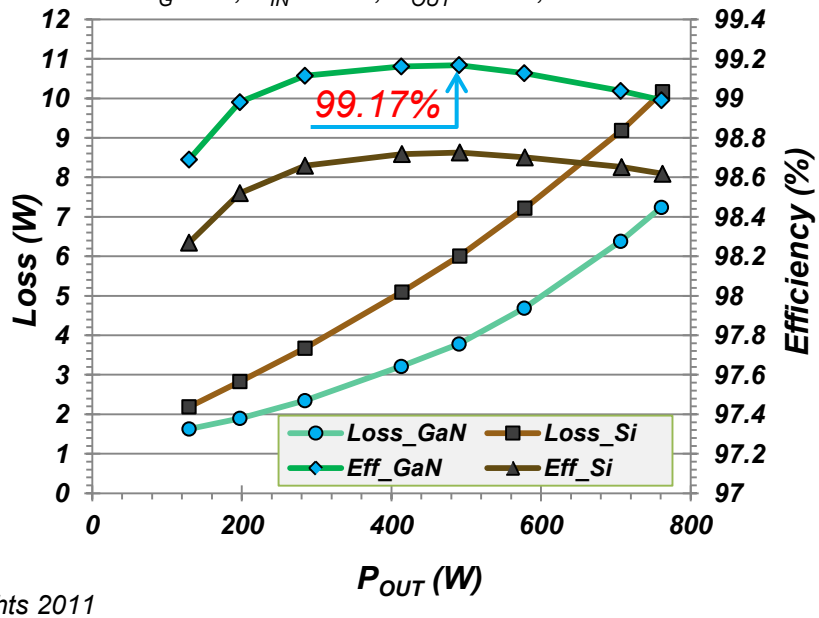

Infrared Imaging Sensors

QmagiQ develops infrared sensors based on quantum wells and superlattices made from compound semiconductors. Part of the process development is carried out at the UCSB node of the NNIN. Shown below is a 1Kx1K (million) pixel chip that produces longwave infrared imagery using InAs/GaSb superlattice photodiodes. With their high quantum efficiency and relative low cost, these sensors hold the promise of revolutionizing infrared imaging. Funded by the Missile Defense Agency, the chip was partly developed at UCSB. Cameras containing such chips find uses in security and surveillance, missile defense, pollution detection and monitoring, and infrared astronomy.

R&D ***Products***

1Kx1K SLS
IR focal plane array

Image from chip

Chip on puck

Sensor Engine

Camera

QmagiQ
Work performed at UCSB and Harvard in 2011

Quantum Cascade Lasers: High-Power Emission and Single-Mode Operation in the Long-Wave Infrared (λ>6 μm)

We present an overview of our recent results on the growth, fabrication, and characterization of high-power long-wave infrared quantum cascade lasers with multimode and single-mode waveguides. Powers of up to 1.2W at wavelengths of λ = 6.1 μm are obtained with InGaAs/InAlAs buried heterostructure lasers grown lattice matched on InP substrates. For longer wavelengths, up to λ = 9 μm, powers of P = 800 mW are delivered from room-temperature-operated devices. Distributed-feedback waveguides have been fabricated with buried grating geometry, leading to single-mode emission of more than P = 150 mW output at λ = 7.74 μm when the device is operated at room temperature in continuous mode

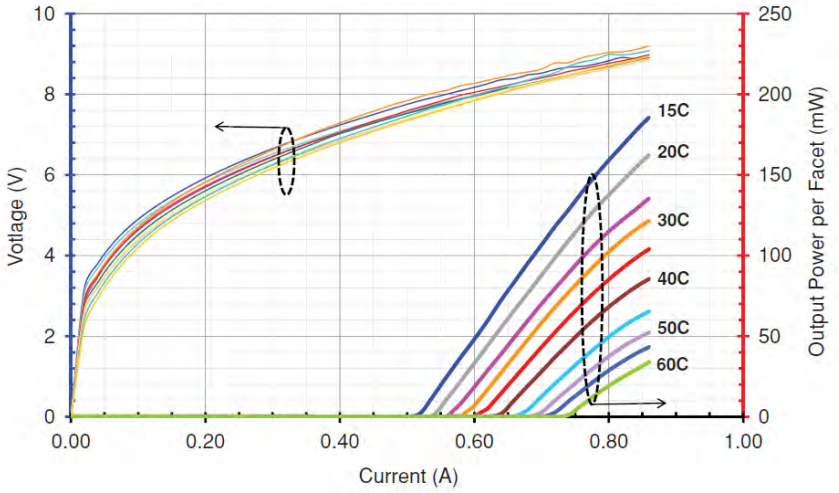

Voltage-current and optical power-current characteristics of QCL-C devices processed as DFB waveguides. The emission in this case is single-mode centered at λ = 7.74 μm. Side-mode supression is 30dB as shown below for low currents (black) and high current (red).

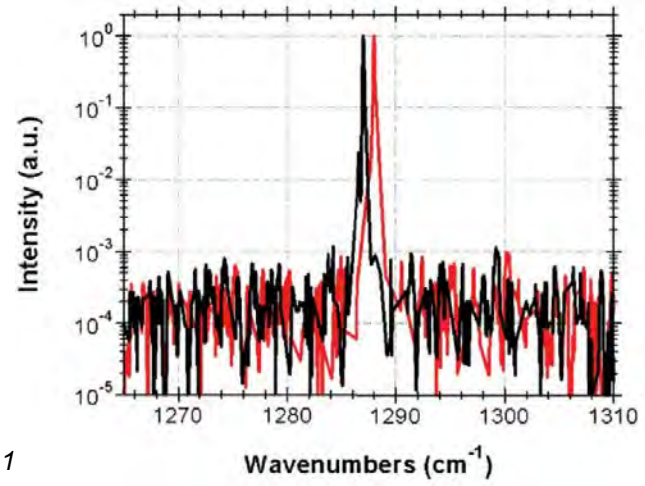

M. Troccoli, et. al.
AdTech Optics, Inc.
Work partially performed at UCSB Facility

M. Troccoli, X. Wang, and J. Fan, "Quantum cascade lasers: high-power emission and single-mode operation in the long-wave infrared (λ>6 μm)", Opt. Eng. ***49****, 111106*

Metal-Oxide Thin Film Transistor with High Performance and Good Operation Stability

Non-InGaZnO based metal-oxide TFT is developed with high performance and good stability. Manufacturability was demonstrated with a high capacity, Gen-2.5 size, color-filter production line. Superb TFT performance was achieved with □>80 cm2/Vsec, Ion/Ioff >1010 and S<0.2 V/dec. This TFT shows high stability under OLED and LCD operation conditions. A 4.8" bottom emission AMOLED is demonstrated with aperture ratio larger than 50%. Power efficiency >6 lm/Watt at >500 nits was achieved with high display uniformity. The average power efficiency under video operation is beyond 20 lm/Watt

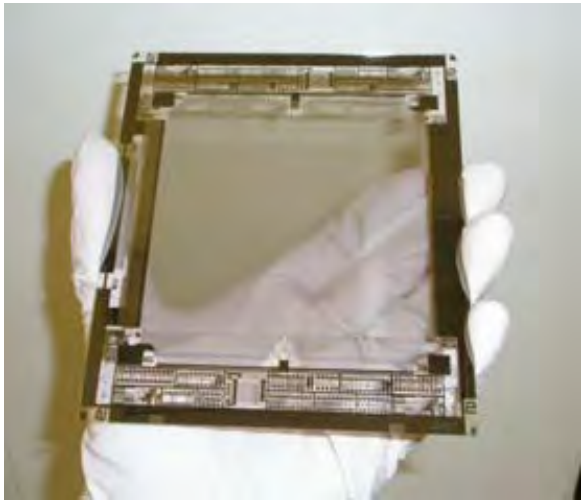

a 4.8" FC AMOLED backpanel on 5"x5" glass (top-right). >50% aperture ratio is well seen from the high transmission of the 4.8" panel.

G. Yu, et. al.
CBrite, Inc., Goleta CA
Work partially performed at UCSB Facility

A photo of the 4.8" AMOLED with a white OLED emitter

Display Size	4.8" diagonal
Display Format	FC QVGA: 320x3x240
Total Pixel Count	230.4K
Pitch Size (sub-pixel)	300 µm x 100 µm
Active Area	96 mm x 72 mm
Architecture	Bottom emission
Aperture Ratio	>50 %
Frame Rate	60, 120, 240 Hz
Sub-pixel current	>3µA @ Vds<3V
Vds(T2)@Ipixel=3 µA	<3V
Peak Brightness	>600 nits
Power efficiency	6 lm/W (~ 20 lm/W Movie)
Homogeneity	>89% (5 and 9 point tests)

Gang Yu, et al., SID Digest, 35(4), 483-485, (2011)

High-Speed SiGe Microcoolers for Study of Ultrafast Peltier Effects

In this work, we have developed integrated microcoolers with SiGe superlattice as the active medium for study of ultrafast Peltier effects at the thermoelectric interface. The metallization was laid out as transmission lines (coplanar waveguides: GND-SIG-GND) to enable high-speed operation. We performed dynamic thermal characterizations with a variety of thermoreflectance imaging techniques

We see from the measurements that Peltier cooling is quicker than Joule heating (as expected from associated thermal mass). A net cooling of 1 to 2 degrees observed with response times down to 100ns

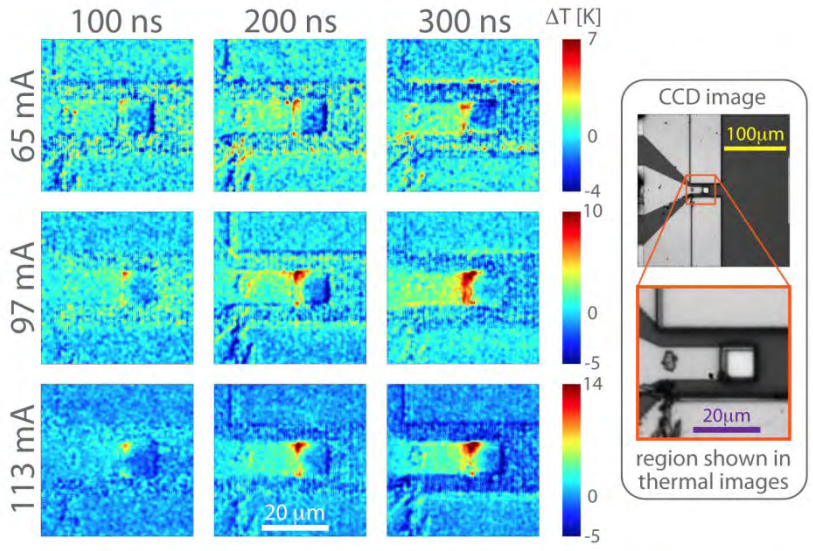

Exemplary thermoreflectance images of 10x10µm² sample. Active cooling is clearly visible; hot spots at electrode neck suggest insufficient metalisation of superlattice side wall.

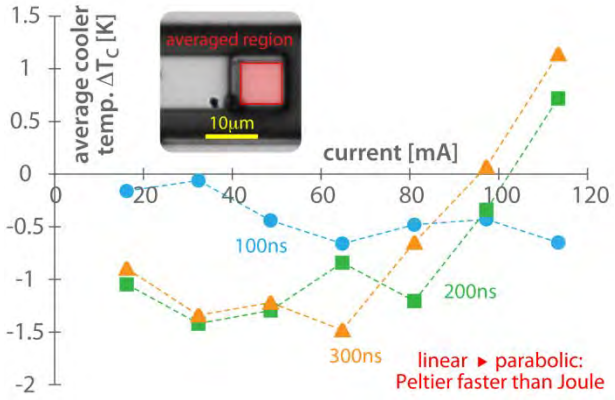

Average temperature of the active cooler area

Bjorn Vermeersch, Je-Hyeong Bahk, Ali Shakouri
UC Santa Cruz

Work partially performed at UCSB Facility

B. Vermeersch, J-H. Bahk, J. Christofferson, A. Shakouri, Proceedings of the MRS Spring Meeting - Symposium I, San Francisco CA, April 2011.

Funded by AFOSR

Parametric Amplification and Self-Oscillation in a Nanotube Mechanical Resonator

"A hallmark of mechanical resonators made from a single nanotube is that the resonance frequency can be widely tuned. Here, we take advantage of this property to realize parametric amplification and self-oscillation. The gain of the parametric amplification can be as high as 18.2 dB and tends to saturate at high parametric pumping due to nonlinear damping. These measurements allow us to determine the coefficient of the linear damping force. The corresponding damping rate is lower than the one obtained from the line shape of the resonance (without pumping), supporting the recently reported scenario that describes damping in nanotube resonators by a nonlinear force. The possibility to combine nanotube resonant mechanics and parametric amplification holds promise for future ultralow force sensing experiments."

A. Eichler, J. Chaste, J. Moser, and A. Bachtold
Catalan Institute of Nanotechnology (ICN) and CIN2, Campus UAB, Barcelona, Spain
Work partially performed at UCSB Facility

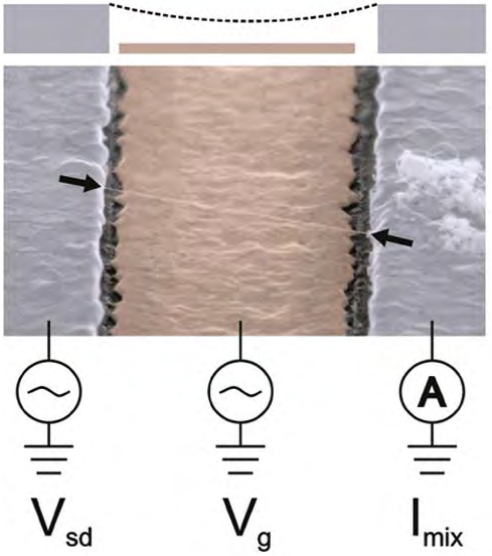

Schematic diagram and false-color scanning electron microscopy (SEM) image of the device. The nanotube (arrows, dashed line in the SEM image) is suspended over a gate electrode (red) between two metal electrodes (gray). The distance between the electrodes is 1 μm. All measurements are performed in an ultrahigh vacuum chamber (about 10^{-10}mbar) at 100 K

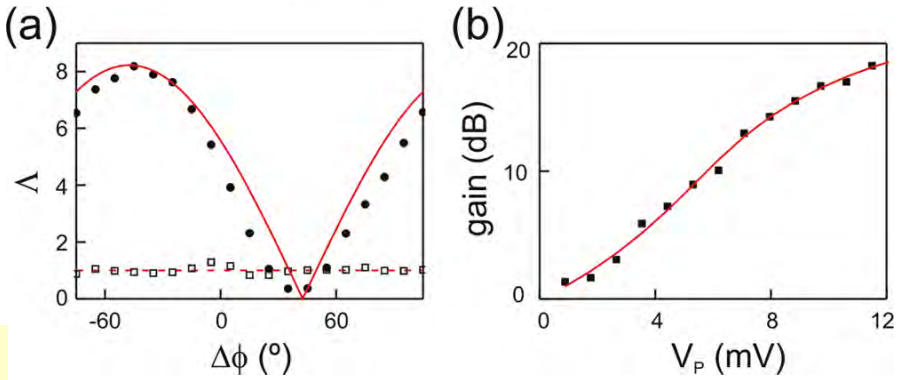

(a) Amplification (Λ) as a function of the phase difference, Δφ, between the driving force and the pump for V_P = 11.5 mV(solid dots) and V_P = 0 (hollow squares). Vg_{AC} = 3 mV and Vsd_{AC} = 1.4mV. Red lines are best fits. (b) Gain as a function of the amplitude of V_P for Δφ at which the amplification is largest. We estimate the motion amplitude to be ~10 nm at the largest gain.

A. Eichler, et. al., Nano Letters 11, 2699 (2011)

Heterogeneous Photonic Integrated Circuits

Aurrion is commercializing a semiconductor integration platform that enables all the elements of photonics systems to be fabricated on a single chip using control and cost-structure of silicon foundries. This technology is disruptive to the current photonics industry, therefore, in both its ability to change the economics of photonics manufacturing and its ability to push photonic integration on a growth curve similar to Moore's law. Aurrion believes that such integration will be critical to the next generations of military systems and communication systems.

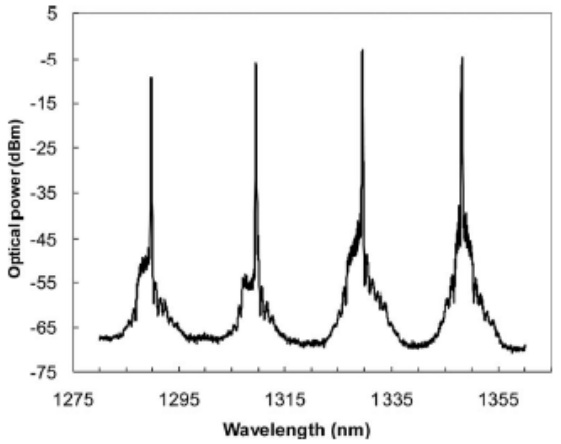

CWDM Laser Spectrum of 50 Gb/s Hybrid Silicon Photonic Transmitter.

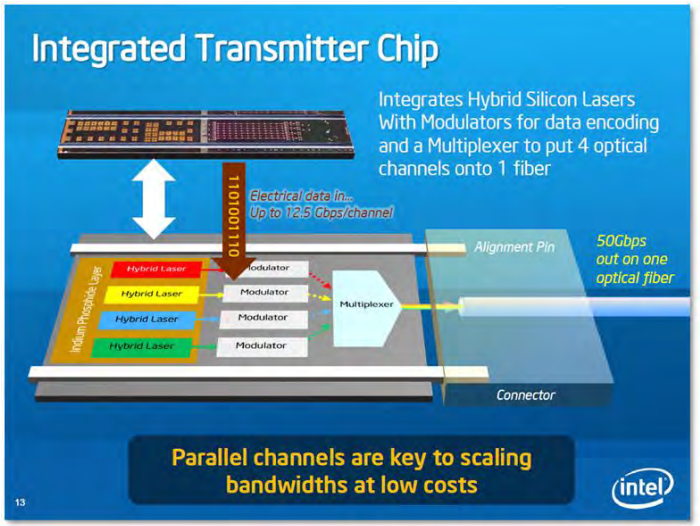

50 Gb/s Hybrid Silicon Photonic Transmitter

Aurrion Inc. - Work performed at UCSB Facility

Aurrion work published in:
IEEE Journal of Selected Topics in Quantum Electronics, 17(3), 671-688, (2011).

Monolithic Nonlinear Pulse Compressor on a Silicon Chip

Optical pulse compression is important for applications auch as ultrafast optical time division multiplexing, optical coherence tomography and time resolved spectroscopy. In this work, pulse compression is achieved at low input peak powers in silicon waveguides through Re-phasing with an anomalously dispersive grating formed by precision electron beam lithography and etching. Dispersion is measured to be 1.3ps/nm resulting in a compression factor of 7 at a low input peak power of 10W.

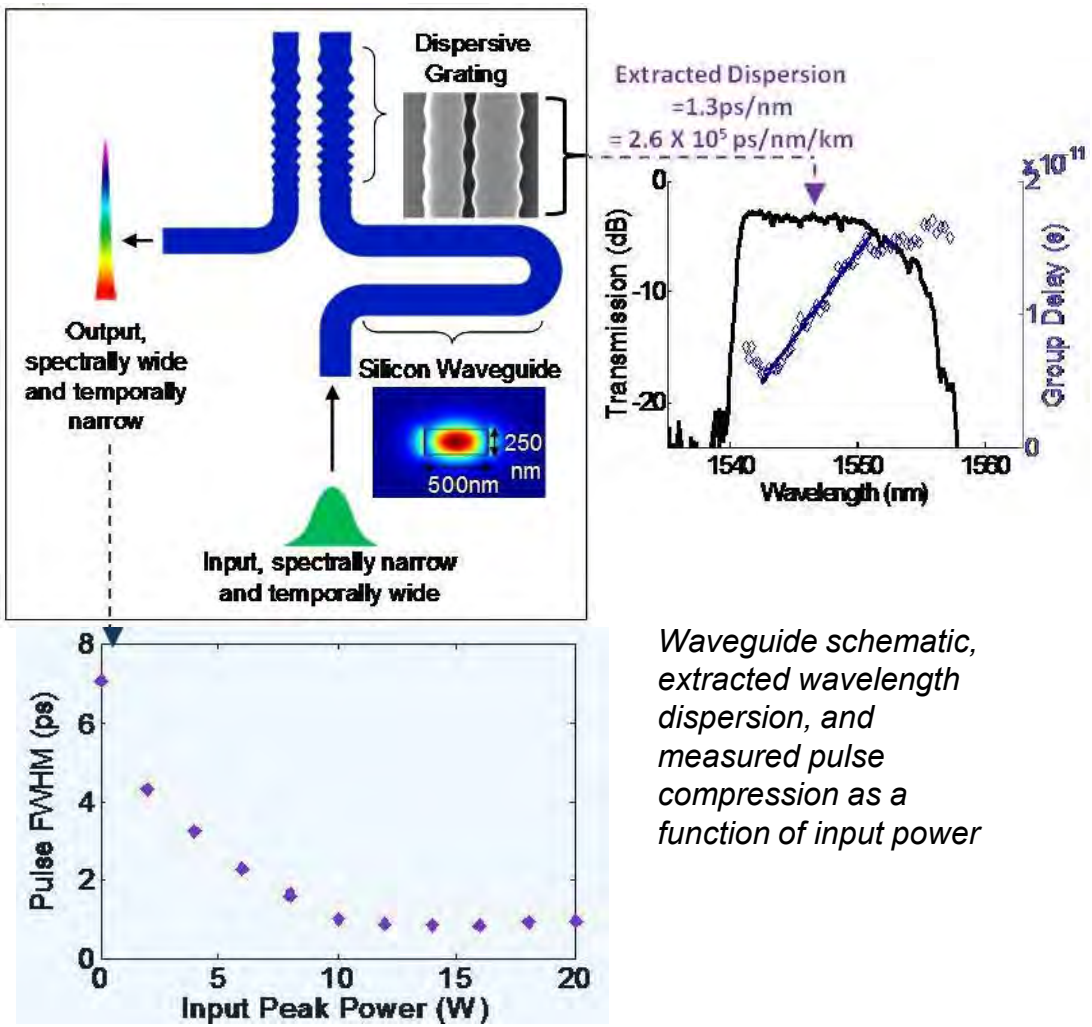

Waveguide schematic, extracted wavelength dispersion, and measured pulse compression as a function of input power

D. Tan, et. al. Fainman Group, UC San Diego
E-Beam Lithography performed at UCSB Facility

D. Tan, et. al. Nature Comunications, 1, 116

CMOS Biosensor system

The portable and sensitive molecular diagnosis platform with large dynamic range is the ultimate goal of a lot of research. This kind of system can enable point-of-care diagnosis and self diagnosis.

We designed a magnetic particle labeled immunoassay system for portable molecule diagnosis. This system uses magnetic particles to label the target molecule and detecting the magnetic particle magnetic field with magnetic sensors.

We used CMOS technology to design the magnetic sensor. Because CMOS technology can integrate large amount of sensors array and read our circuits on the same chip. So the whole system can be made portable and low cost. We also integrate CMOS technology and Microfluidic technology .

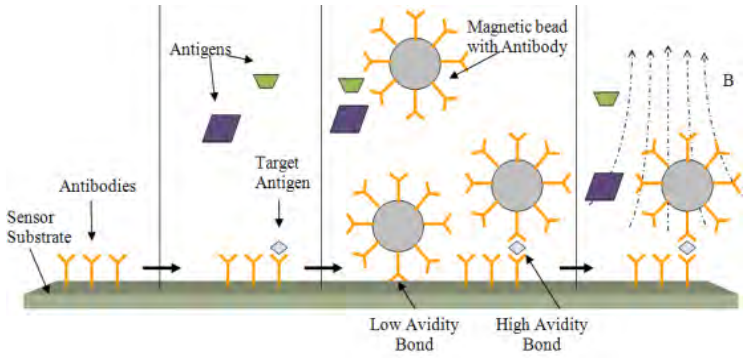

Magnetic Immunoassay procedure

CMOS Magnetic Sensor

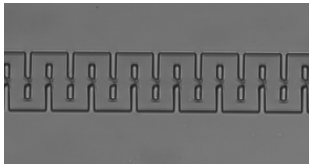
Microfluidic Channel

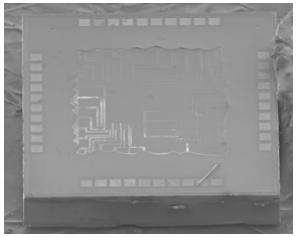
CMOS SENSOR Chip

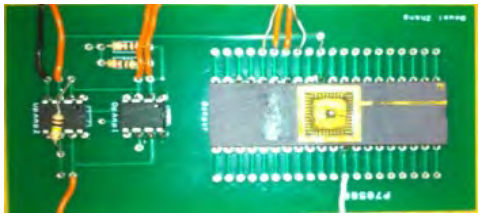
Test board of the CMOS biosensor

Prof. Mona Zaghloul and Bowei Zhang, Institute of VLSI&MEMS Technology, The George Washington University.
Part of work done at UCSB facility.

InP DHBTs in a Refractory Emitter Process for THz Electronics

This work focuses on high frequency InP Double Heterojunction Bipolar Transistor (DHBT) development for use in 0.3-1.0THz imaging, sensing, radio astronomy, and spectroscopy and 100-500 GHz digital logic. *We have made a*dvances in epitaxial design and processing of emitter and base contacts to allow proper device scaling for multi-THz operation. The recent generation of devices using sub-200nm wide emitters and self-aligned base contacts has yielded 480 GHz f_t and 1.0 THz f_{max} HBT transistors.

V. Jain, et. al., Rodwell Group, UCSB
Work partially performed at UCSB Facility

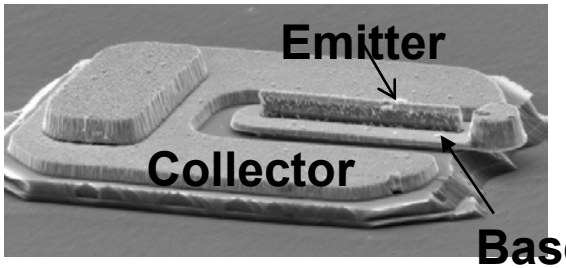

SEM of the completed DHBT before BCB passivation

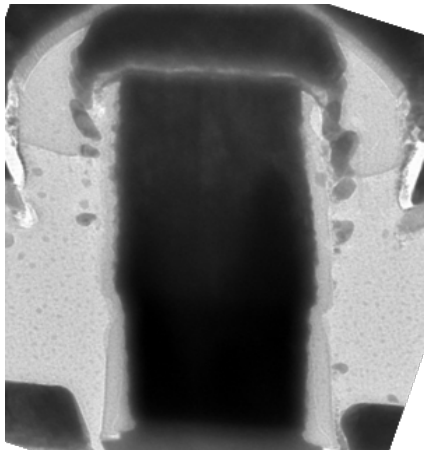

Cross-sectional TEM of the emitter

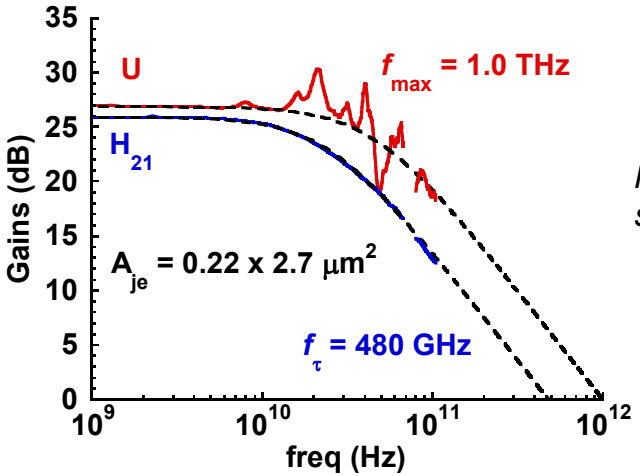

RF gains for the DHBT showing 1 THz f_{max}

Vibhor Jain *et al*., "1.0 THz *f*max InP DHBTs in a refractory emitter and self-aligned base process for reduced base access resistance", *DRC,* 2011
NNIN Research Highlights 2011

Funding: DARPA THETA

Fast Tunable Coupler for Superconducting Qubits

A major challenge in the field of quantum computing is the construction of scalable qubit coupling architectures. Here, we demonstrate a novel tunable coupling circuit that allows superconducting qubits to be coupled over long distances.We show that the interqubit coupling strength can be arbitrarily tuned over nanosecond time scales within a sequence that mimics actual use in an algorithm. The coupler has a measured on/off ratio of 1000. The design is self-contained and physically separate from the qubits, allowing the coupler to be used as a module to connect a variety of elements such as qubits, resonators, amplifiers, and readout circuitry over distances much larger than nearest-neighbor. Such design flexibility is likely to be useful for a scalable quantum computer.

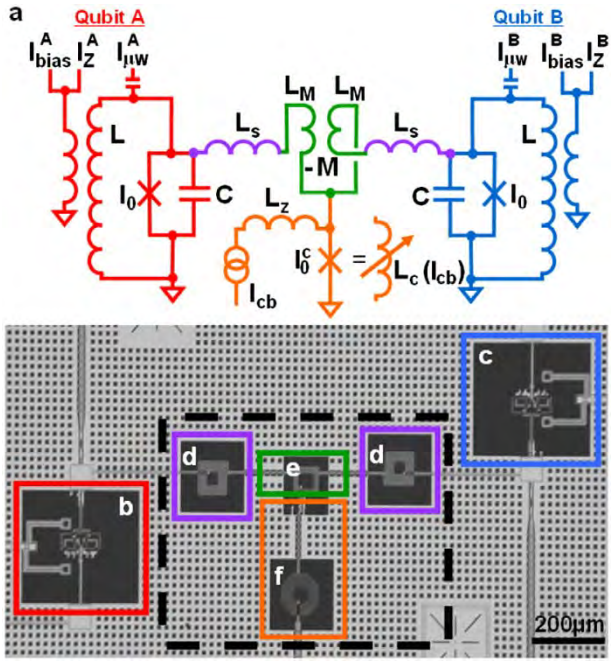

Device circuit and micrograph of two Josephson phase qubits with a tunable coupler. The two qubits are shown in red and blue in the circuit, and boxes b and c in the lower micrograph

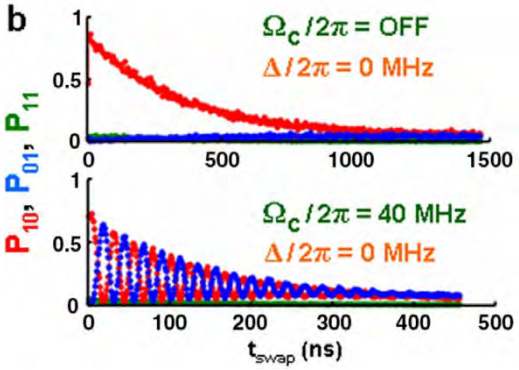

The measured two-qubit probabilities P01, P10, and P11 are plotted versus tswap for qubits on resonance $\Delta/2\pi = 0$ and two sets of coupling $\Omega c/2\pi$, corresponding to off (top) and on (bottom) conditions

R. C. Bialczak, et. al., Martinis and Cleland Groups, Physics Dept., UCSB

Work partially performed at UCSB Facility

R.C. Bialczak, et al., Phys. Rev. Lett. ***106****, 060501 (2011)*

The Mesa Merging Oxidation Method for Creating Low-Loss Dielectrics and Transmission Lines on Low-Resistivity Silicon

A mesa merging oxidation method has been developed to create large low-loss SiO_2 dielectrics on low-resistivity silicon. In the mesa merging method, thermal oxidation converts an array of silicon mesas into a solid block of SiO_2. The SiO_2 dielectrics are combined with further micromachining steps to create high aspect ratio coplanar waveguide (hicoplanar) transmission lines. The large SiO_2 dielectrics enable high-impedance and low-loss hicoplanar transmission lines to be created with this method. Hicoplanar transmission lines with high impedance of 80 Ohms and loss less than 1 dBcm^{-1} up to 67 GHz have been successfully fabricated

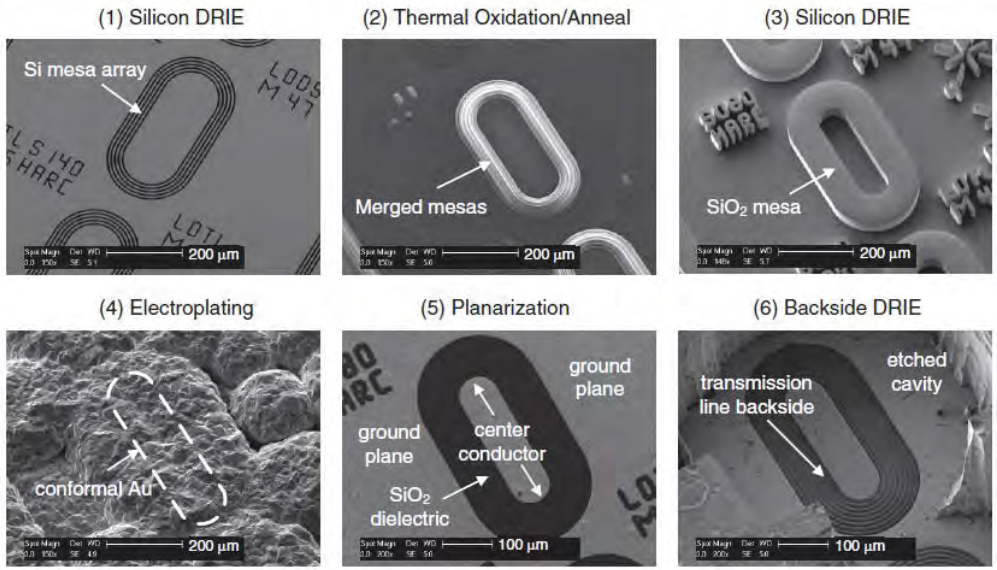

SEM micrographs of a hicoplanar thru line showing critical steps in the fabrication process

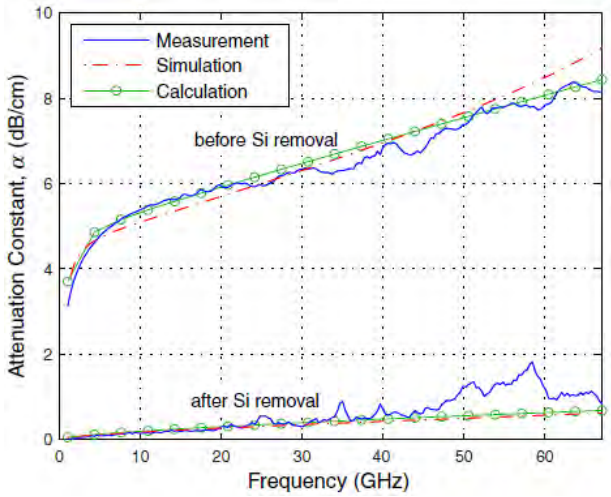

Attenuation constant versus frequency of a 1600 µm long mesa merged hicoplanar line before and after silicon removal

S. Todd, N. MacDonald, J. Bowers, UCSB
Work partially performed at UCSB Facility

S. T. Todd, et. al., J. Micromech. Microeng., 21, 1-10 (2011).

Genetic Analysis of H1N1 Influenza Virus from Throat Swab Samples in a Microfluidic System for Point-of-Care Diagnostics

Microfluidics technology offers compelling tools for integrating multiple biochemical processes in a single device, but despite significant progress, only limited examples have shown specific, genetic analysis of clinical samples within the context of a fully integrated, portable platform. Herein we present the Magnetic Integrated Microfluidic Electrochemical Detector (MIMED) that integrates sample preparation and electrochemical sensors in a monolithic disposable device to detect RNA-based virus directly from throat swab samples. By combining immunomagnetic target capture, concentration, and purification, reverse-transcriptase polymerase chain reaction (RT-PCR) and single-stranded DNA (ssDNA) generation in the sample preparation chamber, as well as sequence-specific electrochemical DNA detection in the electrochemical cell, we demonstrate the detection of influenza H1N1 in throat swab samples at loads as low as 10 TCID50, 4 orders of magnitude below the clinical titer for this virus.

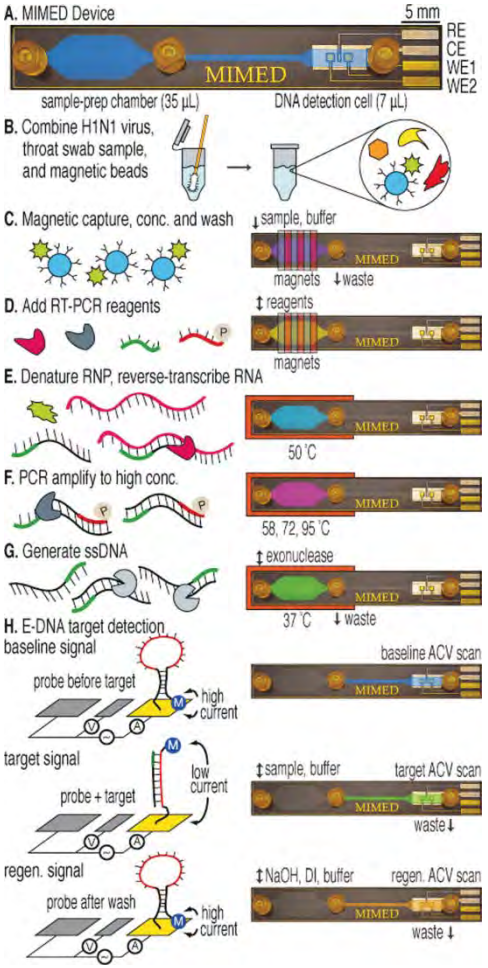

Sample-to-answer genetic analysis of H1N1 virus

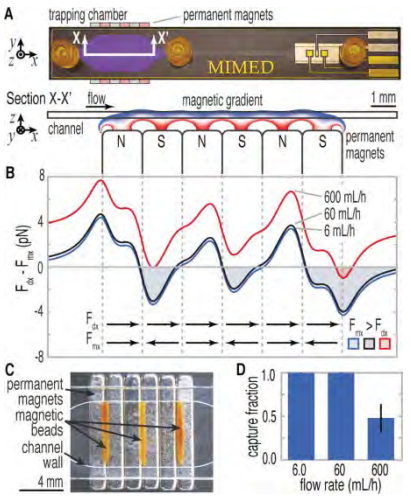

Simulation of magnetic capture

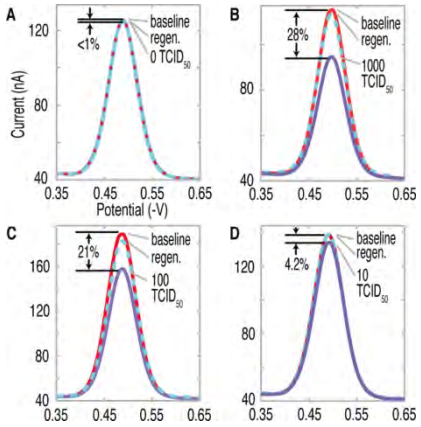

Limit of detection of MIMED is ~10 TCID50. Swab samples containing 1000, 100, and 10 TCID50 returned peak faradic current changes of 28, 21, and 4.2%, respectively, relative to 0.5% for negative control

S. Fergusen, et. al. Soh Group, UCSB
Work partially performed at UCSB Facility

B. Fergusen, et. al Journal of the American Chemical Society ***133****, 9129-9135 (2011)*
NNIN Research Highlights 2011

Gate Tunable Surface Processes on a Single-Nanowire Field-Effect Transistor

In this study we demonstrate how a single semiconducting nanowire whose surface has been decorated with metal nanoparticles and configured as the channel in a field-effect transistor can function as a miniature laboratory. The above device is used to investigate chemical processes occurring at the surfaces both of the metal nanoparticles and of the semiconductor and their effect on the electronic and transport properties of the device, and reciprocally how the transfer characteristics of the FET influence the chemistry occurring at the device's surface. These effects, negligibly small at the surfaces of ordinary materials systems, are enormously amplified when the FET's channel is a nanowire whose radius is comparable to, or smaller than the material's Debye screening length.

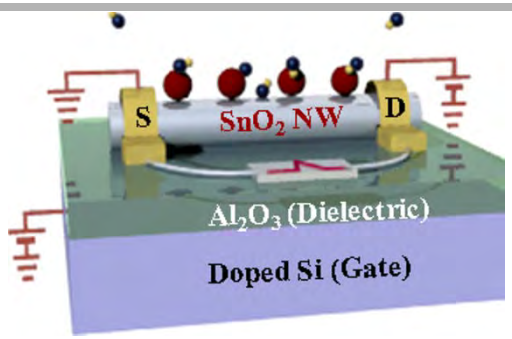

Schematic of the metal-nanoparticle decorated single SnO_2 nanowire FET sensor and its operation

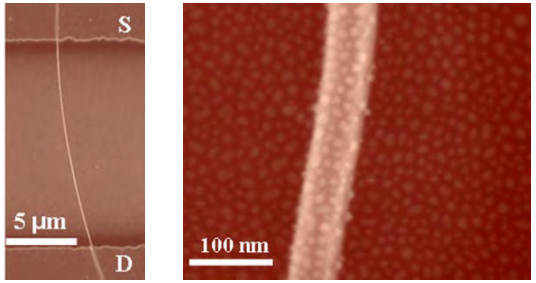

SEM image of Pd nanoparticle-decorated SnO2 nanowire

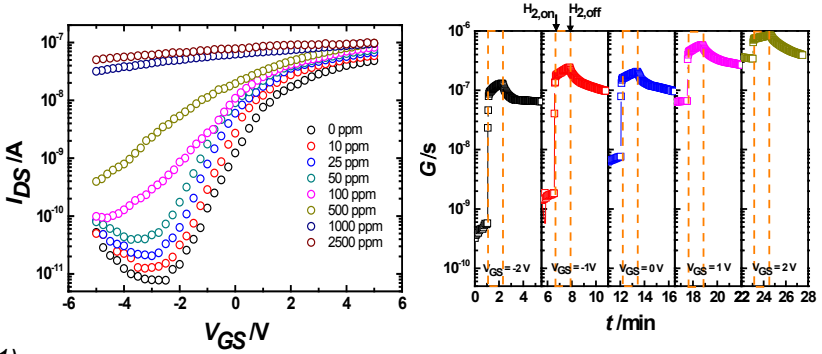

Effect of hydrogen partial pressure on the measured transfer characteristics of Pd-nanoparticle decorated SnO_2 nanowire

Syed Mubeen and Prof. Martin Moskovits,
University of California, Santa Barbara
Work performed at UCSB Facility

*Syed Mubeen and Martin Moskovits, Adv. Mater. **23**, 2306–2312 (2011)*

Spin Control of Drifting Electrons Using Local Nuclear Polarization in Ferromagnet-Semiconductor Heterostructures

We demonstrate methods to locally control the spin rotation of moving electrons in a GaAs channel. The Larmor frequency of optically injected spins is modulated when the spins are dragged through a region of spin-polarized nuclei created at a MnAs=GaAs interface. The effective field created by the nuclei is controlled either optically or electrically using the ferromagnetic proximity polarization effect. Spin rotation is also tuned by controlling the carrier traverse time through the polarized region. We demonstrate coherent spin rotations of 5p rad during transport.

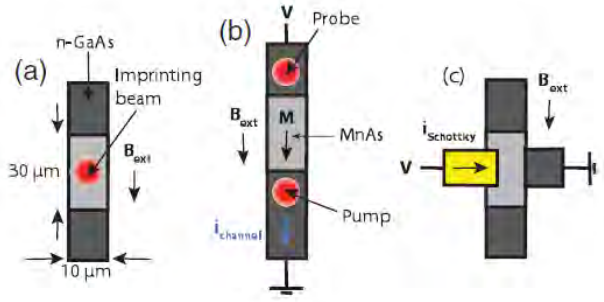

(a) Nuclear spins are polarized at the MnAs=GaAs interface using an optical imprinting beam. (b) Nonlocal TRKR measurement geometry used to inject and detect drifting electron spins in the channel after imprinting the nuclear region. (c) Nuclear spins are also polarized by forward biasing the Schottky junction at the MnAs=GaAs interface.

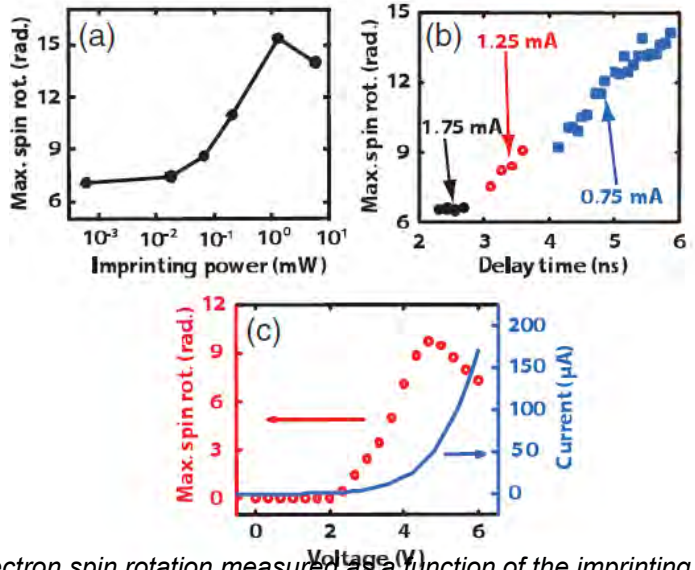

(a) Maximum electron spin rotation measured as a function of the imprinting beam power at Dt = 6 ns, $i_{channel}$ = 0.75 mA after imprinting for 20 min. (b) Maximum electron spin rotation measured as a function of delay time for $i_{channel}$ = 0.75, 1.25, and 1.75 mA after imprinting with a 1.75 mW beam for 20 min. (c) Schottky current and maximum electron spin rotation measured versus forward bias Schottky voltage at Dt = 4.5 ns, $i_{channel}$ = 0.75 mA after imprinting for 20 min. For all data B_{ext} = 0.2850 T and T = 8 K.

M. Nowakowski, et. al., Awschalom Group
Physics Dept., UCSB

Work partially performed at UCSB Facility

M. Nowakowski, et. al., Phys. Rev. Lett. 105, 137206

Versatile Chip Specific Integration Technology (VCSIT)

VCSIT is a novel technique for the integration of small CMOS dies in a large area substrate. A key component of the technique is the CMOS die based self-aligned masking. This allows the fabrication of sockets in wafers that are at most 5μm larger than the die. The die and large area substrate are bonded onto a carrier using BCB such that the top surfaces of the two components are flush. SOG is then applied to fill any small gaps between the chip and the substrate, and to planarize the top surface. The VCSIT platform has been designed with CMOS-, MEMS- and bio-compatible materials and processes. It allows for the integration of macroscale components, such as leads and microfluidics, and post-CMOS micromachining of the packaged chip. Because of its versatility, the VCSIT promises to be a formidable approach to implement next-generation biochips, integrated CMOS RF IC's and photonic CMOS chips.

Ashfaque Uddin, Kaveh Milaninia, Chin-Hsuan Chen, Luke Theogarajan, UCSB
Work performed at UCSB Facility

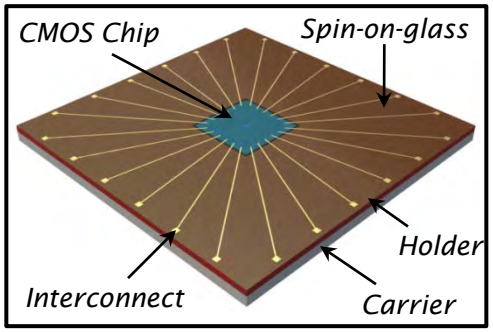

Schematic of VCSIT

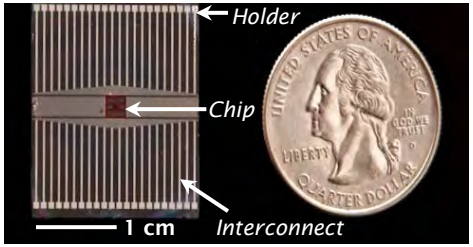

Integrated chip using VCSIT

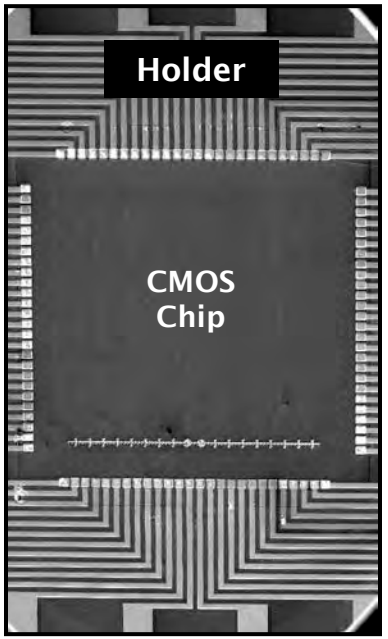

SEM top-view of embedded chip

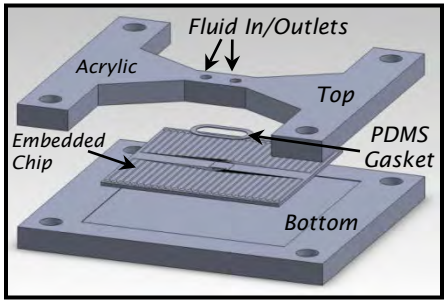

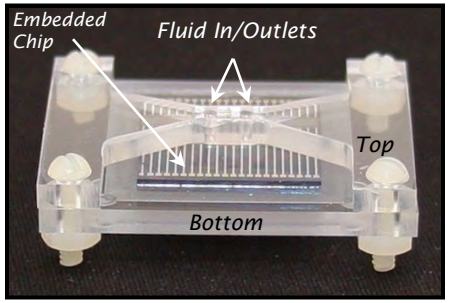

Assembly of a CMOS/Microfluidic hybrid system utilizing VCSIT

A. Uddin, et. al. IEEE Transaction on Components, Packaging and Manufacturing Technology, (2011)

Sponsored by Intel Corporation and NIH

N-polar GaN HEMT Achieving High f_{max} Frequency of Merit

The extremely rapid performance advances of N-polar GaN HEMTs are a significant indication of their relevance and viability in modern electronic device applications. The advantages of HEMTs on N-polar GaN include low contact resistance, built-in back-barrier for improved electron confinement and modulation efficiency, and ability to scale the barrier thickness independently of 2DEG channel charge. The current study highlights a novel high-aspect-ratio T-gate design and its resulting state-of-the-art RF device performance on the N-face GaN material system. We report measured fmax data of over 300 GHz on an MOCVD-grown N-polar GaN HEMT using a high-aspect-ratio T-gate. To our knowledge, this > 300-GHz fmax value is the highest reported to date for N-polar GaN HEMTs.

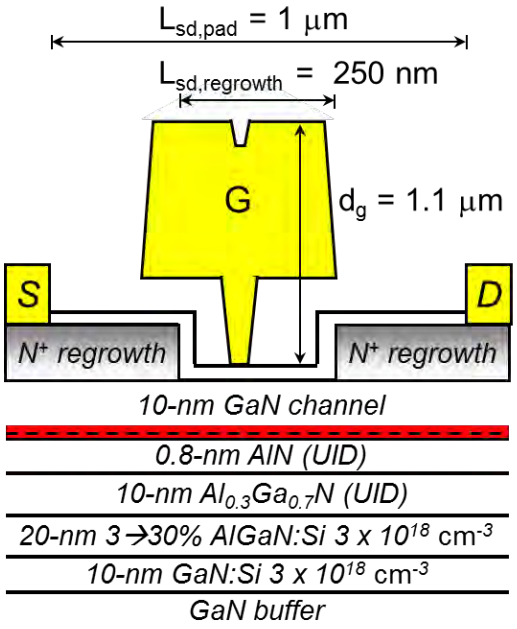

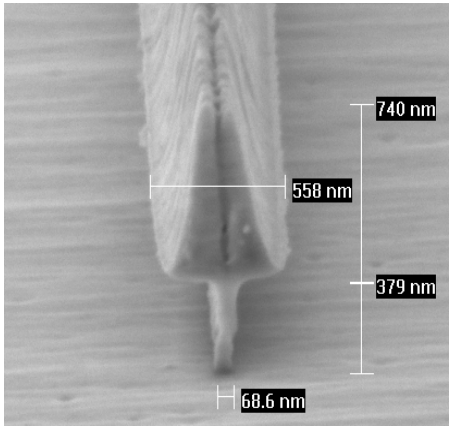

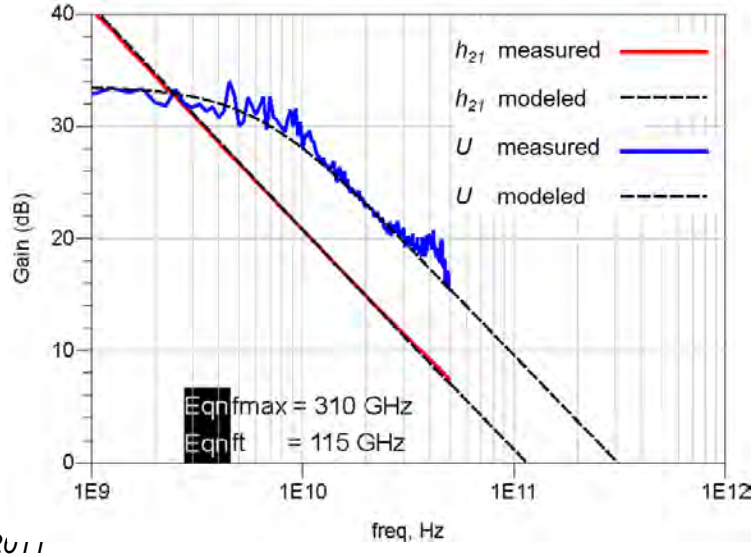

D. Denninghoff, et. al. Mishra Group, UCSB
Work performed at UCSB Facility

DARPA MTO NEXT program
D. Denninghoff, et. al., DRC 2011

High Quantum Efficiency InGaN/GaN Multiple Quantum Well Solar Cells with Spectral Response Extending Out to 520 nm

InGaN-based alloys have also begun to receive considerable attention for photovoltaic applications. This interest has been driven by the favorable physical properties of InGaN-based alloys for photovoltaic applications, including a direct band gap ranging from 0.64 eV for InN to 3.4 eV for GaN, high absorption coefficients of 10^5 cm^{-1} near the band edge, superior radiation resistance compared to other photovoltaic materials, and the potential for integration with existing silicon technology. We demonstrate high quantum efficiency InGaN/GaN multiple quantum well (QW) solar cells with spectral response extending out to 520 nm. Increasing the number of QWs in the active region did not reduce the carrier collection efficiency for devices with 10, 20, and 30 QWs. Solar cells with 30 QWs and an intentionally roughened p-GaN surface exhibited a peak external quantum efficiency (EQE) of 70.9% at 390 nm, an EQE of 39.0% at 450 nm, an open circuit voltage of 1.93 V, and a short circuit current density of 2.53 mA/cm^2 under 1.2 suns AM1.5G equivalent illumination.

R. Farell, et. al. Speck, Nakamura, DenBaars Groups,
Materials and ECE Depts, UCSB
Work performed at UCSB Facility

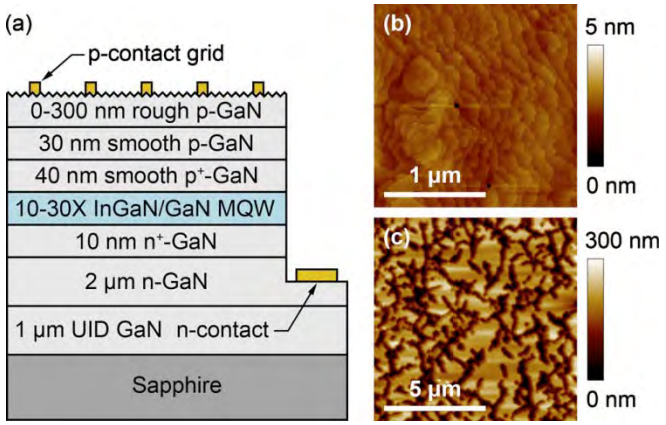

(a) Cross-sectional schematic of the general device structure. (b) 2 x 2 μm AFM image of the surface of sample C (30QW, smooth). (c) 10 x 10 μm AFM image of the surface of sample D (30QW, rough)

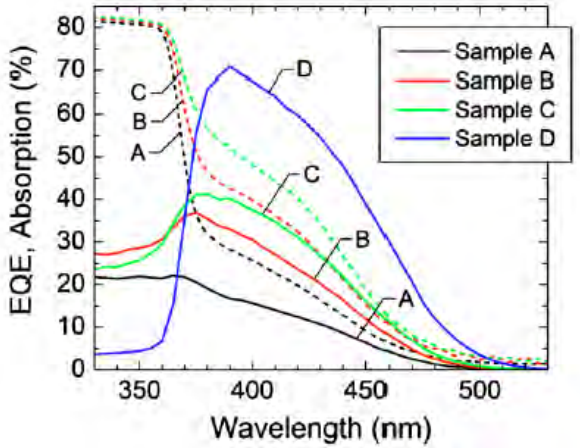

Dependence of EQE (solid lines) and absorption (dashed lines) on wavelength for samples A(10QW, smooth), B(20QW,smooth), C(30QW, smooth), and D(30QW, rough)

*R. M. Farrell, et. al. APPLIED PHYSICS LETTERS **98**(20), 201107*

Continuous-Wave Operation of Pure Blue AlGaN-Cladding-Free Nonpolar InGaN/GaN Laser Diodes

Next generation display technologies, including full color displays and mobile projectors, require light emitters that are spectrally pure, thermally stable, energy efficient, and small in size. For these applications, wurtzite (Al,In)GaN-based laser diodes (LDs) have emerged as the leading candidate for blue and green direct-emission light sources. We present the first reported continuous-wave (CW) operation of pure blue AlGaN-cladding-free (ACF) nonpolar m-plane InGaN/GaN laser diodes (LDs). CW lasing was achieved at a wavelength of 461nm and a threshold current density of 4.1 kA/cm^2 for LDs with an InGaN-based separate confinement heterostructure (SCH) waveguide design. The devices showed a 9 nm/decade blue-shift of spontaneous emission wavelength with increasing current density, a characteristic temperature of 156 K, a red-shift with increasing stage temperature of 0.05 nm/K, and an estimated thermal impedance of 60 K/W

K. Kelchner, et. al. Speck, Nakamura, DenBaars
Groups, Materials and ECE Depts, UCSB
Work performed at UCSB Facility

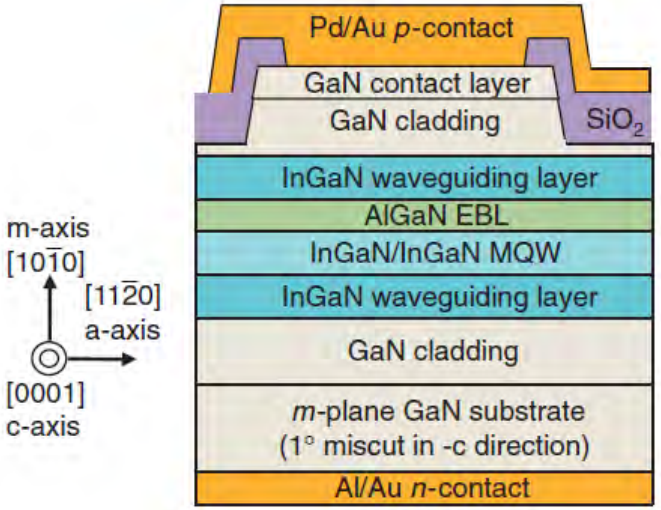

Device Schematic

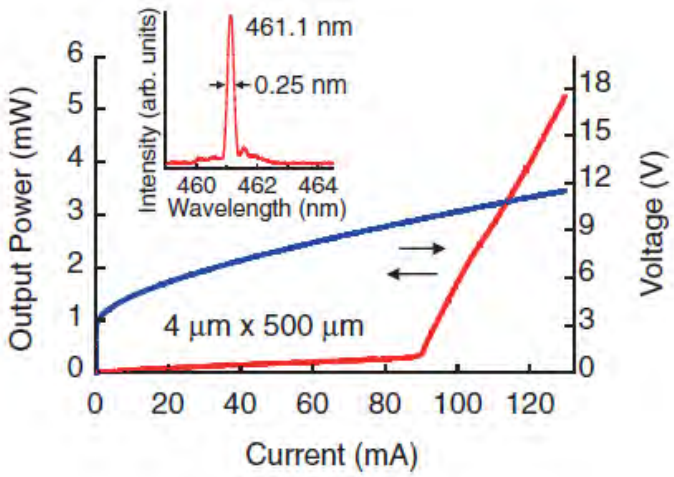

CW Light and Voltage versus Current

Applied Physics Express ***3****, 092103 (2011).*

Programmable Photonic Microwave Filters Monolithically Integrated in InP–InGaAsP

We demonstrate an integrated programmable photonic filter structure capable of producing bandpass filters with both tunable passband bandwidth and center frequency. Such filters could provide dynamic pre-filtering of very wide bandwidth analog microwave signals, essential to the next generation RF-front ends. The photonic filter is constructed froman array of uncoupled identical filter stages, each reconfigurable as a zero or a pole using an asymmetrical Mach-Zenhder Interferometer (MZI) structure with feedback. Integrated on a standard InP–InGaAsP material platform, semiconductor optical amplifiers (SOAs) and current injected phase modulators (PMs) are used to rapidly adjust the individual pole and zero locations, thereby reconfiguring the overall filter function. In this paper, we demonstrate cascaded filter structures with up to four filter stages, capable of producing a variety of higher order filters. Demonstrated filters have a free spectral range (FSR) of 23.5 or 47 GHz.

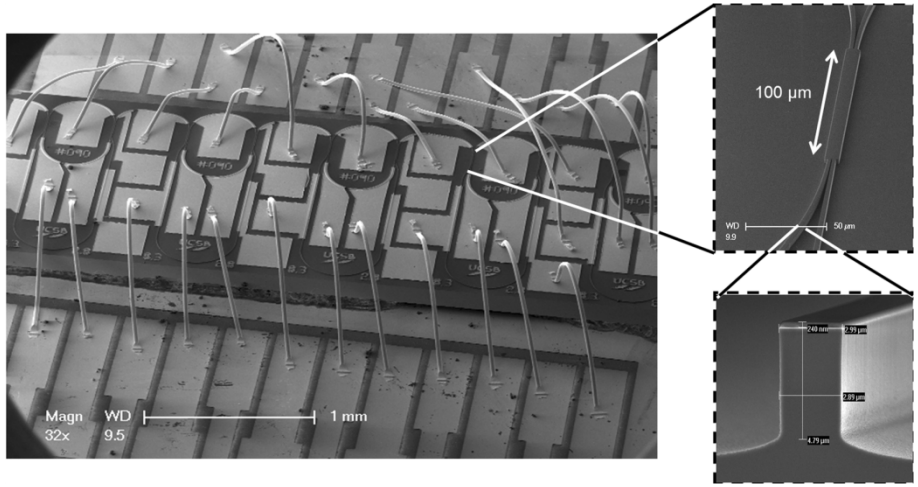

Scanning electron microscopy (SEM) image of a programmable photonic filter device wire bonded to a carrier. Insets show deeply etched MMI coupler (upper) and a cross section of deeply etched waveguide (lower).

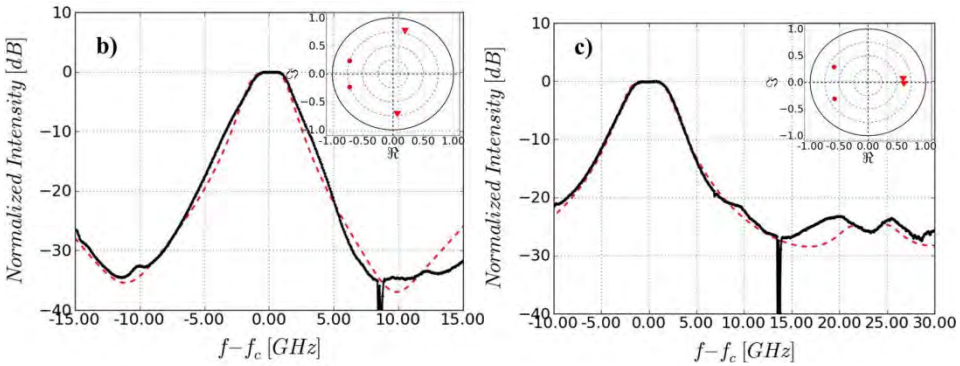

Examples of higher order filters synthesized with our programmable filter device. (b) Bandpass filter utilizing both zeros and poles. (c) 2nd order bandpass filter with zeros placed to eliminate the next filter order and thus double the FSR.

E. Norberg, et. al. Coldren Group, ECE Dept, UCSB
Work performed at UCSB Facility

ournal of Lightwave Technology, IEEE, ***29****(11), 1611-1619*

Forty Gb/s Hybrid Silicon Mach-Zehnder Modulator with Low Chirp

Recent efforts in silicon photonics have focused on developing a wide range of optical components that can be integrated on a single platform. A lot of work has focused on modulators as they are crucial for the generation and transmission of high-speed signals such that increasing demands on data capacity can be satisfied. To be able to efficiently send information at high frequencies, modulators with large optical bandwidth, high-speed operation and good modulation efficiency are required. Modulators based on a Mach-Zehnder interferometer (MZI) architecture are of particular interest because they satisfy several of the aforementioned criteria. In this work, we demonstrate a hybrid silicon modulator operating up to 40 Gb/s with 11.4 dB extinction ratio. The modulator has voltage-length product of 2.4 V-mm and chirp of - 0.75 over the entire bias range. As a switch, it has a switching time less than 20 ps.

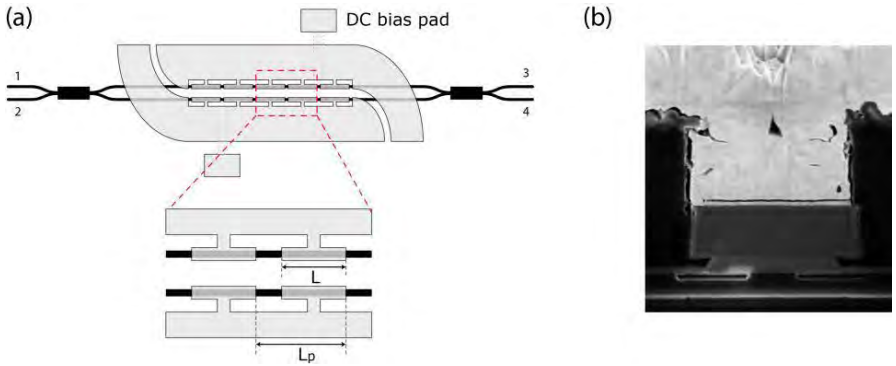

(a) Top schematic of a 500 μm MZM with slotline design. (c) SEM cross section of one arm of the MZM

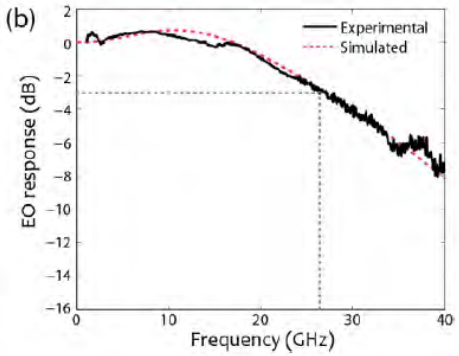

Modulation bandwidth measured at -3 V with 25 Ω termination.

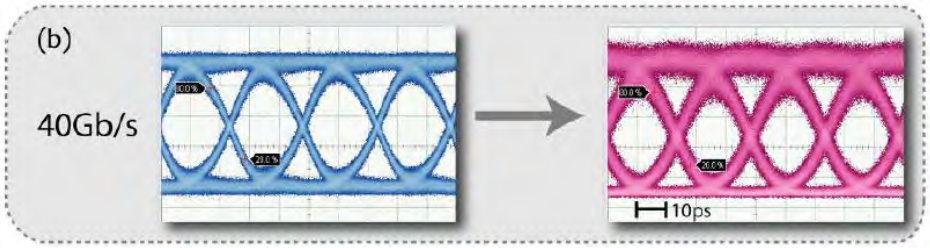

Left: 40 Gb/s electrical driven signal with 2^{31}-1 NRZ PRBS. Right: signal after modulator with 11.4 dB ER

Hui-Wen Chen, J. Peters, and J. Bowers
ECE Dept, UCSB
Work at UCSB Facility

*H-W Chen, et. Optics Express **19** (2), 1455-1460*

supported by Agilent Technologies

Improvement of Barium Strontium Titanate SMR Q-Factor by Reduction in Electrode Surface Roughness

Bulk acoustic wave resonators are used to filter unwanted frequencies in wireless microwave applications such as cell phones. Currently used materials, such as AlN, only allow for fixed frequency and constantly ON filters. At UCSB, novel thin film materials are being explored for these applications, such as $SrTiO_3$ and $(Ba,Sr)TiO_3$. Surface roughness is a scattering loss mechanism that degrades the Quality factor of the resonator. Comparison of the surface roughness between two SiO_2 surfaces deposited by two different methods figure 1 PECVD and figure 2 ICP PECVD in Panel A. The Quality factor improves significantly for the resonator with the smoother electrode surface (Panel B).

G. Saddik, S. Stemmer, R. York
ECE and Materials Depts, UCSB
Work at UCSB Facility

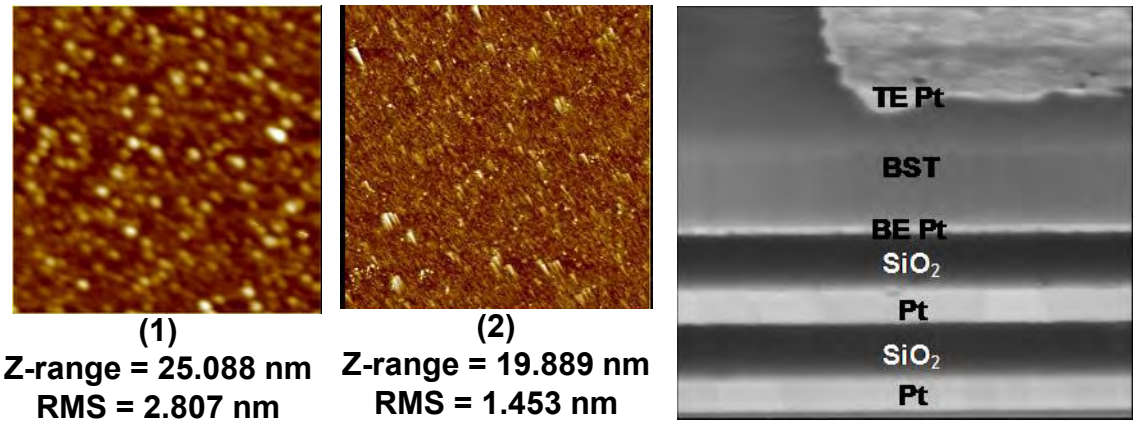

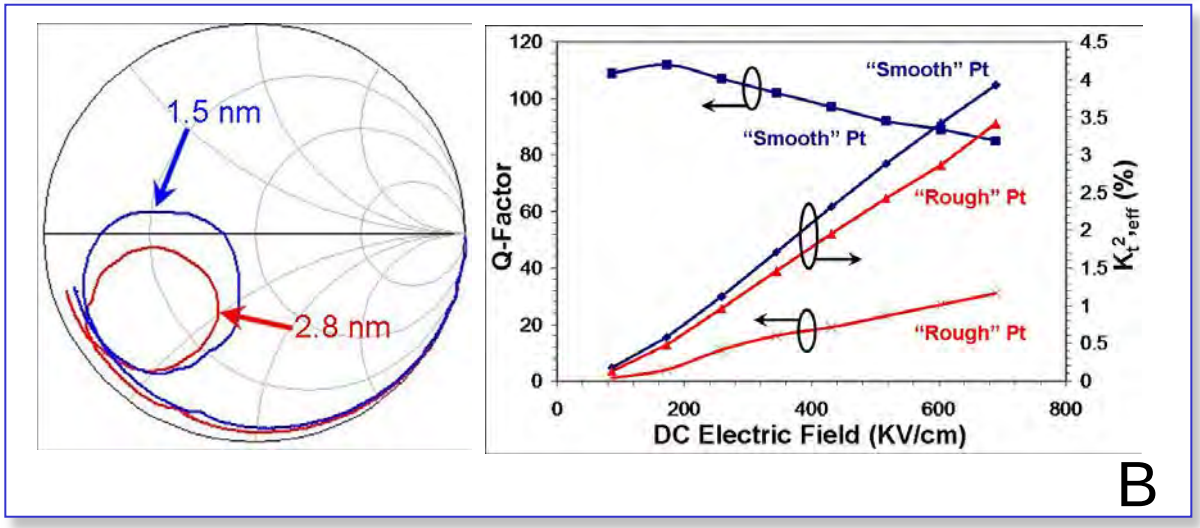

G. N. Saddik, et. al. *Journal of Applied Physics* **109**, 091606 (2011).

NNIN Research Highlights 2011

U.S. Army Research Office (Grant No. W911NF-0601-0431), NSF (Grant No. CCF-0507227)

NNIN Site at the University of Minnesota

Flexible, Low Voltage Organic Digital Circuits

We use printable electrolyte ion gel to achieve these flexible, low voltage digital circuits. Low operational voltage circuits use a printable, high capacitance (~ 10 μF/cm^2) ion gel.
Printed, fast digital circuits are based on carbon nanotubes (CNTs) and have a stage delay of about 50 μs. Printed flexible OTFT circuits are for display applications.

printed carbon nanotube thin film

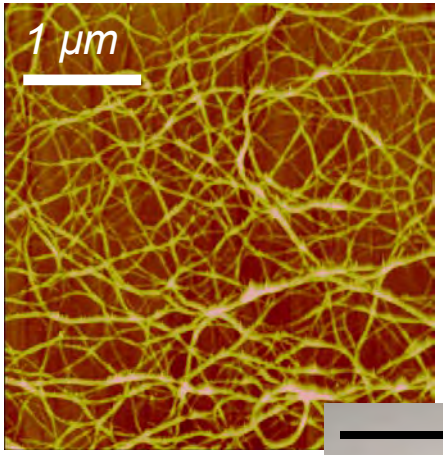

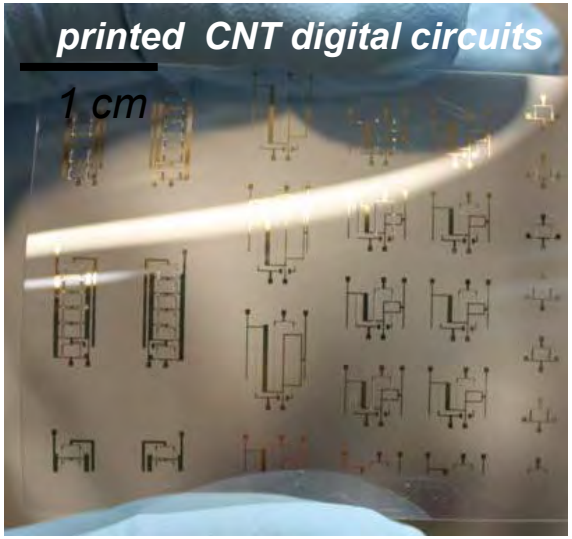

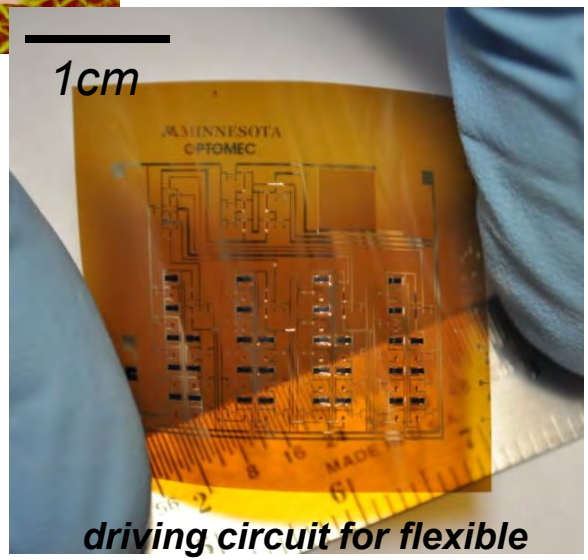

driving circuit for flexible display

C. Daniel Frisbie, Mingjing Ha, Chemical Engineering & Materials Science, University of Minnesota

Work performed at Nanofabrication Center, University of Minnesota

Spin Transport in Nanoscopic Metallic Spin Valves

This work uses spin valves to study spin-dependent transport for ferromagnetic (FM) and normal metals (N). The focus is on the role of material interfaces and surfaces on spin relaxation.

Spin transport is dominated by FM and geometry. Temperature dependent spin-dependent resistance is strongly impacted by the FM injector material. Spin diffusion length increases with increasing device thickness, indicating enhanced spin relaxation at the surfaces.

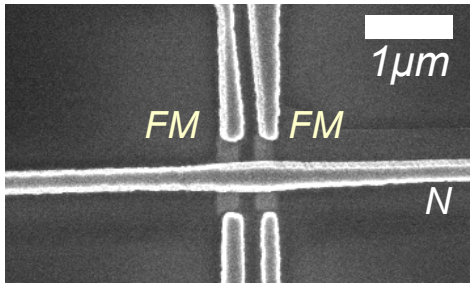

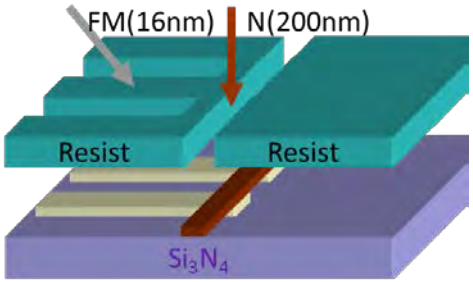

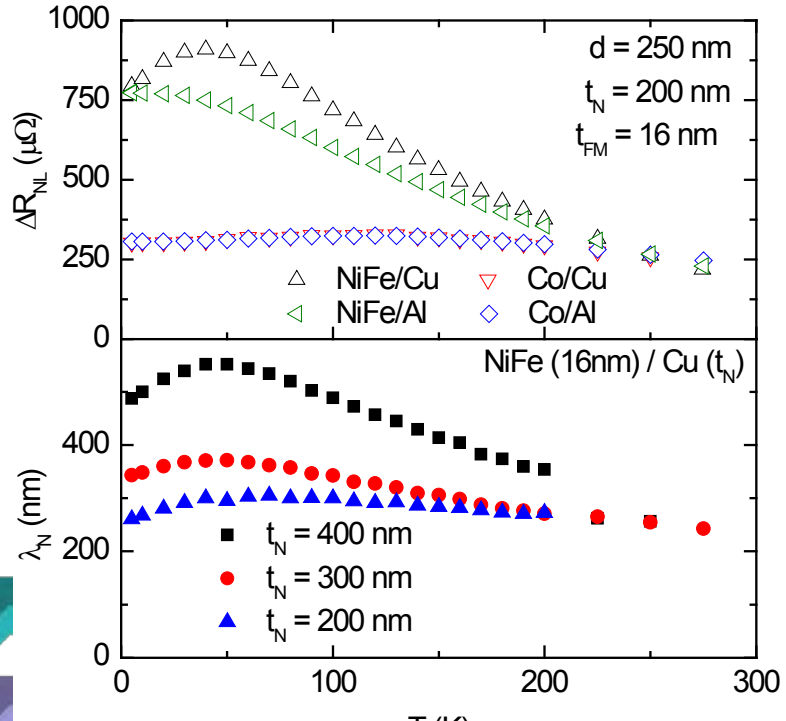

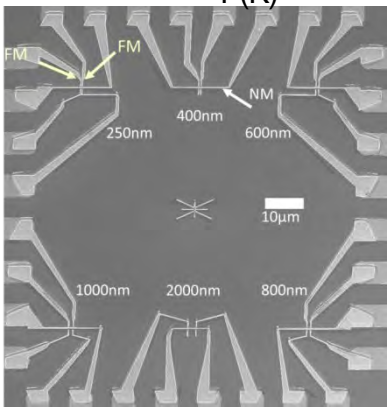

Paul Crowell, Chris Leighton, Mike Erickson
Physics; Chemical Engineering & Materials Science
University of Minnesota

Work performed at Nanofabrication Center, University of Minnesota

Fracture in Core-shell Si-SiC Nanotowers

Si-SiC composite nanotowers were grown to study the small scale confinement of Si. The nanotowers were grown using VLS. Nanocrystalline SiC was deposited using hypersonic plasma partide deposition (HPPD).

VLS Si nanotowers

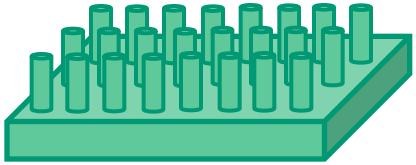

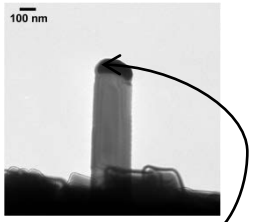

Au catalyst

HPPD nc-SiC coated Si

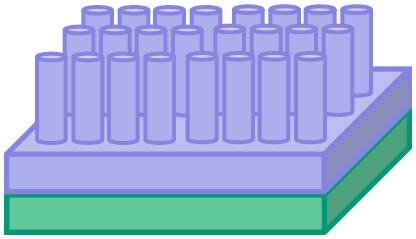

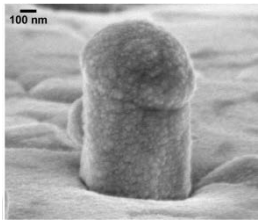

Focused ion beam milling

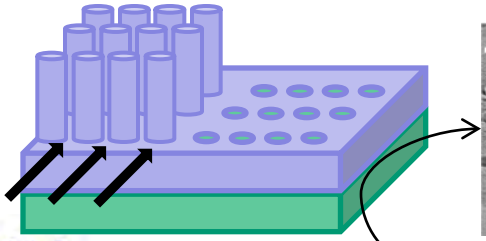

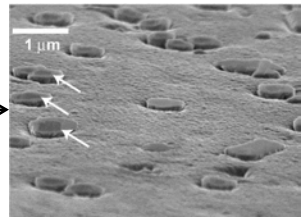

Core-shell structure exposed

- *Nanoindentation is used to probe the confined Si core.*
- *Indentation induced cracks at the indenter vertices are confined to the Si core due to compressive stress imposed by the SiC shell.*
- *Deviation from elastic- plastic unloading suggests Si phase transformation.*
- *An AFM height scan shows significant plastic pile-up at the indentation edges.*
- *Increased composite toughness is due to ductile phase pinning and phase transformation toughening.*

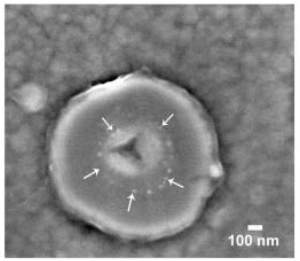

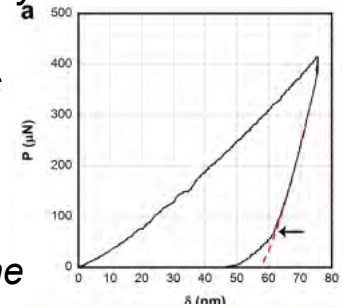

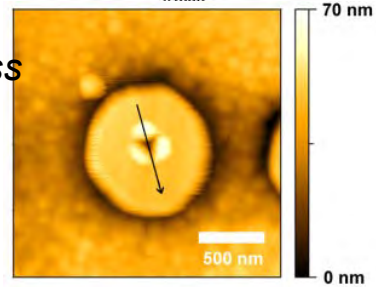

S.L. Girshick, A.R. Beaber, W.W. Gerberich
Mechanical Engineering; Chemical Engineering & Materials Science
University of Minnesota
Work performed at Nanofabrication Center, University of Minnesota

Tunneling and Transport in Nanowires

This work involves the fabrication and characterization of superconducting nanowires. Zn and Al nanowires were fabricated using elctron-beam lithography. They were cooled below the transition temperature and driven resistive by the application of current.

The application of a magnetic field restored the superconductivity. From the angular dependence of the response, it is possible to infer that the generation of quasipartides by the field dampens resistance producing phase fluctuations thus restoring the superconductivity.

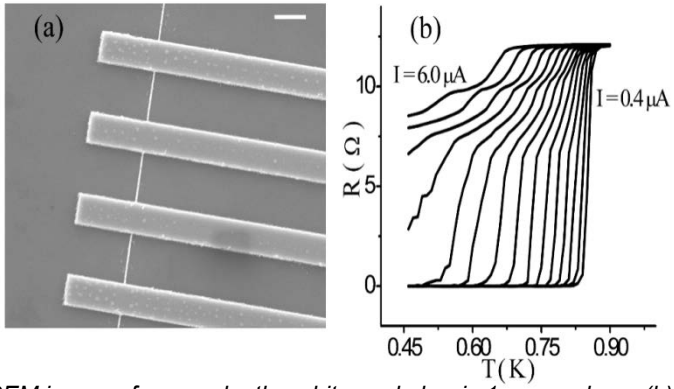

(a) SEM image of a sample, the white scale bar is 1 μχρον long. (b) Temperature dependence of the wire resistance in zero magnetic field with currents ranging from 0.4 microamps to 6.0 microamps in increments of 0.4 microamps.

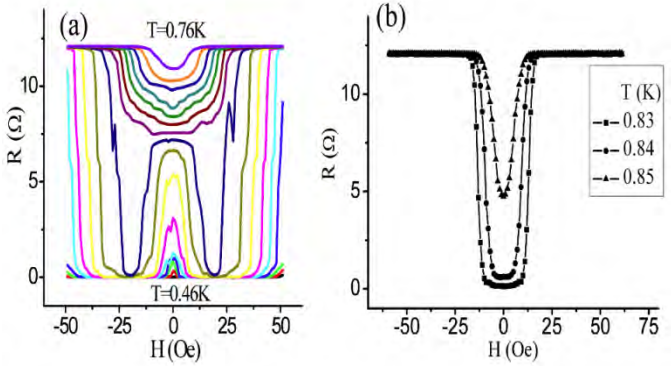

a) Magnetic field dependence of wire resistance, at I = 4.4 μιχροαμπσ, with temperatures ranging from 0.46K to 0.76K, every 0.02K. b) Magnetic field dependence of wire resistance, at I = 0.4 microamps, with temperatures ranging from 0.83K to 0.85K, every 0.01K.

A.M. Goldman, S. Snyder, Y. Chen
Physics, University of Minnesota

Work performed at Nanofabrication Center, University of Minnesota

Block Copolymer Patterning of Magnetic Nanostructures

Solvent annealing of Poly(styrene-b-lactide) leads to well-ordered cylindrical structures. This process leads to high fidelity pattern transfer from self-assembled polymer templates to magnetic metals. Poly(styrene-b-lactide) is spun cast onto a Si wafer. Incorporating solvent annealing leads to self assembled, perpendicularly oriented cylinders. Aqueous degradation of the polylactide minority block (cylinders) leaves a polystyrene template behind. Evaporation of NiFe, in excess, on top of the template fills the dimples (D). Normal incidence Ar ion beam milling planarizes the surface, eventually removing the overlayer (O).

The disparity in milling times for polystyrene (10nm/min) and NiFe (2nm/min) leads to a pattern reversal and the formation of NiFe nanodots.

Chris Leighton, Marc Hillmyer, Andrew Baruth
Chemical Engineering & Materials Science
University of Minnesota

Work performed at Nanofabrication Center, University of Minnesota

Process schematic

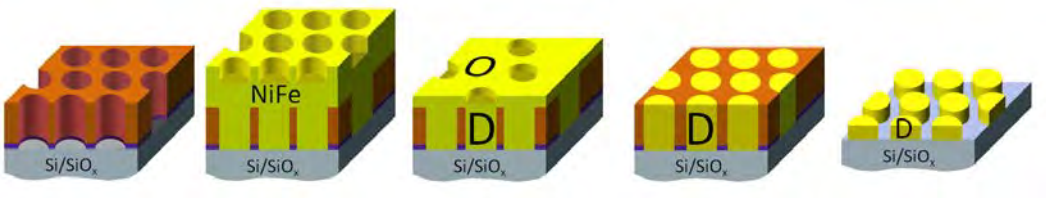

PS template *Intermediate mill time* *Final array*
After metal deposition *Removal of overlayer*

AFM of polystyrene template

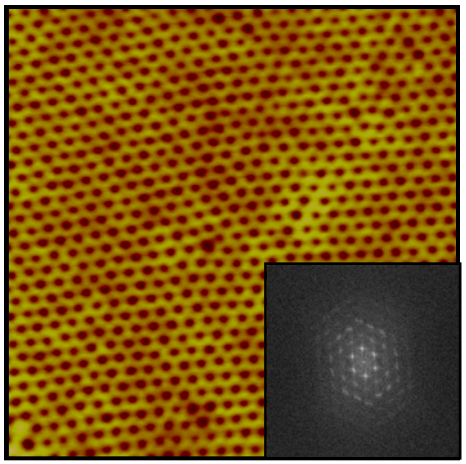

SEM of $Ni_{80}Fe_{20}$ nanodots

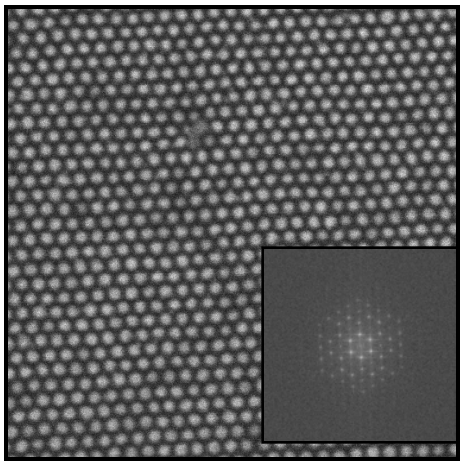

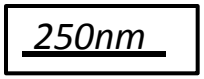

Fiber-optic Photoacoustic Endoscopy

The objective of this research is to create a miniature linear acoustic sensor array for photoacoustic endoscopy. We deposit an optical resonator (etalon) for acoustic detection on the tip of an optical fiber using e-beam evaporation. We produce a resonator on multiple fibers with additional fibers transmitting optical pulses for photoacoustic excitation.

The sensor exhibits optical resonance and compressibility suitable for opto-acoustic ultrasound detection at frequencies up to 50 MHz. We can image photoacoustic targets less than 100 nm in size which gives cause for developing a bundle of sensors. If fabrication is successful, the device will be ready to image live tissue.

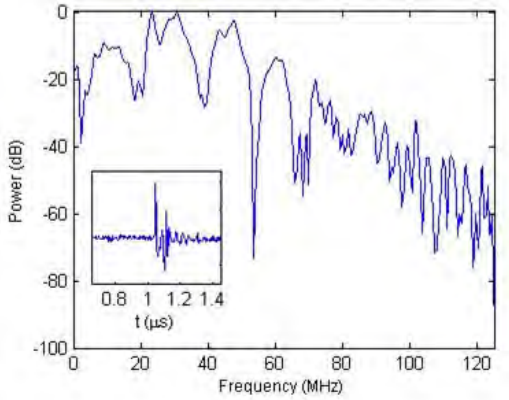

Detection of ultrasound emitted from chromium thin-film irradiated with 532nm opt. pulse

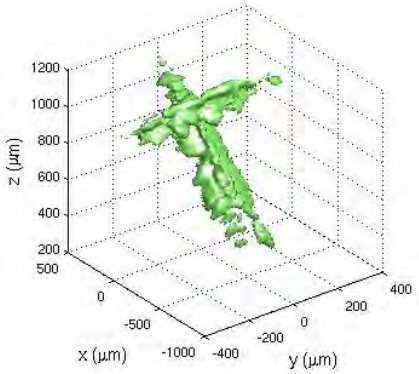

Reconstruction of two strands of 60 μm black hair by scanning sensor to make synthetic aperture

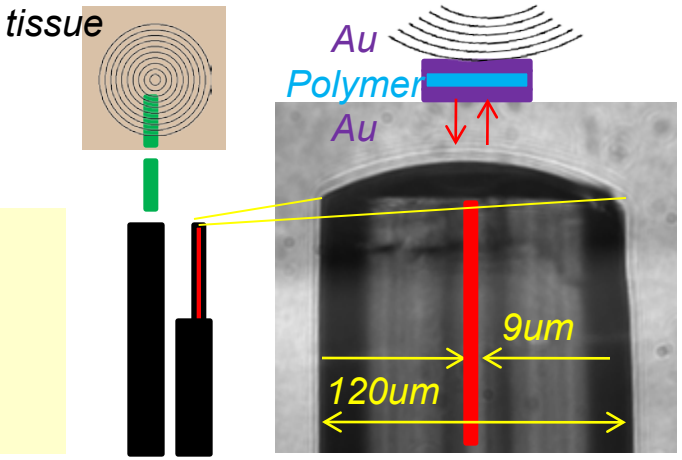

Shai Ashkenazi, Clay Sheaff
Biomedical Engineering, University of Minnesota
Work performed at Nanofabrication Center, University of Minnesota

Imaging Biofilms in Micro-Scale Porous Media Flow Cells

We are working to develop a synthetic porous-media flow cell through photolithography in which biofilm can be grown to be microscopically imaged. We compare confocal laser scanning microscopy and x-ray computed microtomography biofilm imaging methods. We are also evaluating the use of two novel x-ray contrast agents for biofilm imaging: silver coated microsphere and barium sulfate suspensions. These agents rely on size exclusion to capture the 3D features of biofilms.

Photolithography is an effective way to manufacture microscale flow cells for the microscopic study of biofilms in porous media systems. These systems work particularly well with CLSM imaging. The use of silver microspheres as an x-ray contrast agent for CMT is effective at capturing large biofilm features on the scale of 0.5 mm. Barium sulfate captures features but can damage a delicate biofilm during injection due to its high viscosity and mass.

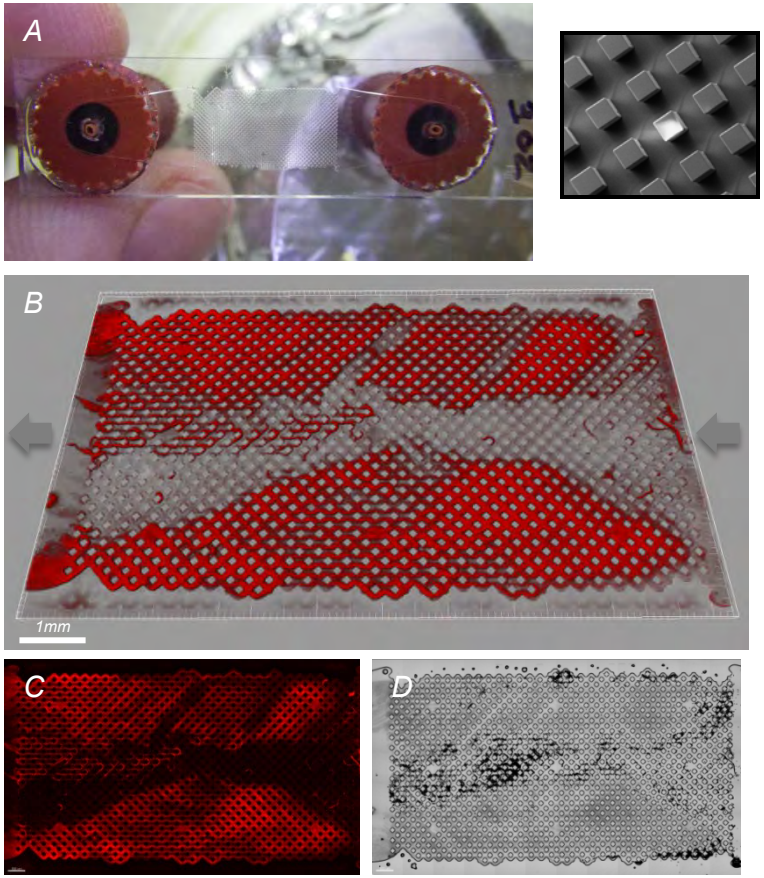

***Figures** – **(A)** Micro flow cell with 100µm porous media features. **(B)** CLSM image of a biofilm grown in the porous media flow cell. **(C)** 2D projection of the same biofilm (fluorescently stained) before x-ray contrast agent addition. **(D)** The same system after the addition of silver microspheres imaged with transmitted laser light.*

James Connolly, Robin Gerlach; Gabe Iltis, Dorthe Wildenschild
Montana State University; Oregon State University
Work performed at Nanofabrication Center, University of Minnesota

An Ultra-Sensitive and Low-Cost Graphene Sensor Based on Layer-by-Layer Nano Self-Assembly

Layer-by-layer (LbL) self-assembled graphene based flexible cancer sensors have a detection limit of prostate specific antigen (PSA) down to 4 fg/ml (0.11 fM). They are label-free and HRP labeled. They are low in cost due to this self-assembly technique and the polyethylene terephthalate (PET) substrate.

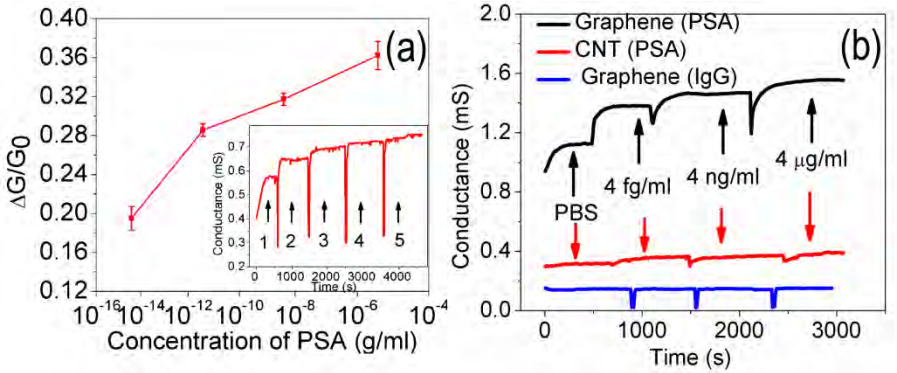

(a) Detection result of label free graphene cancer sensor; inset: real-time detection results. (b) Conductance versus time testing for graphene and CNT biosensors with different PSA concentrations. Normal rabbit IgG is induced to prove the specificity of biosensor.

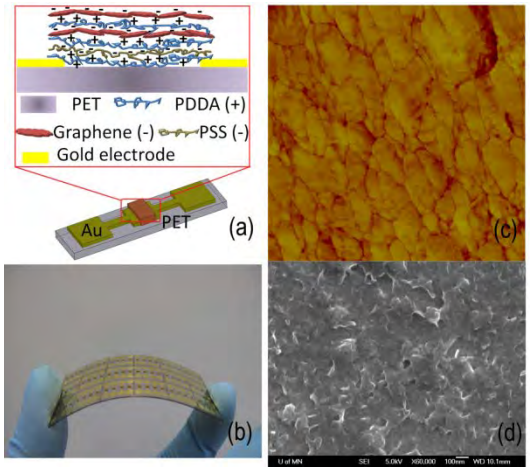

(a) LbL self-assembled graphene nanocomposite before immunization. (b) graphene cancer sensor on a flexible PET substrate. (c) AFM image of LbL self-assembled graphene (scanning area is 1 μm by 1 μm). (d) SEM image of LbL self-assembled graphene displaying its porous defoliation surface profile. The average graphene nanoplatelet is about 100 nm by 100 nm.

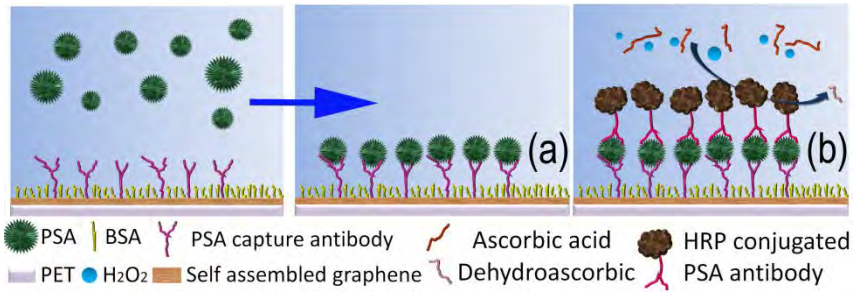

(a) Schematic illustration of interaction between capture antibodies and target protein molecules in a label free detection. After graphene biosensor modified by capture antibodies encounters PSA solution, the immunoreaction will take place, and the conductance of graphene changes due to the absorption of PSA on the surface of the graphene. (b) Schematic illustration of a graphene sensor in a labeled detection. HRP labels the different concentration of PSA, and catalyzes the conversion from ascorbic acid to dehydroascorbic acid, causing the local pH shifts. The conductance of graphene is sensitive to pH shifts.

Tianhong Cui, Bo Zhang
Mechanical Engineering, University of Minnesota
Work performed at Nanofabrication Center, University of Minnesota

Single Molecule Tunneling with Sub-molecular Resolution for DNA Sequence and Fragment Sizing Applications

Our work deals with the fabrication of devices for single molecule electrical detection. We are working on the development of a nanopore-tunneling junction combined platform and the study of DNA for future biomedical applications.

Nanometer-scale pores (nanopores) are versatile single molecule sensors for the label-free detection and structural analysis of biological polymers such as DNA, RNA, polypeptides, and DNA-protein complexes in solution.

We have observed the alignment of a nanopore and a nanoelctrode couple using the Focused Ion Beam technique. We see different dynamics of DNA translocation through the device.

We developed a simple method to fabricate tunneling junctions aligned to a nanopore and proof-of-principle experiments demonstrating simultaneous detection of DNA translocations using both tunneling and ionic currents in a nanopore platform.

J. Edel, T. Albrecht, E. Instuli, A. Ivanov
Chemistry, Imperial College London
Work performed at Nanofabrication Center, University of Minnesota

The "Bumps" – A Device to Measure Touch Sensation

We have constructed a rapid, sensitive method to quantify the tactile threshold of the finger pads for early detection and staging of peripheral neuropathy. The "Bumps" are produced by photolithography and are arranged in a checkerboard-like smooth surface divided into squares with five colored circles in each square. One circle in each square contains a bump which is 550 μm in diameter, and ranges in height from 2.5 to 14 in 0.5 μm increments. We are beginning construction of a master mold for commercial production.

The mean fingertip detection threshold strongly correlates with Meissner's corpuscle sensory receptor density.

The device can lead to earlier diagnosis of neuropathy and allows for inexpensive, fast, easy testing with minimal training.

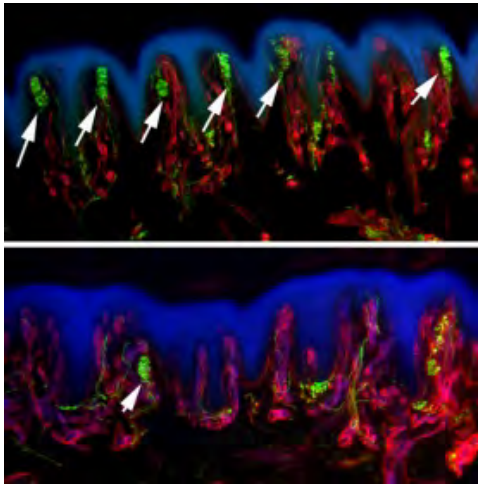

Meissner's corpuscles (arrows) in finger tip skin sections are more numerous in normal skin (top) than in skin from chemotherapy-induced peripheral neuropathy subject's skin

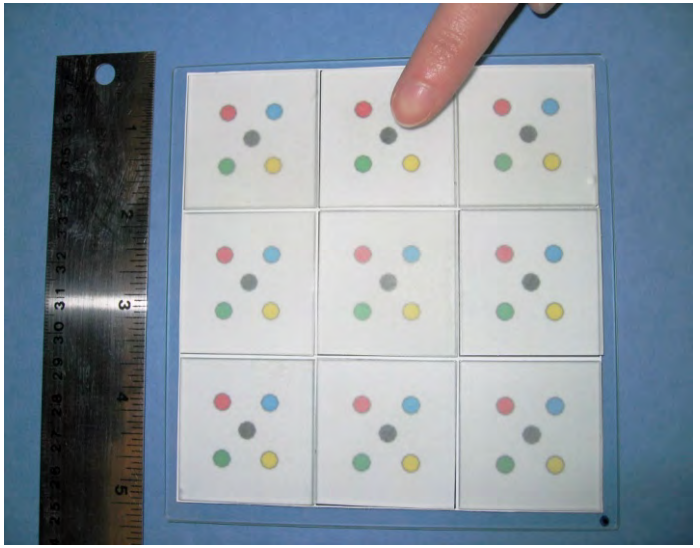

William Kennedy
Neurology, University of Minnesota
Work performed at Nanofabrication Center, University of Minnesota

Long Wavelength VCSELs

Our work centers around vertical cavity surface emitting lasers (VCSELs) for biomedical sensing and stimulation. They have a 1860 nm Wavelength and InP/InGaAsP material platform.

1860 nm laser performance allows power up to 3mW, a single mode spectrum less than 0.1 nm and continuous wave lasing up to 60° C.

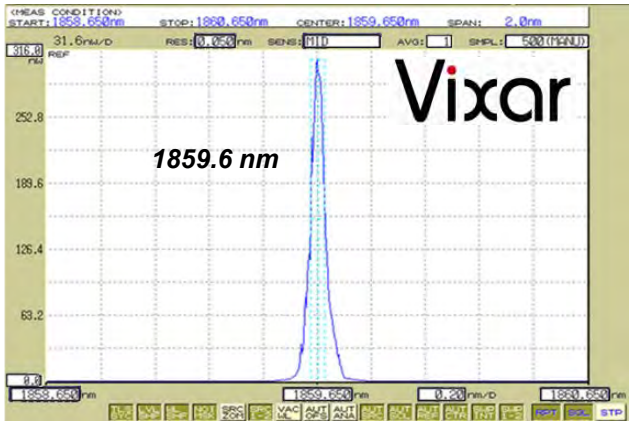

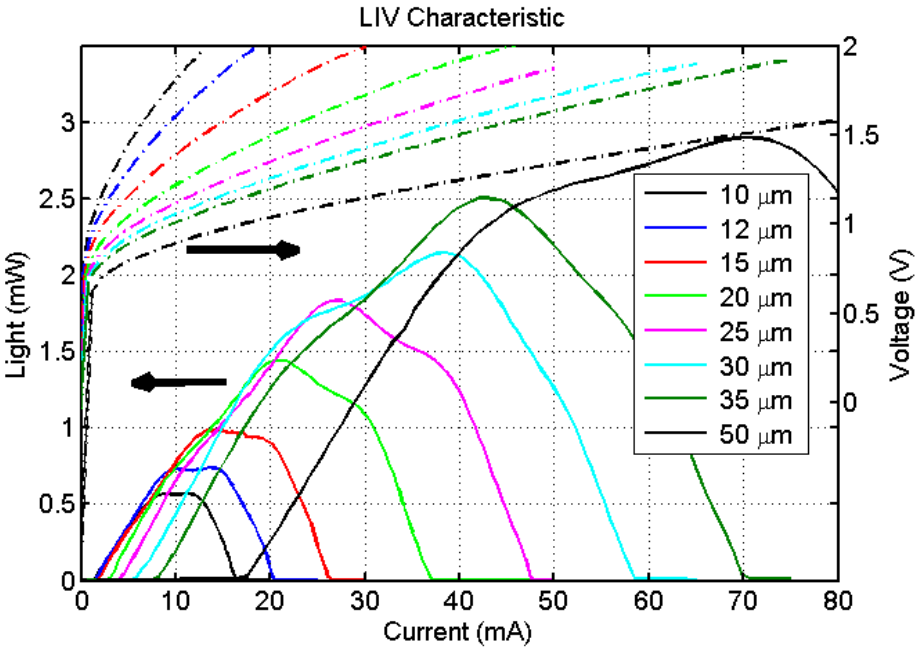

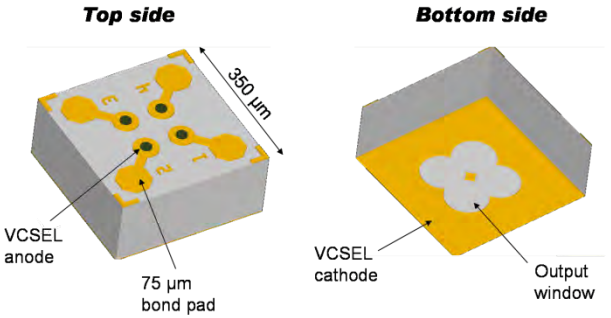

M. Dummer, K. Johnson, W.K. Hogan, M. Hibbs-Brenner
Vixar LLC
Work performed at Nanofabrication Center, University of Minnesota

Low Mass Density RF Actuators

The goal of this project is to develop a Single Walled Carbon Nanotube (SWNT) film using Layer-by-Layer deposition. We want to demonstrate reliable and fast 3-terminal actuators and implement high speed MEMS digital logic circuits.

We have measured Film Resistivity for each annealing condition:
Lowest Resistivity=8.9x10^{-4}Ω·cm@300˚C Annealed. We have measured film Young's modulus(E) and yield strength(Y) by triboindentation from free-standing CNT beams:
Highest E=913GPa@300˚C Annealed

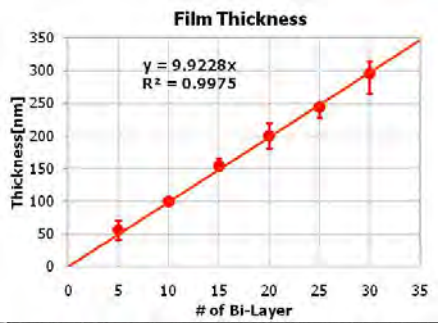

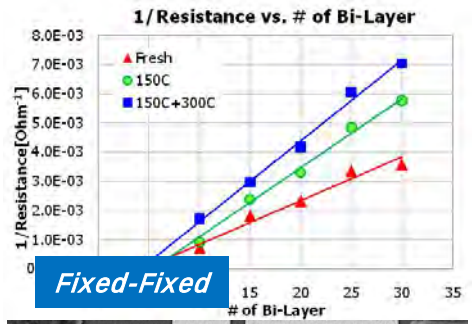

Fixed-Fixed

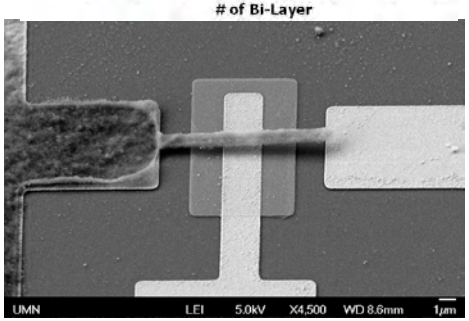

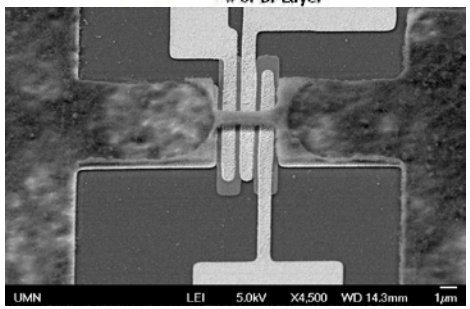

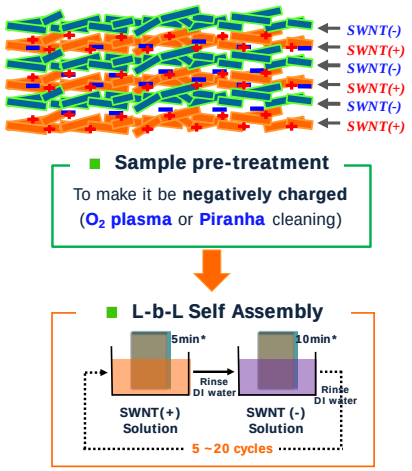

T.A. Taton, W. Partlo; T. Cui, D. Lee, Z. Ye; D.J. Lilja, S.A. Campbell, S. Patil, C.-L. Chen, M.-W. Jang
Chemistry; Mechanical Engineering; Electrical & Computer Engineering
University of Minnesota
Work performed at Nanofabrication Center, University of Minnesota

Monolithically Integrated Two-Axis Micro-Tensile Tester

A monolithically integrated two-axis micro-tensile tester has been developed. The tensile tester consists of a two-axis electrostatic actuator with integrated capacitive position sensors and a two-axis capacitive micro-force sensor. It is fabricated using a bulk silicon micro-fabrication process.

The actuation range is +/-16 µm along both axes with a position resolution of 20 nm. The force sensor is capable of measuring forces up to +/- 60 µN with a resolution down to 60 nN. The position feedback sensors as well as the force sensor are calibrated by direct comparison with reference standards.

The functionality of the tensile tester is demonstrated by the automated stiffness measurement of the elongated cells in plant hairs (trichomes) as a function of their size. This enables a quantitative understanding and a model-based simulation of plant growth based on actual measurement data.

S. Muntwyler, B. Kratochvil, F. Beyeler, B. Nelson
Institute of Robotics and Intelligent Systems, ETH Zurich. Work performed at Nanofabrication Center, University of Minnesota

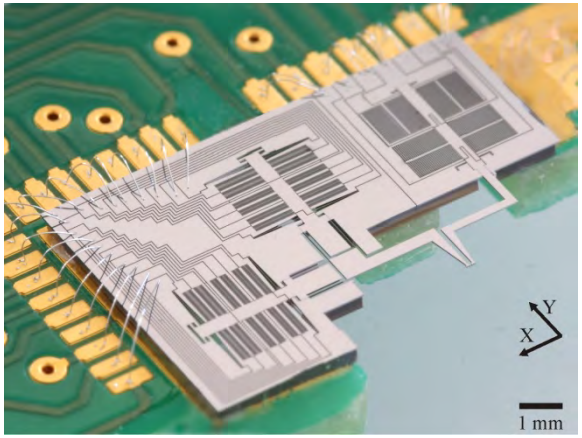

Monolithically integrated two-axis micro-tensile tester.

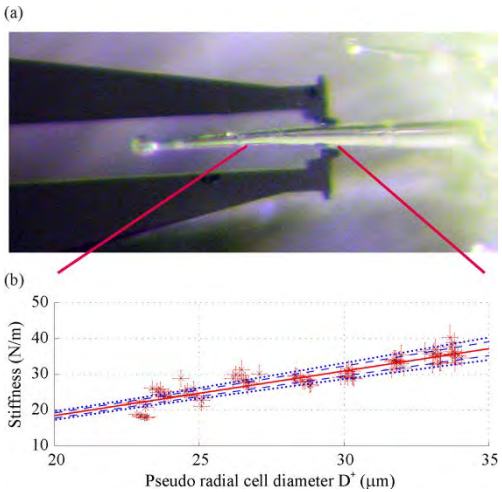

Measurement results of the cell characterization:

Wafer-Level Comb Drive Inspection System

A non-contact method for testing comb drive based MEMS devices based on piezoelectric excitation of MEMS structures on a wafer has been investigated.

Experiments with a wafer with microgrippers have shown that defective devices can be reliably detected by the proposed method. The presented method is not limited to microgrippers. It can also be applied to inertial sensors such as accelerometers and gyroscopes as well as actuators such as electrostatic resonators and MEMS switches. This versatility makes the system a powerful tool for wafer-level testing of unpackaged MEMS dies.

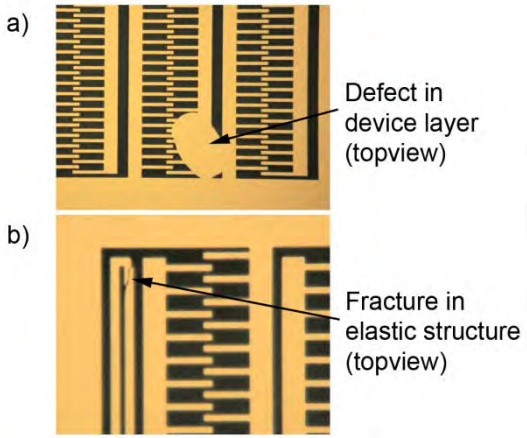

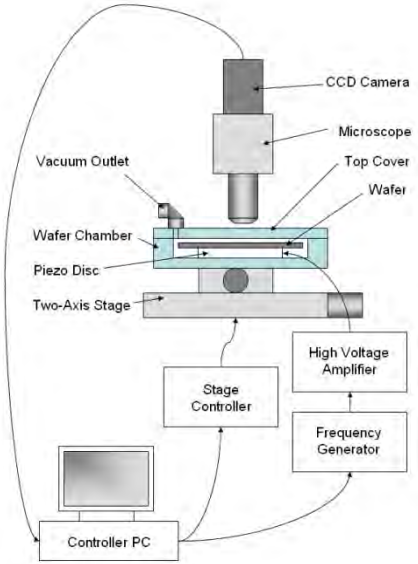

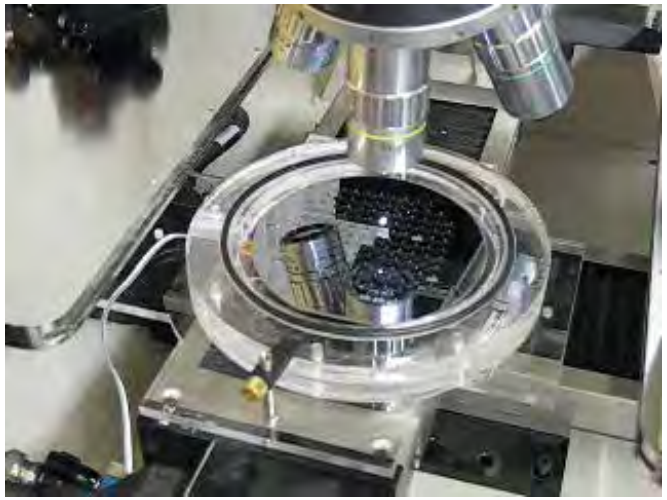

F. Beyeler, S. Muntwyler, B. Nelson
Institute of Robotics and Intelligent Systems ETH Zurich. Work performed at Nanofabrication Center, University of Minnesota

MEMS-based Nanoindentation Transducer

As more nanomechanical testing applications need to measure lower force and smaller scale development with better stability and faster operation speed, further advances in transducer technology are highly demanding. A MEMS-based nanoindentation transducer is developed to meet the demands for more advanced tests. The transducer has high precision actuation and high bandwidth dynamic characteristics as well as low noise level in displacement and force measurements.

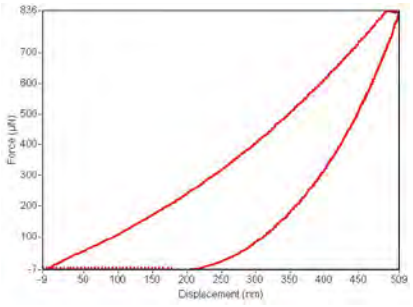

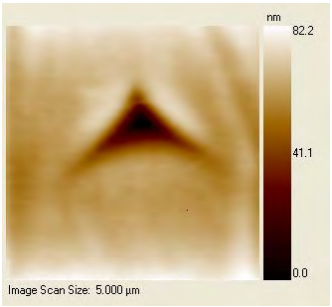

Nanoindentation data taken on a polycarbonate sample and the corresponding indent image. Indentation and the imaging were performed using the developed MEMS transducer.

The advantages of this transducer are tremendous since it has high bandwidth actuation, good controllability, and can be used in many challenging environments such as in high vacuum and under high temperature. Owing to its small scale, the MEMS transducer can be used in instruments allowing extremely small space for transducer placement such as inside transmission electron microscope holders.

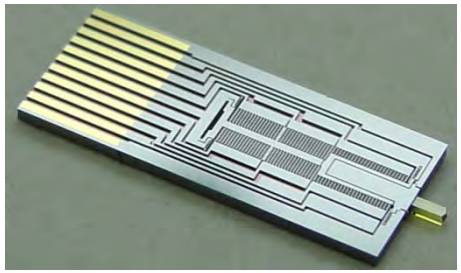

Developed MEMS transducer (patent pending).

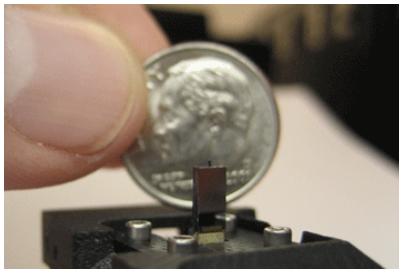

Packaged MEMS transducer for nanoindentation instrumentation.

J.Y. Oh, S.A. Syed Asif, O.L. Warren
Hysitron, Inc.
Work performed at Nanofabrication Center, University of Minnesota

Optimizing Chemo-Mechanical Structure for MEMS Chemical Vapor Sensor

We have developed and optimized an integrated gas sensor system that achieves higher performance and is fabricated inexpensively and reliably. We created a variety of mass sensors, prepared a polymer matrix with sensing probe coating, and incorporated chemical and structural behaviors into a design optimization procedure.

We see a steady state fluorescence response of polymer in the presence of HF and good dynamic performance in atmosphere pressure.

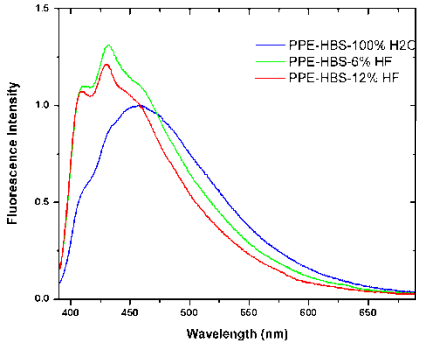

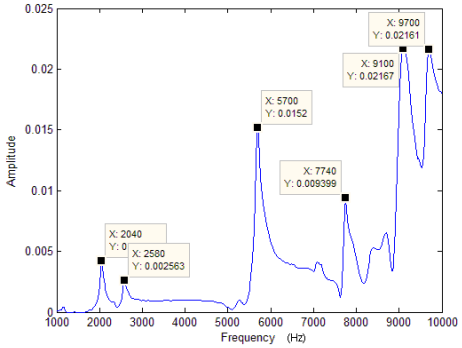

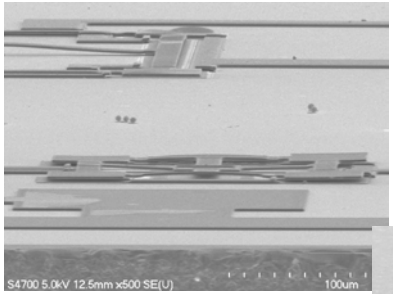

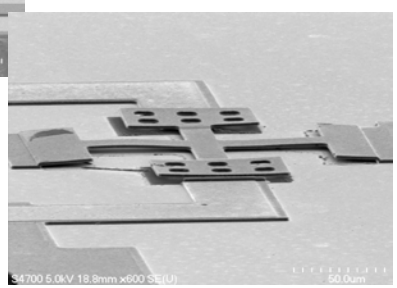

M. Miller, C. Li, J. Singh
Electrical & Computer Engineering; Mechanical Engineering
Michigan Technological University
Work performed at Nanofabrication Center, University of Minnesota

Radiation Sensing for Environment Aware Fault Mitigation

This program exploits reprogrammable hardware fabrics to increase the efficiency of flight computers by improving computational power, increasing fault tolerance and reducing mass. Spatial sensitive radiation sensors were designed and fabricated to detect the location and trajectories of radiation strikes that cause single event upsets and single event functional interrupts. The information is used to more effectively search for radiation induced errors in reconfigurable computing platforms.

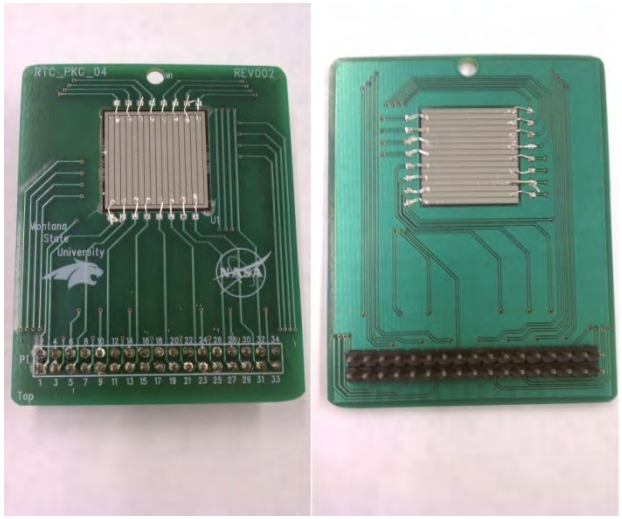

Packaged Sensor

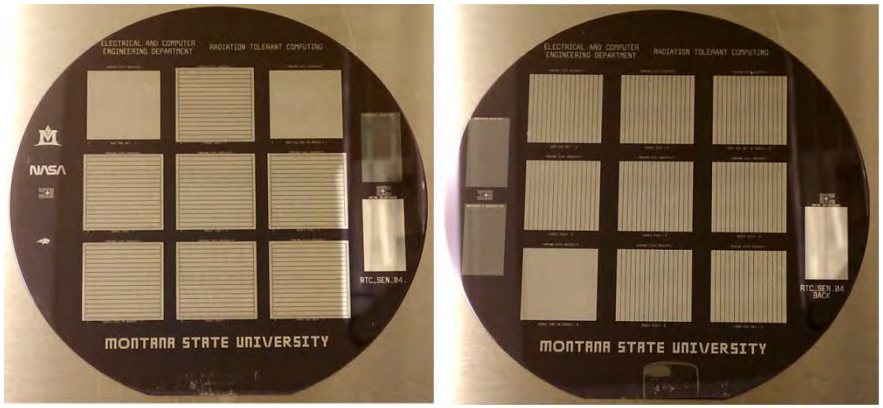

Front and Back of Radiation Sensor Wafer

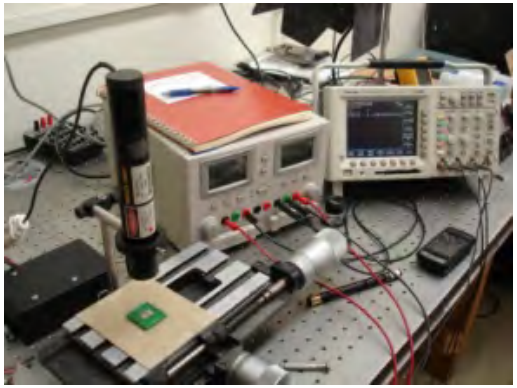

Sensor Characterization and Testing

Todd J. Kaiser, Brock J. LaMeres: Montana State University Mask Set for Position Sensitive Radiation Sensor Fabricated at Nanofabrication Center, University of Minnesota

RoboCulture

We are researching the automated dissociation of the drosophila central nervous system (CNS) in a microdevice. We dissociate the CNS in a microfluidic device under controlled conditions, characterize the conditions required for dissociation (e.g. shear stress, number of cycles), and culture the neuron cells obtained from the dissociation with various drugs to observe the developmental effects. The overall goal is to create an automated system for high-throughput drug screening.

The devices are still in developmental stages, having undergone many evolutions. Early results show that the tissue can easily be dissociated within the microfluidic device and that the cells remain viable and can be cultured afterward.

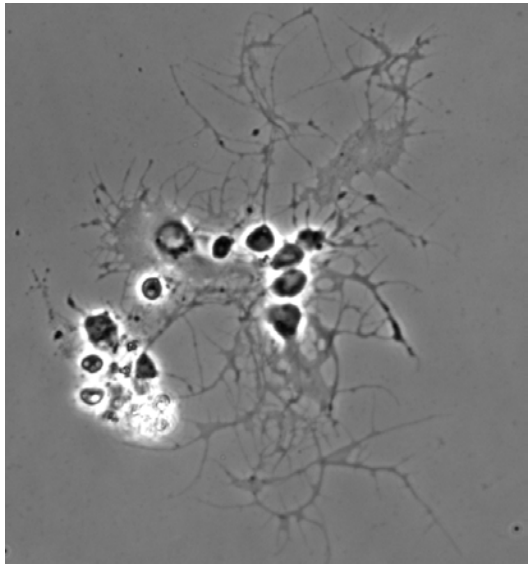

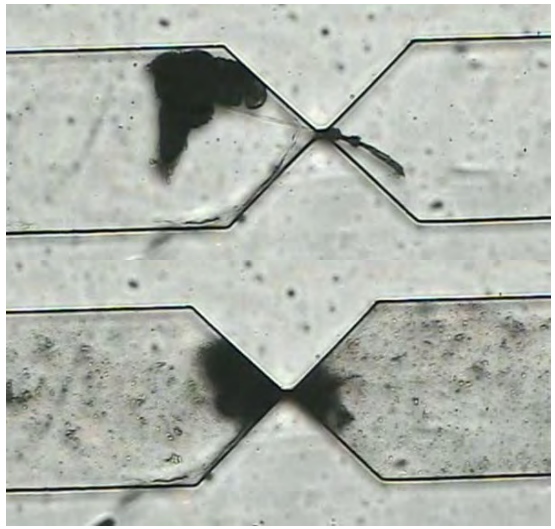

Y. Zohar, M. Stamm; L. Jiang; R. Kraft
Aerospace & Mechanical Engineering; Optical Sciences; Neuroscience
University of Arizona
Work performed at Nanofabrication Center, University of Minnesota

NNIN Site at the University of Texas

Two Dimensional Phonon Transport in Supported Graphene

Suspended graphene has demonstrated ultrahigh electron mobility and thermal conductivity, making it attractive for electronic applications. However, graphene is often supported on a substrate for device applications, and the effect of substrate interaction on thermal transport has not been elucidated. In this work, we showed experimentally that **the thermal conductivity of single layer graphene (SLG) exfoliated on a silicon dioxide support is still as high as about 600 W m^{-1} K^{-1} near room temperature, exceeding that of copper.**

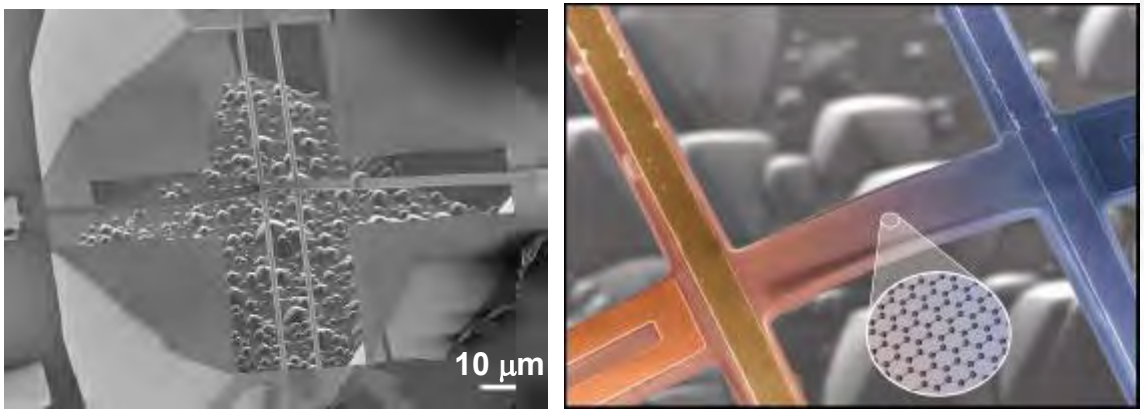

(Left) The suspended microdevice used to measure SiO_2-supported single layer graphene (SLG) samples. (Right) A false-color close-up of the SLG-on-SiO_2 bridge region. The supporting beams are SiO_2 with Au/Cr lines for use as resistance thermometers. Joule heating in one of the lines is used to impose a temperature gradient on the bridge region.

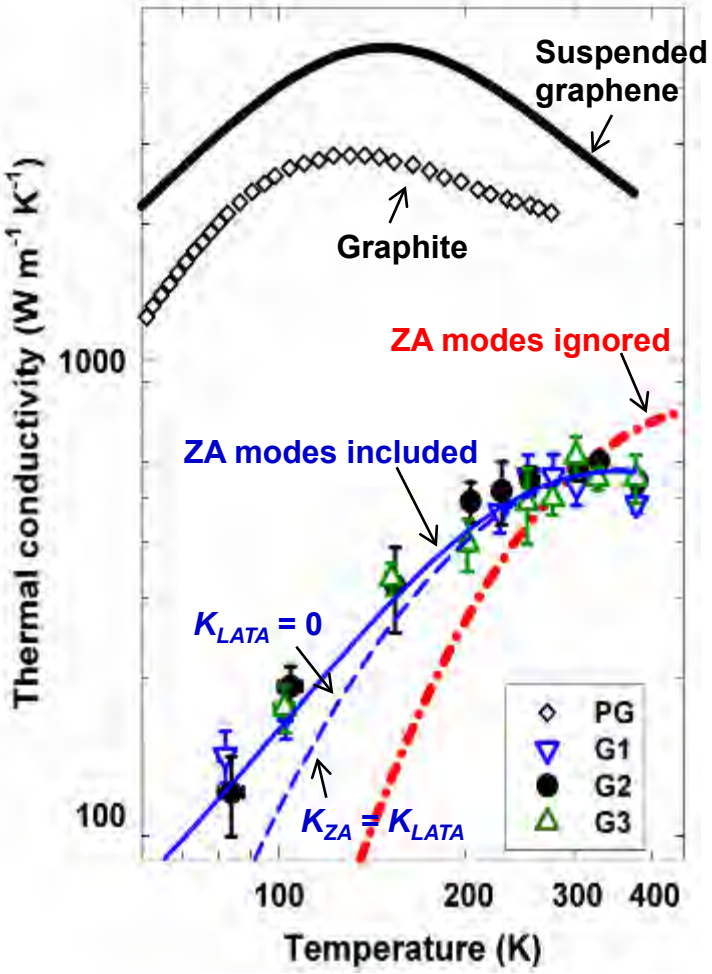

The measured thermal conductivity results for three SLG samples (G1, G2, and G3) along with bulk graphite data and numerical calculation results for suspended and substrate-supported SLG.

Fabrication and measurement performed at UT-Austin
Modeling performed at Boston College, UT-Austin, and CEA-Grenoble

Sub-wavelength Resolution Microspectroscopy

The goal of this project is to identify materials on nanoscale. We are developing photoexpansion microscopy for measuring local infrared (λ=2.5-30 μm) and terahertz (λ=30-300 μm) absorption spectra of chemical/biological samples with sub-100 nm spatial resolution using compact low-power quantum cascade lasers (QCLs). This method detects light absorption by measuring associated local thermal expansion in thin samples with an atomic force microscope (AFM) cantilever in contact with the sample surface.

Photoexpansion signal is greatly enhanced by a Q-factor of an AFM cantilever when the repetition rate of our QCLs is tuned in resonance with the mechanical frequency of the cantilever. As a result, low-power light sources such as QCLs can be used.

Nanostructured Optoelectronics Group
Prof. Mikhail A. Belkin. Work performed at UT-Austin.
Work performed at UT-Austin.

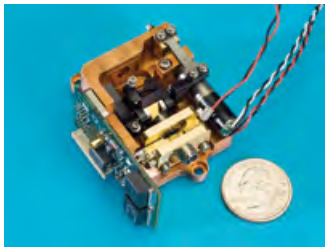

External-cavity QCL

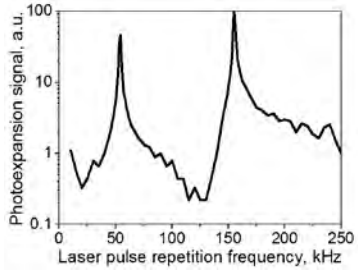

Resonance enhancement of an AFM cantilever

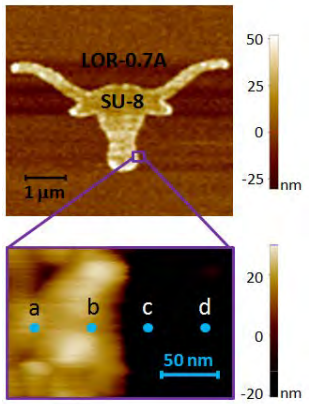

Topographic image

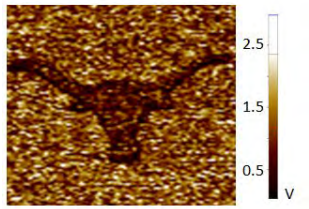

Infrared photoexpansion image @ λ= 8.3 μm

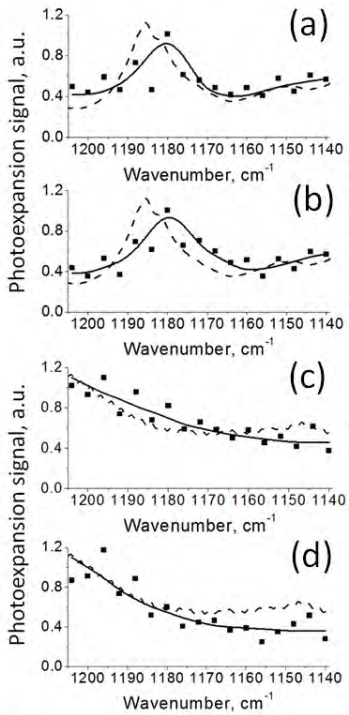

50 nm (λ /170) spatial resolution demonstrated by spectra

Structure-Thermal Relationships of Bi-Layer Graphene

High power dissipation is an increasing important challenge in highly miniaturized electronic devices making high mobility, high thermal conductivity materials such as graphene increasingly attractive for use in nanoelectronic devices and for thermal management solutions.

We have been able to elucidate the structure-thermal property relationship of individual graphene crystals using a suspended microthermometer device fabricated at MRC to allow for a fundamental understanding of thermal transport processes in these materials.

Our findings provide an important insight for the use of graphene as filler materials in polymeric nanocomposites.

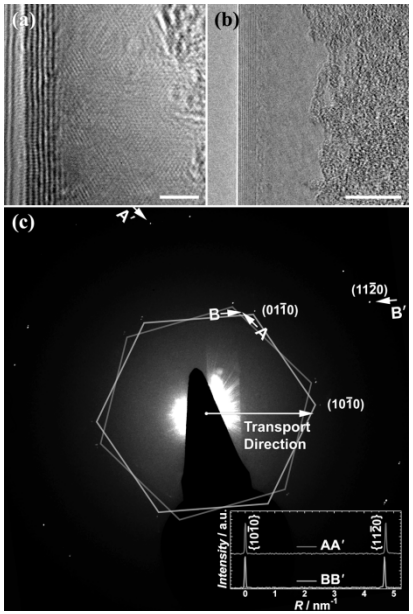

(a) Transmission electron micrograph of a bi-layer graphene sample. (b) Lower resolution reveals a relatively uniform layer of organic residue approximately 10 nm from the quintuple-folded edge. (c) Diffraction pattern using a 335 nm coherent electron beam, revealing turbostratic stacking. (inset) Intensity profiles along AA' and BB' reveal that each set of reflections result from an individual graphene layer. Scale bars in (a) and (b) are 2 nm and 10 nm, respectively.

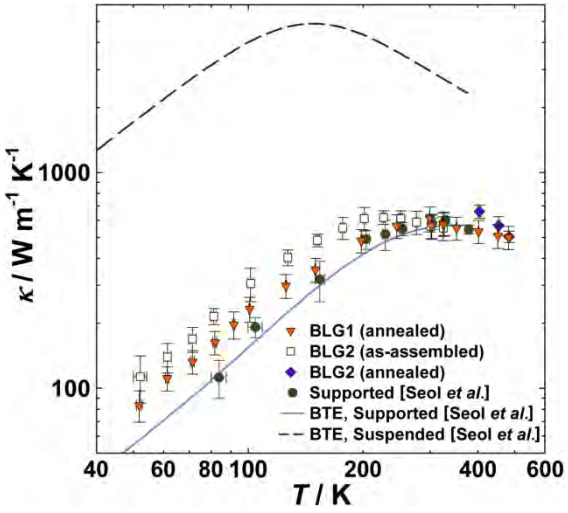

As-measured effective thermal conductivity (κ) versus temperature (T) for the two bi-layer graphene samples in this work. Shown in comparison are the reported κ values of a graphene single-layer supported on SiO_2 along with the numerical solution to the Boltzmann transport equation (BTE) for supported (solid blue line) and suspended (dashed black line) graphene from Seol et al., Science 328, 213 (2010).

Michael Pettes, Insun Jo, Zhen Yao and Li Shi, UT Austin, Work performed at UT Austin

Quasi-Free Standing Epitaxial Graphene Bilayer on SiC

Graphene bilayers in Bernal stacking exhibit a transverse electric field tunable band gap, a property that renders this material attractive for device application.

We fabricated top gated devices using graphene bilayers grown on SiC substrates, and investigated the transport properties in high magnetic fields and at low temperatures. At the charge neutrality point the longitudinal resistance shows an insulating behavior, as a consequence of energy gap opening. Quantum Hall states with filling factors ν=4, 8, observed at high magnetic fields establish the Bernal stacking arrangement of the grown graphene bilayer.

These findings render this system attractive for electronic and optoelectronic device applications, thanks to its high mobility, and tunable energy gap.

Kayoung Lee, Seyoung Kim, Micah S. Points, Emanuel Tutuc
Microelectronics Research Center, The University of Texas at Austin

Taisuke Ohta, Thomas E. Beechem,
Sandia National Laboratories

Work performed at UT-Austin.

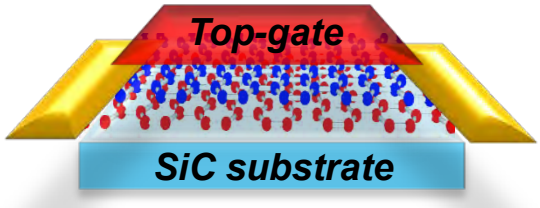

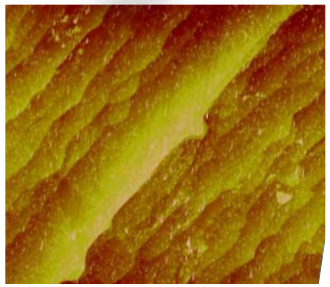

Topography of the SiC probed by atomic force microscopy.

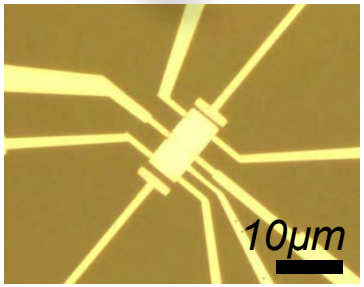

Optical micograph of a top gated graphene bilayer device on SiC.

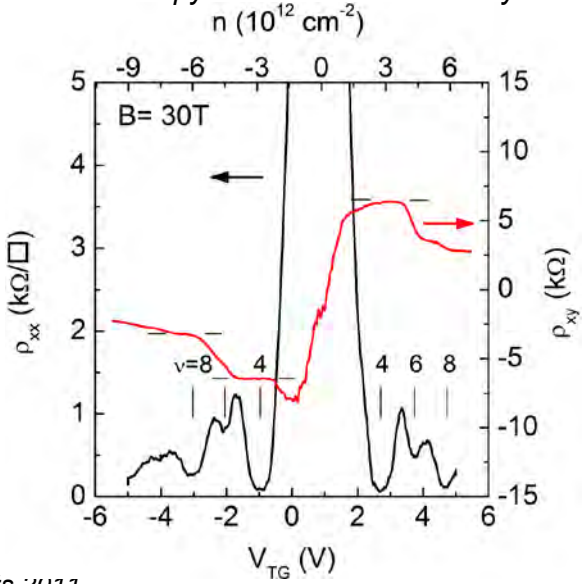

Longitudinal (ρ_{xx}) and Hall (ρ_{xy}) resistance vs. top gate bias (V_{TG}) (bottom axis), and density (n) (top axis), measured at B = 30 T, and T = 0.3 K.

Optical Beam Steering Project

We demonstrated design, fabrication and characterization of an optical phased array implementation on silicon nanomembrane. The array configuration is non-uniform and is designed to avoid grating lobes inside the field of view during beam steering while allowing the separation of the waveguides to be large enough to prevent optical coupling. A 1x12 multimode interference optical beam splitter provides the arrayed waveguides with uniform excitations. Individually controllable micro heaters are used to modulate the optical phase in the arrayed waveguides. An optical beam steering angle of 10.2° in a planar guide corresponding to 31.9° steering in air is demonstrated, which is the largest steering angle presented to date using single-stage phased array systems.

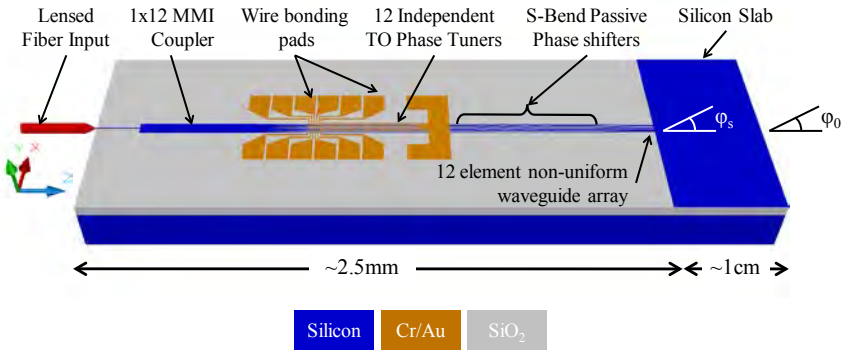

A schematic of silicon photonics based large angle optical beam steering chip

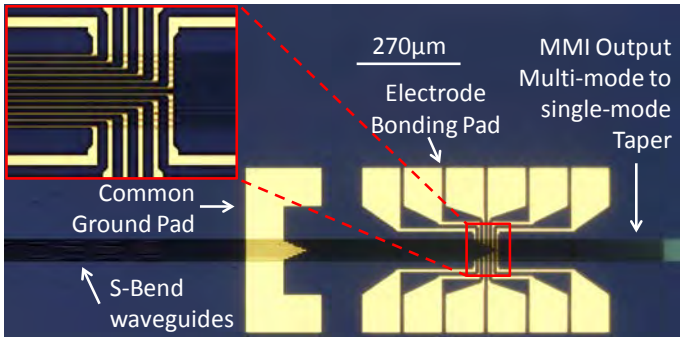

Fabricated photonic and electrical circuits

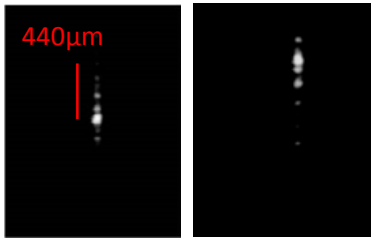

Observed optical beam steering

Prof. Ray Chen
Amir Hosseini, David Kwong, and Yang Zhang
Work performed at UT Austin.

Nanopatterned a-Si thin film solar cell

The purpose of this project is to optimize the nanostructure of the amorphous and micromorph silicon-based solar cells to enhance the light absorption, and then to increase the power conversion efficiency at low cost.

The use J&FIL nanoimprinting technology to fabricate 3D nanostructured substrate provides the opportunity to well control the pitch, shape and roughness of the features to maximize the light trapping while reducing the recombination of excitons. Data have shown a 70% improvement of patterned substrates over plan ones in term of photocurrent

Thin film photovoltaic panels being installed onto a roof

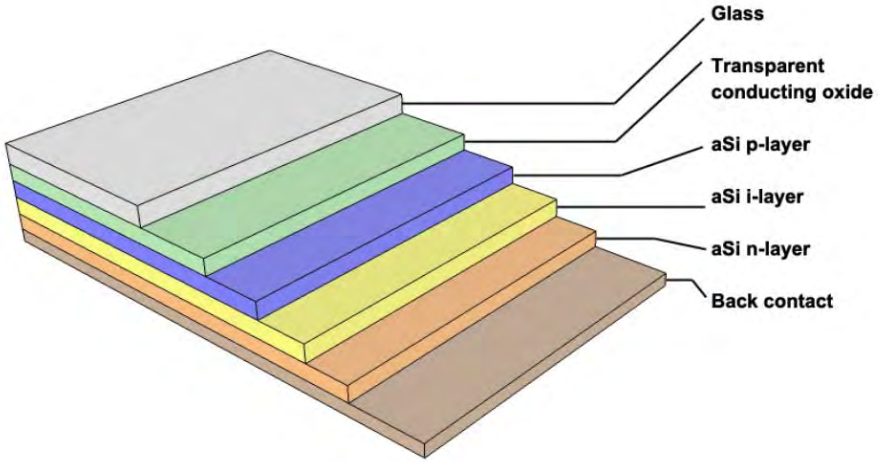

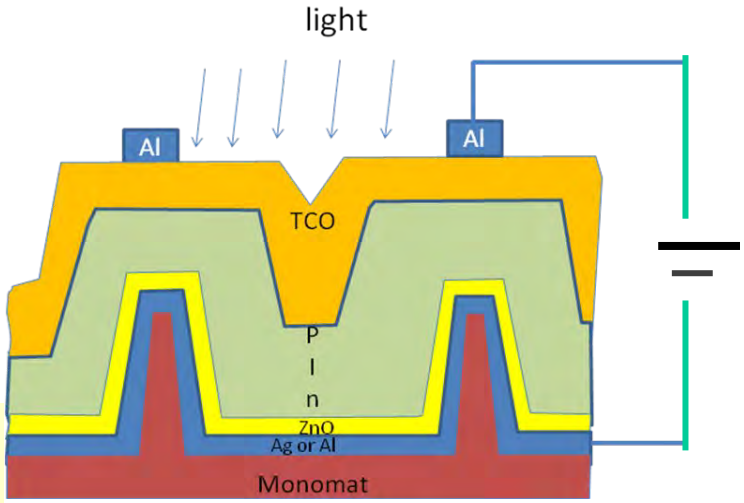

F. Wan, M. Menezes, S.V. Srinivasan, Molecular Imprints, Inc.

Work performed at UT-Austin.

Stabilization of Alkaline Phosphatase with $Au@Ag_2O$ Particles

The purpose of stabilizing Alkaline Phosphatase (AlkP) with core@shell nanoparticles is to protect the enzyme from organic inhibitors and retain catalytic activity for biosensing applications.

The nanoparticle-stabilized AlkP was highly active in the presence of inhibitory chemicals urea and L-phenylalanine (Phe) while wild-type enzyme was largely inhibited. We attribute protection to the Ag_2O shell.

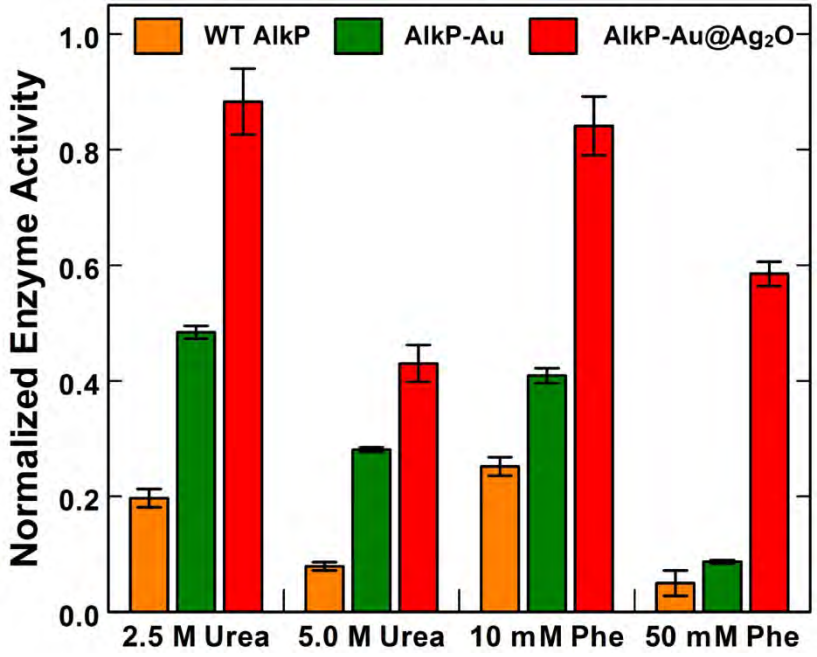

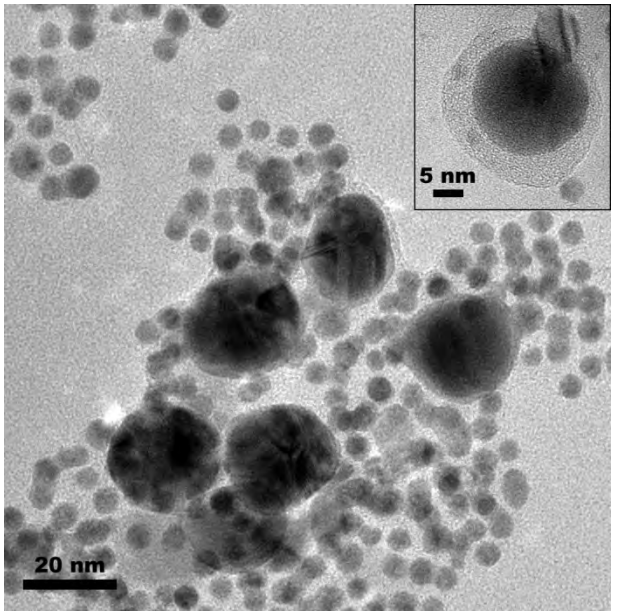

A transmission electron micrograph, (above) and element map, (below) of enzyme-containing nanoparticles having a core@shell structure.

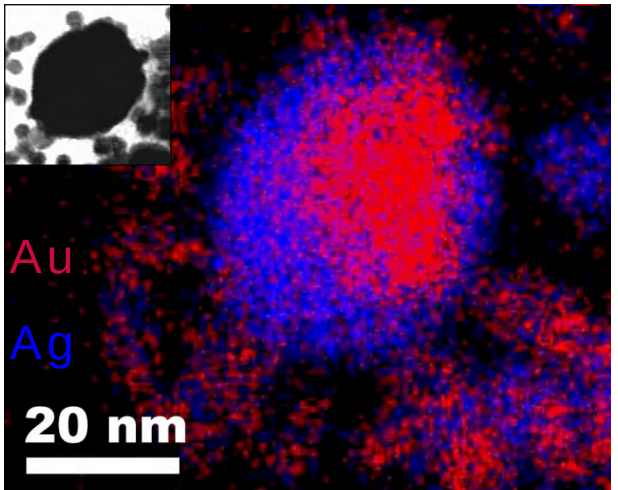

Brian A. Zaccheo and Richard M. Crooks, UT Austin.
Work performed at UT Microelectronics Research Center.

NNIN Research Highlights 2011

Microthermoelectric devices

For this program, Nanohmics is using the lithographic processing capabiltiies of the MRC to fabricate the mold for preparing a flexible thermoelectric cooler devices composed of consolidated nanophase microdice. Solid state heating or cooling devices that can be made more efficient by virtue of increasing the thermoelectric Figure of Merit hold promise in small device heat dissipation (detectors, microchips) as well as larger scale heat recovery process (thermoelectric generators)

Bi2Te3 filled SU-8 cavity molds

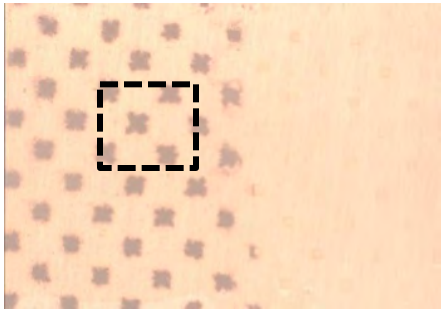

Steve Savoy- Nanohmnics, Inc.
Kevin Stokes- University of New Orleans
Rhonda Willigan- United Technologies

Work performed at University of Texas at Austin Microelectronics Research Center

Hyperspectral Infrared (IR) Windows

Nanohmics is developing methods and materials to coat zinc sulfide windows. Such windows serve as primary protection for sensitive multi-band electro-optic instrumentation or sensors in aerospace platforms. It is critical in most of these applications that the hyperspectral window resist erosion from raindrops and dust encountered during flight, and that spectral transmittance is not degraded as a result.

Zinc sulfide windows have poor erosion resistance and so a protective coating is required for applications where impact with sand, dust, or raindrops is anticipated. Nanohmic's work has been creating and characterizing a patterned surface for windows that reduces optical reflections, in addition to providing enhanced protection from rain and sand erosion.

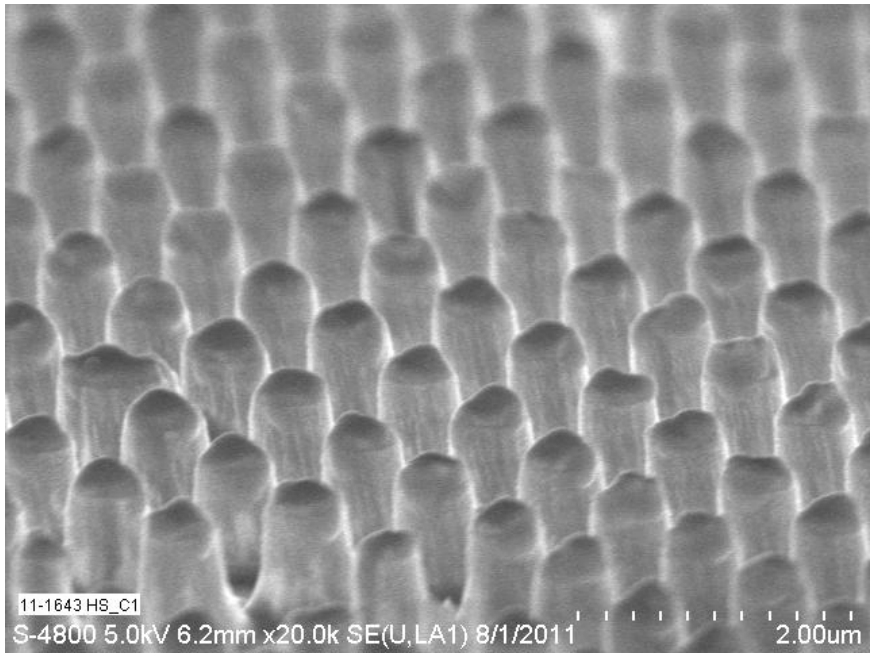

SEM micrograph of Nanostructured Zinc sulfide windows.

Steve Savoy, Byron Zollars Nanohmnics, Inc.

Work performed at University of Texas at Austin.

EpiFlex™ Metamaterial

Nanohmics working in collaboration with Professor Gennady Shvets at The University of Texas at Austin, is developing EpiFlex™ Metamaterial film technology that involves fabrication of precision nanoscale structures on large area flexible films. These films will enable a number of applications in the visible and NIR spectrum such as multispectral mosaic filters, wavelength-specific emitters and wavelength-selective absorbers/reflectors in sensing applications.

Wu et al., Phys. Rev. B 2011 84(7)

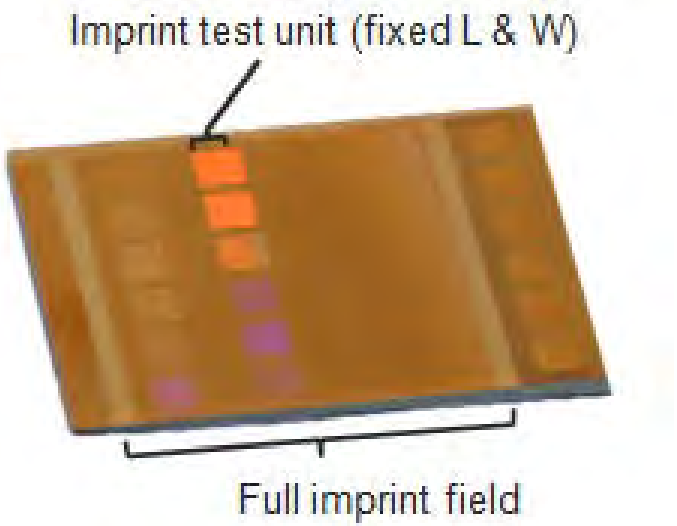

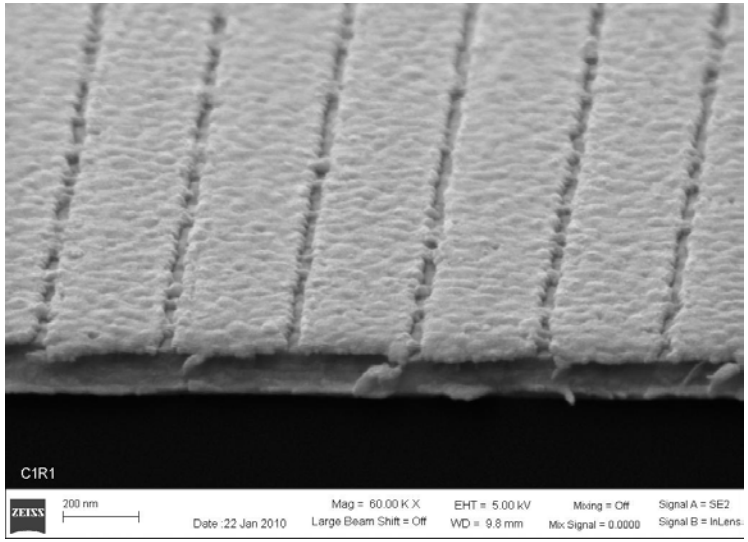

Andrew Milder, Nanohmnics, Inc. and Gennady Shvets at The University of Texas at Austin

Work performed at University of Texas at Austin Microelectronics Research Center

High efficiency, flexible photovoltaics

Nanohmics, working in collaboration with Professor Gennady Shvets of the University of Texas at Austin and Dr. Brad Clevenger at Emcore Photovoltaics, propose to develop Immagen™ Technology, a power generation device that includes integration of state-of-the-art Emcore IMM photovoltaics into a large area conformal device for military remote recharging and lightweight power scavenging applications.

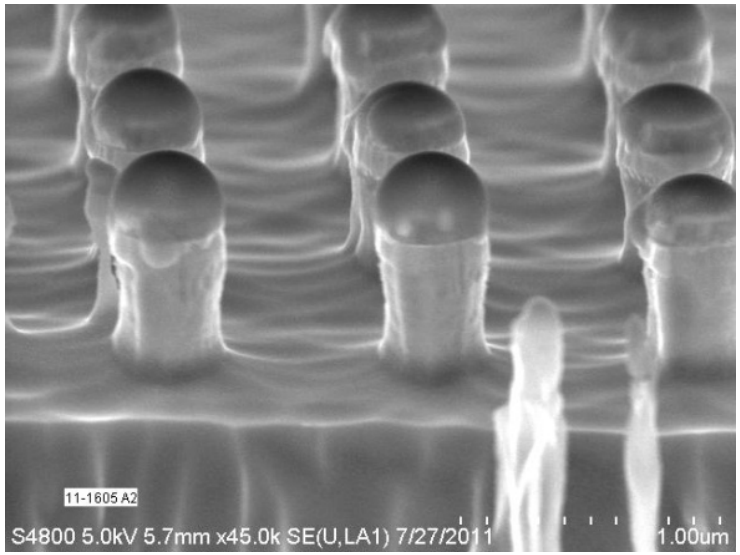

Steve Savoy, Nanohmnics, Inc. and Gennady Shvets at The University of Texas at Austin, *Dr. Brad Clevenger at Emcore*

Work performed at University of Texas at Austin Microelectronics Research Center

Synthesis and combined theoretical/experimental characterization of MoS_2 nanostructures

The purpose of this research project is the understanding of structure/function relations in catalytic active nanostructured materials.

Samples were synthesized using Ammonium Tetra-Thiomolybdate as precursor agent, and under high pressure and low temperature conditions. Optimization of Hydrothermal synthesis parameters has been thoroughly studied. Characterization of samples were done by, XRD, HRTEM/ Transmission and Scanning mode, EDX, Molecular Modeling

M. Ramos, R. Chianelli, The University of Texas at El Paso.

Work performed at University of Texas at Austin.

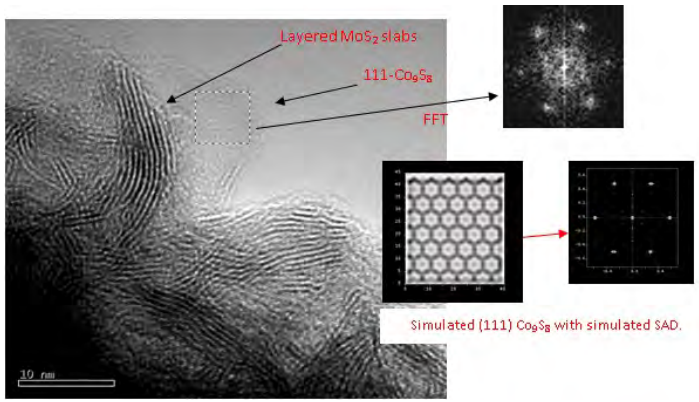

Epitaxial growth of MoS2 over (111)-Co substrate. One can observed laminar MoS_2 getting attach to Cobalt surface, this could be the localization of promoted catalytic area.

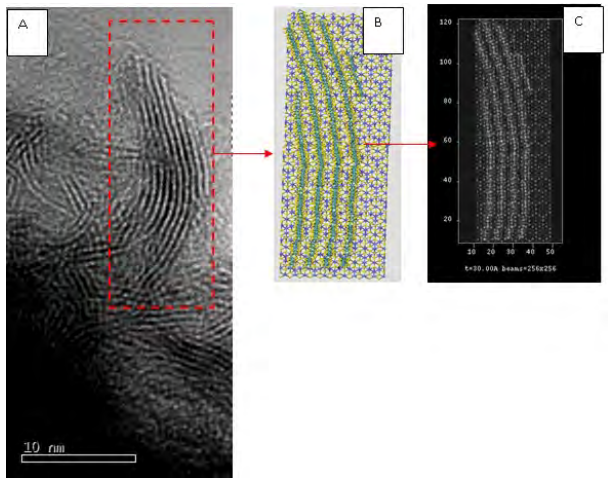

Molecular modeling of epitaxial growth of MoS2 over (111)-Co substrate. In search of resolving observed structure by HRTEM imaging.

Nanomembrane Photonics Project

The purpose of the Nanomembrane (NM) Photonics Project is to provide ultra compact and flexible also high performance photonic devices.

With further process optimizations, transferred NMs can find wider and practical applications in various electronic and photonic device and integration system applications

Frame-assisted membrane transfer (FAMT) process

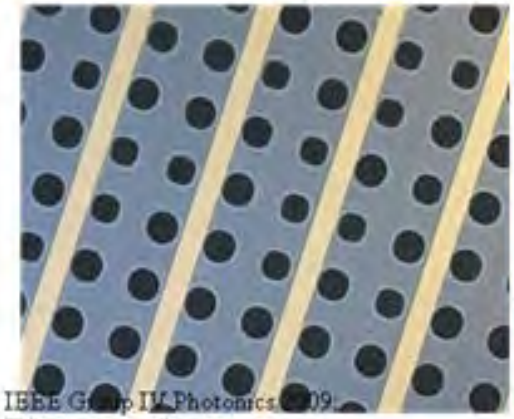

- IEEE Group IV Photonics 2009
- US patent pending

Large area flexible photodetectors and solar cells

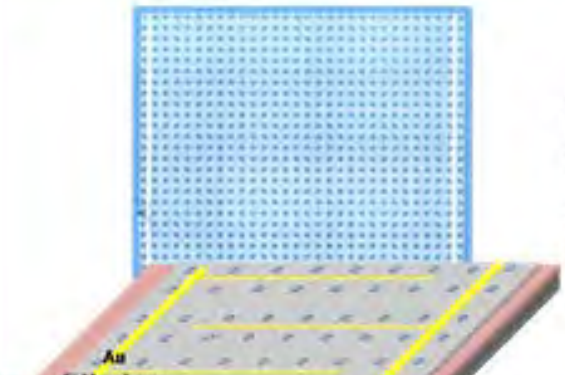

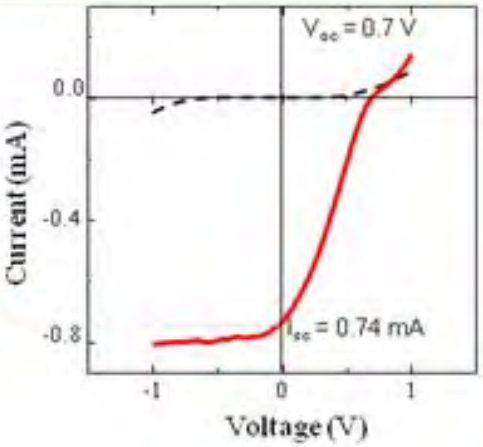

- IEEE Group IV Photonics 2009
- Appl. Phys. Lett. Vol. 96, 121107 (2010)

W. Zhou, Univeristy of Texas-Arlington,, and SiNMs

Work performed at UT-Austin.

New Graphene Wafer-Scale (Shared) Capability

Objective: Wafer-scale growth of graphene for Si/graphene heterogeneous electronics

Capabilities

- 4” wafer capability
- CVD or PECVD growth mode
- Pulsed plasma control
- Independent vapor and substrate temperature control
- CH_4, C_2H_2, and C_2H_4 precursors
- Automated computer control for routine repeatability

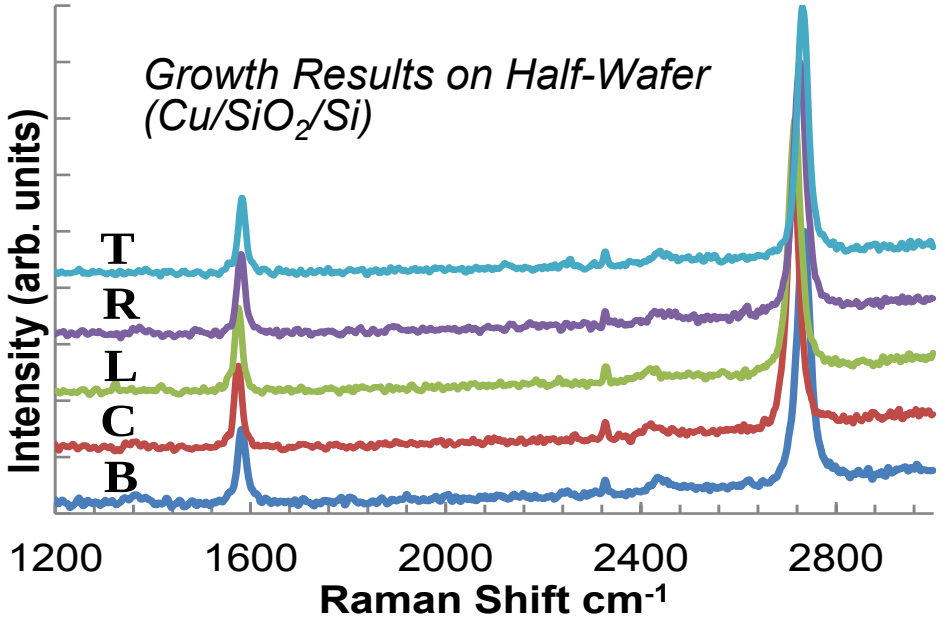

Deji Akinwande, University of Texas-Austin Facility.

Work performed at UT-Austin.

High-throughput method for atom-sized drug-delivery devices

NanoMedical Systems is a medical device manufacturer that produces long-term implantable drug-delivery devices which use a silicon nanofabricated chip to control drug release

- NanoChannel heights 2nm ~ 50+nm
- NanoChannel density over 100,000/mm^2

NNIN Research is focused on removal of protective layers and defects to perfect the cleanliness of the product

Post-fabrication chips are cleaned and exposed to various experimental chemistries for inspection and design of best manufacturing process

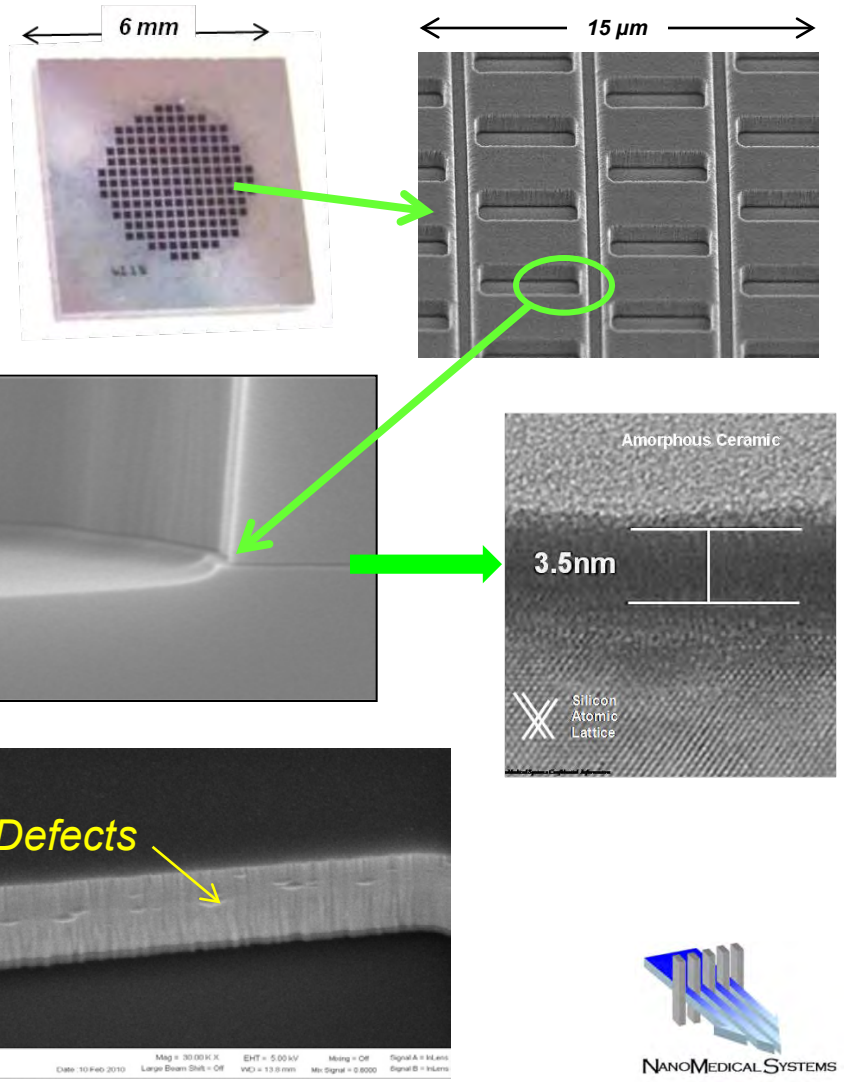

NanoMedical Systems

Work performed at Microelectronics Research Center at the University of Texas at Austin

Evaluation of cleans efficacy of nanofluid chips under the SEM

Surface Plasmon Enhanced Fluorescence and Organic Solar Cells

The purpose of this undergraduate student led research is to tailor the plasmonic properties of metallodielectric gratings for applications including:

•Fluorescence Enhancement – Slot gratings offer multiple modes of plasmons, leading to a broad band of plasmon wavelengths. This allows for multi-color fluorescence enhancement on a single substrate

•Increased Efficiency of Organic Solar Cell – We pattern the metal electrode of organic solar cells with a sinusoidal grating whose plasmons are tuned to the absorption spectrum of the active layer to enhance solar efficiency

Over a dozen undergraduate students have participated in this work over a five year period, most of which went on to graduate school or medical school.

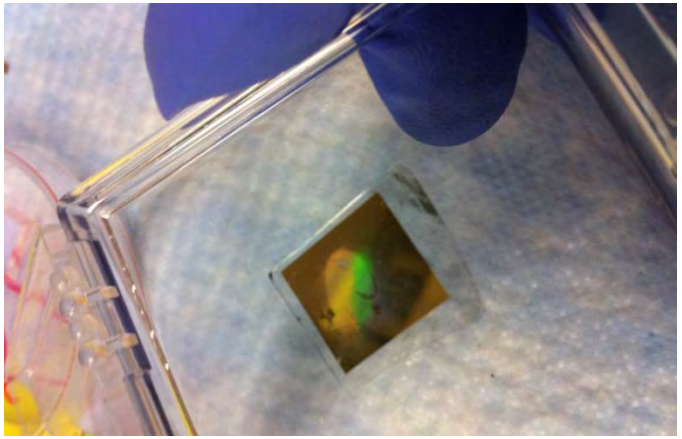

833 nm period gold wire grating made with microcontact printing for fluorescence enhancement.

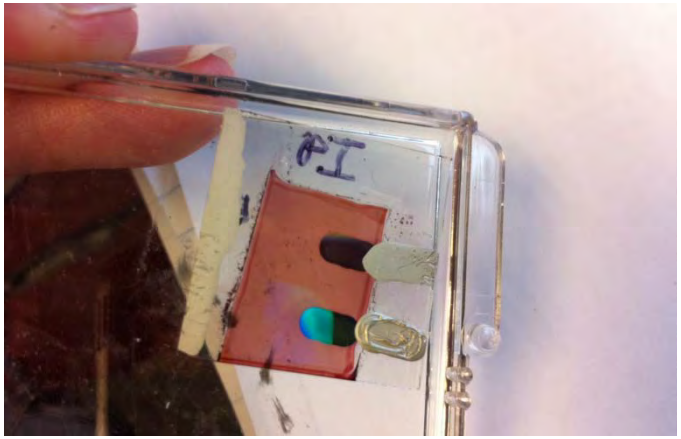

Organic Photovoltaic solar cell with a 416 nm period grating formed on the aluminum electrode.

Jennifer Steele, Department of Physics and Astronomy, Trinity University

Work performed at Microelectronics Research Center at the University of Texas at Austin

NEAT Energy Converters

The goal of our research is to realize high-efficiency electronic energy converters that exploit nonequilibrium transport effects and energy selective tunneling at semiconductor-metal interfaces. These NEAT devices are an enhanced version of thin film thermoelectric coolers, and will be incorporated in the cooling engines designed by Sheetak for compact refrigerator and air-conditioner OEMs in US and India. The NEAT project has been funded by BEET-IT program of ARPA-E for improving air conditioners in buildings and homes.

We use advanced PVD and CVD methods to deposit bismuth chalcogenides and fabricate cooler elements with phonon-blocking tunneling layers that reduce the thermal conductance without affecting the electronic conduction processes.

U. Ghoshal, A. Guha, A. Stautzenberger, and M. Grigas
Sheetak Inc.

Work performed at UT-Austin.

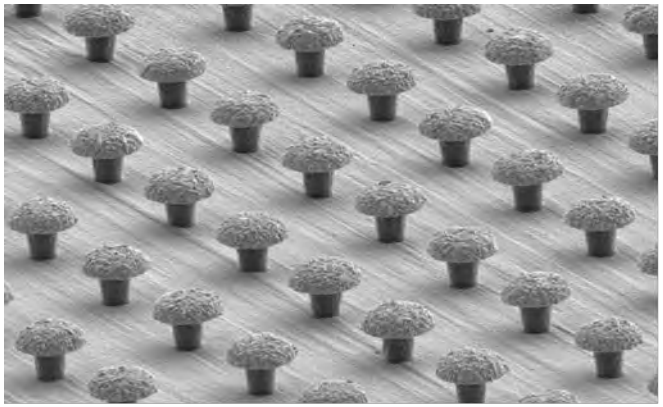

Constellation of constricted contacts for Sheetak's energy converter

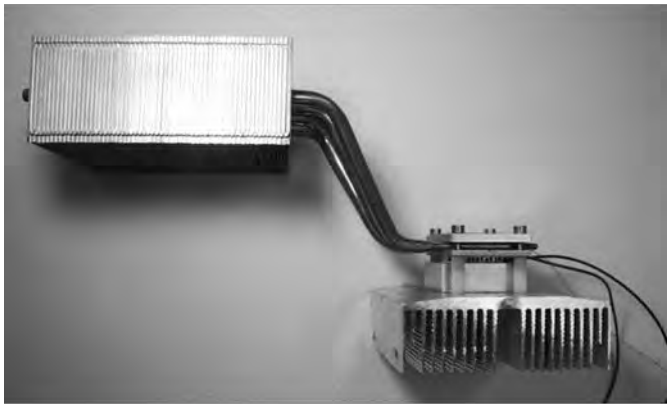

Sheetak's solid-state cooling engine for refrigerators

sheetak

arpa·e
Advanced Research Projects Agency • ENERGY

NNIN
www.nnin.org
Nanoscale Science Engineering & Technology

High Performance MEMS Microphones for Hearing Aids

The purpose of this project is to introduce the first commercialize optical-based MEMS microphone. Semiconductor lasers and diffractive optics enable a robust micro-interferometer, which in turn is used to resolve acoustic waves with 20dB improvement in SNR as compared to conventional miniature microphones. High fidelity MEMS microphones will improve hearing aid performance and the quality of life for those with hearing-impairments.

The ability to apply internal forces to the microphone diaphragm via piezoelectric materials empowers the device with a "self-calibration" feature. Processing of these piezoelectric materials is being developed at UT's MRC.

A MEMS microphone structure fabricated on silicon.

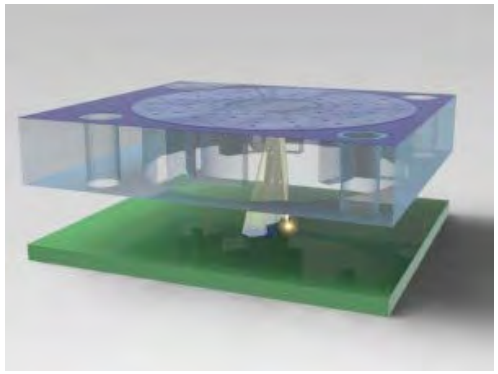

Schematic illustrating optical readout of the microphone diaphragm.

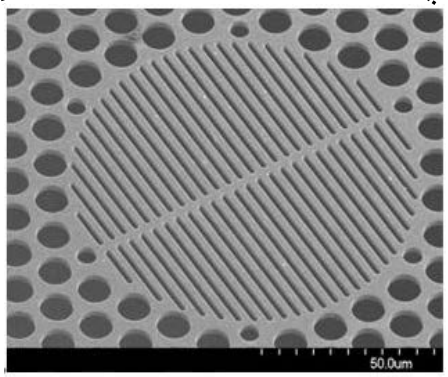

Underneath the diaphragm resides a back-plate consisting of a diffraction grating etched into polysilicon

Neal A. Hall, Arjang Hassibi (UT-PIs), and Silicon Audio, Inc.
Work performed at UT-Austin.

Cancer Cell Imaging with Quantum Dot LEDs

We demonstrate the nanopatterning of multicolored inorganic quantum dot light emitting diodes (QDLED) on silicon for compact multispectral analysis of cancer cells. With well-correlated emission spectra, the QDLEDs works as excitation sources to illuminate cancer cells. Key parameters such as the nucleus-to-cytoplasm ratio of selected cancer cell lines were measured to benchmark cancer progression.

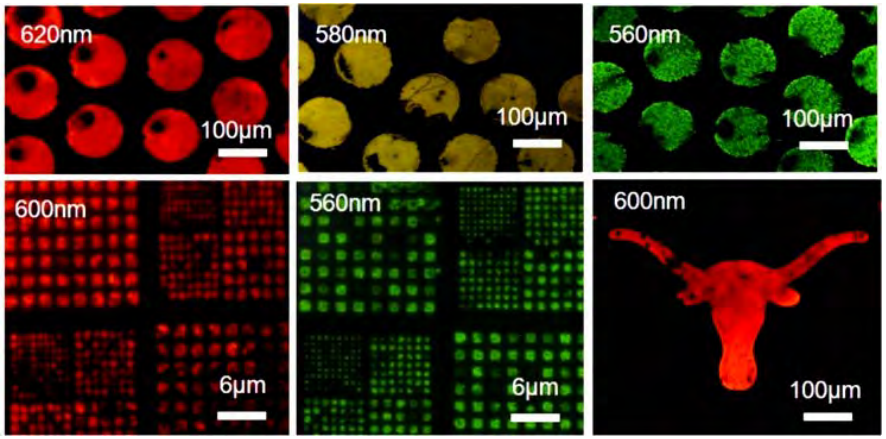

Patterned electroluminescence from the QDLED on created on silicon substrates

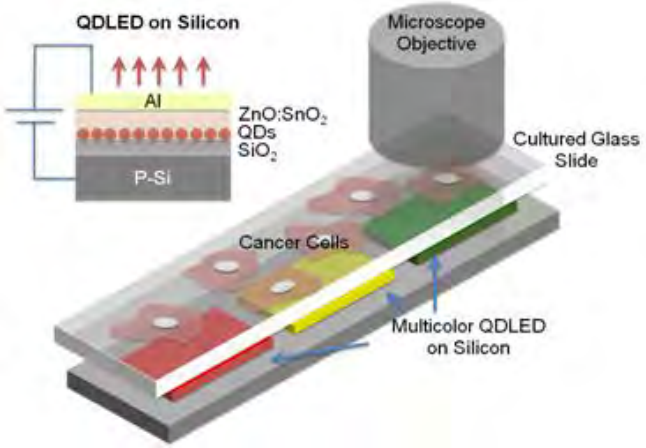

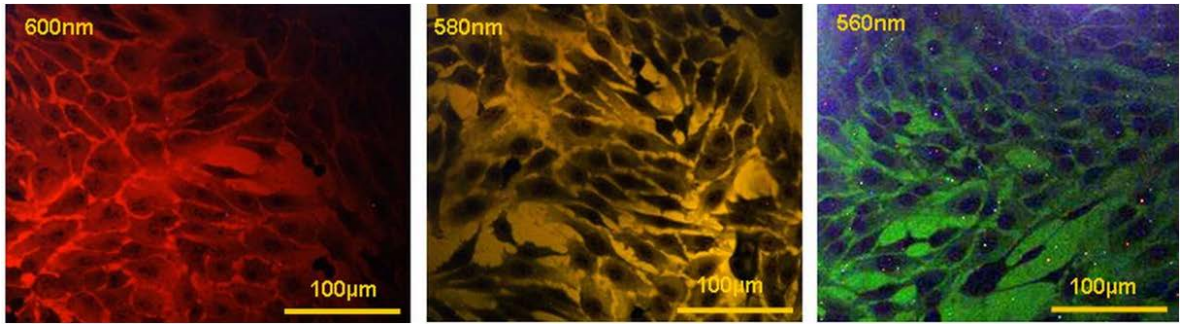

MDA 435 cancer cell illuminated with QD electroluminescence

The John Zhang group, University of Texas at Austin,
Work performed at Microelectronics Research Center, UT Austin

NanoMembrane Photonics Project

The purpose of the nanomembrane photonics project is to develop photonic components based on patterned semiconductor crystalline nanomembranes transferred onto foreign rigid or flexible plastic substrates. Photonic crystal patterning and fabrication process was carried out at NNIN-UT Austin MRC site. High quality flexible photonic filters, ultra-compact membrane reflectors on Si have been fabricated based on membrane printing transfer processes, carried out at both University of Wisconsin-Madison (in collaboration with Prof. Jack Ma) and at University of Texas at Arlington NanoFAB center.

Photonic Crystal structure fabricated at UT Austin MRC site.

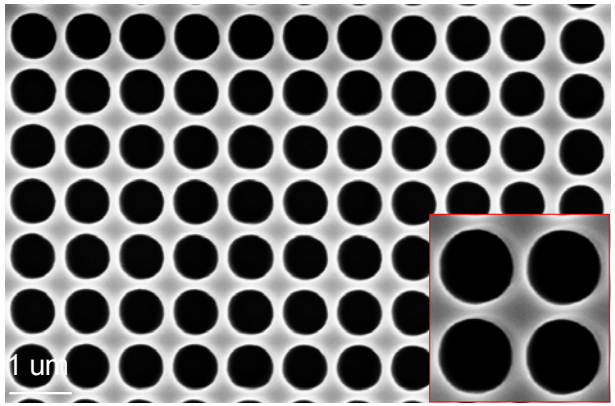

Ultra-compact single layer photonic crystal Fano resonance broadband reflectors on silicon.

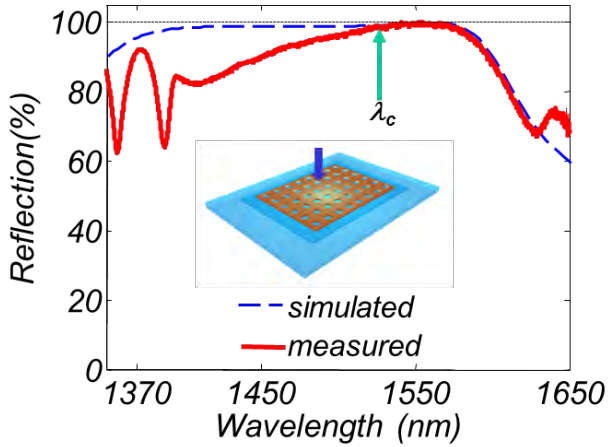

Prof. Weidong Zhou, University of Texas at Arlington, Prof. Zhenqiang (Jack) Ma, University of Wisconsin-Madison

Work performed at UT-Austin.

Enhanced Cooling: Nano-Fins and Nanofluids Integrated with Microchannels & Nano-sensors

Cooling of electronics, lasers, nuclear & solar-power units using nano-scale roughness (nano-fins) and coolants mixed with nanoparticles (nanofluids) are explored. Nano-fins and microchannels enhance the surface area for heat transfer between a hot surface and coolants. Nanofluids enhance the efficacy for heat removal (thermal conductivity) and the heat capacity of various high-temperature coolants. Temperature nano-sensors (TFT) are used for monitoring the coolant performance.

NNIN facilities are used for nanofabrication of nano-fins and temperature nano-sensors (TFT) using nanolithography - Step and Flash Imprint Lithography (SFIL), Electron Beam Lithography (EBL), Physical Vapor Deposition (PVD), Reactive Ion Etching (RIE).

Dr. D. Banerjee (Texas A&M University, College Station, TX, US) and Dr. R. Sadr (Doha, QatarQatar)
PhD Student: Jiwon Yu (US); Post-Doc.: Dr. A. Karanjikarat

Work performed at the NNIN (Univ. of Texas, Austin)

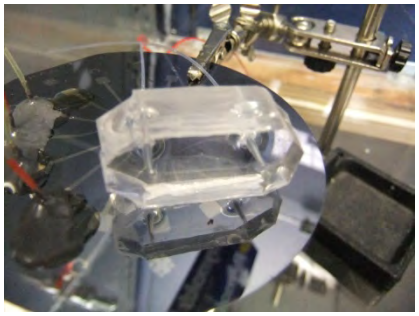

Microchannels integrated with hi-speed temperature nano-sensor array (TFT).

Nano-fins will be fabricated and integrated with micro-channels, temperature nano-sensor arrays as well as nanofluids for enhanced cooling.

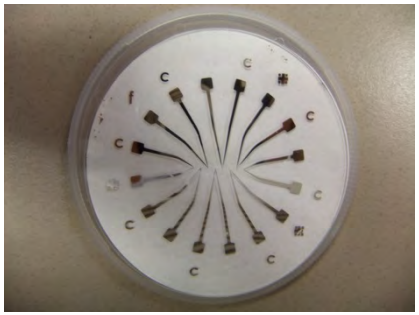

Hi-speed temperature nano-senors (Thin Film Thermo-couples or "TFT") fabricated using PVD and "lift-off" process. The TFT are ~ 200 nm thick and have response speed of ~5-10 MHz.

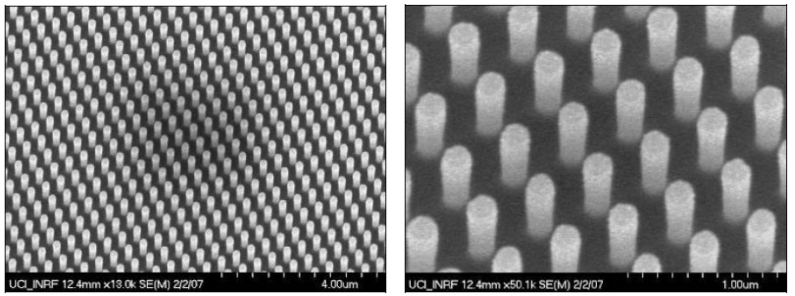

Image showing array of nano-fins with 200 nm diameter, fabricated using nanolithography (SFIL) at NNIN. The nano-fins increased cooling rate by 120%.

NNIN Site at the University of Washington

Self-Assembling Dipolar Chromophores

Organic dipolar chromophores, once aligned in the solid state (usually by an applied electric field) allow electric modulation of light propagation at very high frequency. It has been a major challenge in the last fifteen years to reduce the tendency of the molecules to aggregate into centrosymmetric assembly and enhance head-tail assembly.

Cheng Zhang has been working on molecular engineering of chromophores to make them “fat” at the waist so that the attractive force between antiparallel pairs will yield its dominance to the desired head-tail interaction. The new chromophore CC7a (shown below) appears to be the first dipolar chromophore that no longer has a strong tendency for antiparallel packing as a self-assembled string-like structure has been observed for the first time.

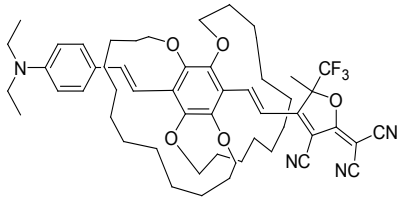

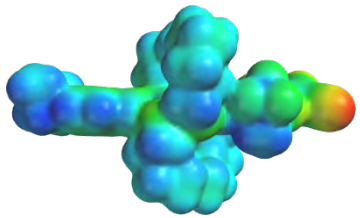

Cheng Zhang, Norfolk State University
(now at South Dakota State University).
Work performed at U. Washington

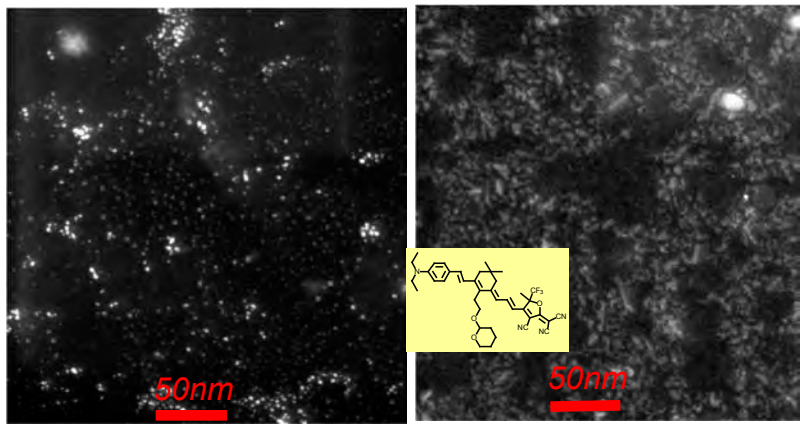

STEM image of CC7a sub-monolayer film showing strings of molecules.

STEM image of a regular chromophore, sub-monolayer film

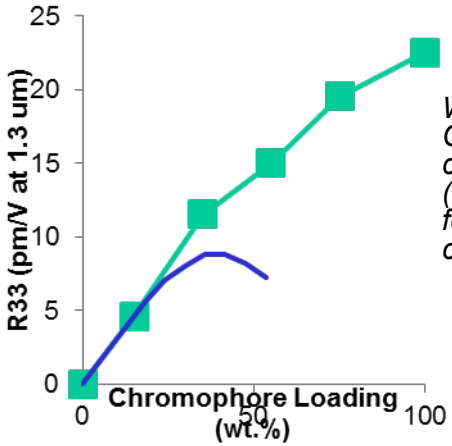

With the new chromphore, CC7a, the EO coefficient ~ chromophore loading curve (green) no longer bends as for a conventional chromophore (blue).

Polypropylene Nanocomposite Foams

The purpose of this project is to produce microcellular foams from polypropylene (PP) mixed with clay or carbon nanotubes (CNT) by sub-supercritical CO_2 process. The process involves saturation of plastic sheets with CO_2 gas, and the foaming occurs by submerging the saturated sheets into a pre-heated oil bath. By changing saturation pressure and oil bath temperature, one can obtaion foams with different morphology, which will affect the final mechanical properties of the material. Smaller cell size of the foams will usually result in lower density (lighter) material with better mechanical properties.

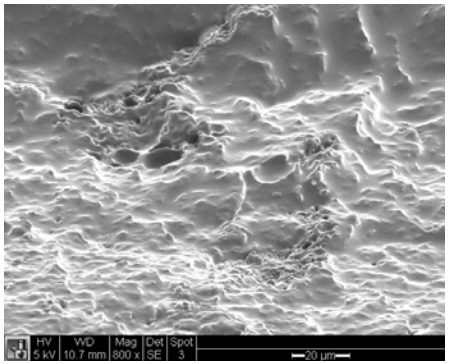

PP/clay

Saturation pressure 3MPa

No foaming occurred

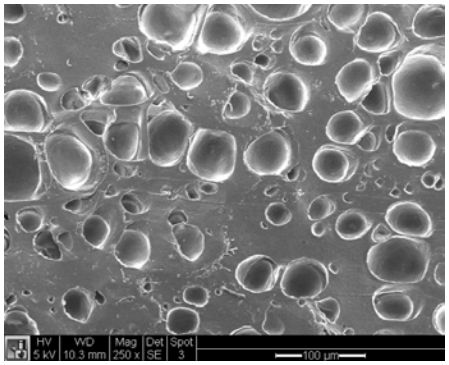

PP/clay foam

Saturation pressure 5MPa

Cell size 20-100 µm

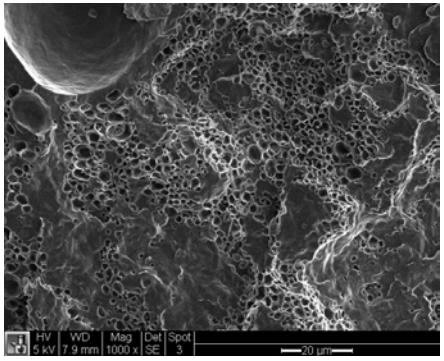

PP/clay foam

Saturation pressure 7MPa

Cell size 2-10 µm

AALBORG UNIVERSITET

Viktoriya Dolomanova, Aalborg University, Denmark.
Work performed at U. Washington

NNIN Nanoscale Science, Engineering & Technology

Visualization of Biomolecular Complexes: Protein-Protein and DNA-Protein Interactions

The Murphy group is working on visual analyzes of the interaction of the glucocorticoid receptor (GR), associated chaperone proteins, and DNA. The GR plays a fundamental role in mediating the body's physiologic response to stress and its therapeutic response to many anti-inflammatory drugs. In order to produce its effects at the cellular level, the GR must sequentially bind to chaperone proteins and specific regions of DNA. Understanding how and where these biomolecular interactions take place allow to better elucidate the molecular signaling process by which the GR functions. Unlike other nanoscale imaging techniques, AFM image acquisition can be performed on unlabeled biomolecules in near-physiological conditions. See video at:
http://www.jove.com/index/Details.stp?ID=3061

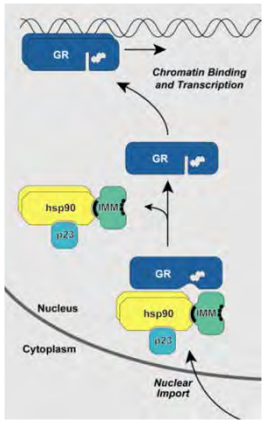

Model of glucocorticoid receptor signaling following cytoplasmic activation and nuclear transport

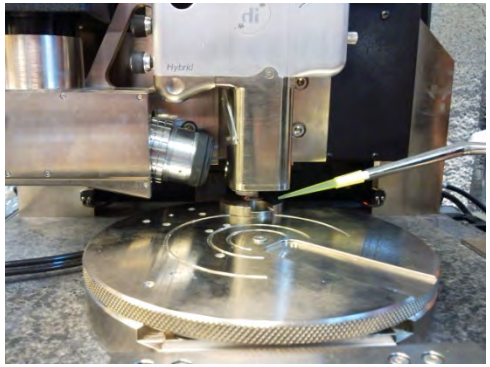

Near-physiological buffer added to mica for liquid-cell AFM imaging

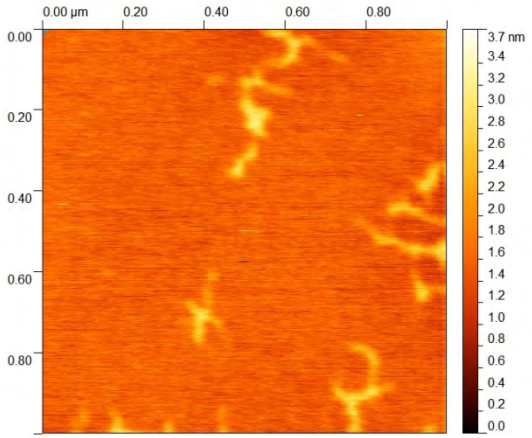

Plasmid DNA on mica, displaying a characteristic two-nanometer height. http://www.jove.com/index/Details.stp?ID=3061. doi: 10.3791/3061

Patrick Murphy, Seattle University
Work performed at U. Washington

Rapid and Efficient Dewatering of Microalgae

For microalgae to be competitive for commercial production, the costs of growing, harvesting , dewatering and processing need to be significantly reduced. Current methods for separating microalgal cells from their growth medium are too expensive to be commercialized.

Seattle University students and faculty designed a batch and a continuous flow system that use small amounts of electric current to rapidly dewater algae. The process cost is significantly smaller than with any known method.

Confocal microscopy results are shown in the figures.

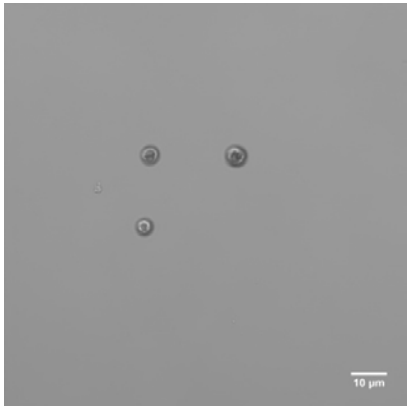

Microalgae cells repel each other when suspended in their growth medium.

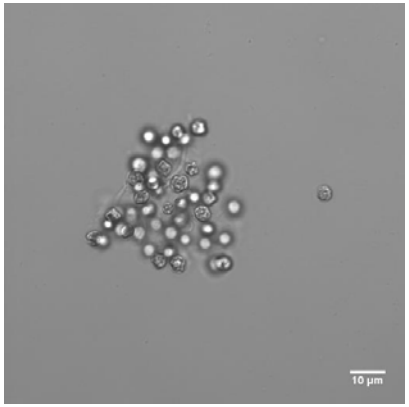

After treatment, algae flocculate and can easily be separated form the growth medium.

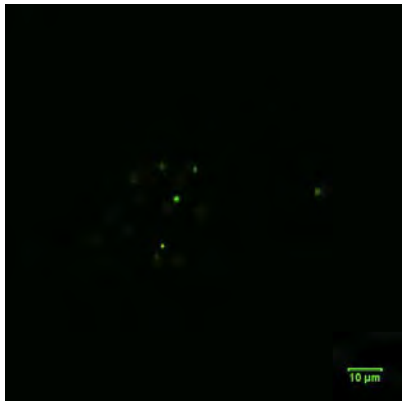

SYTOX Green dye staining shows evidence of small cell membrane disruption during the treatment.

Teodora Rutar Shuman, Seattle University
Work performed at U. Washington

Scalable Solar Power

Integrated Photovoltaics, Inc. (IPV) develops next-generation scalable solar-power solutions. Our innovative silicon photovoltaic (PV) technology dramatically reduces solar generation costs while satisfying the solar industry's requirements for reliability, quality, and high-performance.

Compared with conventional silicon PV devices, IPV's devices use approximately 90% less silicon, require less energy to produce and require less capital to scale up. Our technology is also more environmentally friendly. IPV uses UW-NNIN for developing technologies that manufacturing partners can rapidly integrate into their current PV production lines.

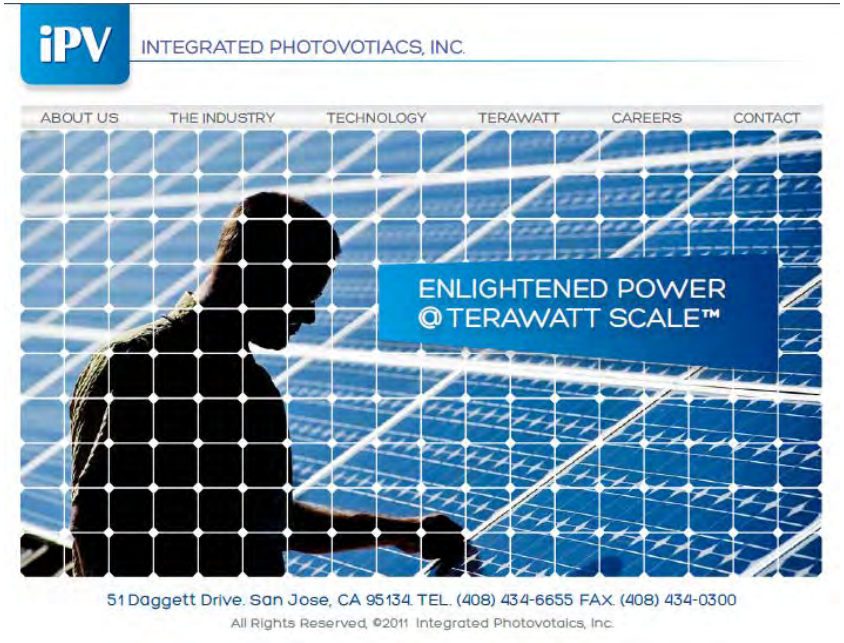

Integrated Photovoltaics, San Jose, CA
Work performed at U. Washington

Electrically Variable Optical Elements

New Light Industries Ltd. is a small research company specializing in optics, holography, document security technologies, and image processing. NLI is developing liquid crystal devices that act as electrically variable lenses or prisms. Applications of the technology will range from inexpensive autofocus eyeglasses to augmented reality eyewear, and from cell phone cameras to 3D displays. The work involves nanofabricated structures to precisely control liquid crystal alignment, proprietary high-volume mass production of nanostructured surfaces, and a revolutionary new adaptive optics architecture for which a patent will be issued in 2011. The nanofabrication resources at UW-NNIN are crucial for production of precisely controlled features ranging from 200 to about 20 nm.

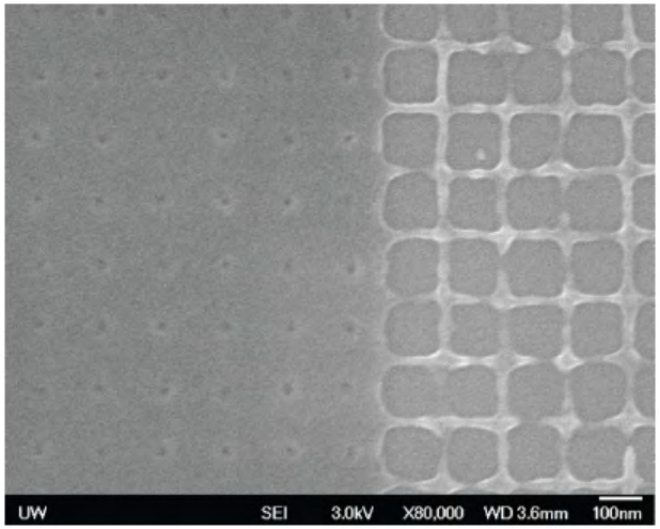

Pattern generated on JEOL 6300FS e-beam writer

NEW LIGHT INDUSTRIES LTD.

New Light Industries Ltd., Spokane, WA
Work performed at U. Washington

NNIN Nanoscale Science, Engineering & Technology

Catalyst Development for Advanced Monopropellant

Advanced (low cost, low-toxicity green) monopropellant technology research has been underway at **Aerojet** for years. Thrusters based upon those propellants require catalyst in order to achieve steady state operation and meet other mission requirements.

Catalyst deactivation at propellant combusting temperature (>1600ºC) is the primary thruster life limiting factor. We use UW-NNIN capabilities to develop new catalyst formulations with enhanced survivability at high temperatures.

Detailed nano/micro-structural studies including XRD and SEM are key to improving catalyst stability, understanding deactivation mechanisms, evaluating projected engine lifetime and, more importantly, selecting new routes in catalyst synthesis.

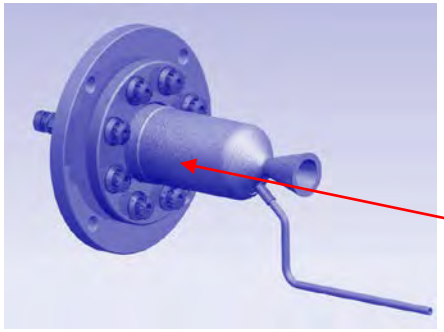

Propellant thruster

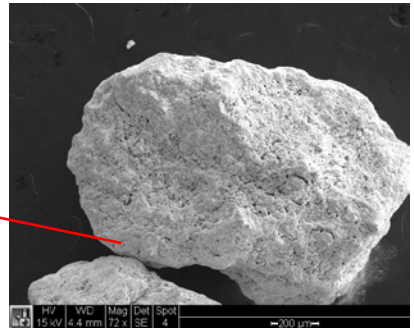

Catalyst Granules Packed in Engine

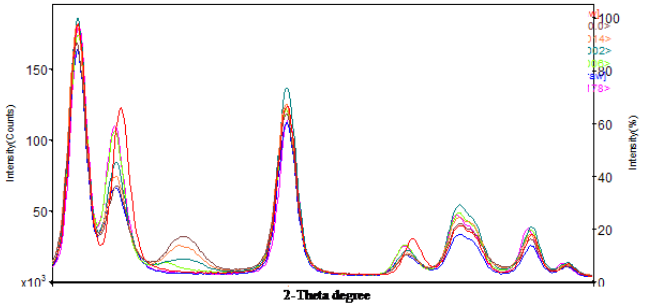

XRD measurements of phase changes in post-fired catalysts, explaining catalyst deactivation mechanism

AEROJET
A GenCorp Company

Aerojet – Redmond Operation, Redmond, WA
Work performed at U. Washington

NNIN Nanoscale Science, Engineering & Technology

Rapid and Inexpensive DNA sequencing

Stratos Genomics is developing a new method that will dramatically reduce time and costs of high throughput DNA sequencing. The technology creates surrogate molecules from DNA targets that comprise a sequential linkage of large reporters. These reporters encode the target DNA sequence information and are measured using nanopore detectors, a silicon-based miniaturized version of Coulter counters.

To be commercially feasible it is necessary to reduce the dielectric noise of these nanopores, improve their durability, and develop a wafer-based production scale-up. Very high signal-to-noise molecular translocations of molecular reporter constructs have been achieved and new concepts for wafer-based production are being explored that utilize E-beam lithography as the 3rd generation of nanopore design begins.

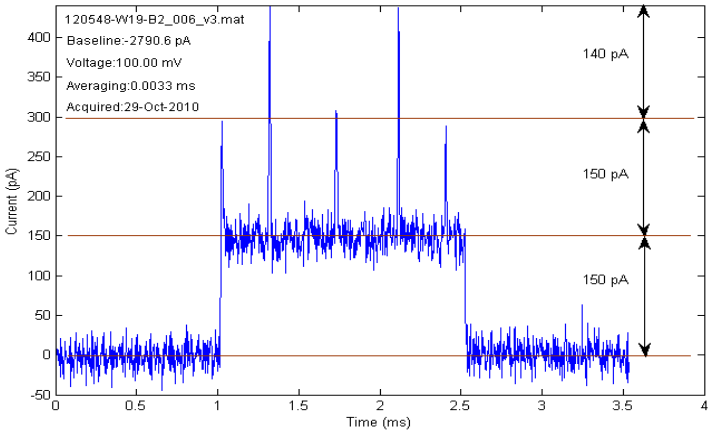

Current trace of a molecular construct with 5 alternating reporters as it trans-locates through a low-noise nanopore.

STRATOS genomics inc.

Stratos Genomics, Inc., Issaquah, WA
Work performed at U. Washington

Nanolaminated Materials

Modumetal builds a revolutionary new class of nanolaminated materials that will change design and manufacturing forever by dramatically improving the structural, corrosion and high temperature performance of coatings, bulk materials and parts.

Our technology is based on the interaction of different materials at interfaces. By laminating metals, we create new ways to influence properties, and by using low-cost electrochemistry, we enable a whole new class of applications for these materials.

Manufacturing is based on a "green" approach which reduces the carbon footprint of metal and parts production. Modumetal relies on UW-NNIN characterization and fabrication tools to develop new materials with unprecedented performance.

MODUMETAL

Modumetal Armor (featured in Inc. Magazine, 2009)

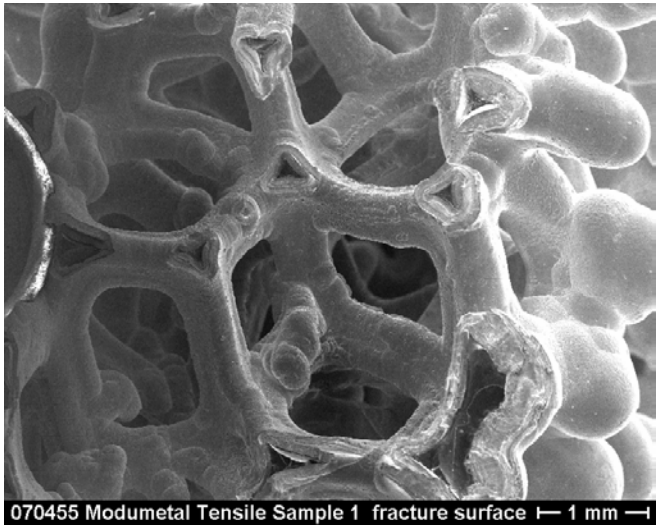

Modumetal structural foam

Modumetal, Seattle, WA
Work performed at U. Washington

NNIN Nanoscale Science, Engineering & Technology

Optimizing Cyanobacteria for Biofuel Production

Targeted Growth, in collaboration with the National Alliances for Advanced Biofuels and Bio-Products, seeks to develop economically viable biofuels and other products from algal biomass. Targeted Growth Inc., has leveraged UW-NNIN facilities, in particular laser scanning confocal microscopy platform and expertise to characterize lipid body formation and dynamics within *Cyanobacteria*, a photosynthetic blue green algae.

Visualization of lipid bodies in genetically engineered strains helps researchers determine how specific biochemical pathways alter lipid body biogenesis, location and life-cycle. Data generated at UW-NNIN is translated directly back to pathway engineers in the lab to inform genetic alteration strategies directed at the development of Cyanobacterial strains with the capacity for enhanced lipid production.

Targeted Growth, Inc.

Targeted Growth, Inc., Issaquah, WA
Work performed at U. Washington

NNIN Nanoscale Science, Engineering & Technology

Silicon Quantum Dot Light-emitting and Detection Devices

Silicon quantum dots (QD) are heavy-metal-free, potentially compatible with well-established Si processing technologies and can be synthesized from almost inexhaustible starting materials in the earth crust. In this project, we demonstrate colloidal Si phosphor materials using electro-chemical etching. Using solution-based process with these materials, we fabricate hybrid Si QD-OLEDs which show electroluminescence across the visible spectrum, as well as thin-film photodetectors that can be made on a variety of substrates.

Colorful Si QD materials fabricated using electrochemical etching

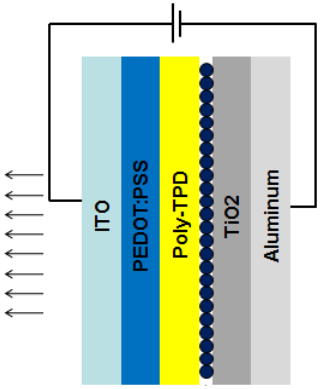

Device structure of the hybrid Si QD-OLED

SHARP LABORATORIES OF AMERICA

Optics Express ***18****, 21622-21627 (2010)*
Applied Physics Letters ***98****, 213102 (2011)*

I-V measurement results of the Si QD thin-film photodetector in dark (circle) and under 405 nm laser illumination (square). The inset illustrates the structure of the device. The shaded area shows the region covered with colloidal Si materials.

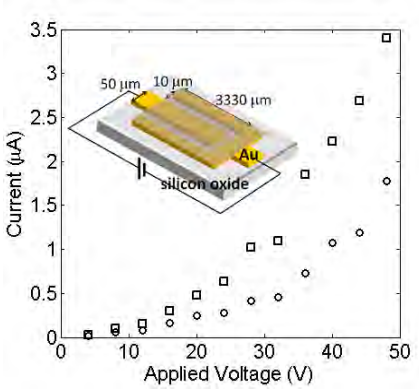

Apostolos Voutsas, Sharp Laboratories of America
and Lih Y. Lin, U. Washington
Work performed at U. Washington

NNIN Nanoscale Science, Engineering & Technology

How Dividing Cells Get the Right Chromosomes: Tension and the Chinese 'Finger Trap' Effect

An exquisite molecular machine, the mitotic spindle, organizes and separates chromosomes during cell division. To uncover how this machine operates, this collaborative group is reconstituting spindle functions and applying new tools for manipulating individual molecules. Recently they found that chromosome-spindle attachments behave like Chinese 'finger-traps': they are more stable when pulled. This helps explain why division is so accurate. Improper attachments, which lack tension, are selectively destabilized.

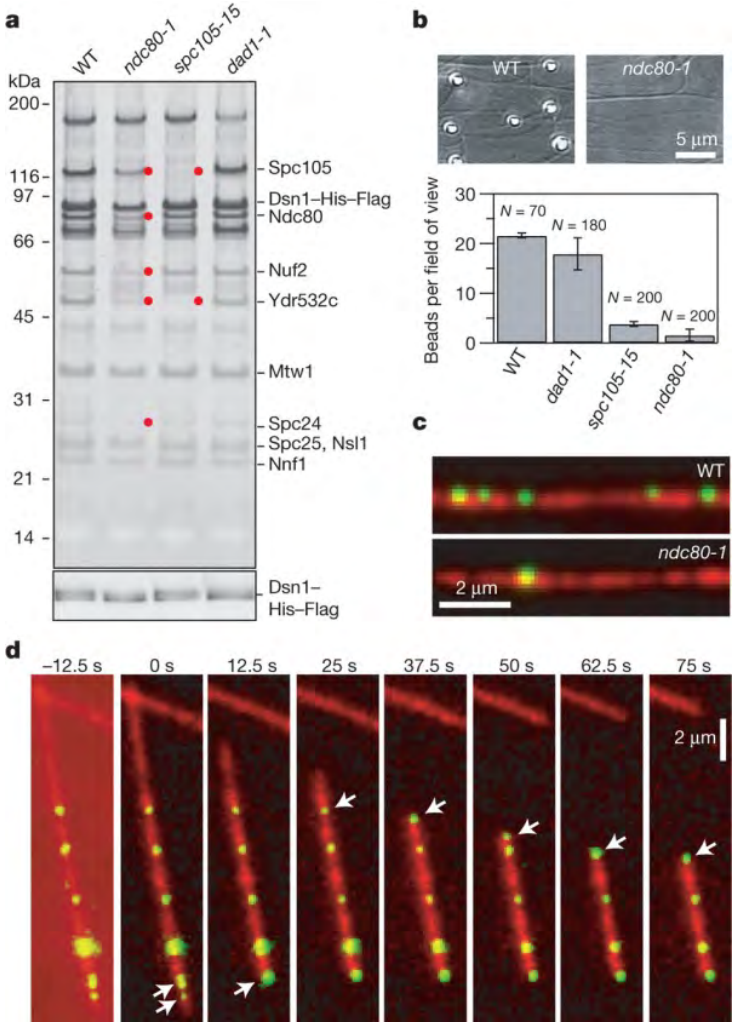

Nature 468, Iss. 7323, 576-579 (2010)

Sue Biggins, Fred Hutchinson Cancer Research Center, Jeffrey Ranish, Institute for Systems Biology, and Charles Asbury, UW Physiology and Biophysics. Work performed at U. Washington

Mid-IR Silicon Photonics

Silicon waveguides for Mid-Infrared (MIR) wavelengths have been proposed in a number of theoretical papers, but not demonstrated past 3.5 μm until recently.

Using Silicon-on-Sapphire material and direct-write electron beam lithography, the Hochberg Lab recently demonstrated working ring resonators at 5.5 μm wavelength. MIR wavelengths have applications in thermal imaging, spectroscopy, and bio-sensing, and ability to fabricate MIR silicon photonics with nanometer precision creates opportunities for new, complex systems at these wavelengths.

Applied Physics Letters ***97****, 213501 (2010)*

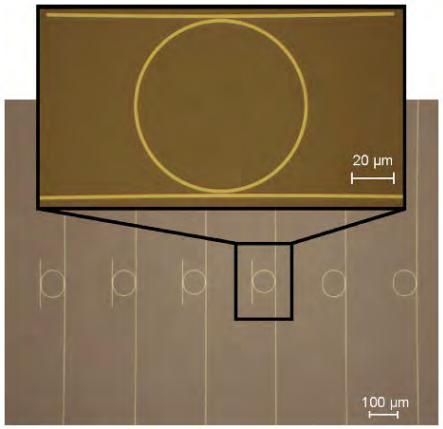

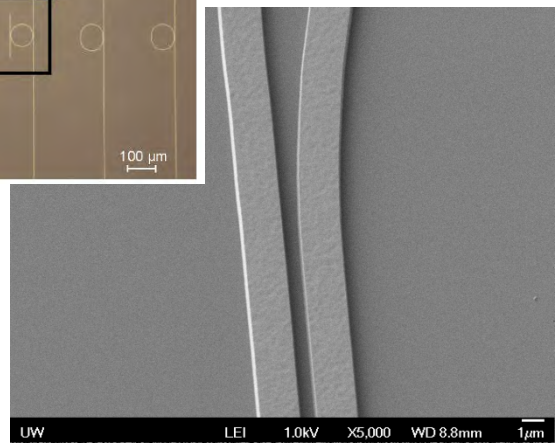

Optical (left) and SEM (below) images of ring resonators fabricated in silicon-on-sapphire for mid-infrared applications.

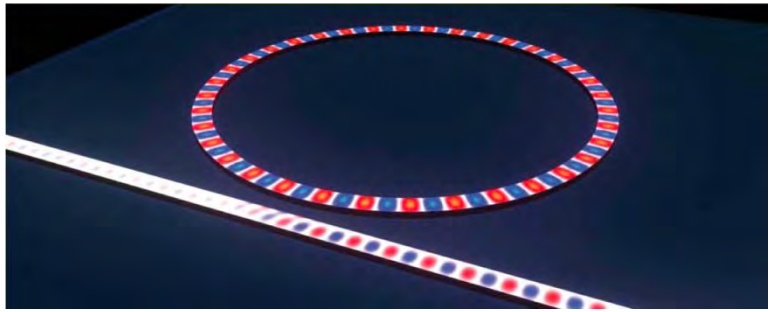

3-D rendering of a ring resonator showing optical mode propagation through a waveguide

Michael Hochberg, UW EE
Work performed at Cornell and U. Washington

Direct Write of Ge Nanostructures in the AFM

The Rolandi lab has developed an AFM strategy to write sub-30 nm germanium nanostructures on Si with deterministic size and placement control. The AFM tip traces desired shapes along the biased silicon sample while immersed in diphenylgermane (DPG). The proximity of the scanning probe to the biased sample generates an intense electric field that injects electrons from the tip into the precursor and fragments the charged precursor to write Ge nanostructures onto the substrate.

Arbitrary shapes 3 nm tall and 80 nm wide Ge nanostructures can be routinely produced at a rate of 1 μm s^{-1}. Increasing write speed to 100 μm s^{-1} yields thinner nanostructures (0.7 nm) that can be as narrow as 25 nm ± 2 nm.

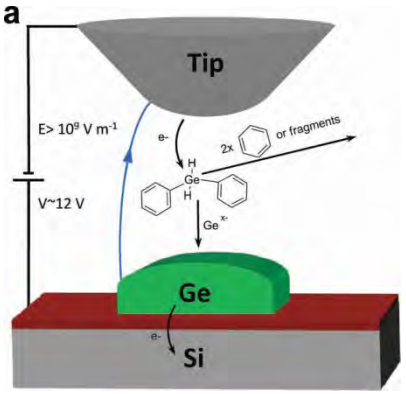

Schematic of the probe sample geometry and proposed chemical reaction for Ge nanostructure AFM direct-write.

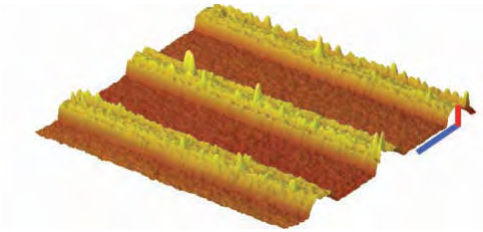

175 nm wide 5 nm lines written at 1 μm/s

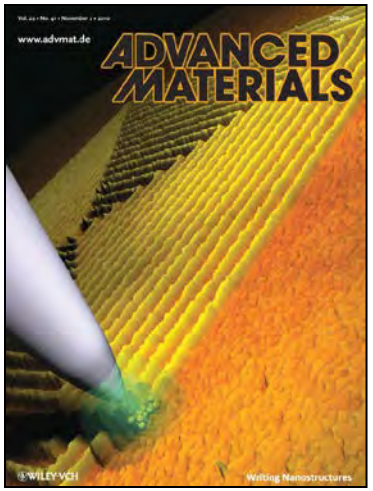

Marco Rolandi, UW MSE
Work performed at U. Washington

NNIN Nanoscale Science, Engineering & Technology

Biofabrication of Doped Quantum Dots

The Baneyx lab has developed a simple and environmentally friendly process for protein-aided mineralization of minimally toxic, transition metal doped ZnS nanocrystals.

The biofabricated ZnS:Mn quantum dots emit bright yellow-orange light upon excitation with standard UV sources and their core does not incorporate cadmium ions that persist for long times in tissues. The capping protein shell incorporates an antibody-binding domain that is stably tethered to the crystalline core through a mineralizing ZnS binding peptide. Thus, the antigen-binding valency of the resulting nanoparticles can be controlled by varying the molar ratio of antibodies to fusion protein.

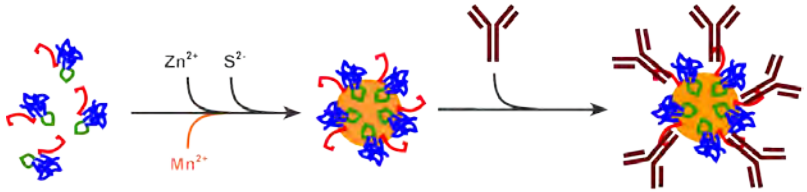

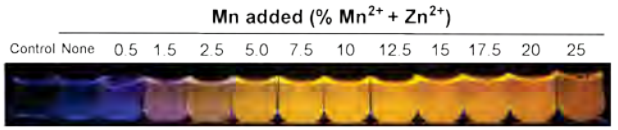

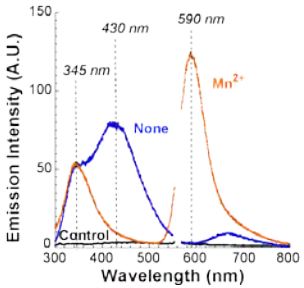

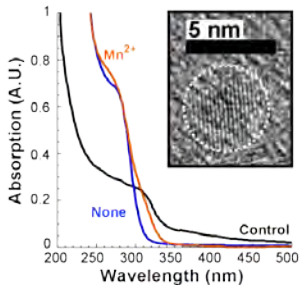

François Baneyx, UW ChE
Work performed at U. Washington

Graphene pn Junction Optoelectronics

The pn junction is the backbone of electronic and optoelectronic devices. The Xu group has fabricated pn junctions in monolayer graphene using a local top gate and a global bottom gate to electrically bias different areas of graphene to form the junction. This device structure has been demonstrated both on individual graphene flakes and on large sheets of chemical vapor deposition grown graphene. With these devices they study the ultrafast response of Dirac fermions with pump-probe photocurrent techniques for applications in new light harvesting and light detecting technologies.

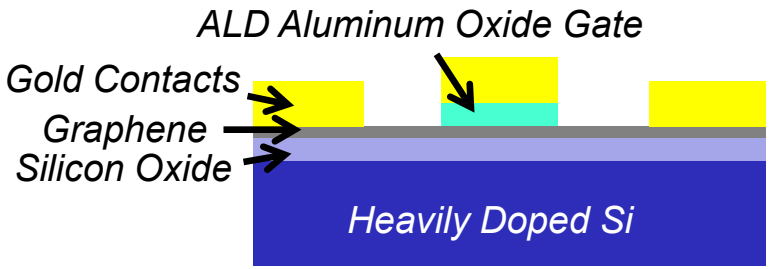

Schematic of PN junction devices. Dual gate structure allows for the creation of a PN junction on either side of the top gate.

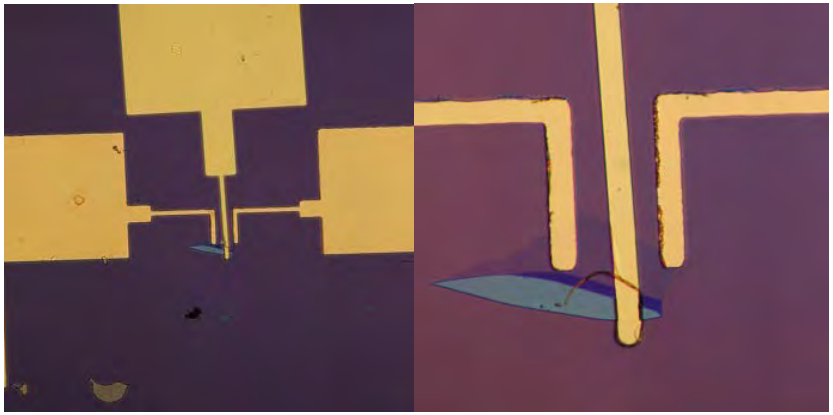

The device fabricated using direct write photolightography on an exfoliated graphene flake.

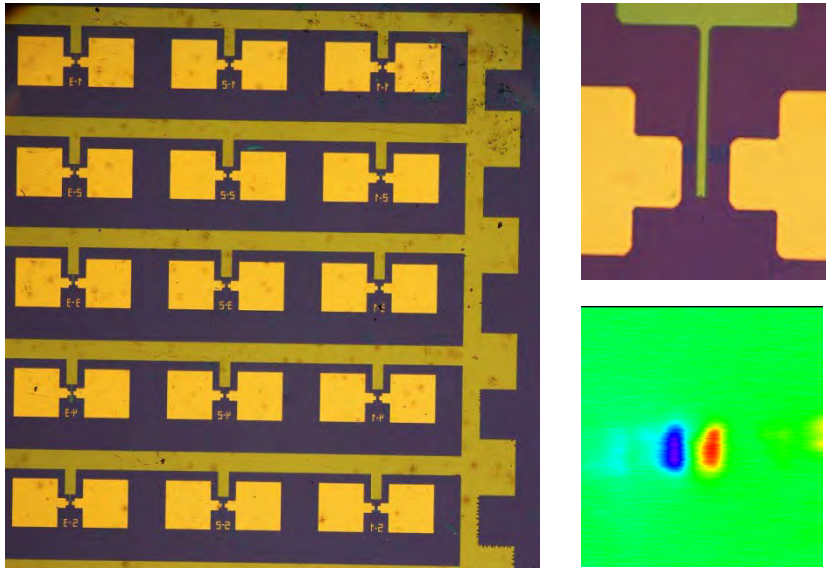

Devices on CVD grown graphene show the scalability of this structure (left). The magnified image of a typical device (top right). A map of generated photocurrent (bottom right).

Xiaodong Xu, UW Physics
Work performed at U. Washington

NNIN Nanoscale Science, Engineering & Technology

Fabricated Nanostructures for SERS Sensing

Local electric fields can be dramatically tuned by varying the diameter of gold nanostructure arrays. The Yu lab has fabricated quasi-3D arrays exhibiting “hot” spots either at the bottom or top of their structure. These arrays allow for optimal surface-enhanced Raman scattering (SERS) sensitivity for the detection of small molecules or large microorganisms. The precisely fabricated and optimized SERS-active quasi-3D nanostructure arrays make it possible to quantitatively and reproducibly detect chemical and biological species, leading to a new sensing platform with molecular specificity for ocean science applications.

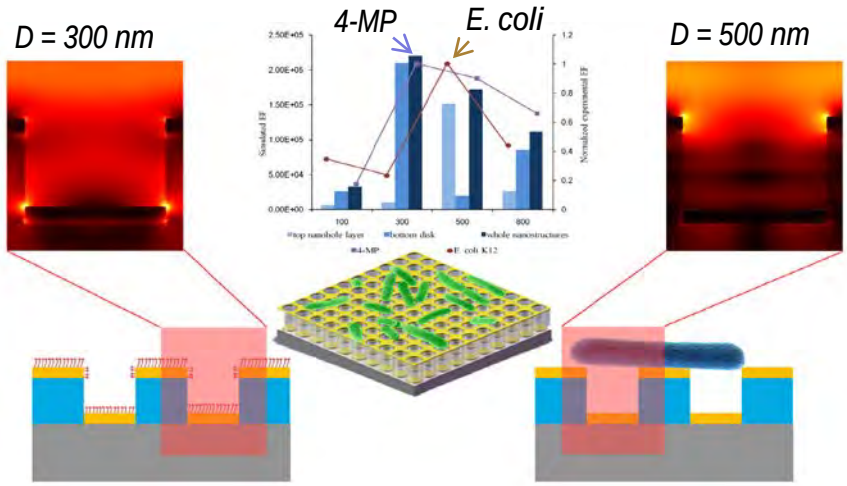

Qiuming Yu, UW ChE
Work performed at U. Washington

Type 2 secretin binds to cholera toxin

The type II secretion system (T2SS) is a macromolecular complex spanning the inner and outer membranes of Gram-negative bacteria that secretes folded proteins, including cholera toxin from Vibrio cholerae. The major outer membrane T2SS protein is the 'secretin' GspD.

Cryo-EM reconstruction of the V. cholerae secretin reveals a dodecameric with a large channel at its center that contains a closed periplasmic gate (left below)

The GspD periplasmic domain (purple, blue, green) binds to cholera toxin pentamer (gold below, right) as shown by surface plasmon resonance (SPR, upper and center, middle below).

SPR also shows that the periplasmic domain of GspD interacts with the KIJ tip of the T2SS piston.

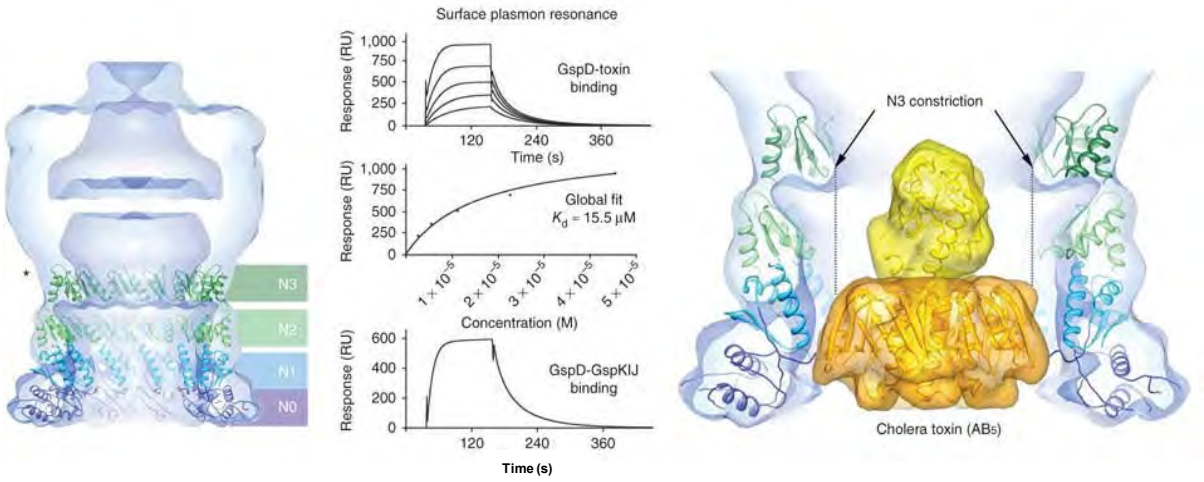

Nature Structural & Molecular Biology ***17,*** *1226 (2010)*

Wim Hol, UW Biol. Structure &
Tamir Gonen, UW Biochemistry
Work performed at U. Washington

NNIN Nanoscale Science, Engineering & Technology

Nanoscale Fluidic Channels

The Parviz Lab has fabricated and electrically characterized arrays of fluidic nanochannels. The electrical properties of the nanochannels were found to be predictably dependent on their geometry, thus allowing us to speculate about the use of such nanochannels in sensing of various biologically important molecules. Electron beam lithography was used to pattern all of the components of the nanochannel arrays. Nanoscale characterization of the system was performed on Atomic Force and Scanning Electron Microscopes.

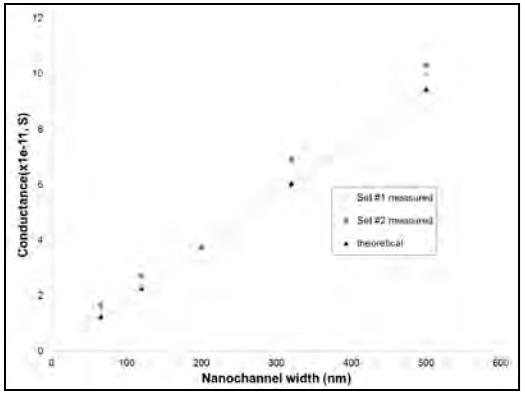

Nanochannel conductance was found to be linearly proportional to the width of the nanochannels

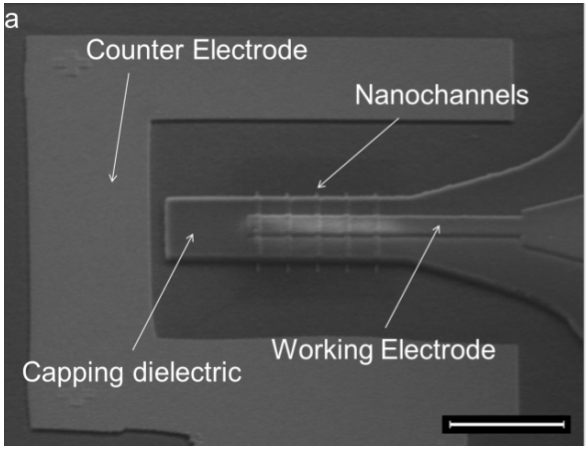

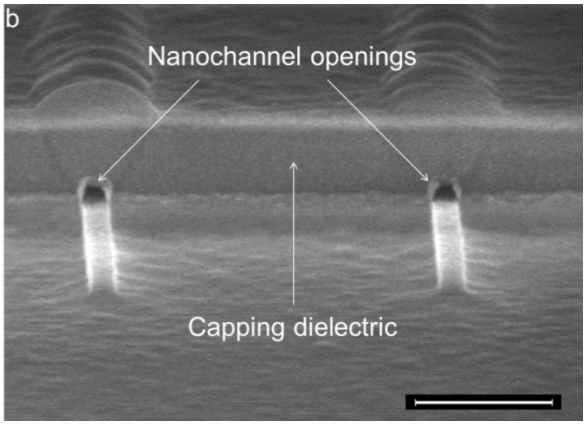

Arrays of 2.25 µm long and 60 nm tall nanochannels with widths ranging from 60 nm to 500 nm were microfabricated in SiO2 with Au electrodes embedded inside and outside of the nanochannels. The scale bar is 5 µm and 500 nm in figures 'a' and 'b', respectively.

Babak Parviz, UW EE
Work performed at U. Washington

NNIN Nanoscale Science, Engineering & Technology

NNIN Site at Arizona State University

Plasma Lithography for Cell Networks Formation

Example----A versatile plasma lithography technique is developed to generate stable surface patterns for guiding cellular attachment. This technique is applied to create cell networks including those that mimic natural tissues and has been used for studying several, distinct cell types. In particular, we have applied this method to form diverse networks with different cell types for transformative investigations in collective cell migration, intercellular signaling, tissue formation, and the behavior and interactions of neurons arranged in a network.

Plasma lithography defined patterns for probing geometric control in cellular networks

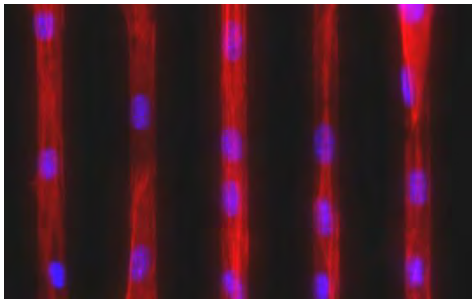

Formation of single myotubes to study cell-cell interactions in myogenesis

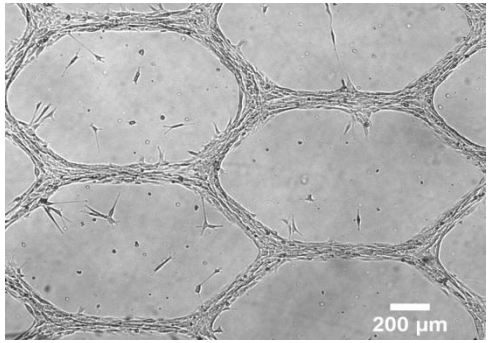

Architecture dependence in artificial cell networks

M. Junkin and P. K. Wong. "Probing Cell Migration in Confined Environments by Plasma Lithography" *Biomaterials*, vol. 32, pp. 1848-1855, 2010

Pak Kin Wong, The University of Arizona
Work performed at Arizona State University NanoFab

Microfabricated Ionizer Project

The purpose of the Microchip Ionizer Project is to create an efficient, low power, low form factor ion source for mass spectrometry and ion pump applications. The device is fabricated using an SOI wafer and consists of a cathode electrode and an anode electrode separated by a sub-micron gap. Application of voltage, either AC or DC, between the electrodes generates high electric field that ionizes gas molecules that passes through the electrode apertures.

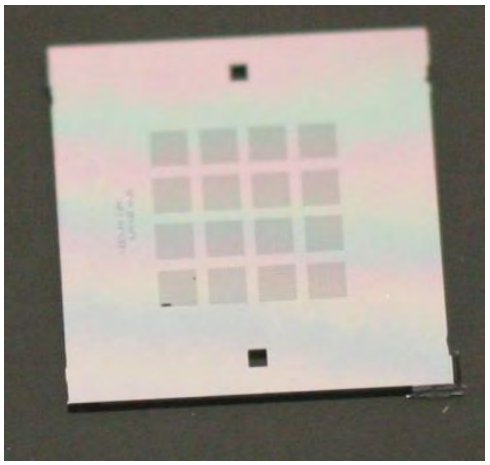

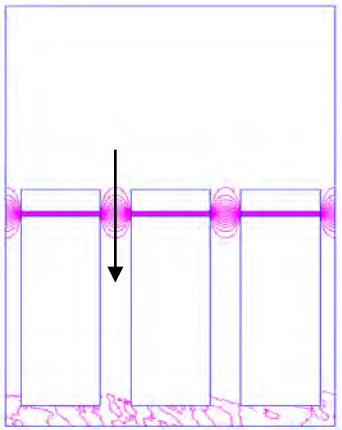

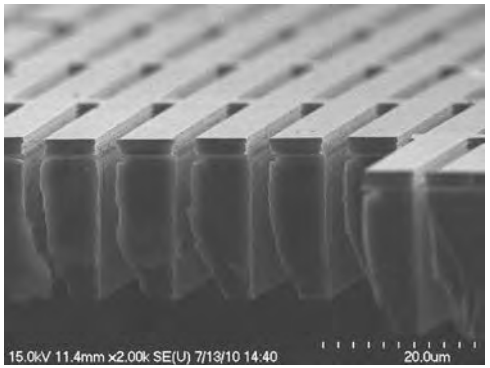

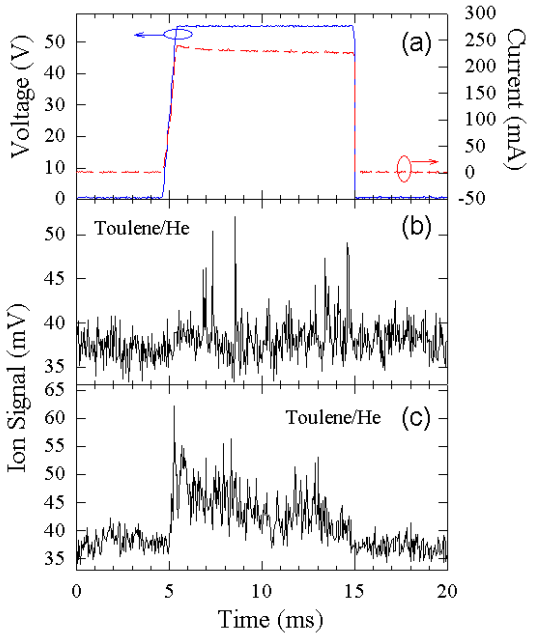

Stanley Pau, University of Arizona
Work performed at Arizona State University Nanofabrication Facility

DC Bias – AC Electroosmotic Pump

The DC bias – AC electroosmotic micropump may be used to induce bi-directional fluid flow in MEMS devices. The structure of the device consists of an array of electrodes deposited on a Si wafer and a PDMS channel, with an input and output port, deposited on top of the electrode's array.

The device features range from micro- to macro-scale, making the fabrication very challenging. The electrodes' width ranges between 40 and 120μm, while the channel's length and width are in the tens of millimeter range.

Constantin Ciocanel and Nazmul Islam, Northern Arizona University and University of Texas at Brownsville
Work performed at ASU NanoFabFacility

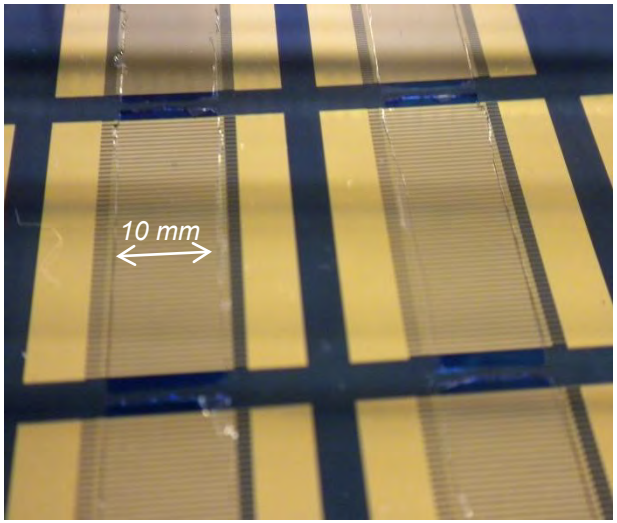

Several electrode array geometries are created to evaluate the best configuration for a desired flow rate.

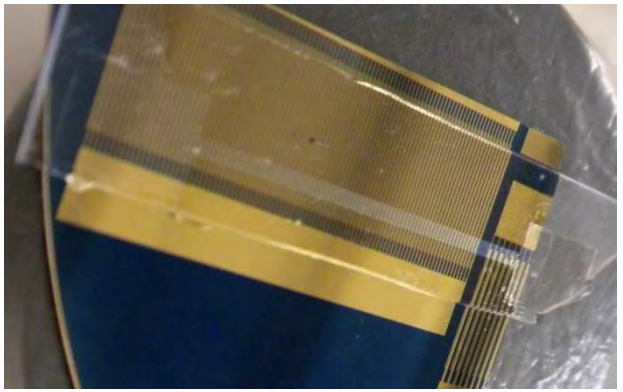

PDMS channel with inlet and outlet ports on top of one electrode array.

NNIN
www.nnin.org
Nanoscale Science, Engineering & Technology

Organic Nanogap Diodes

Nanogap electrodes were fabricated using a combination of direct-write lithography and focused ion beam milling as shown top right. The electrodes are used for measuring the electronic transport properties of polymer thin films, namely poly(3-hexylthiophene): phenyl-C61-butyric acid methyl ester (P3HT: PCBM) blends used in organic solar cells.

Following laser lithography and metallization, a mask is ion milled in the Ti layer (Leroy Center for Solid State Science, ASU). The exposed Au area is etched using ion beam milling through the Ti mask (performed by Jerry Drumheller at CNF). This process was adapted from Nagase et al: Thin Solid Films, 438-439: 374, 2003.

Dr. Tricia Youngbull
Advisors: Dr. Christine Luscombe, Dr. Samson Jenekhe
University of Washington Seattle, WA
Collaborator: Dr. Ghassan Jabbour, KAUST, Saudi Arabia
Work performed at ASU & Cornell NNIN sites

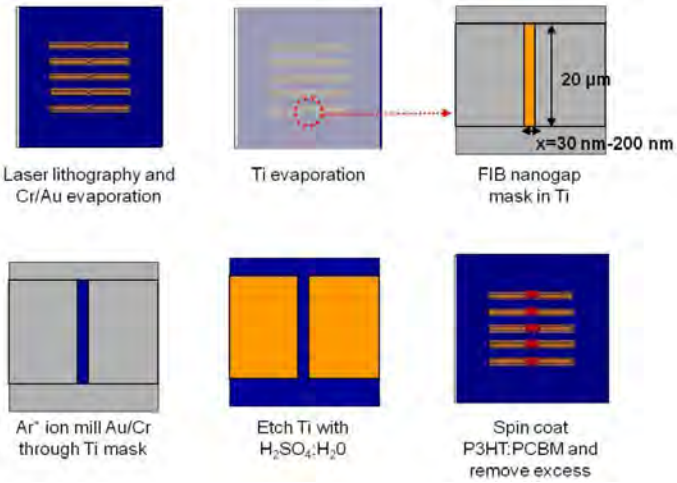

Nanogap diode fabrication process steps.

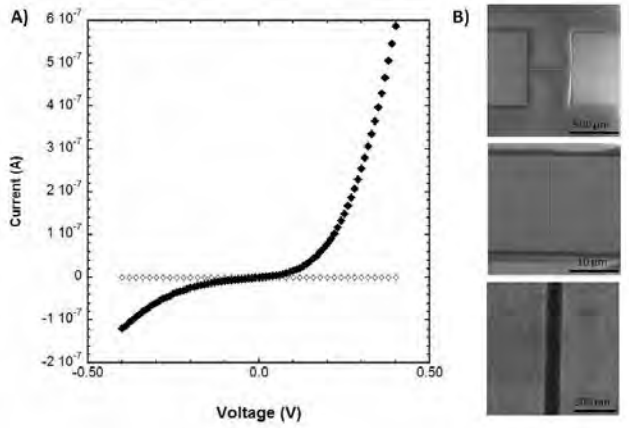

A) IV characteristics of open nanogap electrodes (open diamonds) and P3HT:PCBM nanogap diodes (filled diamonds). B) SEM images of nanogap electrodes after fabrication.

Multifunctional FET

In order to sustain the speed and density of modern ICs, we are investigating a novel approach based on increasing the functions of an individual MOSFET device rather than shrinking its dimensions. This will be possible by using a new CMOS technology, for the manufacturing of high-density integrated circuits, invented by the University of Padova. Such technology, said CMOS WMJ, utilizes field effect devices that have the functionality of two classical transistors (nMOS and pMOS) connected together.

Prototypes of these multifunctional FETs have been fabricated by the ASU Nanofab team and are under tests at the University of Padova. More information about this research can be found in:

F. A. Marino, G. Meneghesso, “Multifunctional Field-Effect Transistor for High-Density Integrated Circuits”, *IEEE Electron Device Letters*, Vol. 32, No. 3, March 2011, pp 264-266.

Dr. Fabio Alessio Marino, UNIPD, Padova, Italy
Work performed by ASU Nanofab

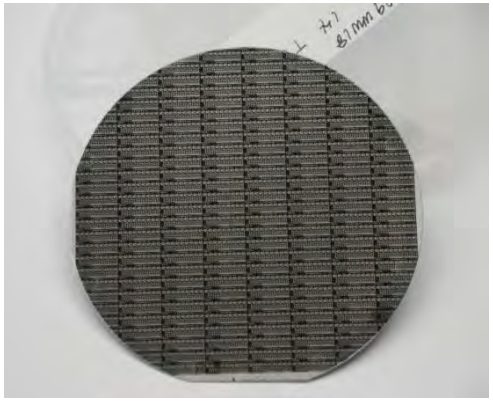

Wafer containing the first prototype structures of the new technology.

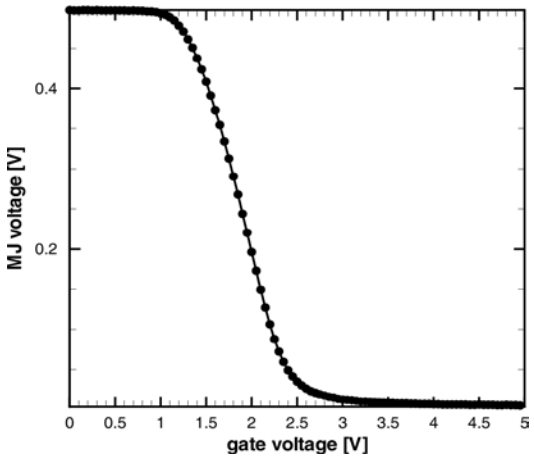

Experimental transfer characteristic of a single WMJ device: a single device behaves as a conventional inverter.

Single Photon Counting Module

Laser Components new COUNT series Single Photon Counting Modules has been developed to offer a unique combination of high detection efficiency (> 70%) over wide wavelength range i.e. 810 nm (RED Count Module) as well as at yellow and green wavelengths (BLUE Count Module), wide dynamic range and ease of use for photon counting applications. Dark counts of 10 photons per second have been achieved in the best devices to date.

Module performance is based on Laser Components' ultra-low-noise VLoK silicon avalanche photodiode developed using the full suite of advanced tools in the cleanroom at the Center for Solid State Electronics Research at Arizona State University.

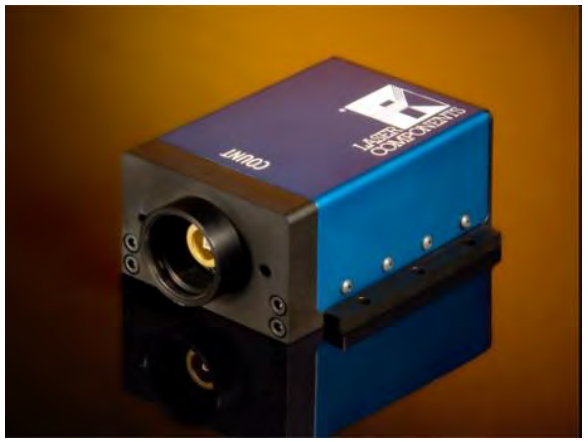

Fabricated Single Photon Counting Module

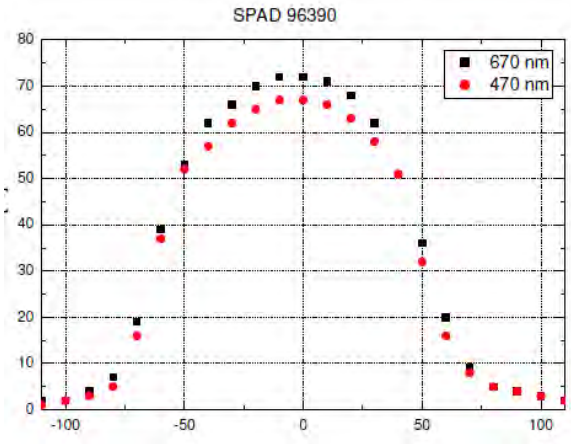

Typical Photon Detection Efficiency (%) Scan Measured Along the Detector Surface

Viet Nguyen and Dragan Grubisic
Laser Components DG, Inc.
Work performed at ASU NanoFab

FDEC Nano Wires

INanoBio is an early stage spin-off company formed to commercialize a revolutionary new nanowire sensor technology developed at Arizona State University. We have invented the first of its kind exponential sensor applications. In our sensor the chemical signal is not diminished, like typical sensors, but internally amplified up to an order of magnitude. This enables ultra-high sensitivity, coupled with exceptional selectivity for single molecular level detection.

The fully depleted exponentially coupled (FDEC) sensors will find applications in industrial process control and leak detection, military and DHS for explosive and toxic gas detection, environmental quality control systems, in-vitro diagnostics and related applications.

Novel prototype nano sensors have been fabricated using proprietary techniques.

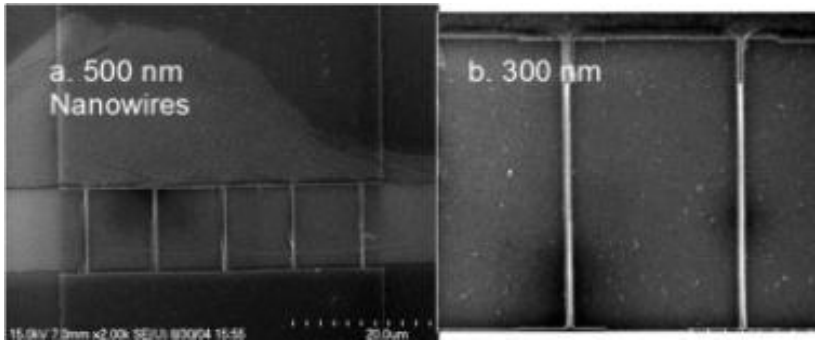

FESEM images of FDEC nanowires

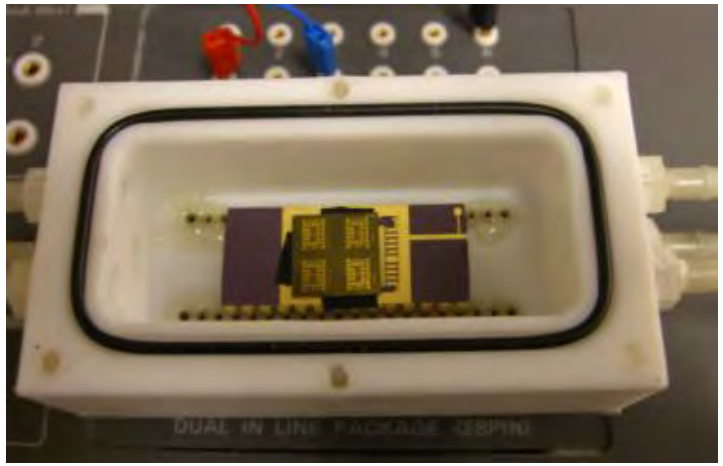

Prototype FDEC Nano Sensors

Bharath Takulapalli and Mukilan Mohan, INanoBio
Worked Performed at ASU NanoFab

Printed Solar Cells

Nth Degree is developing a printed solar cell that will be grid-competitive without subsidies. Prototyping is currently being enabled by ASU's Center for Solid State Electronics Research (CSSER). Spherical silicon micro-diodes are the active component, which are self-tracking and operate in diffuse lighting conditions. Standard rapid annealing, metal deposition, and reactive ion etching used at CSSER are implemented for prototyping. These processes, as well as a multitude of printing and coating techniques, are combined in an entirely atmospheric, continuous roll-to-roll manufacturing line operating at 20 ft/min. This enables flexible, lightweight solar panels with a total manufacturing cost per Watt well below current photovoltaic technologies.

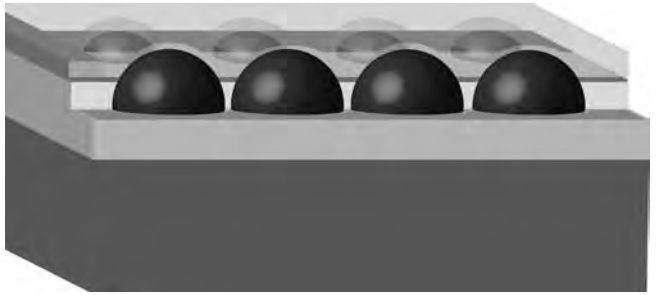

Cutout 3D schematic of Nth Degree's printed solar cells

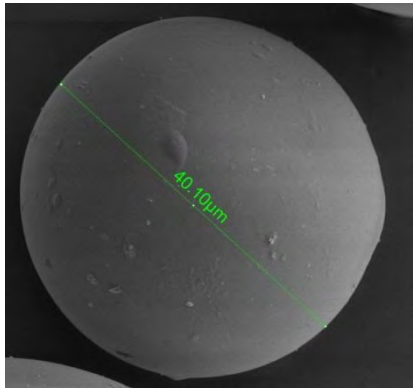

SEM image of spherical silicon which is dispersed in an ink system and printed over a flexible substrate

Dr. Tricia Youngbull and Dr. Lixin Zheng
Nth Degree Technologies Worldwide, Inc.
Work performed at ASU NanoFab

Novel Electrodes For Microfluidic Structures

The next generation microfluidic devices for improved performance will require enhanced materials.

We investigate the feasibility to modulate the electrical attributes of sputtered SiC films by in-situ doping with aluminum and nitrogen, in conjunction with rapid thermal processing under different gaseous ambience. As-deposited SiC films have too high a nominal resistivity for conventional electrode use in microfluidic structures.

Preliminary results show better electrical modulation to in-situ doping with nitrogen coupled with thermal treatment in a reducing atmosphere.

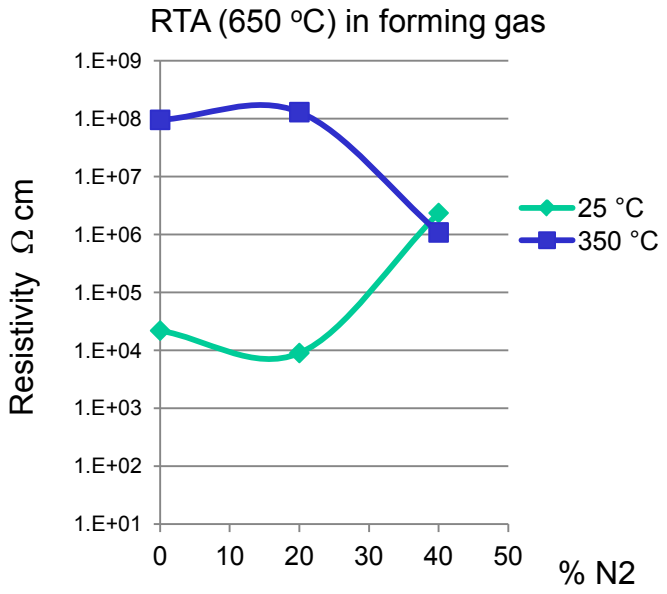

Nominal film resistivity (Ω cm) versus nitrogen doping (ratio of N2/Ar flow) as a function of deposition temperature (25 °C and 350 °C) and rapid thermal processing at 650 °C in forming gas.

Frank Jahnke, Sonata Biosciences
Work performed at ASU NanoFab

Characterization of SOI MESFETs at the 45 nm Node

Silicon-on-insulator (SOI) MESFETs have been fabricated using a commercial 45nm CMOS foundry. The devices, which were designed and subsequently tested using the ASU NanoFab facilities, have superior RF characteristics as expected for this shorter gate length technology. Preliminary measurements confirm f_{max} values in excess of 100 GHz, making these devices ideally suited to power amplifier applications at X-band frequencies.

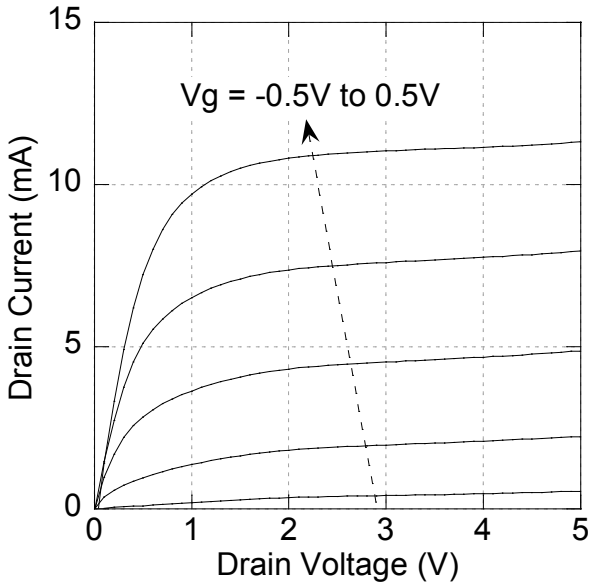

MESFET exceeds the 1V breakdown of the CMOS

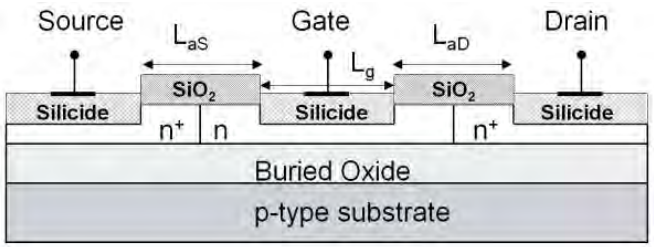

Cross-section of the prototype MESFETs

Seth Wilk and William Lepkowski, SJT Micropower Inc.

Work performed at ASU NanoFab

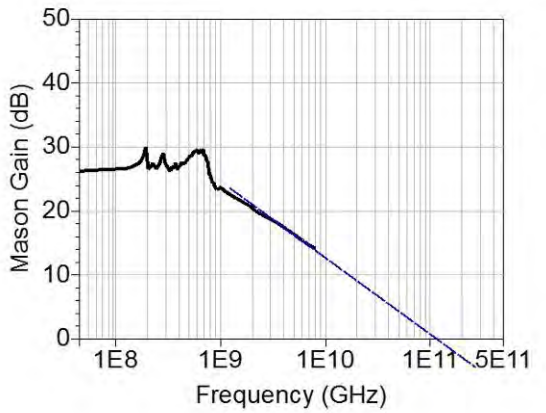

Extrapolated power gain shows that f_{max}>100 GHz

CNT Nanofluidics Project

Carbon nanotube (CNT) has attracted enormous interest for its application in nanofluidics in recent years, owing to its atomically smooth and hydrophobic surface and high aspect ratio geometry. The purpose of this project is to fabricate CNT based nanofluidics devices, understand the fluidic dynamics at sub 2nm, explore the applications of CNT based nanofluidics in DNA sequencing, chemical and biosensing.

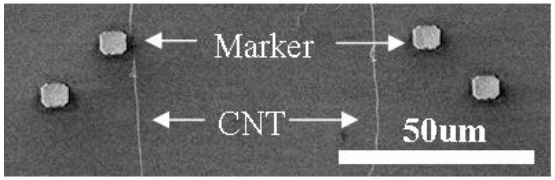

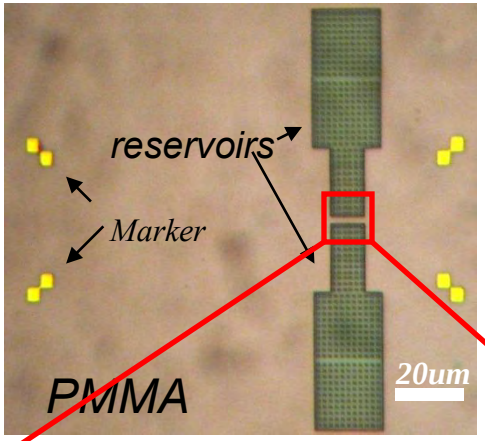

One CNT connects two reservoirs as fluid conduit

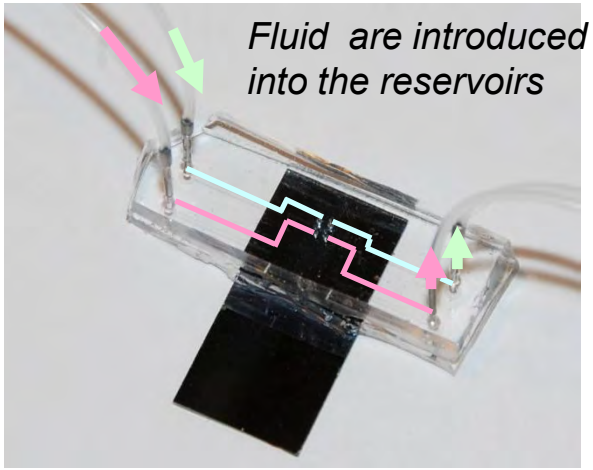

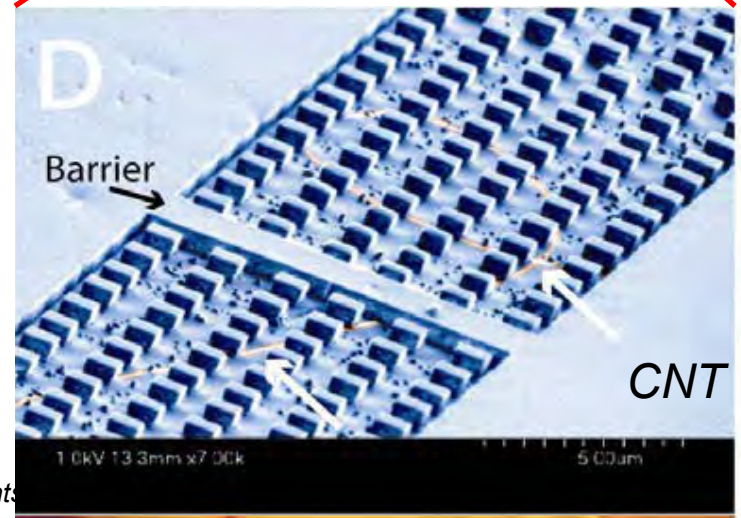

Jin He and Stuart Lindsay, ASU
Colin Nuckolls, Columbia University
Predrag krstic, Oak Ridge National Lab
Work performed at ASU nanofab Facility

Neural Interfaces

A) Autonomous brain implant - The overall goal of this NIH funded research is to develop a novel MEMS technology that will allow sensors to seek and monitor single neurons of interest in the brain over long periods of time. A novel packaging technique for MEMS implantable devices is developed at ASU and the interconnect components are fabricated at ASU Nanofab.

B) Biochip for gene delivery -The overall goal of this project is to develop a technology for delivering genetic material to spatially restricted population of primary neurons in culture. To accomplish the aforementioned goal a novel optically transparent microelectrode array based biochip was fabricated at ASU Nanofab.

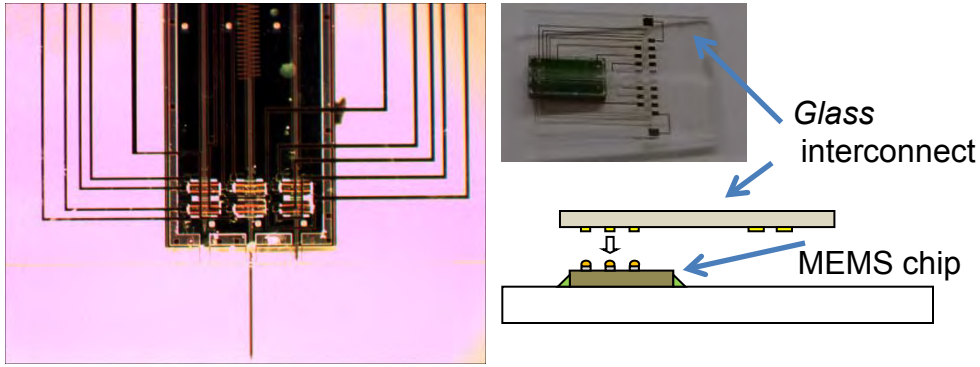

A novel flip-chip packaging and non-hermetic encapsulation technique for MEMS implantable devices

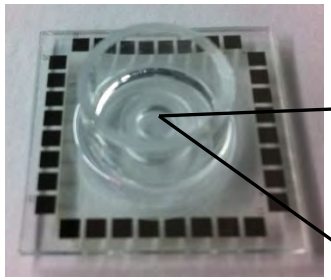

A microelectrode array based biochip for targeted gene delivery to primary neurons in culture

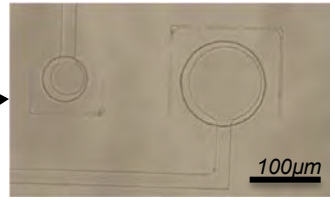

Optically transparent micro-electrodes on the biochip

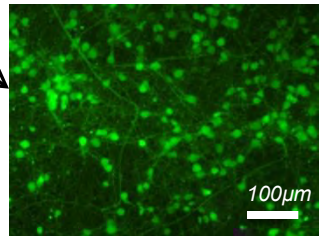

Live culture of primary neurons on the biochip

Jit Muthuswamy, ASU, Tempe, AZ
Murat Okandan, Sandia National Laboratories, NM
Work performed at ASU and Sandia National labs

A Contour-mode MEMS Resonator for Monitoring Blood Coagulation in Real Time

The goal is to demonstrate a small-size, light-weight, low-power, and disposable device for monitoring blood coagulation in real time. The ASU Nanofab was used to fabricate the device except for the piezoelectric (AlN) thin film. The piezoelectric thin film is sandwiched by two electrodes, top and bottom, to generate contour-mode resonance, which is sensitive to the viscosity of the contact media. As a droplet of blood coagulates due to the cascade chain of fibrin reaction, the viscosity increases and consequently lowers the resonant frequency of the resonator.

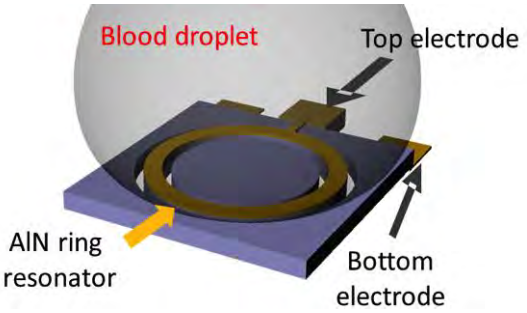

a MEMS contour-mode film bulk acoustic resonator (C-FBAR) with a blood droplet dispensed directly on top of the C-FBAR

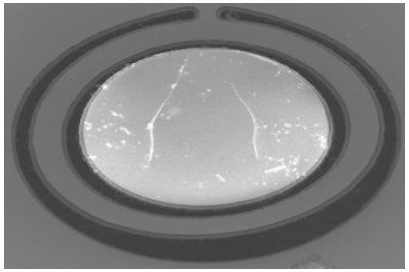

An SEM image of a fabricated single-anchor C-FBAR. The central circle is to avoid liquid smearing beneath of the AlN ring composite

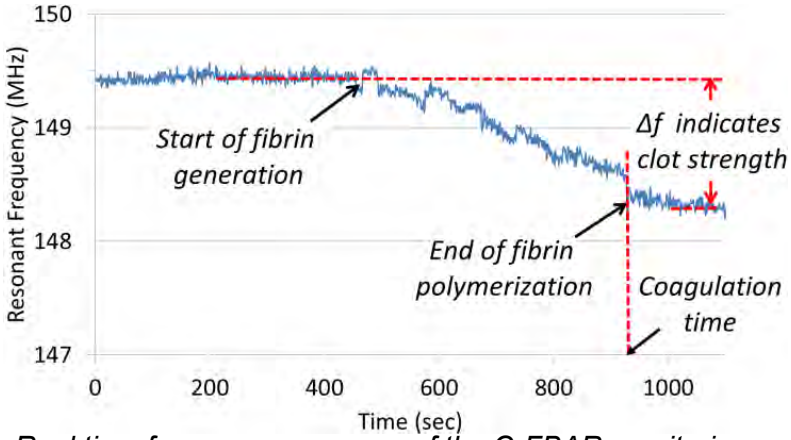

Real time frequency response of the C-FBAR monitoring the coagulation process of a citrated blood with 10 mg/mL Ca^{2+} concentration

W. Xu, X. Zhang, S. Choi, and J. Chae, "A High Quality Factor Film Bulk Acoustic Resonator in Liquid for Biosensing Applications," IEEE J. of MEMS, vol. 20, p. 213 (2011).

Junseok Chae, Arizona State University
Work performed at Arizona State University Nanofab Facility

Advanced Silicon Heterojunction Solar Cells

To provide large scale, low cost power production silicon photovoltaics must shift from high temperature diffusions to low-temperature (<300C) induced junction cells, in which a deposited material inverts the surface of the silicon, providing a high quality, thin junction with excellent surface passivation. Utilizing CSSER lithography, cleans, and deposition capabilities partly in collaboration with an industry partner, test structures are fabricated to validate modeling efforts aimed at understanding these heterojunctions. The goal is to develop novel cell designs such as the rear point contact sketch shown here which are compatible with ultra-thin silicon substrates.

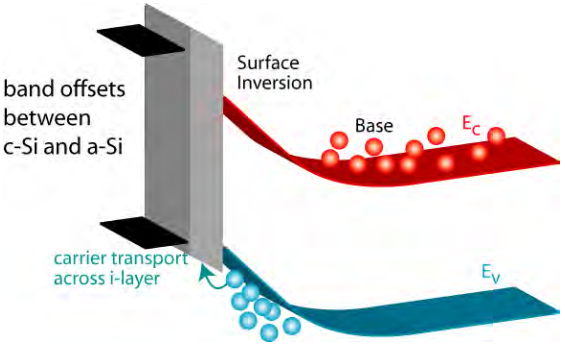

Band structure of silicon heterostructure showing the key features.

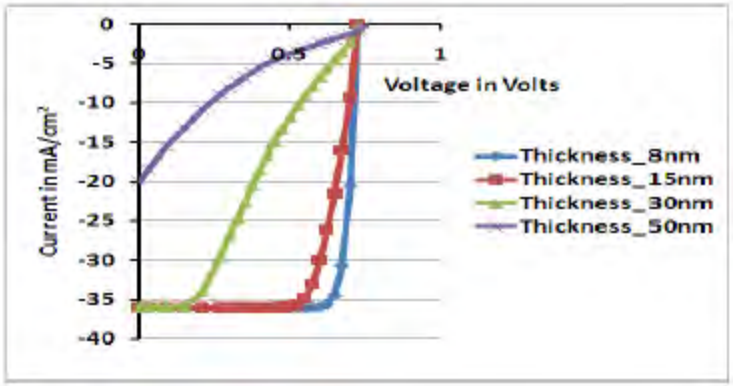

Illuminated IV curve for different intrinsic layer thicknesses

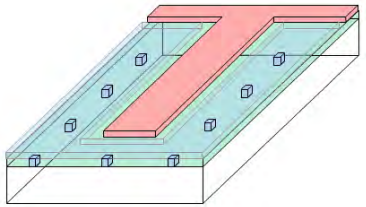

sketch of design sub-element for silicon heterojunction inter-digitated back contact (SHJ-IBC)

Kunal Ghosh, Clarence Tracy, Stanislau Herasimenka, and Stuart Bowden, ASU / Solar Power Laboratory
Work performed in part at ASU CSSER

3D flexible device fabrication project (NSF) and micro lunar seismometers project (NASA)

Fabricate flexible and stretchable 3D micro devices using 1) surface micromachining of polymer with full flexibility, 2) thin film transferring technology with fully stretchability, 3) laser dynamic forming on 3D surface to deform or bond pre-fabricated thin film flexible micro devices on 3D micro surface structure. (Supported by NSF)

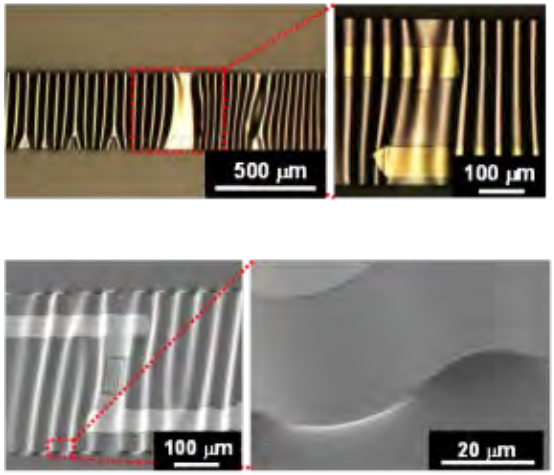

Fully stretchable and flexible temperature sensors

Develop high performance, light weight, low power consumption, robust seismometer for Lunar and Mar Exploration collaborating with seismologists and ASU and MET technology Inc. using molecular electronic transducers for seismology measurement. (Supported by NASA)

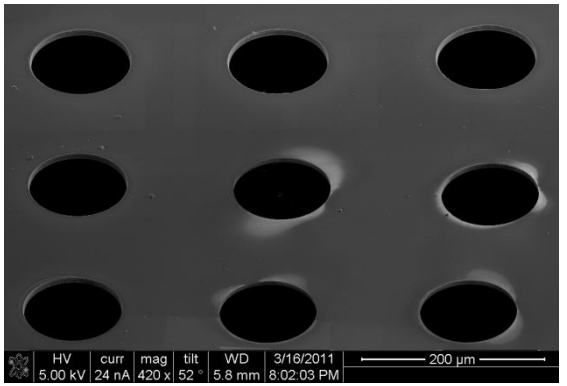

The sensing elements for micro seismometer

Hongyu Yu
Work performed at ASU NanoFab

Silicon Anodes on Soft Substrates in Lithium-Ion Batteries

This research project aims at developing silicon (Si) anode lithium (Li) ion batteries by utilizing Si nanostructures on elastomeric substrates as anodes to release the stress induced by Li ion diffusion during charge-discharge cycles. Si anode is being closely investigated for use in Li-ion batteries because of its highest-known theoretical charge capacity of 4,200 mAh/g. However, the development of Si-anode Li-ion batteries has lagged behind because of their large volumetric change (400%) upon insertion and extraction of Li, which results in pulverization and early capacity fading. The objective of this work is to resolve the stress issue and manufacture Si-anode Li-ion batteries.

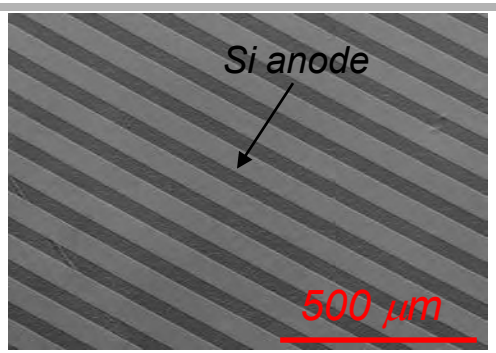

As-fabricated Si anodes on soft substrates are crack-free before lithiation.

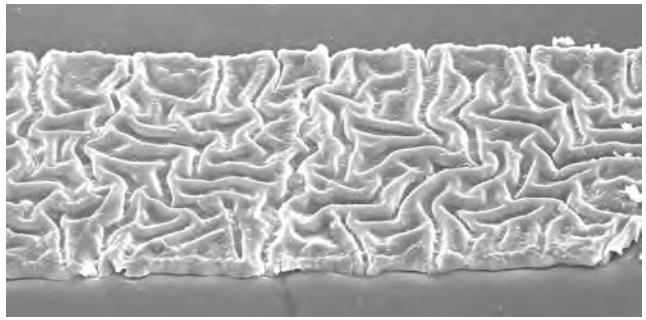

After lithiation: buckled

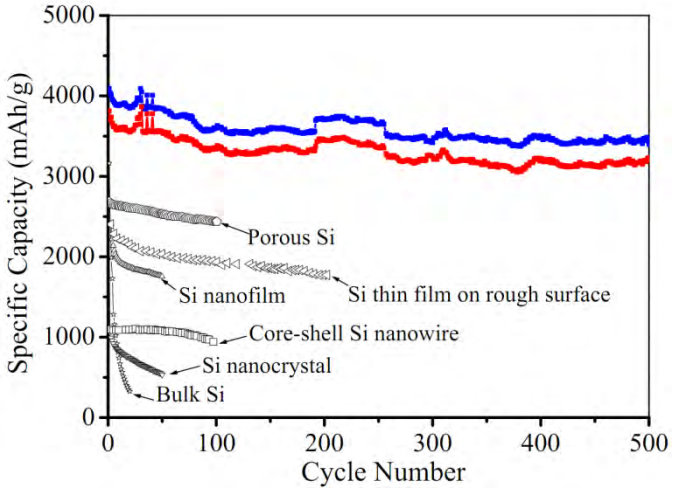

Very stable cyclic charge/discharge performance for over 500 cycles.

Hanqing Jiang, ASU
Work performed at ASU CSSER Facility
Supported by NSF

Ultra-Fast, Low Sample-Volume Microfluidic Switch

Current Surface Plasmon Resonance detection platforms are limited by how quickly a microfluidic sample can be delivered to the sensing region. This limitation prevents the measurement of small-molecule binding events, *i.e.* drug and therapeutic medicines.

Using soft photolithography, we have built a microfluidic system that can detect binding events that occur 20-100x faster than the current limit of commercial SPR. Overcoming this obstacle has opened the doors to fast and low sample volume molecular affinity/kinetic analysis.

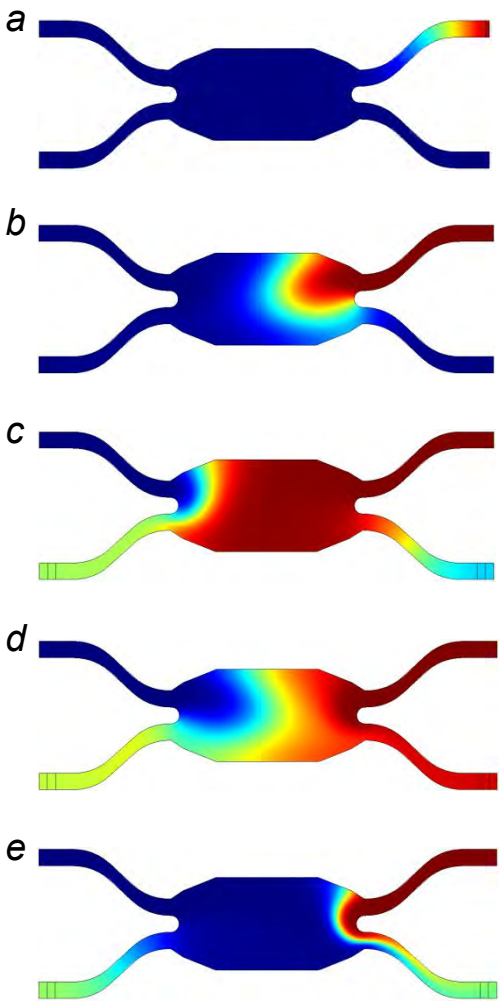

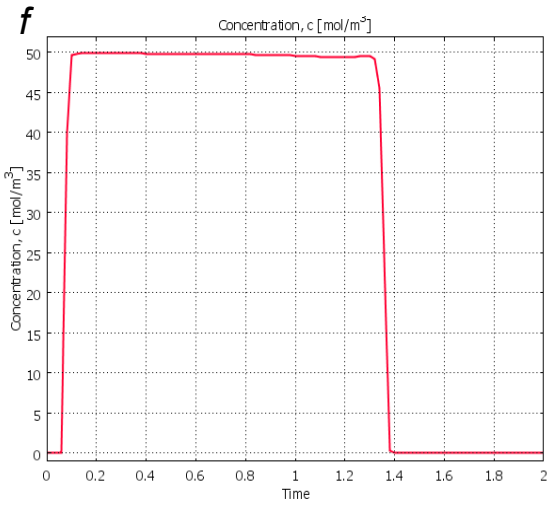

Sample concentration at 5 different times during a switching event as modeled by COMSOL. ***a*** *Buffer flows from the upper left arm and sample flows from upper right. The lower right valve is open and the lower left valve is closed (not shown).* ***b,c*** *Lower left valve is opened and lower right valve is closed. The fluid in the cell changes direction and exits to the lower left. The sample is introduced into the sensing area of the microfluidic device.* ***d,e*** *The valves return the their original state and the fluid flow reverses direction again. Buffer covers the sensing area.* ***f*** *Concentration profile as a function of time in the center sensing region of the microfluidic device*

Christopher MacGriff and N.J. Tao Arizona State University

Nanoporous Diatom Shells on Silicon Chips

Biomineralized Diatom shells exhibit impressive features, such as a hierarchical pore structure with the smallest pores having a diameter of 40 nm. This structure makes them extraordinarily mechanically stable, while allowing a short pore length. This makes them very attractive for nanoparticle filtration applications, the study of cell-cell-communication and ion channel sensors based on nanoscale bilayer lipid membranes.

The purpose of the project is to combine the advantages of the Diatom shells with silicon-based MEMS devices. At the ASU NanoFab photolithography and deep reactive ion etching is used to create through-wafer vias in silicon to allow fluidic access to the thin nanomembranes.

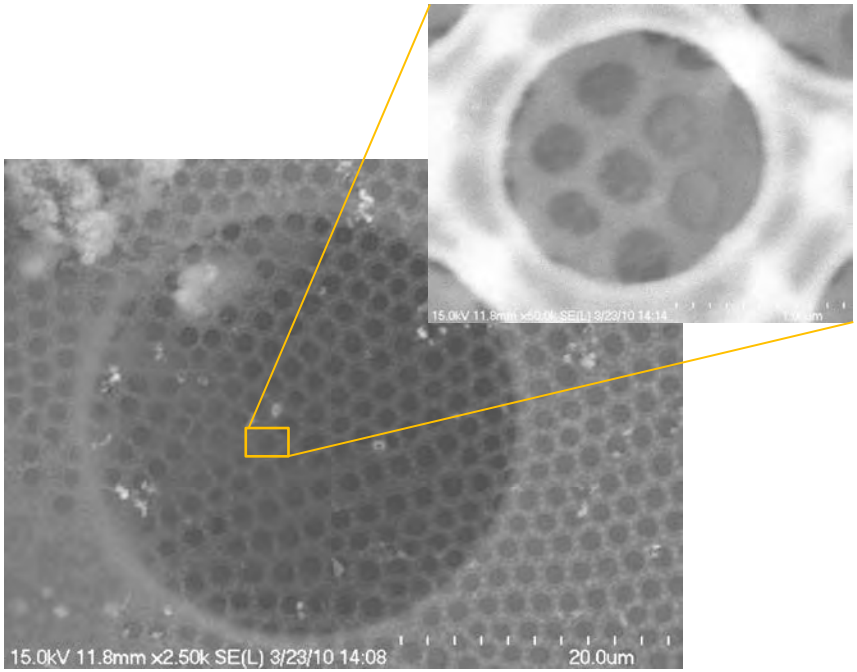

Scanning electron microscopy image of a Diatom shell mounted on a silicon micropore substrate.

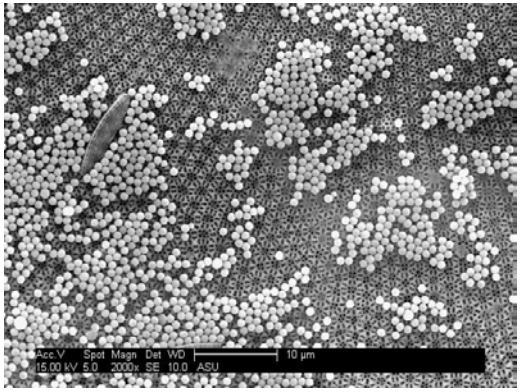

1 µm Polystyrene particles do not migrate through the Diatom and are efficiently retained by the nanopore matrix.

M. Goryll, B. L Ramakrishna and Sandwip K. Dey, ASU SECEE and SEMTE
Work performed at ASU NanoFab

Interconnecting Gold Islands with DNA Origami Nanotubes

Scaffolded DNA origami has recently emerged as a versatile, programmable method to fold DNA into arbitrarily shaped nanostructures that are spatially addressable, with sub-10-nm resolution. Toward functional DNA nanotechnology, one of the key challenges is to integrate the bottom-up self-assembly of DNA origami with the top-down lithographic methods used to generate surface patterning. In this report we demonstrate that fixed length DNA origami nanotubes, modified with multiple thiol groups near both ends, can be used to connect surface patterned gold islands (tens of nanometers in diameter) fabricated by electron beam lithography (EBL). Atomic force microscopic imaging verified that the DNA origami nanotubes can be efficiently aligned between gold islands with various inter-island distances and relative locations. This development represents progress toward the goal of bridging bottom-up and top-down assembly approaches.

Baoquan Ding, et al., Nano Lett. 10, 33073 (2010).

Hongbin Yu
Work performed at ASU NanoFab

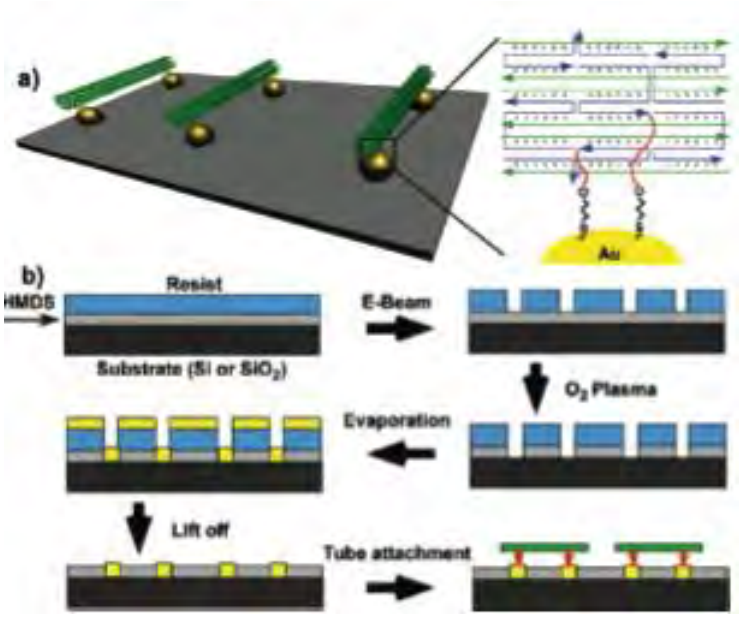

Schematic drawing of gold islands connected by DNA origami tubes on the substrate surface.

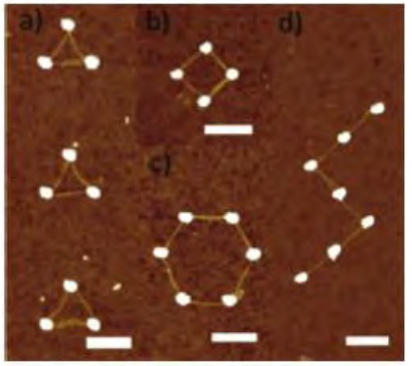

Various structures formed by connecting gold islands with DNA origami tubes

Novel Tunnel Junctions for Multi-Junction Solar Photovoltaics

To enable cost-effective concentrator photovoltaics, higher concentrations of 1000 suns or more, and higher efficiencies, and lower series resistance must be achieved. Additionally, in order to enable lattice-matched solar cells, investigation into the 0.61 nm material system is of great interest. Simulations from this group show that solar efficiencies for a four-junction solar cell based on the 0.61nm material system can reach 55%. In order to create such a solar cell, tunnel junctions for connecting the subcells must be demonstrated.

Our group has fabricated tunnel junctions using combinations of InAs-GaSb, ZnTe-InAs, ZnSe-GaSb, and ZnTe-GaAs. The InAs-GaSb results show very low contact tunnel junctions. The II-VI on III-V tunnel junctions do not yet yield as promising results.

Yong-Hang Zhang,
Center for Photonics Innovation,
Arizona State University

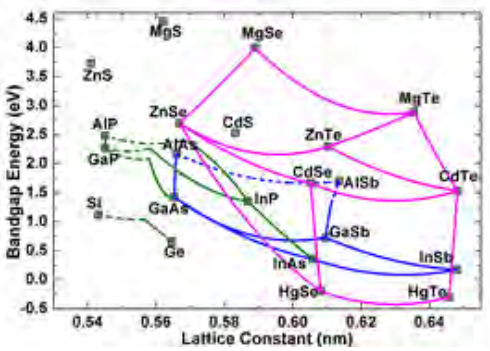

Bandgaps of compound semiconductors as a function of lattice constant

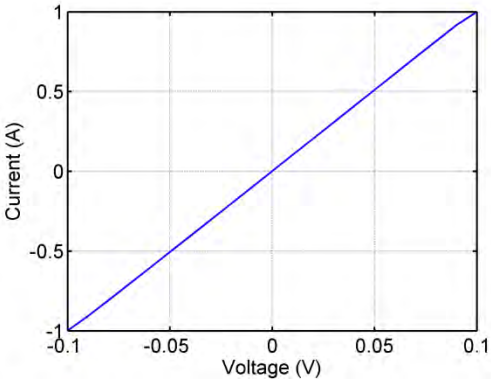

InAs-GaSb tunnel junction showing a resistance of 0.22 mΩ-cm² (Very good)

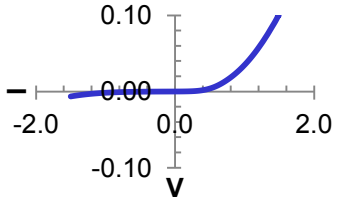

Non-Ohmic ZnTe-GaAs Junction

Electric Cell-substrate Impedance Sensing

The purpose of this project is to understand the interaction between cells and their substrates by measuring AC impedance changes due to cell-substrate separation and the projected area when cells spread and adhere. These two properties are related to the survival rate and level of Ca^{2+} in the cell nucleus. Measuring individual cells allows the study of heterogeneity in cell populations which will help our understanding of disease including cancer.

One of the key components of this project is to develop the micro-electronic device for live cell trapping and impedance sensing. The device consists of eight microwells with gold electrodes at the bottom of each well. Single cells were loaded into the micro-well, and the impedance changes were continuously monitored for 1-2 days or when sufficient data sets were obtained. Microfabrication techniques, such as photolithography, PVD, wet etch, and bonding were developed to fabricate this sensing device and to optimize its geometry and shape.

Roger Johnson, Haixin Zhu and Deirdre Meldrum
Center for Biosignatures Discovery Automation
The Biodesign Institute at Arizona State University
Device fabrication performed at ASU CSSER NanoFab Facility

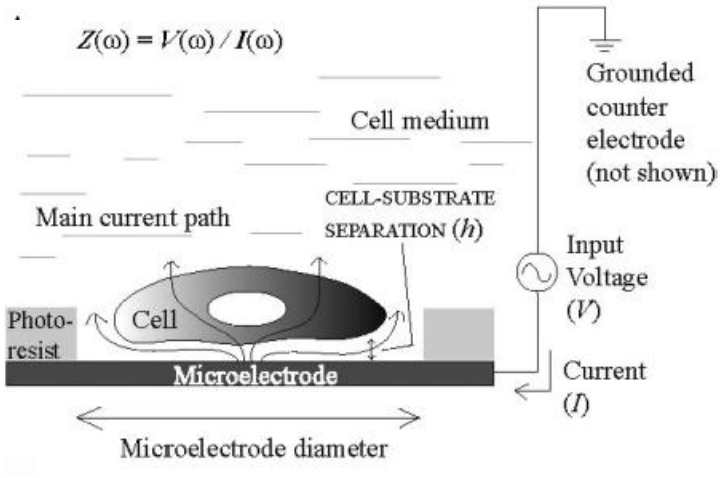

Schematic View of the ECIS technique

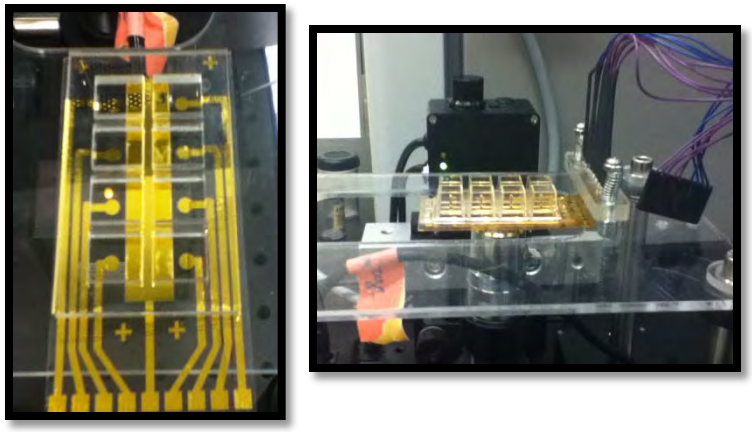

Microfabricated Sensing Device (left) and Experiment Setup (Right)

NNIN Site at the University of Colorado

Micropatterned Treads for In Vivo Robotic Mobility

This work explores micropatterned treads that may enable mobile capsule crawlers inside the body. Current research efforts into providing contact locomotion using micro-tread tracks are explored with an in vivo porcine evaluation and comparison of two leading tread designs.

It was found that a smooth PDMS tread outperformed all other tread patterns. There were no significant differences between the performance of square and circular pillars.

An in vivo comparison of a smooth PDMS covered wheel and a patterned (equally spaced circular pillars) PDMS covered wheel was performed, and the patterned wheel outperformed the smooth wheel.

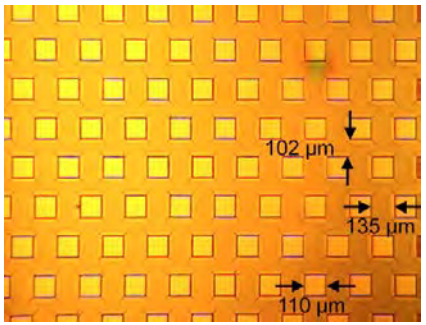

Optical microscope view of micro-tread pattern with 1:2 aspect ratio (height:width)

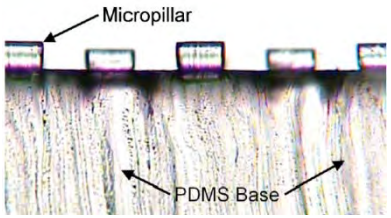

Profile view of micro-tread pattern with 100x magnification

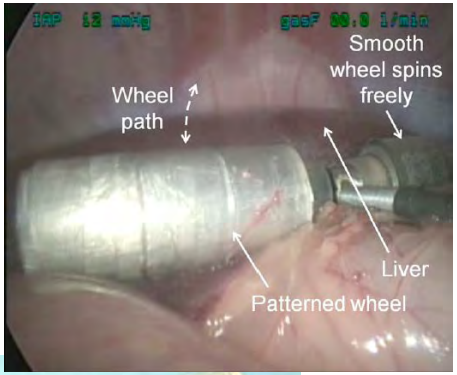

In vivo robot on liver (view from laparoscope)

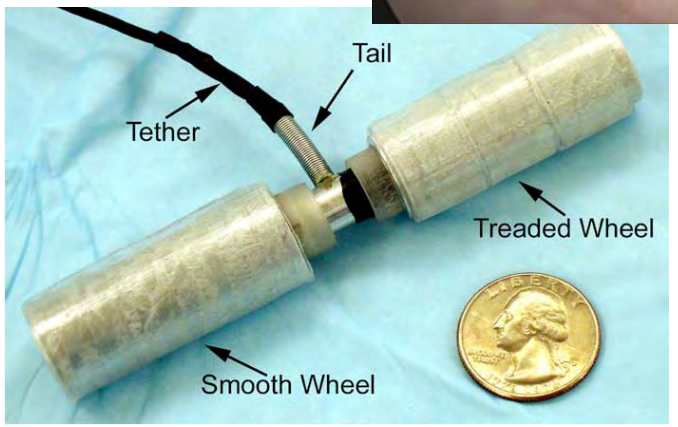

Robot used for in vivo comparison of micropatterned versus smooth wheels

L. Sliker, X. Wang, J. Schoen, M. Rentschler, Univ. of Colorado. The micropatterned treads were fabricated at the Colorado Nanofabrication Laboratory

Atomic layer deposition enabled interconnect technology for vertical nanowire arrays

This work demonstrates an atomic layer deposition enabled interconnect technology for vertical, c-axis oriented gallium nitride nanowire arrays encapsulated by benzocyclobutene (BCB).

The nano-scaled ALD multilayer is essential to provide conformal co-axial dielectric (ALD-alumina)/conductor (ALD-tungsten) coverage and precise thickness control for nanowire metallization.

This interconnect technology can be applied to various vertical nanowire-based devices, such as nanowire light emitting diodes, nanowire-based field effect transistors, resonators, batteries or biomedical applications.

J. Cheng, D. Seghete, M. Lee, J. Schlager, K. Bertness, N. Sanford, R. Yang, S. George, Y.C. Lee, Univ. of Colorado/NIST
Fabricated was performed at the Colorado Nanofabrication Laboratory

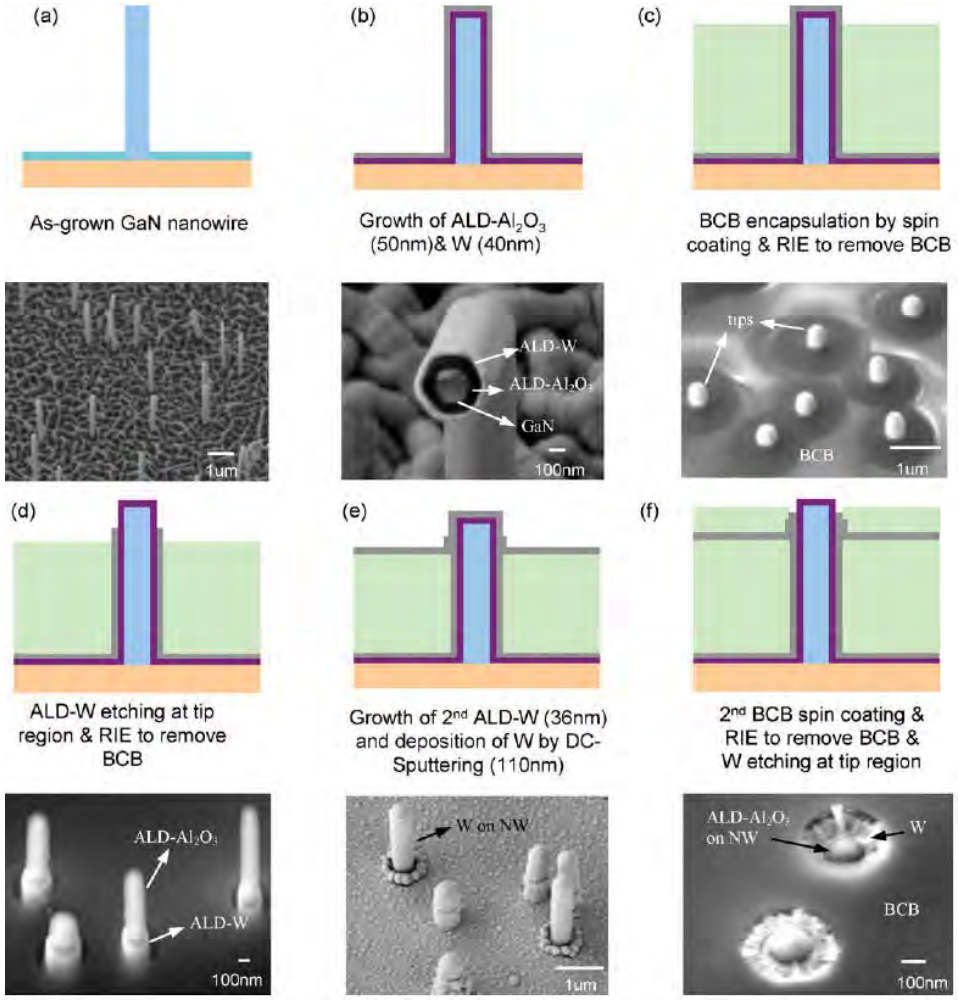

Fabrication process flow and corresponding experimental results of a local interconnect process that results in nanowires interconnected with tips exposed (no W-layer on the nanowire tip).

The Development of Polymer-Based Flat Heat Pipes

This work involves the fabrication and testing of polymer-based flat heat pipes. Liquid-crystal polymer films with copper-filled thermal vias are employed as the case material. A copper micropillar/woven mesh hybrid wicking structure was designed and fabricated to promote evaporation/condensation heat transfer and the liquid supply to the evaporator of the PFHP.

The test data demonstrated that the heat pipe can operate with a heat flux of 12 W/cm^2 and results in effective thermal conductivity ranging from 650 to 830 W/m · K.

With the employment of flexible liquid crystal polymers as casing material, the heat pipe can be integrated into a printed circuit board or flexible circuits for thermal management of heat-generating components.

C. Oshman, B. Shi, C. Li, R.Yang, Y. Lee, G. Peterson, and V. Bright, Univ. of Colorado.
Work was performed at the Colorado Nanofabrication Laboratory

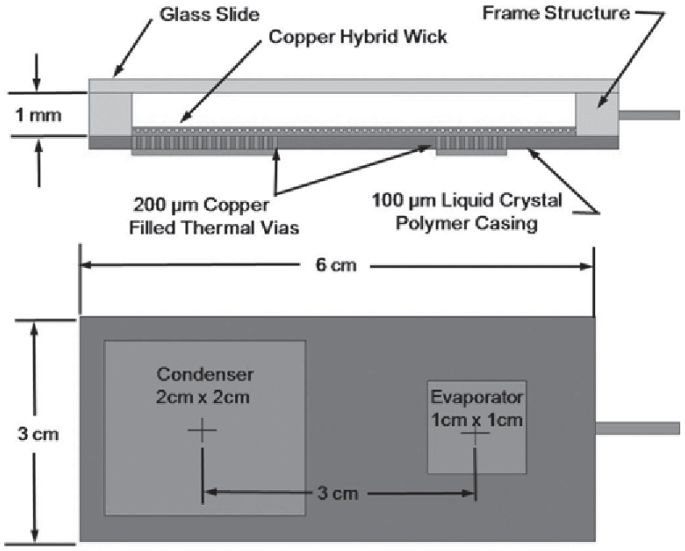

Cross-sectional and bottom view schematic of heat pipe

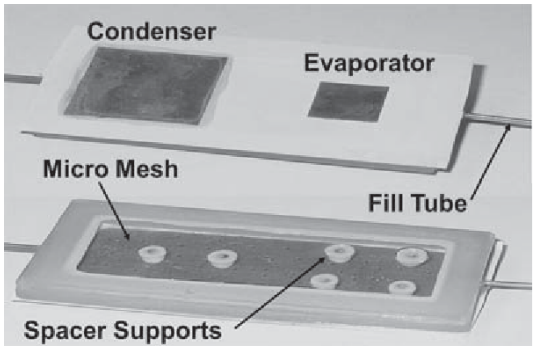

Top and bottom views of the finished device showing the evaporator and condenser regions located on the liquid crystal polymer substrate

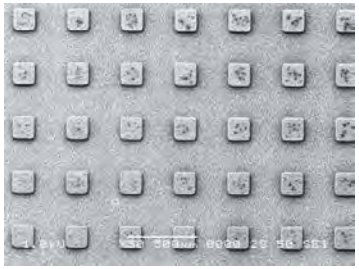

SEM image of the copper wet-etched 200-µm evaporator wicking channels

ALD tungsten NEMS switches and tunneling devices

This work demonstrates a a novel low-temperature, CMOS compatible, top-down nanofabrication process employing ALD tungsten (WALD) as a structural material for nano-electro-mechanical systems (NEMS). Using this process, doubly-clamped suspended NEMS switches/tunneling devices have been successfully fabricated and demonstrated.

A lifetime of ~50,000 cycles has been observed when these devices are operated in full contact switching mode, and a lifetime in excess of 5×10^6 cycles has been observed under low-current-limited operating conditions.

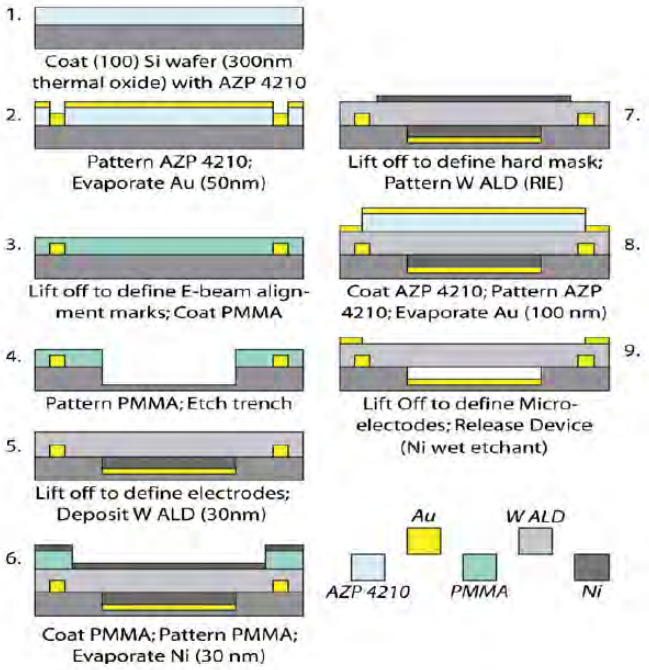

Fabrication process of NEMS switches.

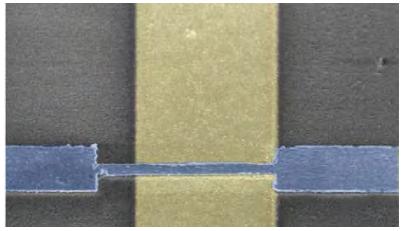

NEMS switch with 3μm electrode width, 32 nm beam thickness, and 32 nm gap

B. Davidson, D. Seghete, S. George, V. Bright, Univ. of Colorado.
Fabricated was performed at the Colorado Nanofabrication Laboratory

NNIN Site at Washington University St. Louis

Magnetomotive Enhanced Thrombolysis in Stroke Patients

Stroke is the third largest killer and the leading cause of long-term disability in the US, impacting over 800,000 Americans each year. Although the US offers the most advanced therapies for stroke, there is less than a 10% chance the victim will see little or no disability, and over 65% chance they will die or become severely disabled. It is currently estimated that stroke represents a $73B economic cost to the US. Pulse Therapeutics is developing a technology to improve stroke outcomes by providing a minimally-invasive, compact, and safe magnetic technology to the emergency room which will mechanically amplify the effects of clot-busting drugs in the treatment of stroke using an external magnetic field coupled to magnetic nanoparticles at the site of the clot. Magnetic nanoparticles used in the study were synthesized at the NRF.

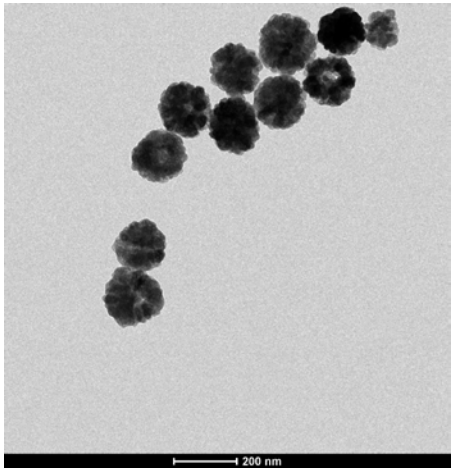

Magnetic nanoparticles synthesized at the NRF for Pulse Therapeutics, Inc.

Prototype magnet system developed by Pulse Therapeutics, Inc. for use with magnetic nanoparticles in the treatment of stroke patients.

Francis M. Creighton, PhD. and Rogers C. Ritter, PhD.,
Pulse Therapeutics, Inc.
Work performed at Washington University in St. Louis Nano Research Facility

Embedded Catalytic Metal Colloids

The purpose of the Embedded Catalytic Metal Colloid Project is to grow metal colloids within silicone polymer matrices and to use these systems as catalysts. These systems could combine the catalytic capabilities of the colloidal metal particles with the ability to recover the catalytic particles at the end of the reaction. To analyze the structure of the metal colloids, the polymer matrix is dissolved in hydrofluoric acid, cleaned, and the metal particles are deposited on a Cu grid for remote transmission electron microscopy at the NRF.

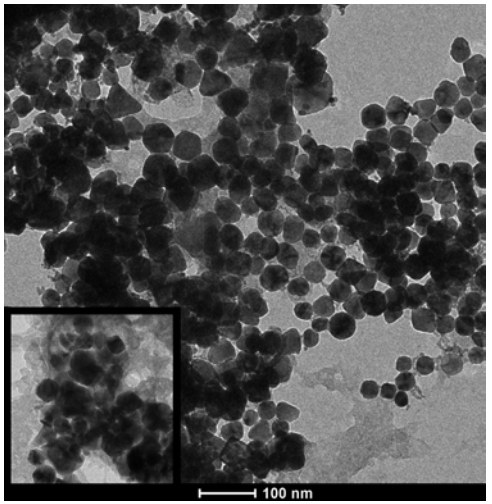

Transmission electron microscope image of palladium colloids before and (inset) after use as catalysts for hydrogenation.

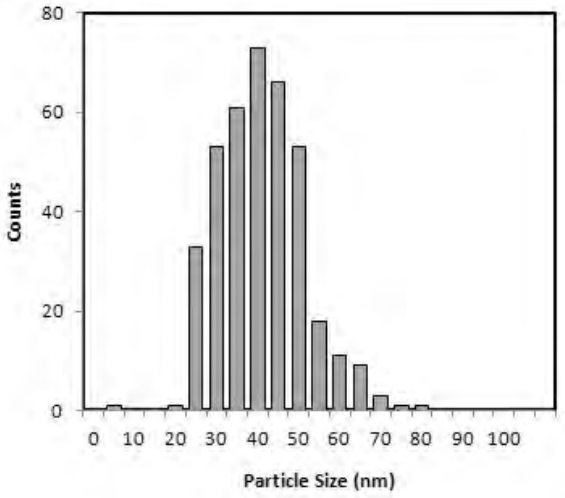

Size distribution of palladium colloid particles.

Dean Campbell, Bradley University
Work performed at Washington University in St. Louis Nano Research Facility

Patterned BZ Gels by PDMS Stamps

The Epstein and Xu groups at Brandeis University are evaluating the fundamental effects of the localization of active species in non-equilibrium soft materials during chemomechanical conversion. A theoretical study by A. C. Balazs has established that heterogeneity and hierarchical structure will be beneficial and advantageous for constructing chemomechanical soft materials. Micron sized heterogeneous BZ polymer gels that implement the design principles obtained from the theoretical study will be generated using PDMS stamps fabricated at the NRF.

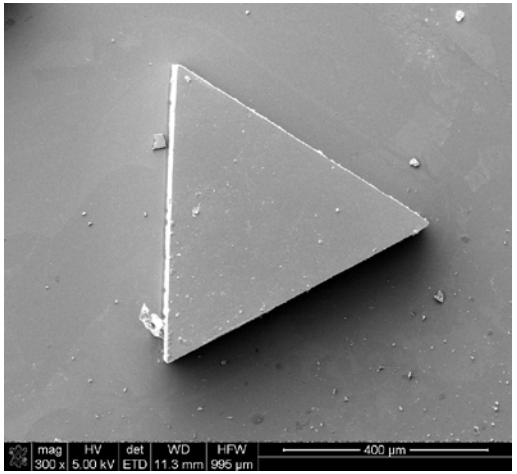

Triangular post on a master used to fabricate the PDMS stamp utilized for BZ gel generation.

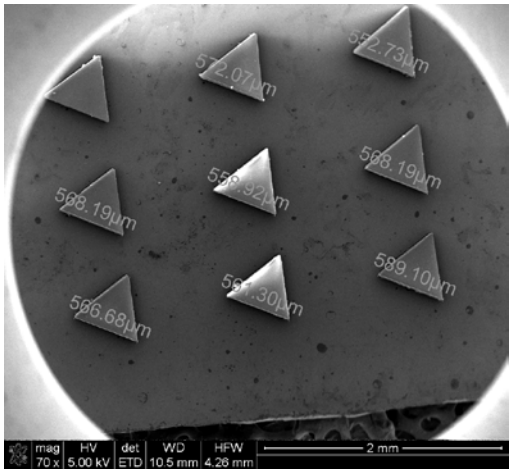

BZ gel particles generated using the PDMS stamp are equilateral triangles with edge lengths of approximately 560 µm. Over 2,000 particles can be generated at a time using the PDMS stamp.

Bing Xu and Irving Epstein, Brandeis University
Work performed at Washington University in St. Louis Nano Research Facility

Nanocatalysts for Fuel Cells

Nanocatalysts can have higher activity than their counterpart bulk catalysts. This makes them ideal candidates for fuel cell development. The size and shape of nanocatalysts can have a significant effect on their activity. The imaging performed at the NRF allows for accurate screening of nanocatalysts based on size, shape, and distribution in order to optimize their activity before they are added to fuel cells.

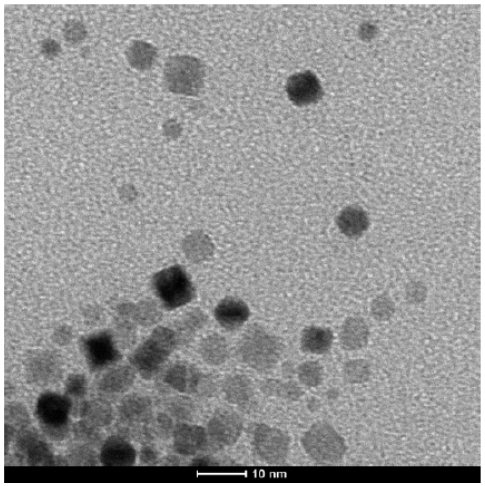

Nanocatalyst with non-uniform particle distribution.

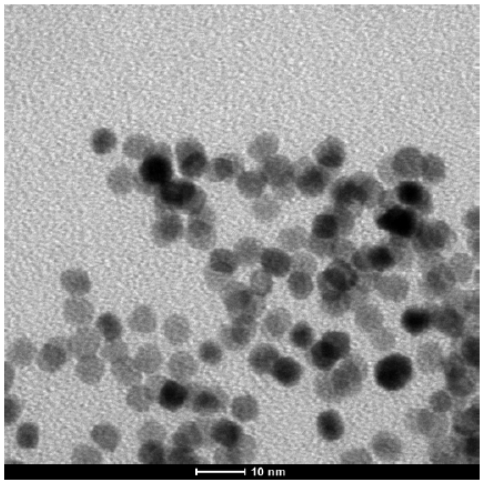

Nanocatalyst with uniform particle distribution.

Minhua Shao, Undisclosed Company
Work performed at Washington University in St. Louis Nano Research Facility

Self Assembled Gold Nanoparticles for Biosensing Applications

Noble metal nanoparticles exhibit localized surface plasmon resonance (LSPR) when excited by incident light of a specific wavelength. The LSPR wavelength is extremely sensitive to changes in the refractive index, and consequently, to the nanoparticle environment. The LSPR wavelength shift can be measured and used to detect molecules adsorbed on the surface of the nanoparticle. Assembly of nanoparticles generates plasmonic coupling between adjacent particles which can greatly enhance sensitivity. In this project rapid self-assembly of gold nanoparticles is achieved using aminothiols (p-ATP). The self-assembled gold nanoparticles are transferred to solid substrates while preserving the assembly structure and optical properties.

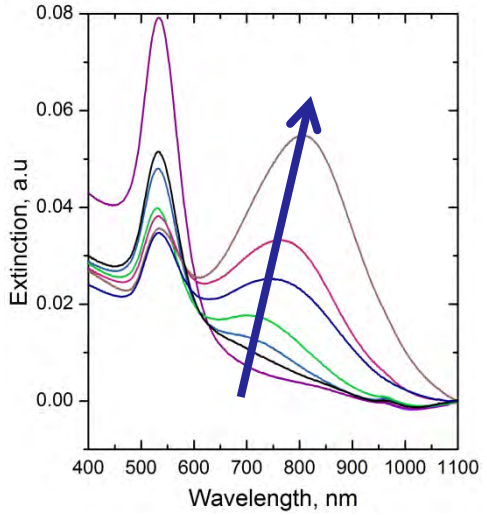

UV-Vis extinction spectra of self-assembled gold nanoparticles on silicon substrates with increasing p-ATP concentration from bottom to top.

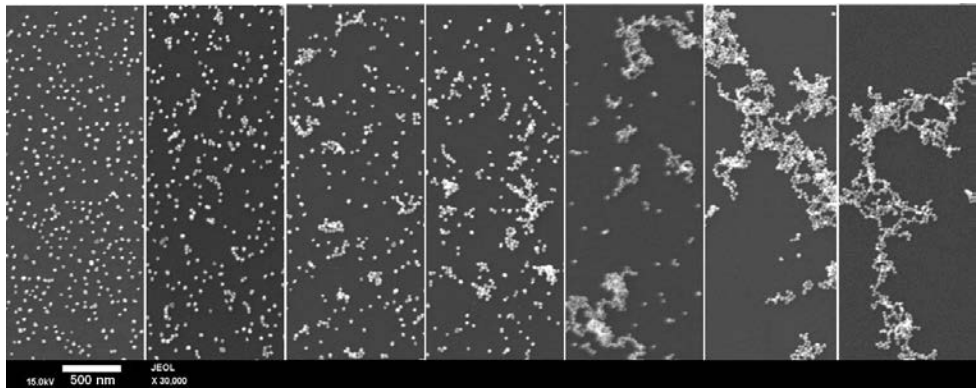

SEM images of self-assembled gold nanoparticles on silicon substrates with increasing p-ATP concentrations from left to right.

Srikanth Singamaneni, Abdennour Abbas, and Abigail Halim, Washington University in St. Louis
Work performed at Washington University in St. Louis Nano Research Facility

Fe(II)-Activated Trace Element Cycling through Crystalline Iron Oxides

Biogeochemical Fe cycling causes nanoscale surface transformations of Fe oxide minerals driven by coupled electron transfer and atom exchange between aqueous Fe(II) and the Fe(III)-oxide surface. This cycling affects the speciation of redox-active trace elements. However, it is unclear how Fe cycling influences redox-inactive trace elements, which may be essential micronutrients or water contaminants. We have shown for the first time that aqueous Fe(II)-activates trace element cycling through Fe(III)-oxides, which involves the incorporation of adsorbed species and the release of pre-incorporated species. Such cycling affects micronutrient availability, contaminant transport, and the distribution of both redox sensitive and redox-inactive trace elements in natural and engineered systems.

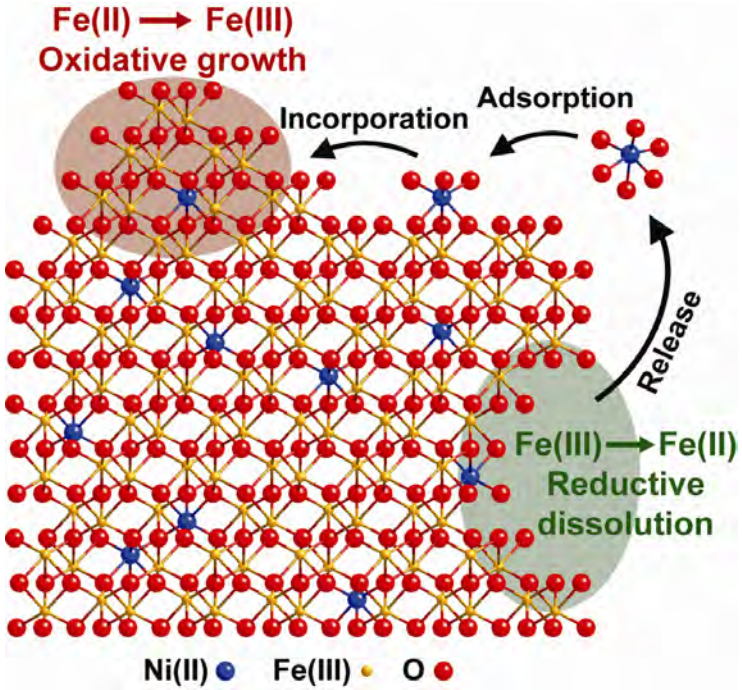

Mechanistic illustration of Fe(II)-induced recrystallization of Ni-substituted hematite. Aqueous Fe(II) catalyzes the simultaneous growth and dissolution on a single crystal. Areas of oxidative Fe(II) adsorption lead to localized surface growth and cause incorporation of adsorbed Ni. Regions exhibiting Fe(III) reductive dissolution cause the release of Ni. Fe(II) is not shown but assumed to be present in excess on the solid and in solution. View is along [100]. From Frierdich et al., 2011.

Andrew J. Frierdich and Jeffrey G. Catalano,
Washington University in St. Louis

Work performed at Washington University in St. Louis Nano Research Facility

Polarization Imaging Sensor with Aluminum Nanowires

The purpose of the Polarization Imaging Sensor is to capture linear polarization properties of the imaged environment in real-time and in high resolution. The sensor monolithically integrates aluminum nanowires with an array of CCD imaging elements. The CCD imaging die serves as a substrate for depositing metallic nanowires at four different orientations. The aluminum nanowires are fabricated via e-beam deposition, e-beam lithography and reactive ion etching. The final imaging sensor records angle and degree of linear polarization at 40 frames per second with 1 million photodetectors.

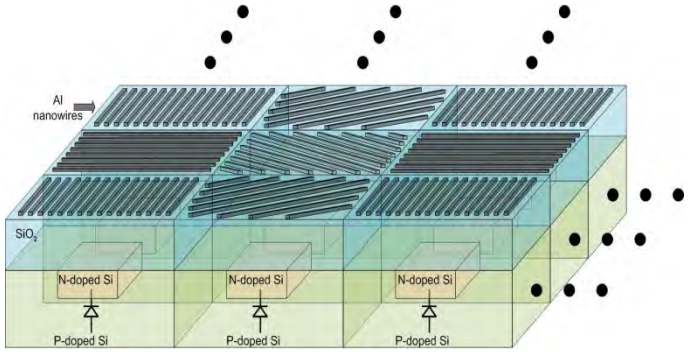

CCD imaging array with aluminum nanowires acting as polarization filters.

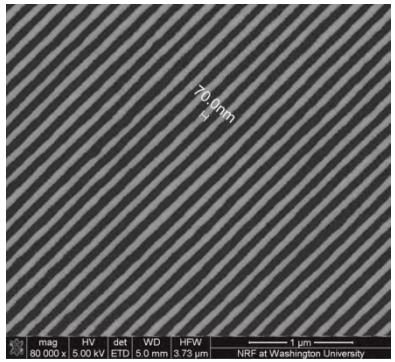

SEM image of the aluminum nanowire optical filters deposited directly on top of the CCD imaging sensor

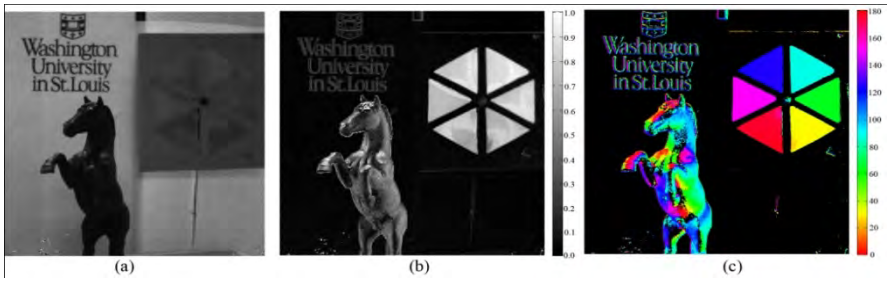

Single-frame excerpts of video recordings from a CCD polarization imaging sensor and linear polarization filters. (a) intensity information; (b) degree of linear polarization and (c) angle of linear polarization of the imaged scene.

Viktor Gruev, Washington University in St. Louis
Work performed at Washington University in St. Louis Nano Research Facility

Gold Nanohexapods with Tunable Photothermal Properties for Cancer Treatment

Many gold nanoparticles have tunable electromagnetic absorption characteristics. They can be tuned to the near-infrared (NIR) region which exhibits low water and tissue absorbance with ease allowing for photothermal therapy in biological settings. Photothermal treatment has been studied for gold nanorods and gold nanocages in the past, but not for gold nanohexapods, a novel class of nanoparticle only recently synthesized. The observed properties of nanohexapods indicate they have comparable or better properties for photothermal applications in comparison to nanorods and nanocages and have great potential in cancer therapy.

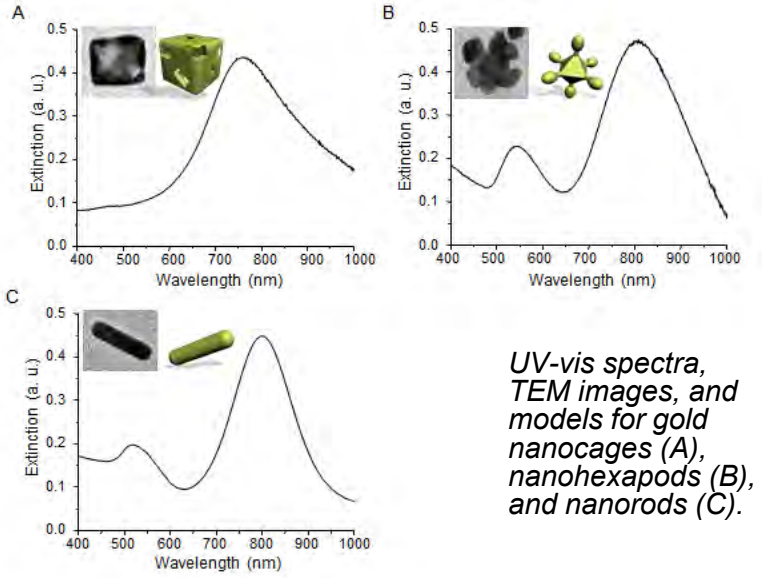

UV-vis spectra, TEM images, and models for gold nanocages (A), nanohexapods (B), and nanorods (C).

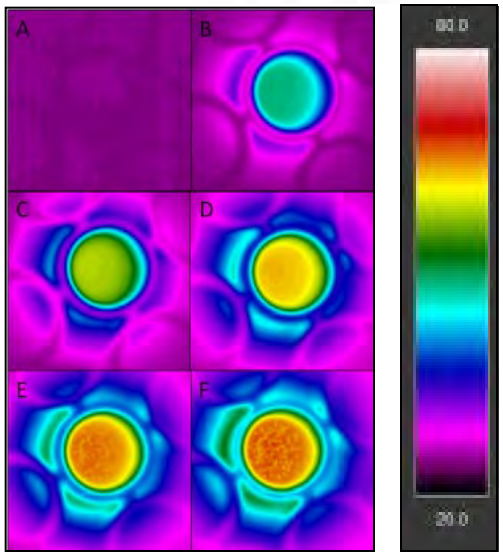

Thermal images of gold nanohexapods in solution after 0(A), 45(B), 90(C), 135(D), 180(E), and 225(F) seconds of laser irradiation. Temperature is in degrees Celsius.

Younan Xia, Yucai Wang and Max Li,
Washington University in St. Louis
Work performed at Washington University in St. Louis Nano Research Facility

NNIN Site at Harvard University

Center for Nanoscale Systems

Detecting Non-Abelian Statistics in the Fractional Quantum Hall Effect

Statistics refers to a quantum property of particles: what happens when two are exchanged. For example, when two fermions changing place, a minus sign is added to the wave function, leading to the Pauli exclusion principle. In two dimensions, exotic excitations can occur, including ones with non-abelian statistics: when two excitations are swapped, a new state is formed. Thus braiding these excitations can be used to encode information. Particles with non-abelian statistics are predicted to exist in certain states in the fractional quantum Hall systems. This project aims to identify them by their predicted interference effects.

Doug McClure, Angela Kou, Patrick Gallagher, Marcus Lab, Harvard University. High mobility GaAs material from Pfeiffer Lab, Princeton University. Devices fabricated using electron beam lithography and deposition systems at Harvard's Center for Nanoscale Systems.

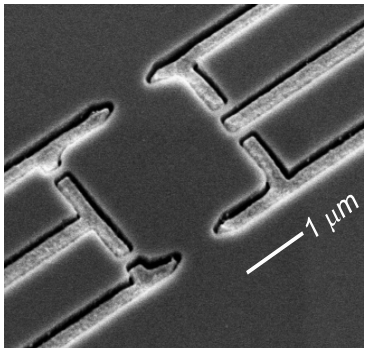

A 4 μm² quantum dot, defined by aligned etching and metallic gates.

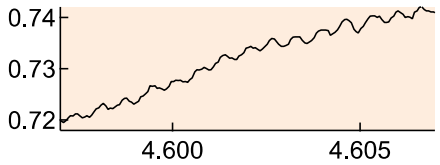

Conductance through the dot in e/h² as a function of magnetic field in tesla, showing oscillations in the 4/3 fractional quantum Hall state.

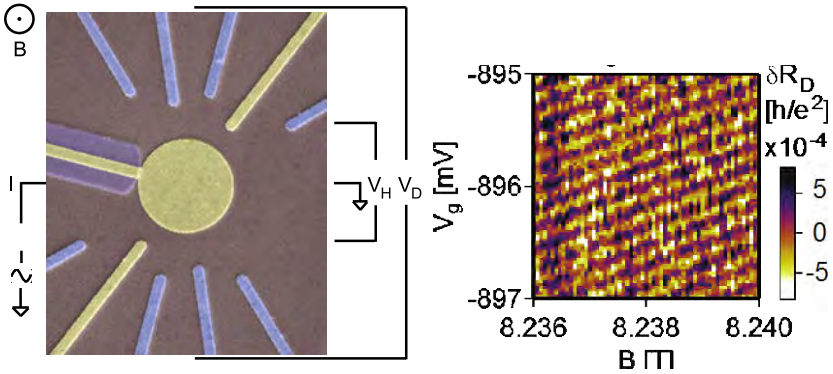

An anti-dot geometry using multilayer aligned lithographic layers of metal, separated by atomic layer deposition oxide. Oscillations of conductance through the antidot system (yellow gates), in the 2/3 fractional quantum Hall state.

Hybrid Integrated Circuit / Microfluidic Chip

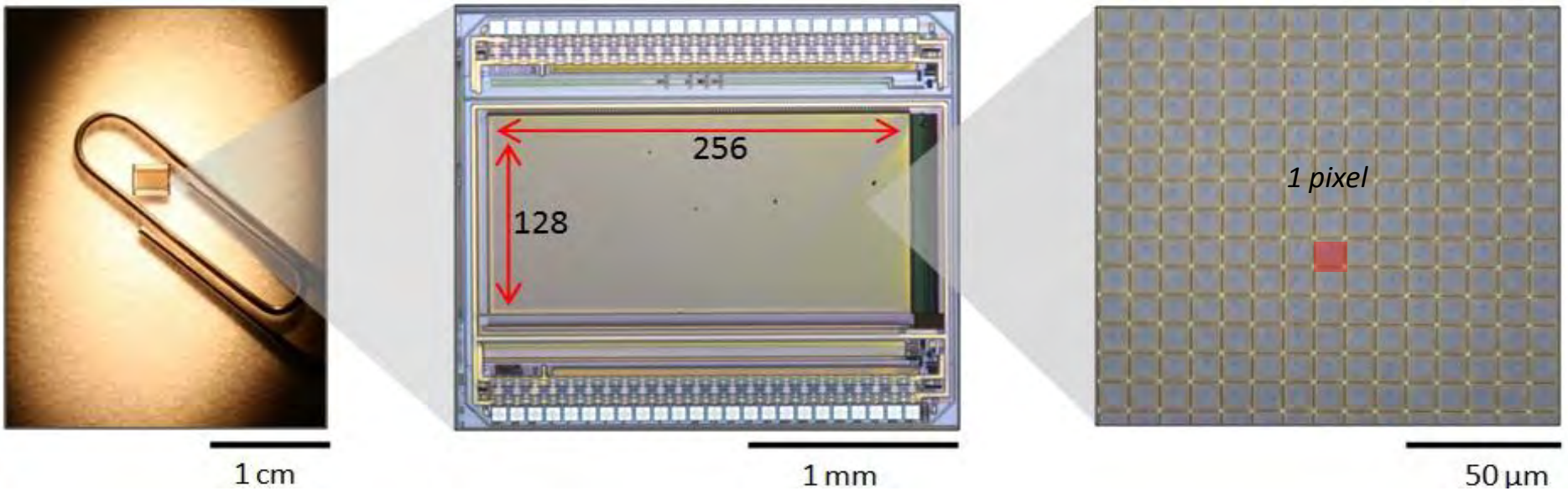

The hybrid integrated circuit / microfluidic chip contains a display of 128 x 256 pixels. Each pixel is 10 x 10 µm in area and can be individually energized to 0 or 5V.

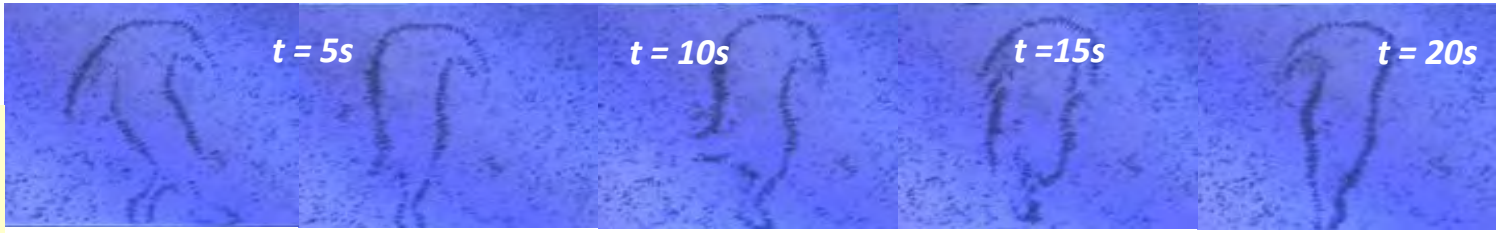

Work performed by Caspar Floryan, Robert Westervelt at Harvard's Center for Nanoscale Systems.

Suspended yeast cells are transported to large electric fields by dielectrophoresis. A video played on the chip creates a dancer composed of yeast cells.

Nanostructured doped TiO_2 for water splitting

The purpose of the nanostructured doped TiO_2 is to produce a material for efficient water splitting for hydrogen fuel production. The titanium thin films are evaporated in the Harvard Center for Nanoscale Systems (CNS) and then laser treated. After laser irradiation, we image the samples with Scanning Electron Microscopy and make cross-sections with the Focused Ion Beam (FIB). We hope to produce efficient water splitting devices with our nanostructured surfaces.

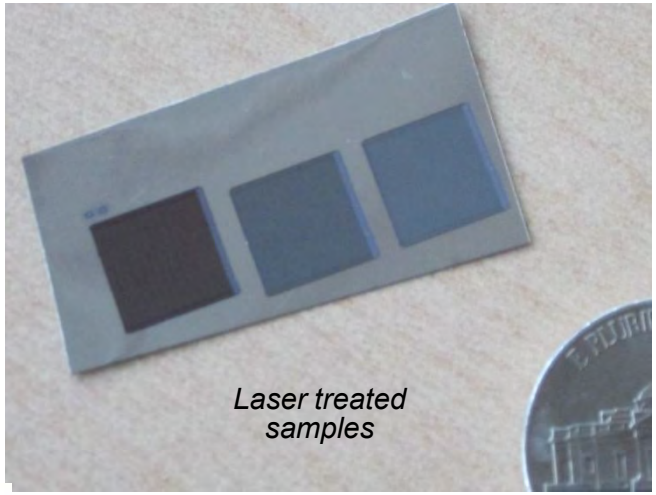

Laser treated samples

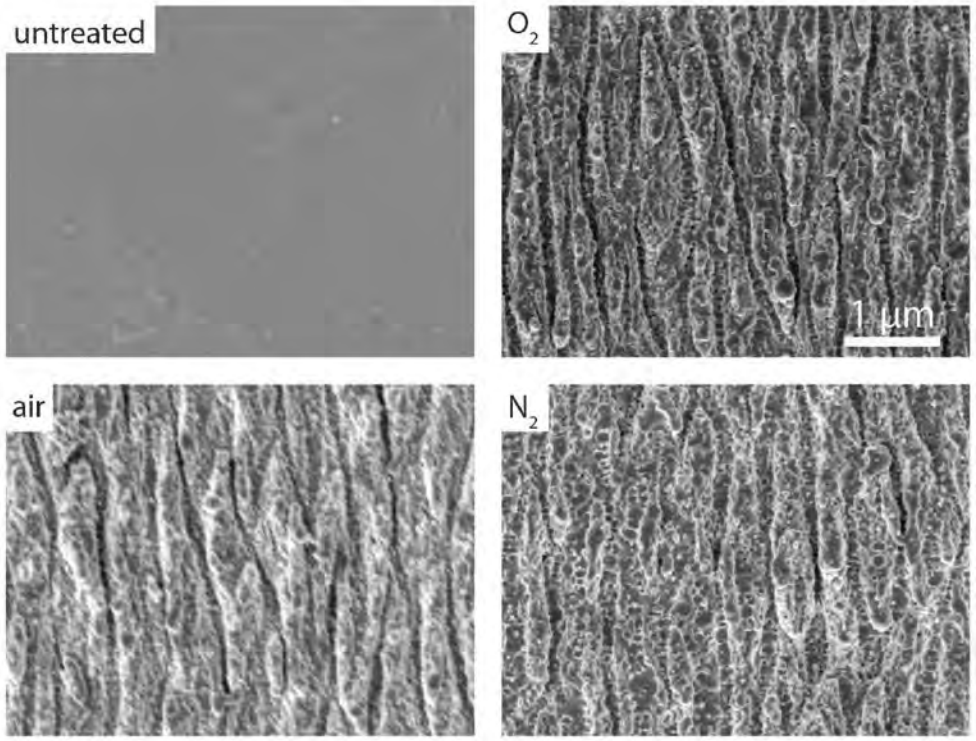

SEM images of the untreated and laser treated samples in various gases (O_2, air, N_2)

Katherine Phillips, Elizabeth Landis, Cynthia Friend, and Eric Mazur, Harvard School of Engineering and Applied Sciences and the Harvard Department of Chemistry.
Site used: Harvard Center for Nanoscale Systems

Landau level crossings in trilayer graphene

Charge carriers in single-layer graphene behave like massless particles whereas, those in bilayer graphene act as massive particles. In Bernal-stacked trilayer graphene (TLG), both of these massless and massive particles coexist.

When these charge carriers are subjected to high magnetic field, they start to form quantized energy levels. However, these energy levels for massless and massive particles depend differently on the magnitude of the magnetic field. As a result, they should cross at finite magnetic field and density.

In this work, we have measured for the first time such crossings, unique to TLG. The position of these crossings in magnetic field and density also allows us to determine the parameters necessary to describe TLG, which is useful in modeling TLG for further study.

Work performed at Harvard Center for Nanoscale Systems by Jarillo-Herrero group, MIT.

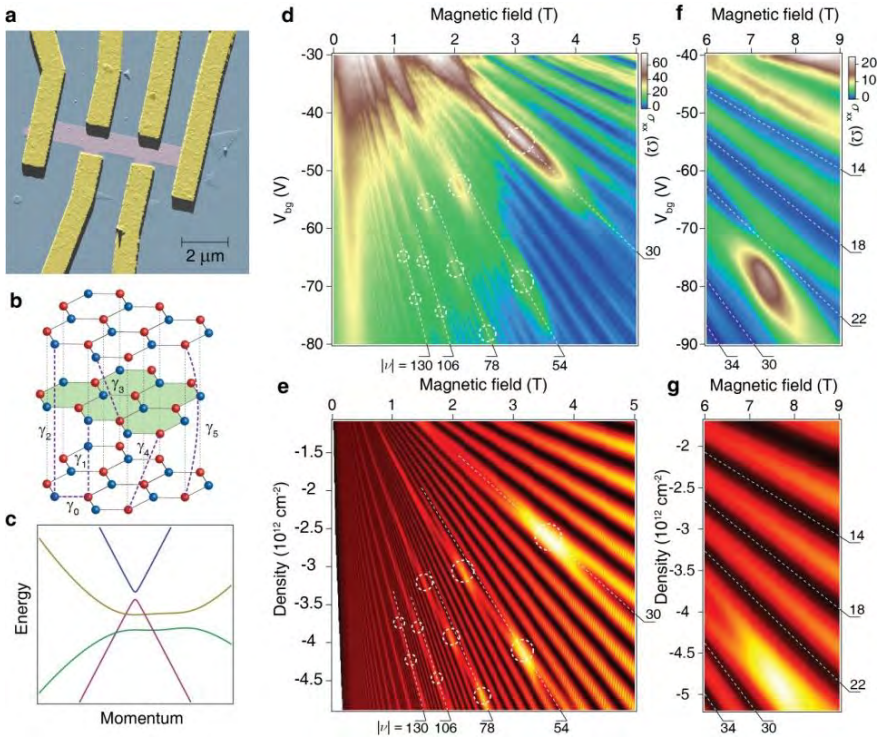

(a) AFM image of a TLG Hall-bar device on hBN. (b) Bernal-stacked TLG atomic lattice. (c) Band structure of TLG within a full-parameter model. (d, f) Color map of Landau fan diagram as a function of back-gate voltage and magnetic field at 300 mK. White dashed lines are guides to the eye with filling factors labeled on the edge and the white dashed circles indicate crossing points. (e, g) Calculated density of states as a function of density and magnetic field

T. Taychatanapat, K. Watanabe, T. Taniguchi, P. Jarillo-Herrero, *Nature Physics* **7**, 621-625 (2011)

Revolutionary Silicon Power Cell™ for Portable Consumer Electronics

Massachusetts-based Lilliputian Systems Inc. (LSI) is developing a revolutionary miniature fuel cell for the $50 billion portable power market.

LSI is pursuing a radically different technical approach (relative to other fuel cells) by implementing its fuel cell in silicon, using thin-film Solid Oxide Fuel Cell (SOFC) technology and Micro Electrical Mechanical System (MEMS)-based fabrication methods

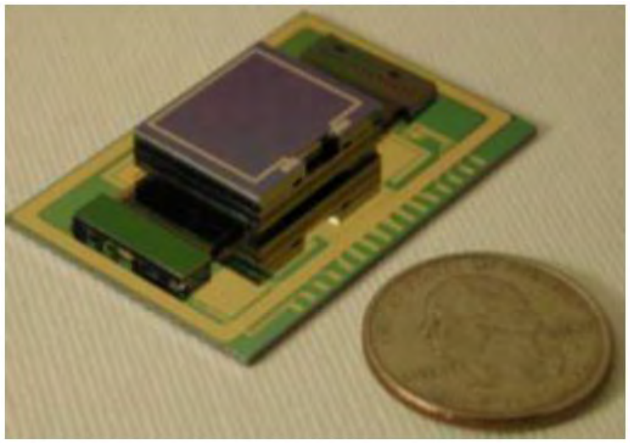

Work performed at Harvard Center for Nanoscale based on technology developed at MIT.

High Resolution Lithography on cured polydimethylsiloxane (PDMS) surfaces

- The low surface energy of PDMS causes most photoresists to dewet.
- Other methods of patterning on PDMS require damaging surface treatments or can only provide low resolution and alignment.
- We have developed a processing method allowing high fidelity lithography directly on cured PDMS surfaces without modification using a commercially available material (polydimethylglutarimide).

Work performed at in part at Harvard Center for Nanoscale Systems by R.M. Diebold (David Clarke group), Harvard University.

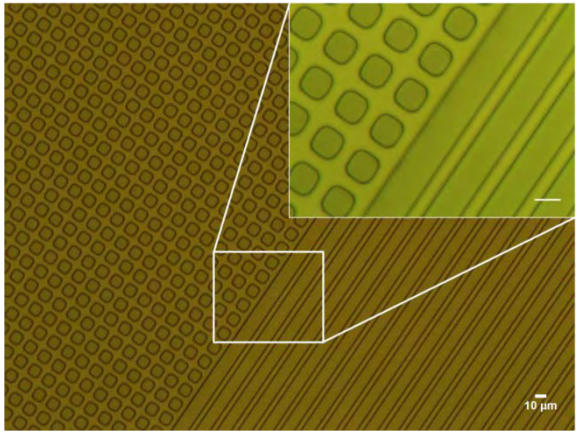

Optical micrograph of 1D and 2D diffraction gratings made of PMGI/Novolak photoresist patterned directly on cured PDMS. Scale bars are both 10µm.

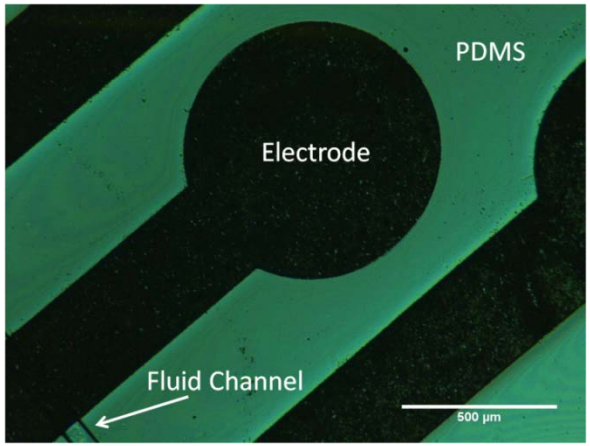

Flexible carbon black/PDMS electrodes can be defined directly on cured PDMS as part of the fabrication of an electrostatically actuated microfluidic peristaltic pump. Scale bar is 500µm.

Bio-inspired Design of Submerged Hydrogel-Actuated Polymer Microstructures Operating in Response to pH

A bio-inspired hybrid materials system has been developed by utilizing pH-responsive, hydrogel as the "muscle" that dynamically and reversibly actuates embedded microstructures (as "bone") while the sample is submerged. The chemo-mechanical actuation system is designed to provide uniform directional bending over a large area by utilizing asymmetric "microfin" structures which have a structurally-determined preferred bending orientation. Such a chemically responsive, reversibly actuating surface that functions in a fluidic environment shows promise for applications ranging from propulsion to microfluidics.

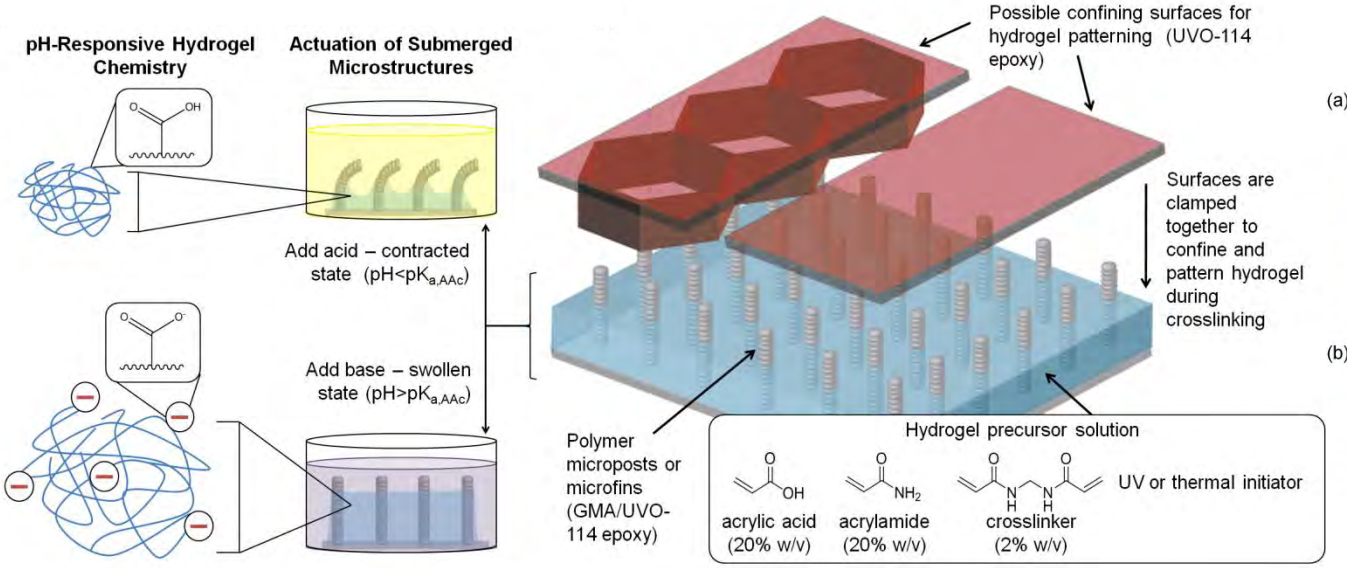

Overview of pH-responsive actuation system. Structures reversibly bend in acid or base, and we can control the direction of actuation by topographically patterning the hydrogel using 3D structured confining surfaces.

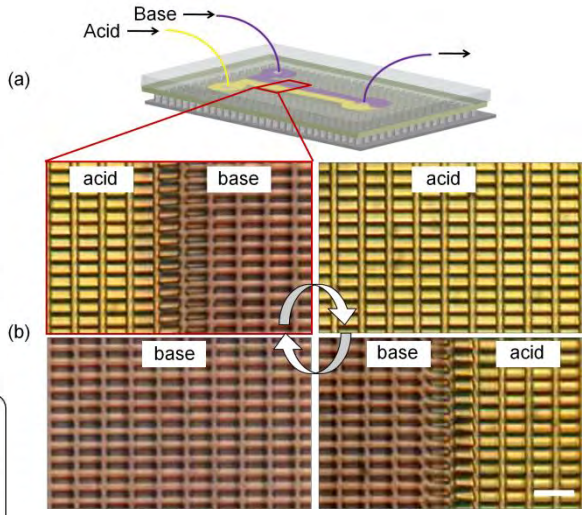

Actuating microfin structures within a microfluidic channel. Laminar flow of acid and base determines where the structures actuate

L. D. Zarzar, P. Kim, J. Aizenberg, *Adv. Mater.* **2011,** *23,* 1442-1446.
Work performed at Harvard Center for Nanoscale Systems

Wetting-In-Color (W-Ink)

We developed a technique for patterning multiple chemical functionalities throughout them inner surfaces of a highly ordered 3D photonic crystal, generating complex wettability patterns. When immersed in a liquid, the pores are selectively infiltrated in a unique spatial pattern – creating an optical fingerprint of that liquid through the color contrast between wetted and non-wetted regions. A remarkable selectivity of wetting is observed over a very broad range of fluids' surface tensions. These properties, combined with the easily detectable optical response, allow us to also exploit this system as a colorimetric indicator for liquids based on wettability.

Work performed at Harvard Center for Nanoscale Systems.

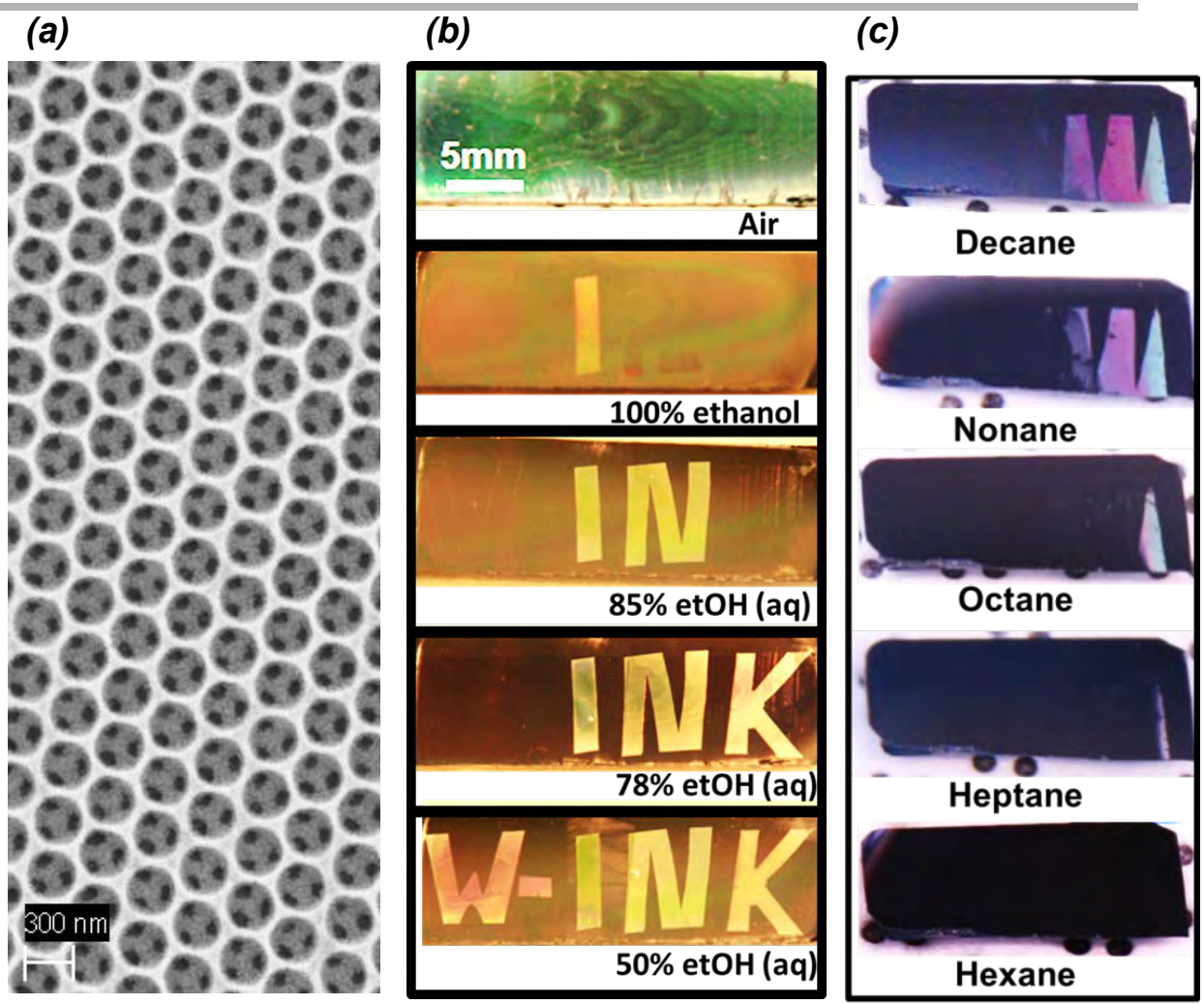

Multilevel Encryption and a colorimetric indicator for liquids
(a) Scanning electron micrograph of the highly regular inverse-opal structure (b) Multilevel encryption displaying the words "I", "IN", "INK", "W-INK" in different ethanol-water mixtures. (c) A strip that allows colorimetric distinction of decane, nonane, octane, heptane, and hexane.

Reference: I.B. Burgess, L. Mishchenko, B.D. Hatton, M. Loncar, J. Aizenberg, J. Am. Chem. Soc., ***133*** *,12430–12432 (2011).*

Microstructure Design in PVD Hard Coatings

The purpose of this project is to develop new microstructures in hard coatings applied to tools and other wear-resistant devices. Coatings are produced by physical vapor deposition system at the CNS and microstructural changes evaluated by transmission electron microscopy after sample preparation by focused ion beam.

By changing the film composition and the sputtering parameters, intense refinement and densification was promoted in the deposited film.

Tool Coated with PVD compound

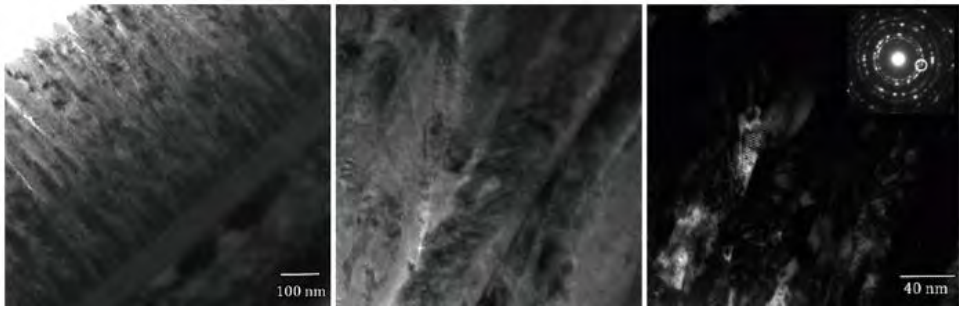

Initial Microstructure: columnar grains with about 20 nm x 100 nm

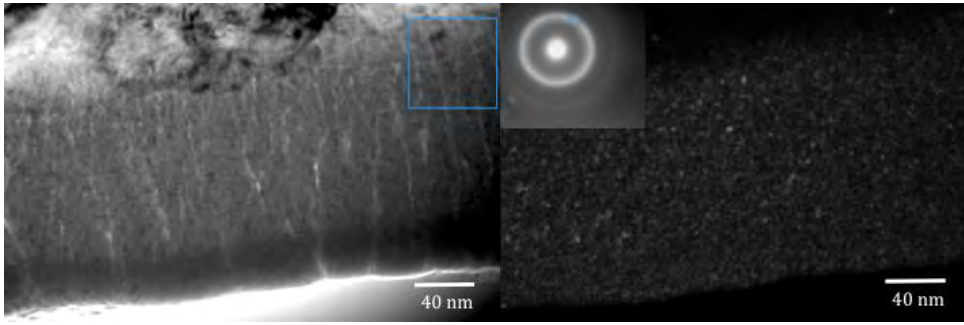

Refined Microstructure: Equiniaxied 3 nm grains

Rafael A. Mesquita and Christopher Schuh, MIT, Materials Science and Engineering Department.

Films deposition performed at Harvard Center for Nanoscale Systems, being the mechanical and microstructural characterization done at the MIT.

Programmable Nanowire Nanoprocessor

We demonstrate the first programmable and scalable logic circuit by bottom-up assembly of nanometer-scale elements. First, nonvolatile nanowire field-effect transistors (NWFETs) were built from Ge/Si core/shell nanowires coupled with designed dielectrics. Second, an architecture was developed to integrate the NWFETs into a multifunctional logic tile. Lastly, the tile was programmed to demonstrate both combinational and sequential logic functions. Our work significantly advanced the complexity of nanoelectronic circuits built from bottom up, and can be cascaded into ultra-low-power nanoprocessors that serve as embedded controllers for integrated nanosystems such as sensors and therapeutic devices.

Hao Yan, Hwan Sung Choe, SungWoo Nam, Yongjie Hu & Charles M. Lieber, Harvard University.
Shamik Das, James F. Klemic & James C. Ellenbogen, MITRE Corporation.

Circuit fabrication and TEM performed at Harvard Center for Nanoscale Systems.

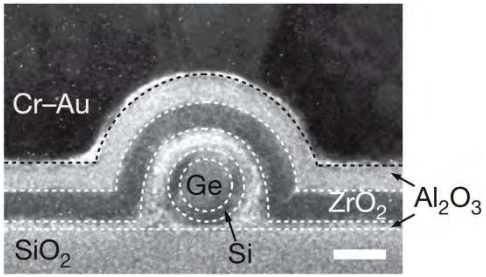

Cross-sectional TEM image of a Ge/Si core/shell nanowire programmable field-effect transistor. Scale bar, 10 nm

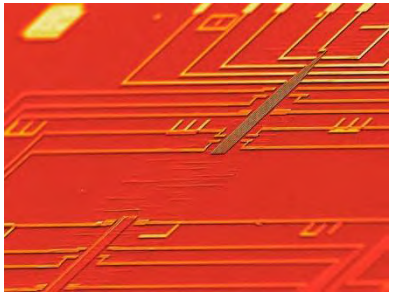

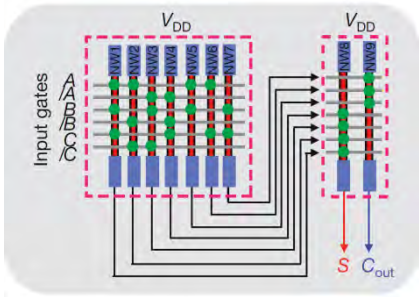

SEM image of a nanowire crossbar array (left) and the corresponding circuit diagram implementing a 1-bit full adder (right).

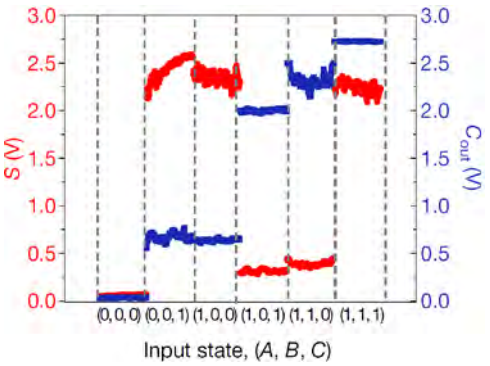

Output voltage of sum (S, red) and carry-out (C_{out}, blue) of the nanowire full-adder circuit

Related publication: Yan, H. *et al*. *Nature* **470**, 240-244 (2011).

Plasmonics Enhanced Performance on Quantum Dot Infrared Photodetector

This project aims to enhance performance of Quantum Dot Infrared Photodetector (QDIP) by fabrication of plasmonics structure on top of QDIP mesas. Metal thin film with array of holes in various patterns has been investigated to increase the photocurrent on the QDIP detector. By an interaction of electric field on patterned metal film, such as periodic array of sub-wavelength apertures, photocurrent can be extracted more than one with regular bare opening surface. Over 100% enhancement is observed at specific wavelength due to the first order plasmonic mode. This development will improve the performance of commercial focal plain array QDIP sensors.

Xuejun Lu, University of Massachusetts at Lowell
Work performed at Harvard Center for Nanoscale Systems

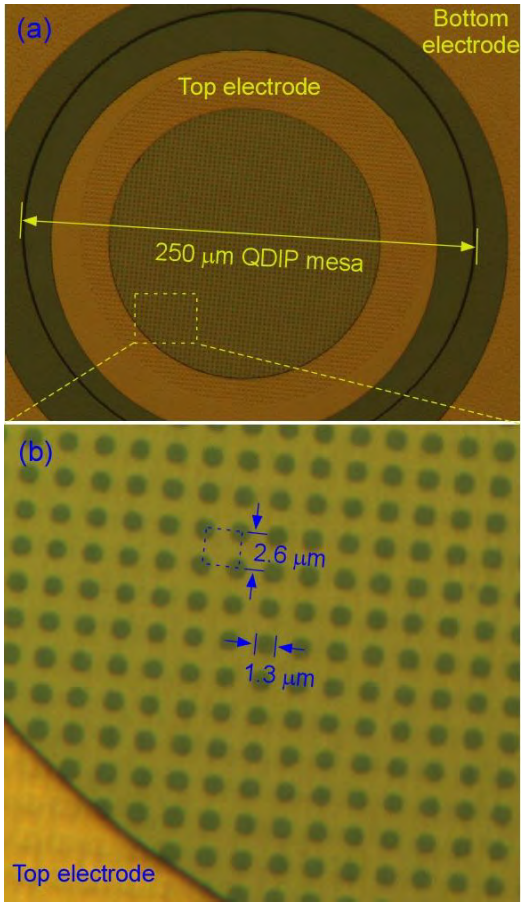

Images from optical microscope
(a) Standard QDIP mesa with plasmonics structure on top surface
(b) Zoom-in image of patterned metal film

Tested device image

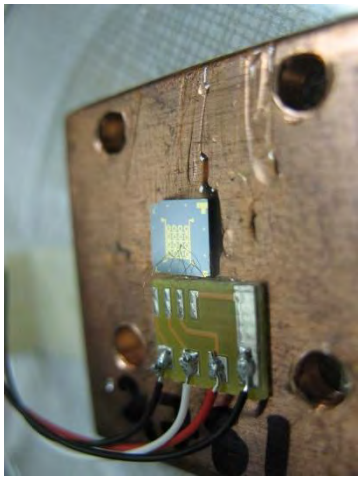

Balloon Catheter with Integrated Electronics

Stretchable electronic materials can be incorporated into or be direct structural elements of balloon catheters. These materials afford the potential to convert catheter systems from largely passive or manually activated systems to active, digital, smart systems, thereby significantly improving outcomes in cardiac interventions.

The CNS-fabricated components of this system have been the stretchable electrodes which are created via conventional electronics fabrication techniques. These electrodes are then transferred onto elastomeric substrates using the soft materials facility and are subsequently integrated into balloon catheters. In a similar manner, active electronic devices may be fabricated in stretchable arrays and transferred to the balloon surface.

Work performed at Harvard Center for Nanoscale Systems by MC10 Inc.

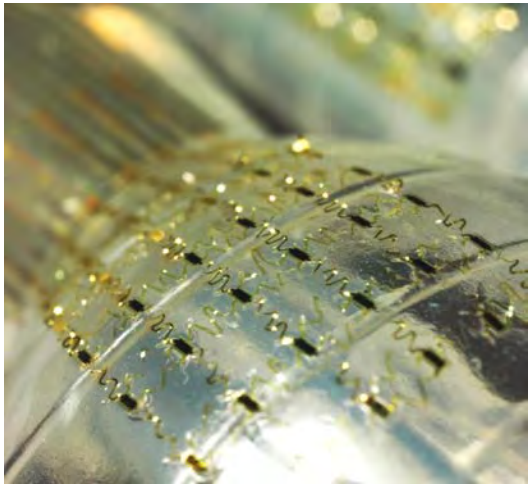

Stretchable electrodes distributed on the surface of a balloon catheter for measuring electrical signals generated by the heart.

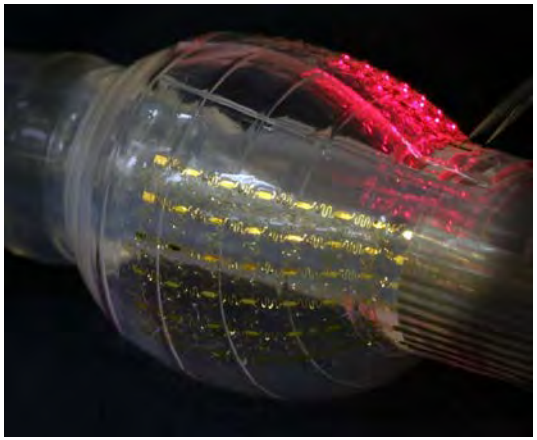

Demonstration of LEDs arrayed on the surface of a balloon. Numerous other electronic devices may be deployed in this format.

Pixtronix Inc. Digital Micro Shutter DMS™ Technology

At the heart of Pixtronix technology is a MEMS-based Digital Micro Shutter device that enables ultra low power consumption and high speed light modulation to create a pioneering display technology.

Pixtronix ultra low power display technology enables displays that consume ¼ of the power compared to conventional LCD Displays. Furthermore, Pixtronix technology allows low power consumption while maintaining exceptional display performance: 145% NTSC color gamut (CIE 1976), 24-bit color, +1,000:1 contrast ratio and 170° view angles.

Pixtronix utilizes the Harvard CNS facility for process/product fabrication and metrology.

Tim Brosnihan and Javier Villarreal, Pixtronix Inc.

Work performed at Harvard Center for Nanoscale Systems

Pixtronix DMS™ Technology Demo Display

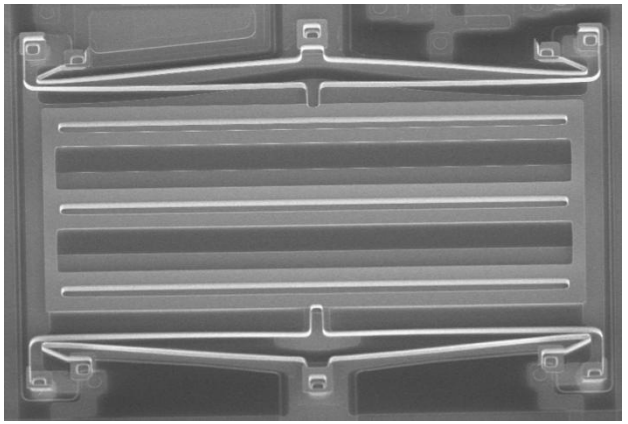

Pixtronix Digital Micro Shutter DMS™ Technology Pixel designed to open and close and allow light modulation

Suspended, Dual-Gated Graphene Layer

We investigated the underlying order of the various broken-symmetry states in bilayer graphene suspended between top and bottom gate electrodes.

We deduced the order parameter of the various quantum Hall ferromagnetic states by controllably breaking the spin and sublattice symmetries.

We used a three step electron-beam lithography process in which Cr/Au contacts are first fabricated on the bilayer graphene.

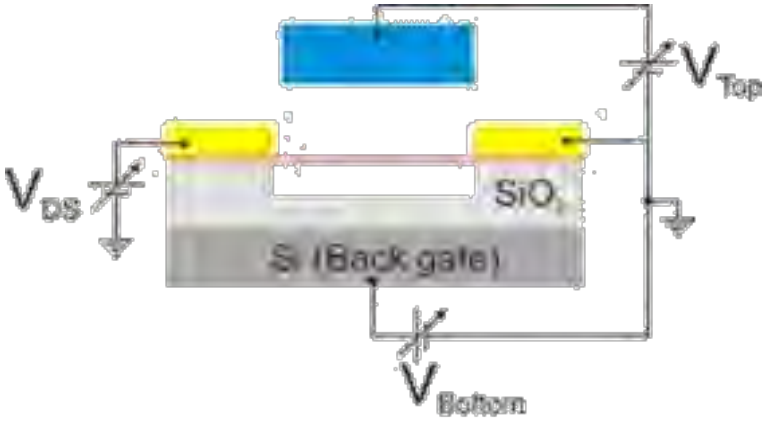

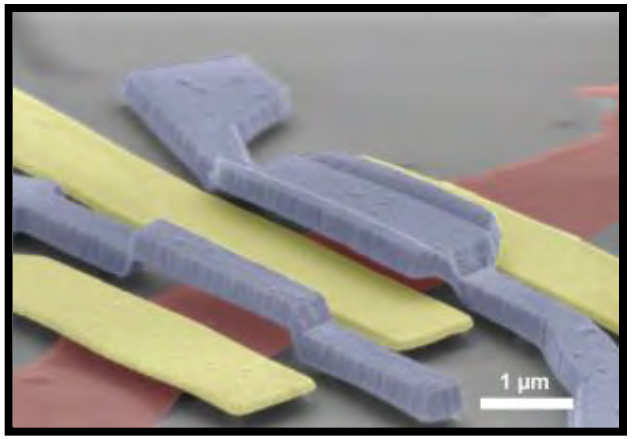

Work performed at Harvard Center for Nanoscale Systems. Yacoby group, Harvard University.

R. T. Weitz, M. T. Allen, B. E. Feldman, J. Martin, A. Yacoby, "Broken-Symmetry States in Doubly Gated Suspended Bilayer Graphene", Science 330, 812-816 (2010).

Cell transfection using Plasmonic Devices

The goal of this project is to develop a plasmon-mediated method for cell transfection that is efficient, low toxic and high in throughput. We propose to facilitate the introduction of molecules into cells, by porating the cell membrane with irradiation of a plasmonic substrate underneath the cells.

The plasmonic device is obtained by template stripping fabrication and consists of a nanopatterned polymer covered with a thin layer of gold.

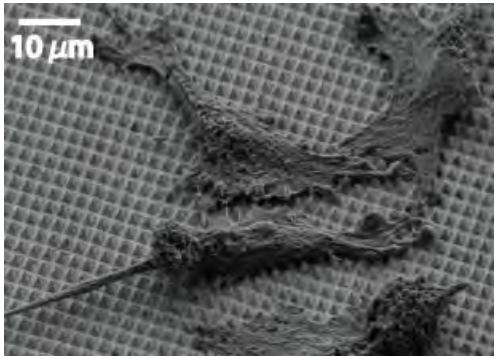

SEM image of HeLa cells sitting on *top of a nanopatterned plasmonic substrate*

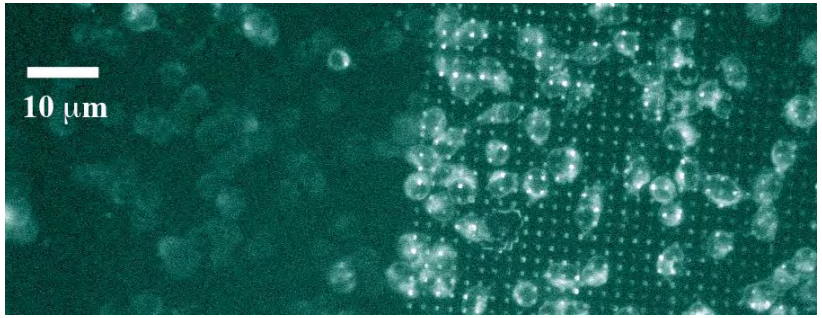

Irradiation of the plasmonic substrate induces *uptake of fluorescent molecules by cells (right side)*

Eric Mazur's research group, Harvard University
Work partially performed at Harvard Center for Nanoscale Systems.

TiO_2 Nanowire Waveguides

We are attempting to achieve all-optical logic switching at a nanoscale. These TiO_2 films are entirely grown and fabricated in the Harvard Center for Nanoscale Systems (CNS). We hope to create integrable and reproducible low power all-optical logic gates using TiO_2.

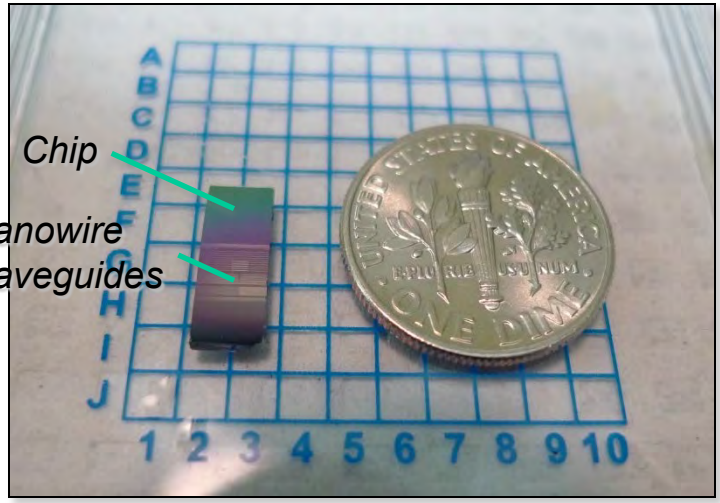

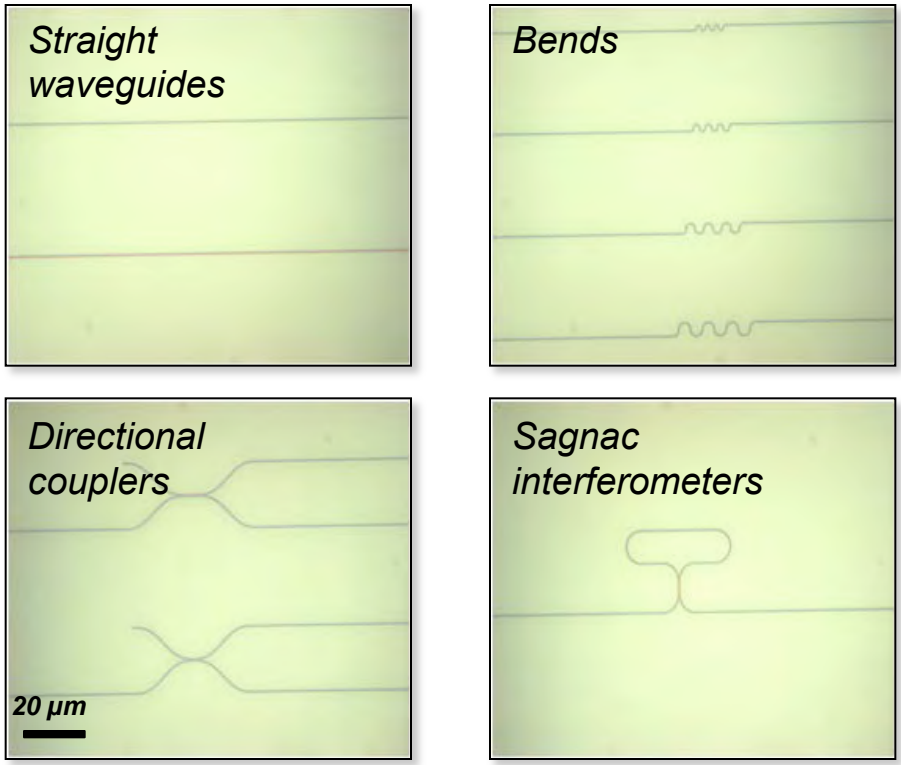

Images of features on TiO_2 chip, including linear devices (couplers) and nonlinear devices (interferometers)

Jonathan Bradley, Christopher Evans, Orad Reshef, and Eric Mazur.
Harvard School of Engineering and Applied Sciences
Site used: Harvard Center for Nanoscale Systems

Branched Nanowire Heterostructures with Synthetically Encoded Function

Branched nanostructures represent unique, 3D building blocks for the 'bottom-up' paradigm of nanoscale science and technology. A rational, multi-step approach has been developed toward the general synthesis of branched nanowire heterostructures. Single-crystalline semiconductor, including groups IV, III-V and II-VI, and metal branches have been selectively grown on core or core/shell nanowire backbones, with the composition, morphology and doping of core (core/shell) nanowires and branch nanowires well-controlled during synthesis. This leads to the encoding of diverse device function, such as light-emitting diodes, transistors, and biological sensors, at the branch/backbone nanowire junctions.

X. Jiang, C.M. Lieber & coworkers, Proc. Natl. Acad. Sci. USA, published online 5 July 2011. DOI: 10.1073/pnas.1108584108.

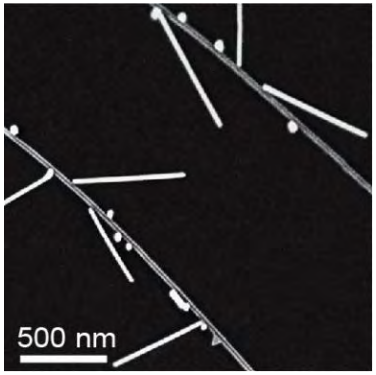

SEM image of Si/Au branched nanowire heterostructures

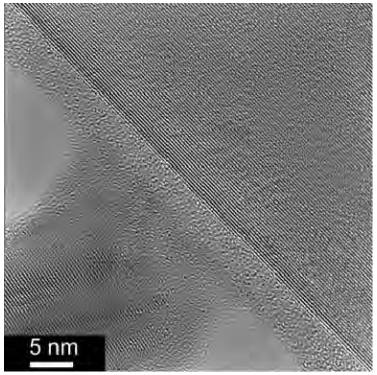

HRTEM image of $Si/SiO_2/Ge$ branched nanowire heterostructure

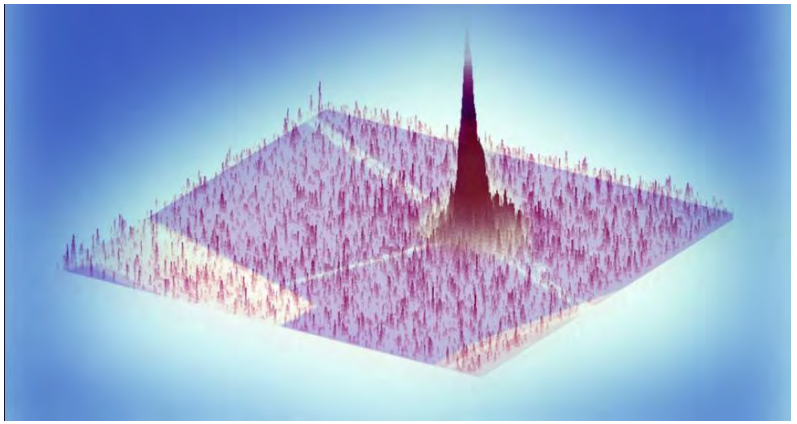

p-Si/n-GaAs branched nanowire LED with peak denoting strong light emission at the nanowire junction.

Lieber group at Harvard University
Work performed at Harvard Center for Nanoscale Systems

Carbon Nanotube Based Energy Storage
FastCAP Systems

FASTCAP SYSTEMS™

Boston-based FastCAP uses carbon nanotubes to improve an energy storage device called an ultracapacitor. Unlike batteries, which store energy via chemical reactions, ultracapacitors store energy in electric fields. The devices possess enormous advantages over conventional battery technologies, including extremely long lifespans (over a million cycles, as compared to 10,000 for conventional batteries), unsurpassed ruggedness and durability, and low environmental impact due to their non-toxic internal components. However, ultracapacitors have fallen short of batteries in one key metric: energy density (energy density is a measure of how big or heavy a battery or capacitor needs to be to store a particular amount of energy). FastCAP's ultracapacitor technology addresses this key metric by improving the internal electrode structure and processes to produce them – improvements which allow us to combine the benefits of ultracapacitors and conventional batteries into one device, with none of the drawbacks of either technology.

Work performed in part at Harvard Center for Nanoscale Systems

NNIN
www.nnin.org
Nanoscale Science, Engineering & Technology

Copyright FastCAP Systems 2011

Optically Manipulated Casimir Force using a Photonic Crystal Slab

"Casimir forces" on neutral objects arise due to quantum fluctuations of the electromagnetic field. The force is always attractive between two surfaces of the same material in air or vacuum. Because the force often dominates when small objects are placed in close proximity, it leads to an undesirable phenomenon known as "stiction" which is a common issue in MEMS and NEMS devices. For combating stiction, we focused on inducing an optical force for compensation and manipulation of the Casimir force, because it can be repulsive with two adjacent plates. We fabricated a double-membrane structure with PhC slab and confirmed that light could be coupled to the structure.

*Eiji Iwase[*1], Pui-Chuen Hui[*1], Alejandro W. Rodriguez[*1*2], David Woolf*1, Mughees Khan[*1], Steven G. Johonson[*2], Federico Capasso[*1], Marko Lončar[*1]*
*[*1]Harvard University [*2]Massachusetts Institute Technology*
Work performed at Harvard Center for Nanoscale Systems

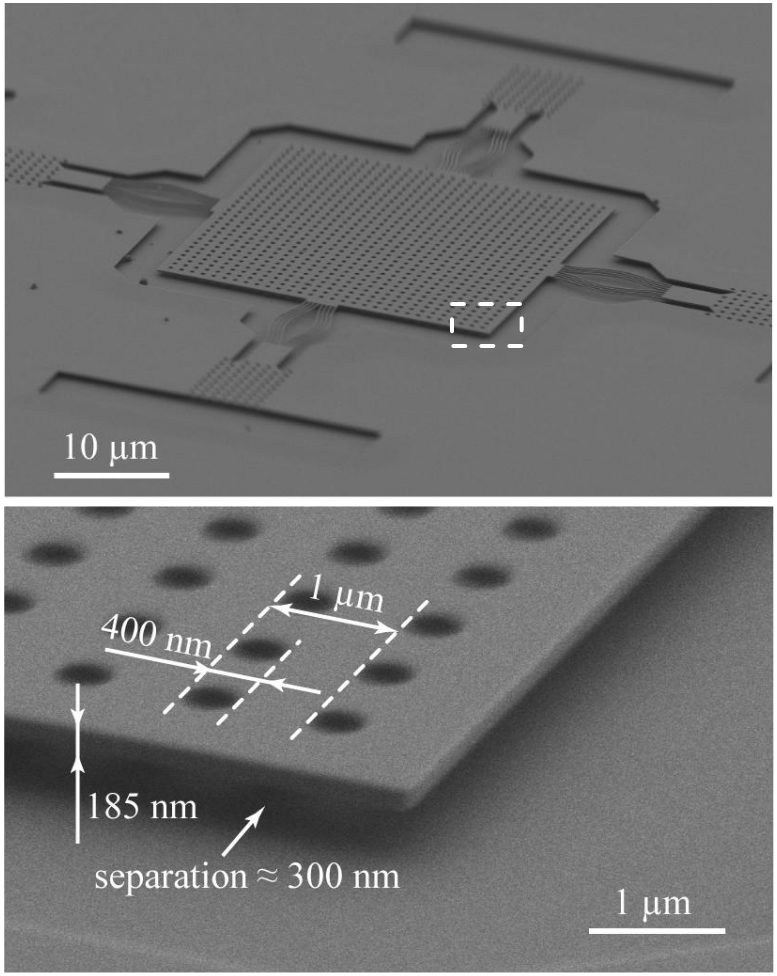

Freestanding PhC slab structure with 30 µm in length and width, 185 nm in thickness, and around 300 nm in separation distance.

Lifetime Modification of Color Centers in Diamond

Color centers in diamond, including the nitrogen-vacancy (NV) center, can be robust nonclassical light sources and are potentially useful in applications such as quantum cryptography, quantum information processing, and nanoscale magnetometry. In many of these applications, it is desirable to modify the spontaneous emission rate of the color center.

We have demonstrated modification of the lifetime of the NV center by embedding the dipole inside a nanostructure (a cylindrical nanopost etched in single crystal diamond). This led to a reduced density of states for the optical transition and hence quenched emission and long emitter lifetime in comparison to the bulk. Finally, by surrounding the nanoposts with metal, we formed a plasmon cavity, which enhanced the spontaneous emission decay rate of the enclosed emitter, allowing for lifetimes much shorter (~5x) than the bulk to be observed.

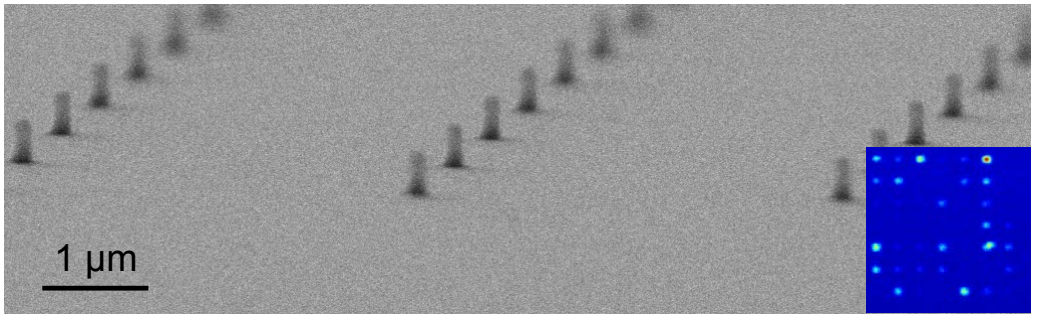

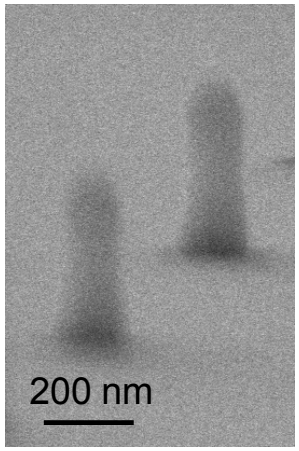

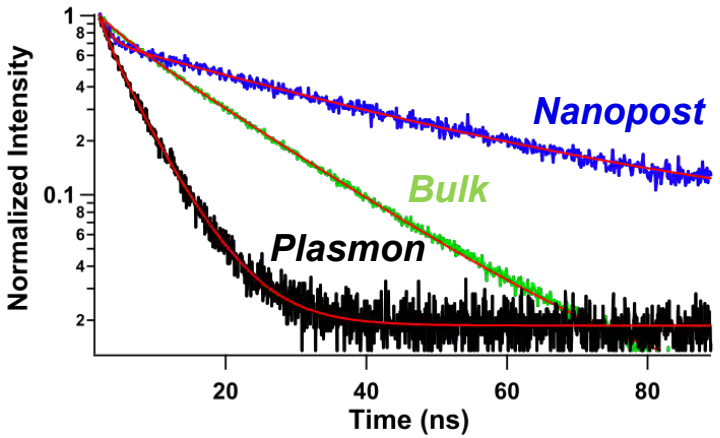

Figure Captions: (Top) Arrays of nanoposts (of diameter ~ 100nm and height ~ 200nm) fabricated in a single crystal diamond crystal. The inset shows a confocal scan image of a set of nanoposts, in which many contain the NV center. (Bottom Left) Zoomed-in view of the diamond nanoposts. (Bottom Right) Fluorescence decay curves for NV centers in the bulk, nanopost, and plasmon cavity show that the nanopost geometry leads to quenched emission while the cavity enhances the spontaneous emission rate.

Lončar Group, Harvard University
Work performed at the Center for Nanoscale Systems at Harvard University

NNIN Site at Penn State University

MEMS Membranes for Biosensing

Thomas Alava, Fabrice Mathieu and Liviu Nicu, LAAS-CNRS, France

A chip of circular micromembranes for biosensing applications

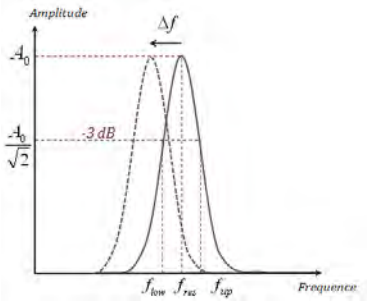

Principle of detection: change of the membrane resonant frequency in the presence of pathogenic agents.

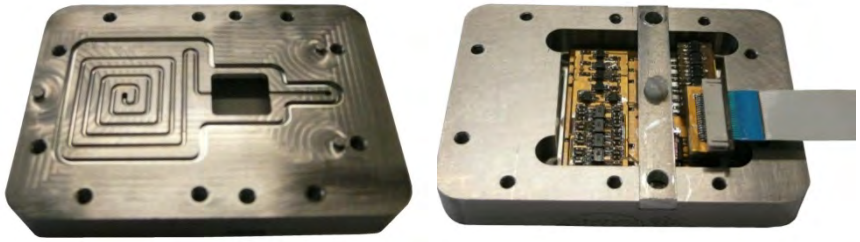

Integration of the chip: fluidic cell and onboard electronics for the detection of pathogenic agents

The Penn State NNIN site has fabricated resonant micromembranes to detect pathogenic agents that mimick bacteriological threats.

Each microfabricated chip includes several circular micromembranes for multiplexed sensing. The actuation and sensing scheme is based on the integration of a Lead Zirconate Titanate (PZT) piezoelectric thin film and a Boron-doped Silicon piezoresistor, respectively. The fully integrated device includes a fluidic cell and onboard electronics.

The devices were fabricated using the Penn State NNIN baseline PZT process.

The Penn State NNIN baseline PZT process was used to fabricate a MEMS biosensor that detects the presence of pathogenic agents by measuring a shift in the micromembrane resonant frequency.

Flexible Medical Systems

J. Marcanio, Flexible Medical Systems LLC, Rockville MD

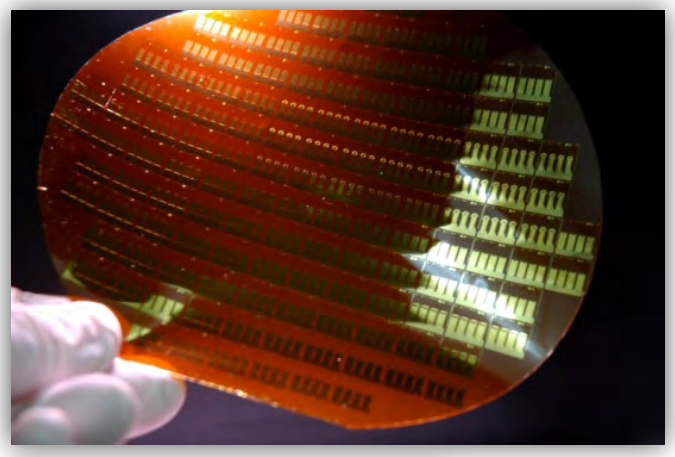

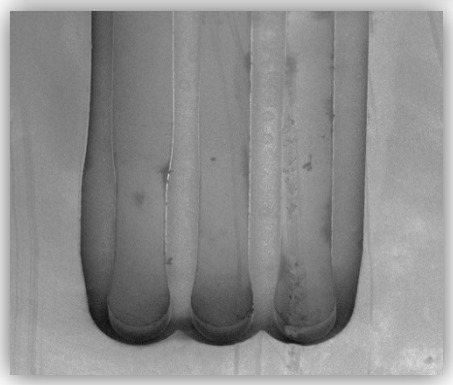

devices fabricated on metallized polyimide film

collection chamber is formed in epoxy photoresist.

FMS has developed technology to extract interstitial fluid (ISF) for analysis without penetrating the skin. This transdermal approach eliminates the pain, needles, and blood associated with typical assays.

Continuity of the phospholipid bilayer is disrupted by a thin film metal transducer on the micro-device, resulting in permeabilization of the skin membrane.

A carefully designed microfluidic system transports the fluid to a micro-electrochemical cell for *in situ* analyte measurement.

A new technology has been developed to extract interstitial fluid for analysis without penetrating the skin, which eliminates the pain, needles, and blood associated with typical assays.

Low-Cost Pyroelectric Detector Arrays

Howard Beratan, Bridge Semiconductor, Pittsburg, PA

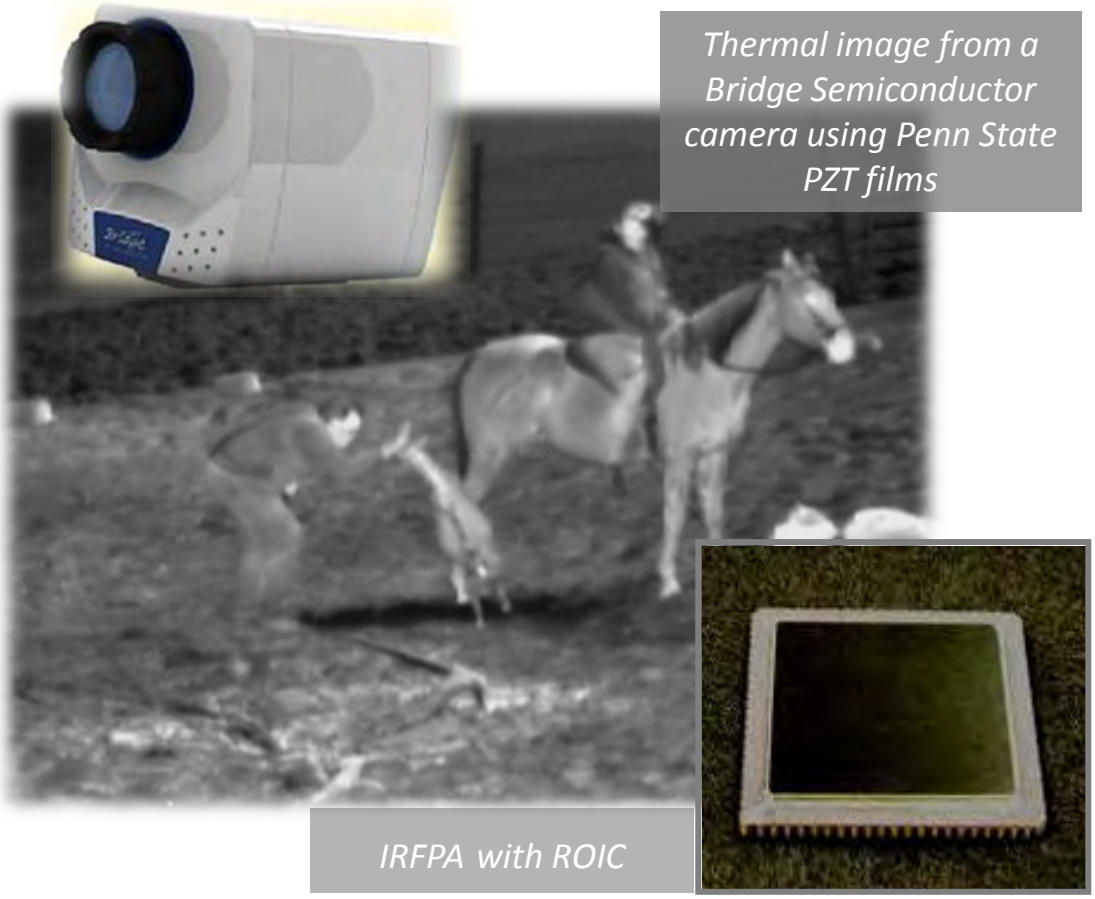

Thermal image from a Bridge Semiconductor camera using Penn State PZT films

IRFPA with ROIC

The Penn State NNIN site is being used to deposit, pattern, and etch doped $Pb(Zr_{0.30}Ti_{0.70})O_3$ (PZT) pyroelectric films for uncooled thermal imaging systems.

Video frame-rate imaging has been demonstrated upon integration with CMOS read-out integrated circuit (ROIC) electronics.

Ultimately, image quality is expected to be superior to other uncooled thermal imagers, including resistive bolometers.

Penn State

Integrating pyroelectric films to a CMOS ROIC with associated system electronics enables high-performance, low-cost infrared cameras.

Low-Cost Sub-Miniature Oxygen Sensor

Ken E. Fosaaen , Fosaaen Technologies, LLC, Greenville, NC

The severe smog problem in China, India, and other developing countries is caused by low-cost vehicles with poor emission control.

Motorcycles are the major mode of transportation throughout the world. Better emissions control is needed to combat severe air pollution problems.

Sub-miniature oxygen sensor. Low cost, small size, low power make this suitable for many small engine applications.

There is a global need to improve the emissions performance in small engines. The low cost, small size, and limited power of these engines provides a challenge that requires a new technology.

Fosaaen Technologies designed a low-cost sub-miniature oxygen sensor, and used the Penn State NNIN Site to produce the first functional prototypes. This reduction to practice allowed the submission of an international PCT patent, which was filed in December 2010.

A low-cost sub-miniature oxygen sensor was prototyped using the Penn State NNIN Site to improve emission performance in small engines.

Micrometric Microbial Fuel Cell

J. Prieto Rojas, J. Mink, and M. Hussain, King Abdullah University of Science and Technology, Thuwal, Saudi Arabia

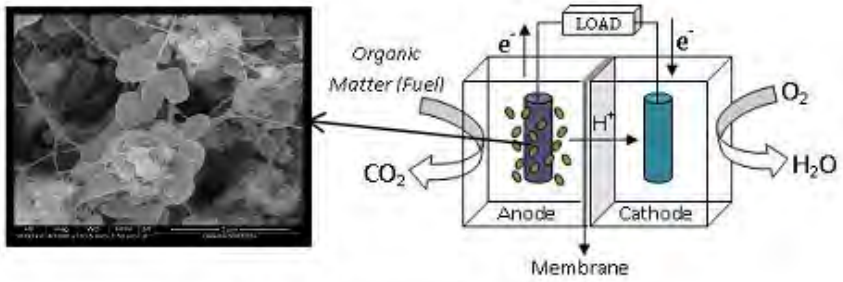

MFC Principle of work

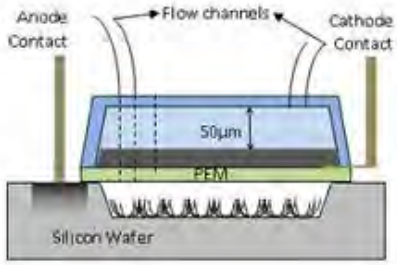

µMFC Assembly

The PSU NNIN Site was used to fabricate micro-sized Microbial Fuel Cell (MFC) with a 1.25µL volume.

A MFC is an innovative device for energy production based on bio-electrochemical reactions made by bacteria when decomposing organic matter in anaerobic conditions.

The breakthrough of this design includes the microfabrication of the smallest MFC reported thus far, and the use of a CNT-based anode with a high surface area-to-volume ratio.

This new configuration attained higher power per surface area as well as per volume of liquid used than previous microfabricated MFCs.

Alternative electricity sources are being developed for low power-consumption devices by combining novel nanomaterials with microfabrication techniques.

High Resolution Ultrasound Imaging

Y. Liang, K. Snook, and W. Hackenberger, TRS Technologies, Inc., State College
X. Geng, and R. Liu, Blatek Inc., State College, PA.

Completed transducer

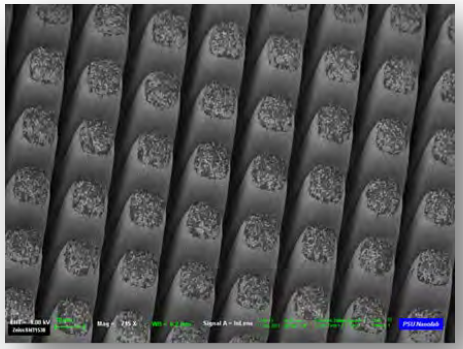

PMN-PT Pillars

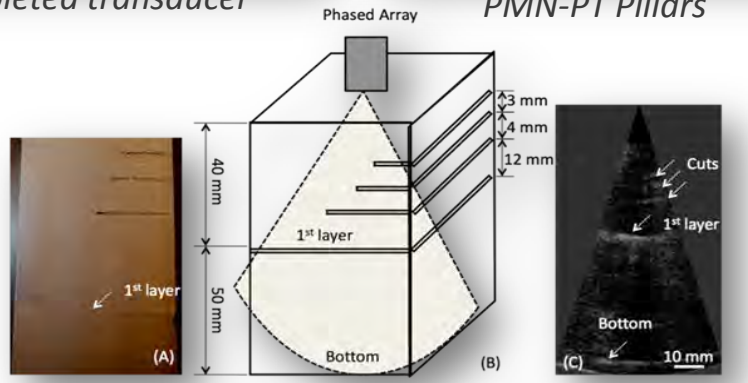

NDE Imaging Application

High-performance 30-40 MHz composites are being developed at the Penn State NNIN Site. The high-aspect ratio, micron-scale pillars fabricated from PMN-PT single crystals provide state-of-the-art performance for high-resolution ultrasound imaging.

The PMN-PT microfabrication capabilities provided by NNIN are enabling advancements in leading-edge ultrasound transducer technology with broad bandwidth for high resolution medical and nondestructive examination applications.

Defining micron-scale, high-aspect ratio pillars in PMN-PT is advancing leading-edge ultrasound transducer technology with broad bandwidth for high-resolution medical and NDE applications.

Shape Memory Alloy Transfer Printing

Chi-Mon Chen, Chang-Lung Chiang and Shu Yang, Materials Science and Engineering, University of Pennsylvania, Philadelphia, PA

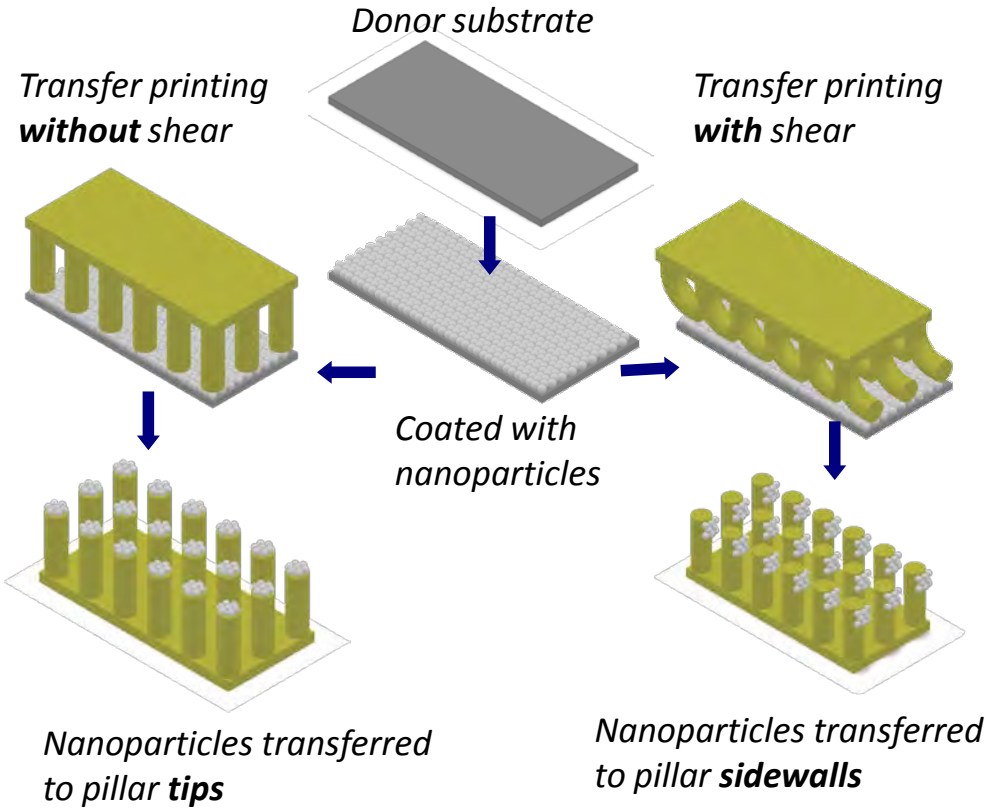

The Penn State NNIN Site created Si masters to fabricate shape memory polymer pillar array.

Selective transfer-printing is achieved by tuning the relative adhesion between the shape memory polymer and the nanoparticle assembly vs. the donor substrate. It allows for:

1) *Spatially controllable contact.*
2) *New patterns on donor substrate.*
3) *Recoverable shape and tunable adhesion of the shape memory polymer pillars.*

A new method was developed to selectively assemble nanoparticles on topographic patterns using shape memory polymer pillars as "sticky fingers".

Piezoelectric Transducer Development

Eastman Kodak Company, Rochester, New York

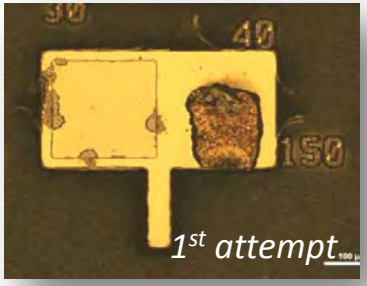

Etch damage and templating

Templating

Good etch

PZT electrical properties (PE loop)

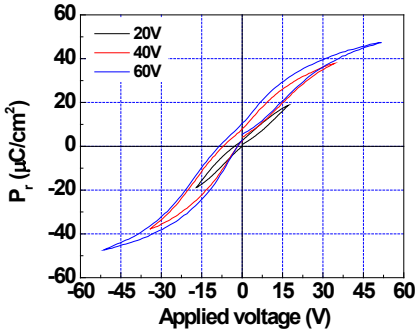

Before etch optimization

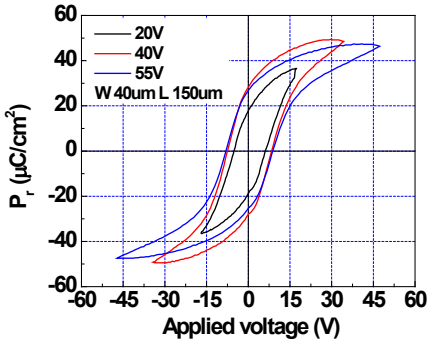

After etch optimization

A thin-film piezoelectric film etch process was developed for an experimental MEMS platform being developed by Kodak.

Unoptimized etch processes resulted in a pinched ferroelectric response as shown by the polarization-electrical (PE) hysteresis loop.

The ferroelectric response of the PZT is greatly improved following etch optimization.

Pinched PE hysteresis loops that result from reactive ion etch damage can be minimized by optimizing the processing conditions.

Radiation Sensitive Gd_2O_3 Capacitors

Joshua Robinson and Doug Wolfe, EOC/ARL, Freeport, PA

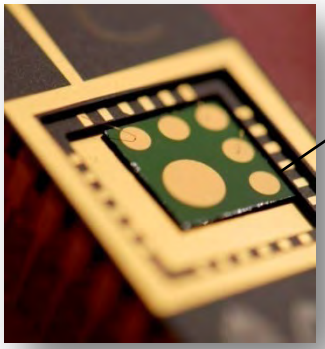

Packaged Gd_2O_3 capacitors

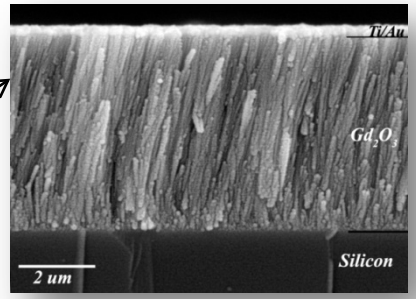

SEM cross-sectional image of a Gd_2O_3 capacitor

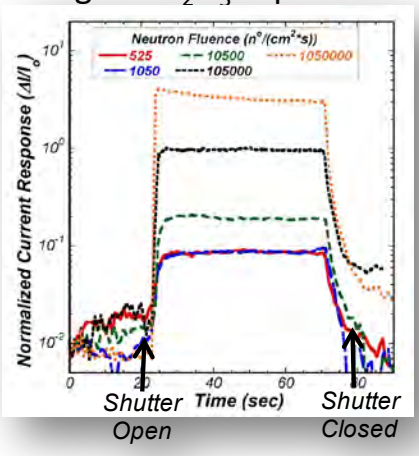

Real-time current response of a metal/Gd_2O_3/Si capacitor

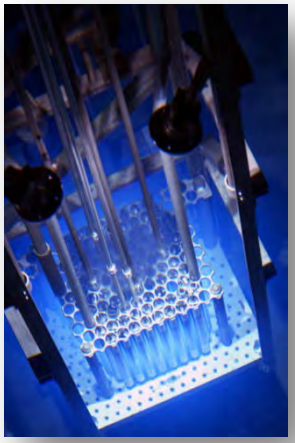

PSU-Breazeale Nuclear Research Reactor

Thick Gd_2O_3 films have a number of applications in the electronics, optics, and nuclear industries. Specifically, Gd-based materials are particularly attractive for neutron detection due to Gd's high thermal neutron capture cross section.

Measuring changes in the conductance provides a basic understanding of the electronic response to radiation. Our research indicates that Gd_2O_3 experiences significant modulation in dielectric conductivity, when exposed to thermal neutrons.

Gd_2O_3 capacitors were fabricated and used as neutron detectors with a rapid detection, high modulation, and full recovery.

Penn State NNIN www.nnin.org Nanoscale Science Engineering & Technology

Epitaxial Graphene Transistors

Joshua Robinson and David Snyder, Electro-Optics Center, Freeport, PA

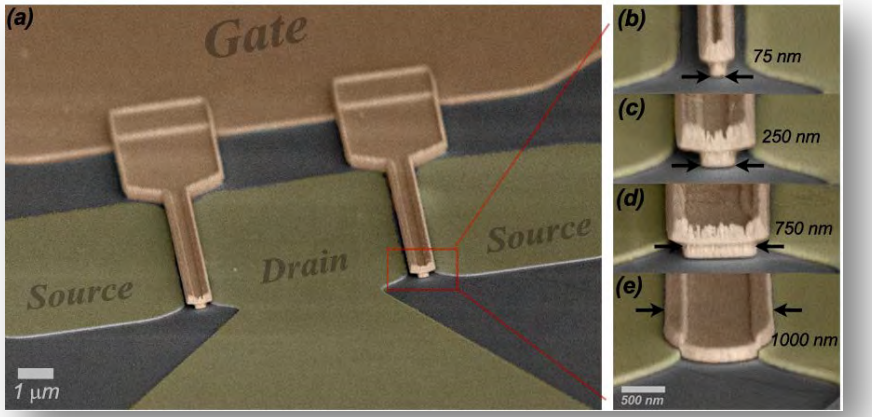

SEM of graphene rf transistors with various gate length

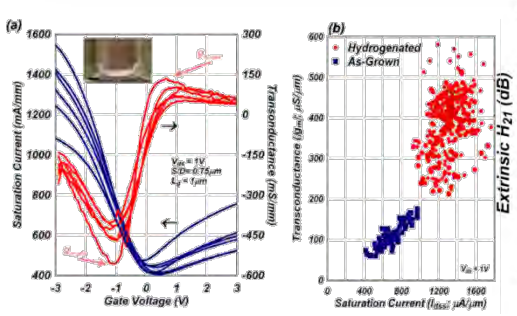

2x increase in FET's saturation current and transconductance

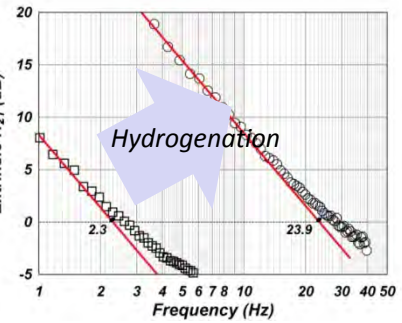

10x Improvement in FET's frequency response

Through a process of hydrogenation, we demonstrate the importance of buffer elimination at the graphene/SiC(0001) interface for high frequency applications.

Upon successful buffer elimination carrier mobility increases from an average of 800 cm^2/Vs to >2000 cm^2/Vs. Additionally, graphene transistor current saturation increases from 750 to >1300 mA/mm, and transconductance improves from 175 mS/mm to >400mS. Finally, we report a 10X improvement in the extrinsic current gain response of graphene transistors, with optimal extrinsic current-gain cut-off frequencies of 24 GHz.

Through a process of hydrogenation, we have achieved 10x improvement of extrinsic cut-off frequency to 24 GHz.

Penn State NNIN
www.nnin.org
Nanoscale Science, Engineering & Technology

High-K Gate Dielectrics on Epitaxial Graphene

Joshua Robinson and David Snyder, Electro-Optics Center, Freeport, PA

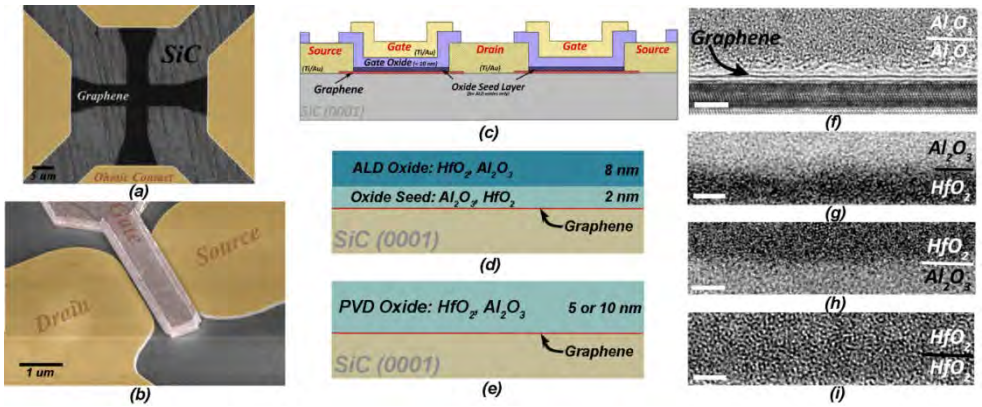

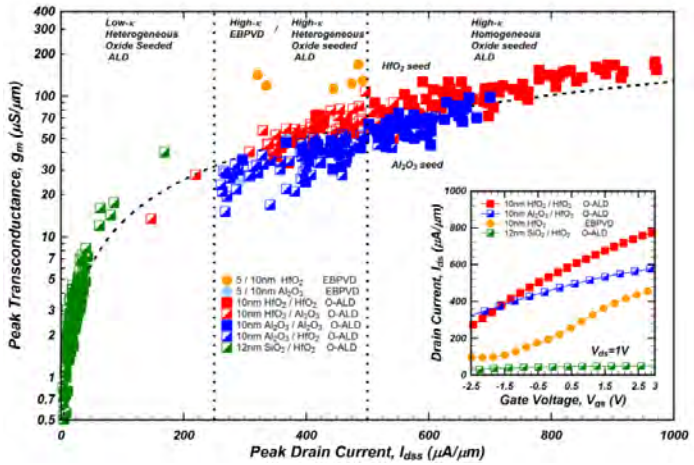

Electrical properties of gFET with various gate oxide structure

A novel seeding technique was developed to dielectrics by ALD that uses direct deposition of high-κ seed layers, and can lead to an increase in Hall mobility up to 70% from as-grown.

Additionally, high-κ seeded dielectrics are shown to produce superior transistor performance relative to low-κ seeded dielectrics ,and the presence of heterogeneous seed/overlayer structures is found to be detrimental to transistor performance, reducing effective mobility by 30 – 40%.

Improvements in carrier transport are obtained by using a high-purity oxide seed to deposit uniform ALD gate dielectrics on epitaxial graphene.

Surface Acoustic Wave Light Shutters

Y.J. Liu, X. Ding, S.-C. Lin, J. Shi, I-K. Chiang, and T.J. Huang, The Pennsylvania State University

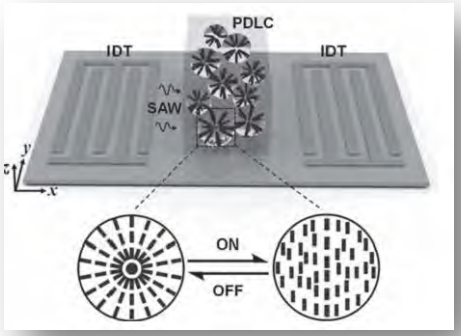

device structure

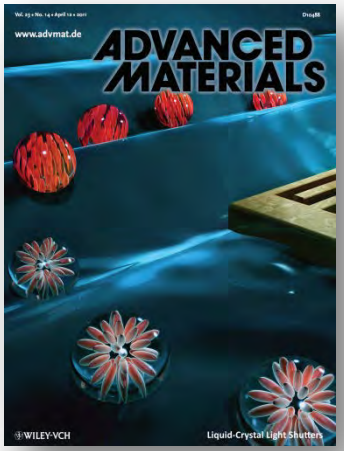

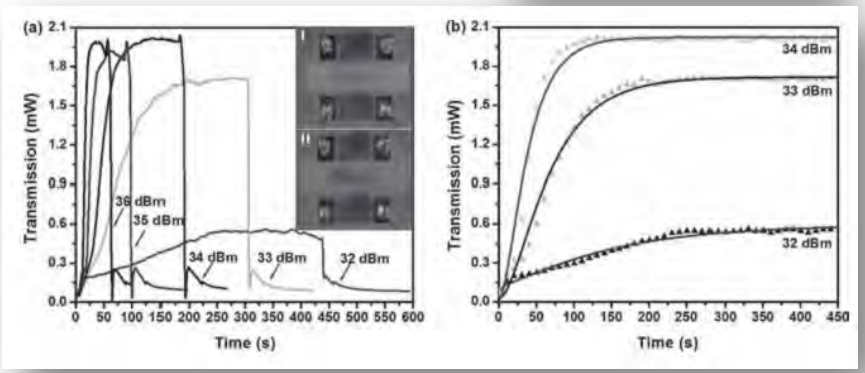

device performance

We demonstrated a SAW-driven polymer-dispersed liquid crystals (PDLCs) light shutter based on the acoustic streaming-induced realignment of LC molecules as well as absorption-related thermal diffusion.

This device shows excellent performance in terms of energy consumption and optical contrast, which is important for applications such as displays and smart windows. In addition, the IDTs fabricated by standard photolithography are highly compatible for future system integration.

Y.J. Liu, et al, Advanced Materials, Vol. 23, pp. 1656-1659 (2011).

This light shutter device shows excellent performance in terms of energy consumption and optical contrast, which is important for applications such as displays and smart windows.

Fluorinated Graphene: Wide Gap Material

S.-H.Cheng, K.Zou, F.Okino, H.R.Gutierrez, A.Gupta, N.Shen, P.C.Eklund, J.O.Sofo, and J.Zhu, The Pennsylvania State University, University Park, PA

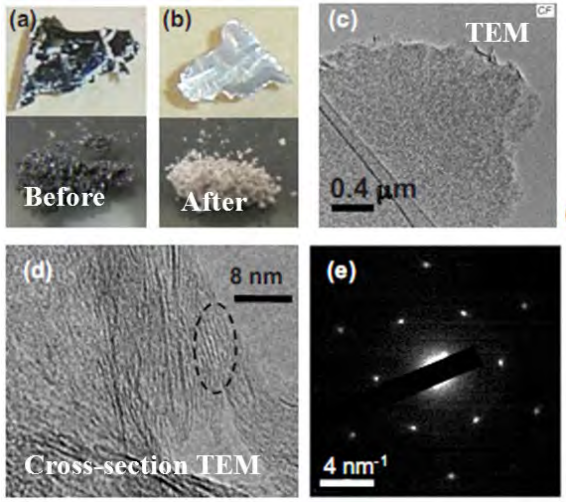

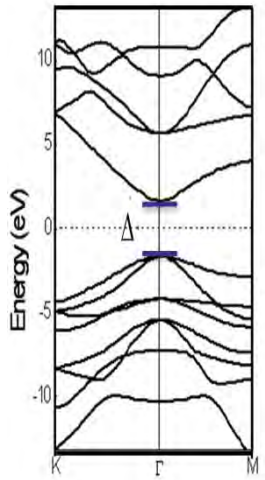

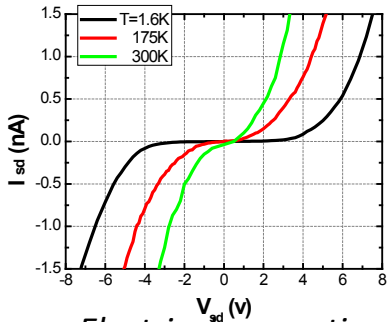

Electrical properties

Calculated band gap 3.5-7.4 eV

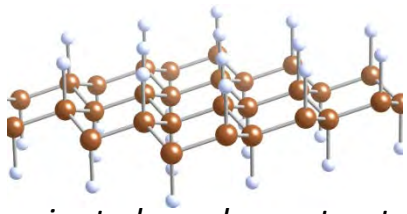

Fluorinated graphene structure

Fluorinated graphene is large band gap, ultrathin insulating material.

In addition to power electronics, graphene fluoride can potentially be used as a deep ultraviolet (UV) light emitter, similar to hexagonal boron nitride or diamond. Such devices may be effectively integrated with carbon electronics to achieve compact assembly and optoelectronic functionalities.

B. Wang et al, Appl. Phys. Lett. 97, 141915 (2010).
S. Cheng et al, Phys. Rev. B 81, 205435 (2010).

Large band-gap and insulting graphene fluoride can be potentially integrated with carbon electronics to achieve compact assembly and optoelectronic functionalities.

Insect Eyes Inspire Improved Solar Cells

F. Chiadini, V. Fiumara, A. Scaglione, D.P. Pulsifer, R.J. Martín-Palma, C.G. Pantano and A. Lakhtakia, Penn State University, University Park, PA

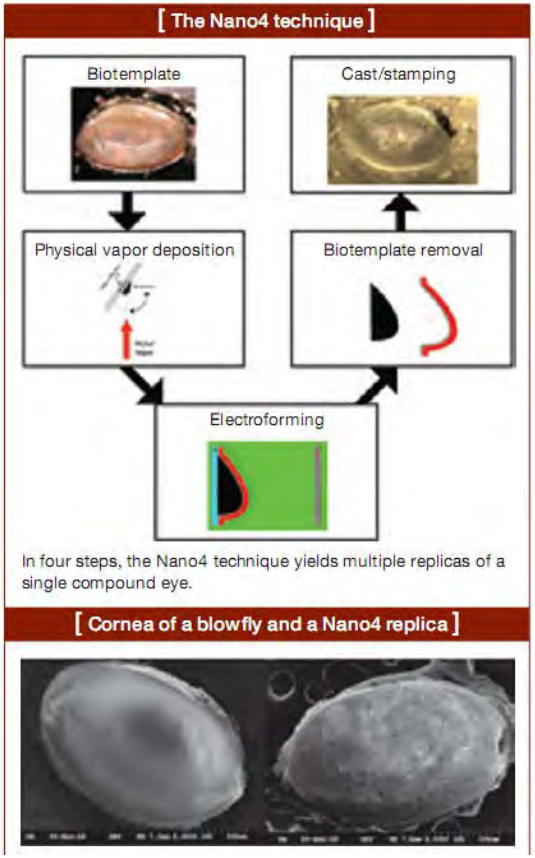

Taking a cue from nature, we have developed a unique approach to replicate the structure of the compound eyes of insects to harvest sunlight.

Nature suggests useful strategies for highly efficient solar cells since natural selection has, over eons, resulted in species endowed with biological structures that allow the capture of light from a large range of directions.

Nanocasting methods, which are analogous to the ones used in a steel foundry but on a much smaller length scale, work very well.

F. Chiadini, et al., OSA Optics and Photonics News, 22(4), 38-43 (2011).

A unique approach has been developed to replicate the structure of the compound eyes of insects for harvesting sunlight.

Complementary Patterned Metallic Membranes

Q. Hao, Y. Zeng, X. Wang, Y. Zhao, B. Wang, I-K. Chiang, D. H. Werner, V. Crespi, and T. J. Huang, Penn State University, University Park, PA

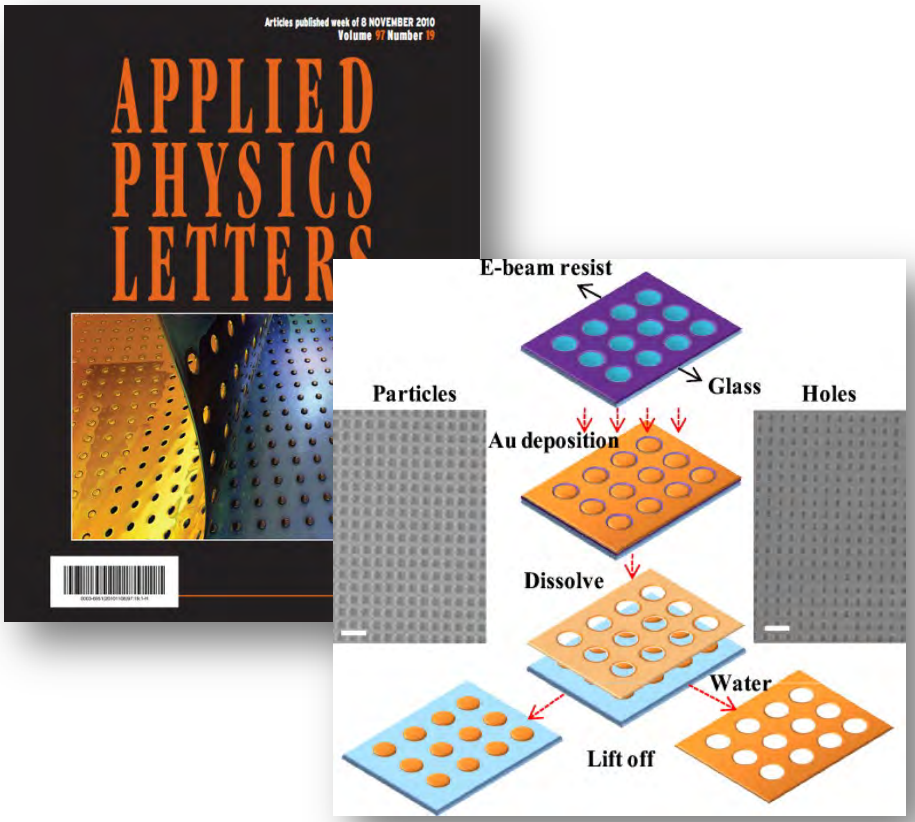

We demonstrate an efficient dual fabrication process to simultaneously produce optically complementary patterned metallic membranes.

It is shown that Babinet's principle qualitatively holds to good approximation at visible and near-infrared optical wavelengths despite the finite conductivity of gold.

We believe that the dual fabrication process together with Babinet's principle can provide a pathway to creating better optical devices, including filters and metamaterials.

Q. Hao et al, App. Phys. Lett. 97, 19301 (2010)

An efficient dual fabrication process was developed to simultaneously produce optically complementary patterned metallic membranes.

Columnar ChG Thin-Films for Fingerprint ID

A. Lakhtakia, R.C. Shaler, R.J. Martín-Palma, M.A. Motyka, and D.P. Pulsifer,

Penn State University, University Park, PA

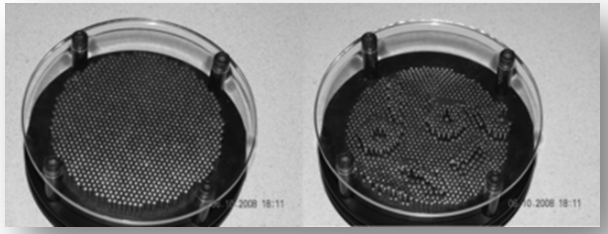

Illustration of the concept

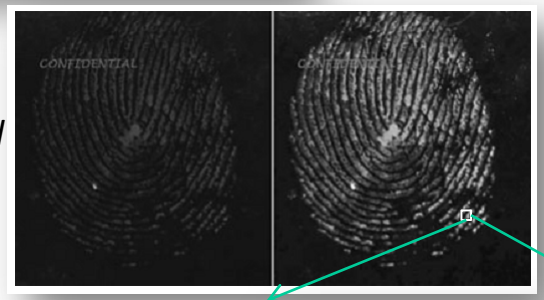

Optical images of chalcogenide-coated fingerprint

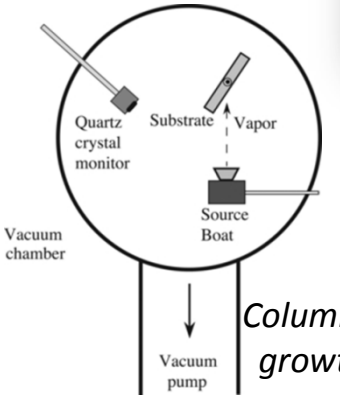

Columnar-thin-films growth schematic

SEM of columnar thin film

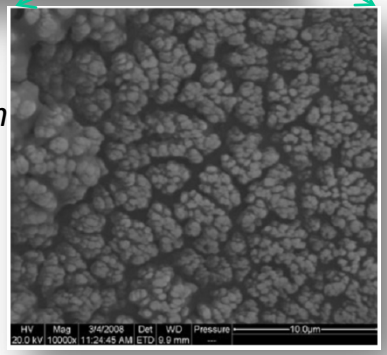

Visualization of fingerprints obtained from physical evidence taken from crime scenes for subsequent comparison typically requires the use of physical and chemical techniques.

We have developed a different vacuum technology: the conformal-evaporated-film-by-rotation technique to deposit dense columnar thin films (CTFs) on latent fingerprints on different types of surfaces.

Thermal evaporation of the solid ChG material leads to the formation of a dense CTF on the fingerprint, thereby capturing the topographical texture with high resolution.

A. Lakhtakia, et al., J. Forensic Sciences, 56, 612-616 (2011).
R. C. Shaler, et al., J. Nanophotonics, 5, 051509 (2011).

A new method has been developed to acquire the topology of latent fingerprints on nonporous ChG surfaces with high resolution.

NNIN Site at Howard University

Development and Investigation of Neural Probes with Microelectrode Array and Vertically Aligned Nanowires

- *Research Goals and Approach*
  - *To aid the pathologic study of virus infection and evaluation of therapeutic treatment in the brain, a chronic and in-vivo sensing method is developed.*
  - *In order to measure neurotransmitter concentration and molecular transport in the brain, nanoelectrodes design is employed, which distinguishes them from 2-dimensional planar electrode configuration.*
  - *The efficacy of the 3-dimensional nanoelectrode is investigated using an electrochemical analysis.*

- *Images of Fabricated Neural Probes on a Flexible Substrate and Vertically Aligned Nanowires*
- *Impedance Analysis of Nanoelectrodes*

Hargsoon Yoon and Courtney S. Smith
Electronics Engineering, Norfolk State University, VA

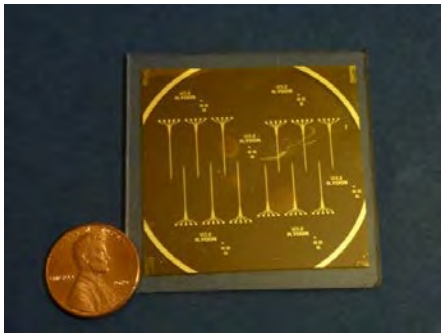

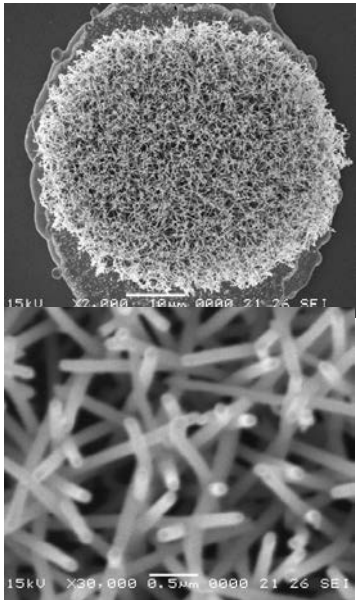

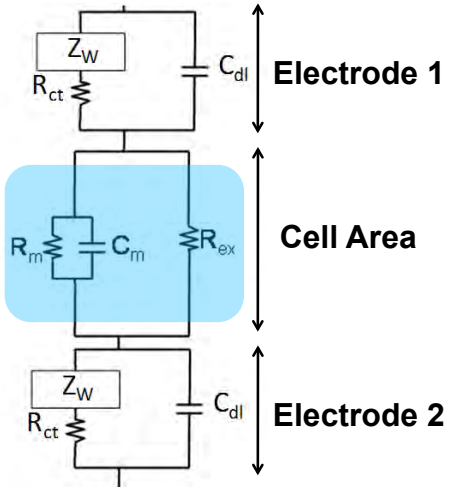

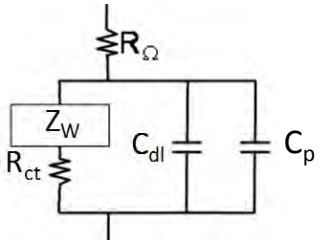

$$C_p = \frac{1}{\omega^{\alpha}\sigma}$$

C_{dl}: Double layer capacitance

Z_w: Warburg Impedance

R_{ct}: Charge transfer resistance

R_m: Cell membrane resistance

C_m: Cell membrane capacitance

Si-Ag Composite Fabrication for Infrared Detector

Significant Findings

Objective:

1. Fabricating an infrared detectors covering three atmospheric windows;
2. Compatible with current processing technology;
3. Easy for integration;

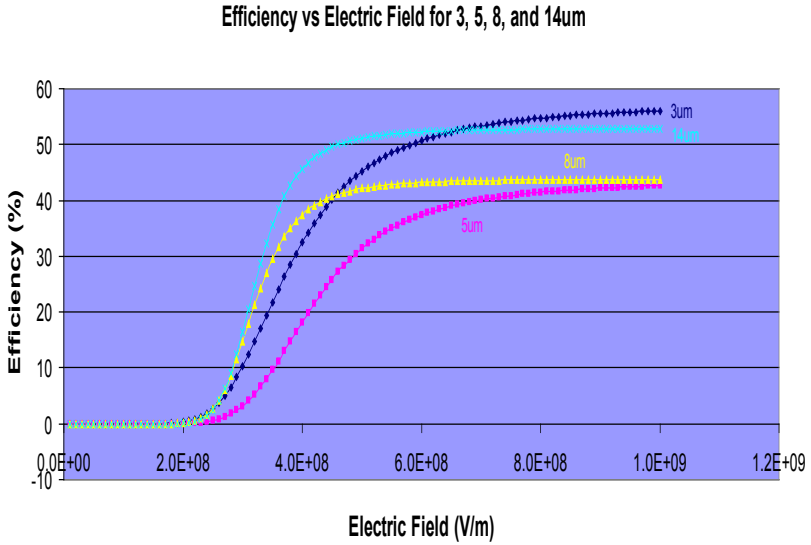

Dr. Chichang Zhang and Clayton W. Bates Jr.
Department of ECE, Howard University, Washington, D.C.

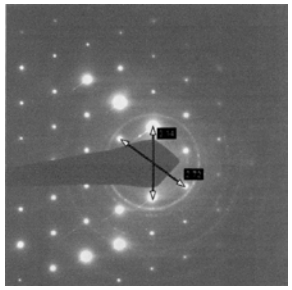

TEM/Electron diffraction pattern for sample Ag/n-Si deposited at 550°C.

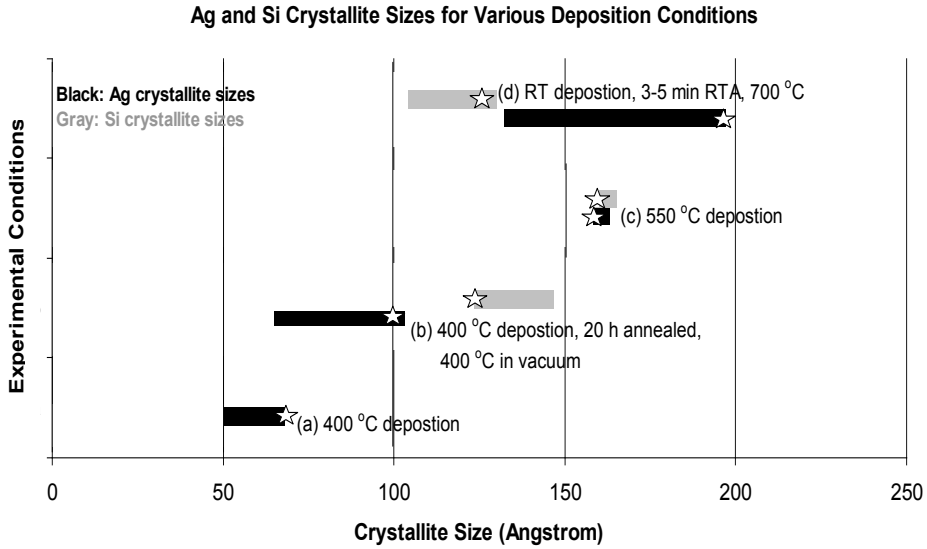

Ag and Si crystallite sizes under various experimental conditions. (a) 400°C deposition; (b) 400°C deposition followed by 400°C 20 hours annealing in vacuum; (c) 550°C deposition; (d) Room temperature (RT) deposition followed by RTA at 700°C for 3-5 minutes. The average crystallites sizes were marked with stars.

HNF-Technical Highlight: Advanced Water Purification Processes to Remove Trace Organics

EPA has identified the need to remove classes of chemical contaminants

- Emerging organic contaminants
- Pharmaceutical and Personal Care Products
- Heavy metals

Jones Group at Howard research group has developed hybrid processes to remove these contaminants

- Modified nanofiltration and reverse osmosis membranes can remove trace concentrations of contaminants with minimal fouling

Integration of nano-silver in the structure of membranes to reduce organic and biological fouling

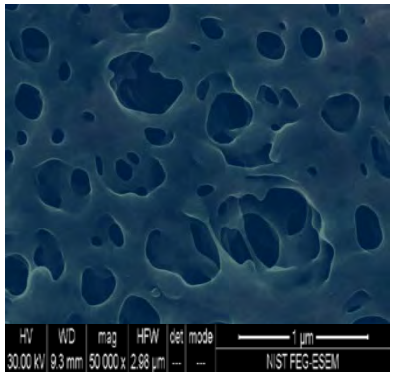

Commercial membrane

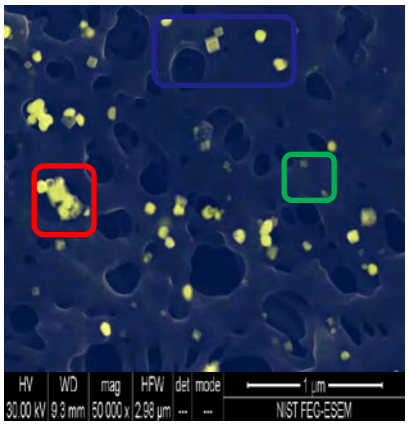

Nano-silver impregnated membrane; Silver particles are in yellow

Biocompatible SiC RF Antenna for In-vivo Sensing Applications

The goal of this research is to develop, fabricate and characterize a fully biocompatible (SiC) RF antenna sensor that can remain functional in the body for years and will not require additional encasing.

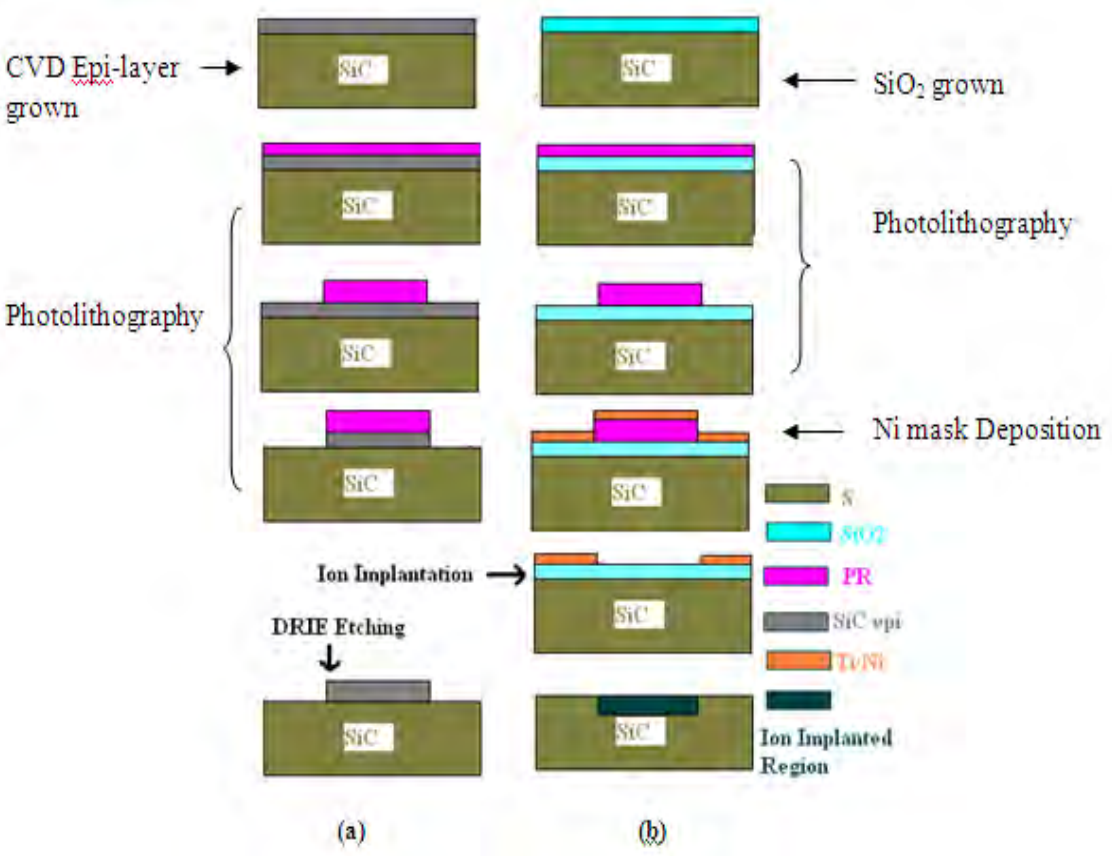

Shamima Afroz , S.W. Thomas
University of South Florida
Work performed at Howard Nanoscale Facility

Modification of sheet metal forming fluids with dispersed nanoparticles for improved lubrication

The tribological properties of dispersions of MoS_2, WS_2, and hBN nanoparticles of varied concentration for metal working fluids applications are studied. The mechanisms by which nanoparticles may contribute to the improved tribological behaviour of these systems are explained in light of the experimental results.

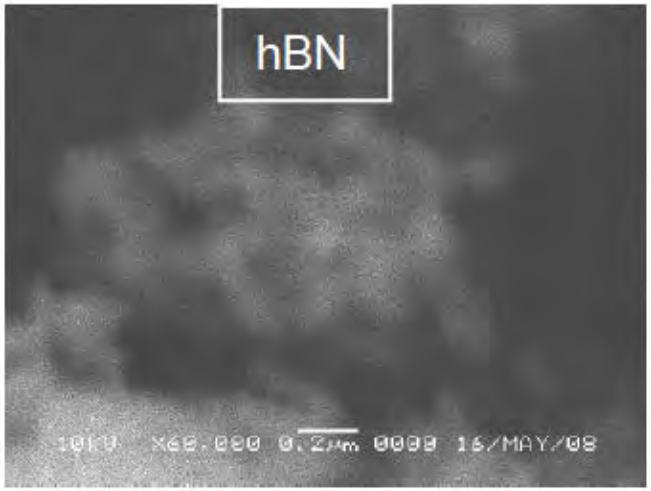

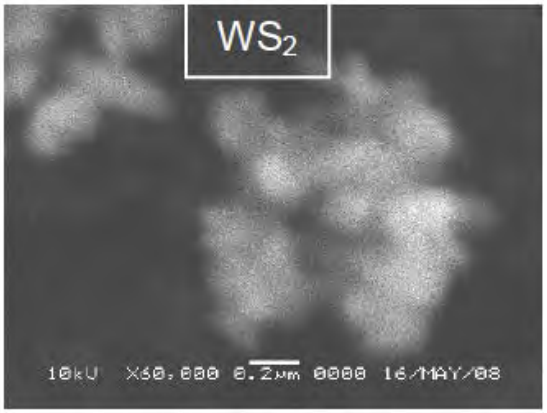

SEM micrographs of MoS2, WS2, and hBN nanoparticles

Mohsen Mosleh, Neway D. Atnafu John H Belk and Orval M. Nobles Howard U. /Boeing Company

Work performed at Howard Nanoscale Facility

Modeling and Simulation of Nanobubbles on Material Substrates

Nanobubbles are extremely small gas bubbles that form at the solid-liquid interface of hydrophobic solids submerged in water. An equivalent effect results from either increasing the strength of the solid or decreasing the surface tension. A model of a substrate formed by layers of materials is proposed to obtain a nanobub-ble with a particular contact angle.

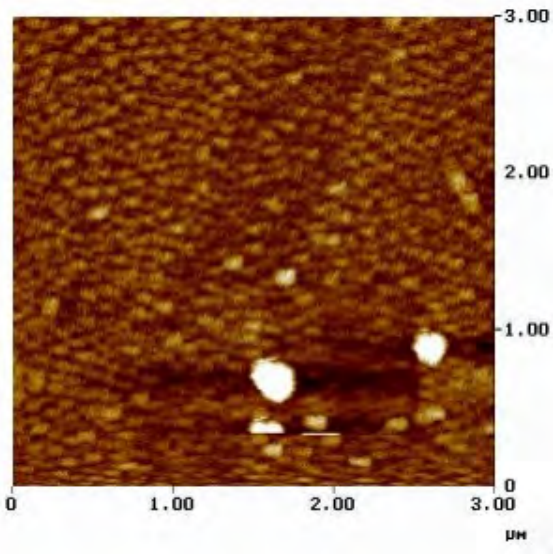

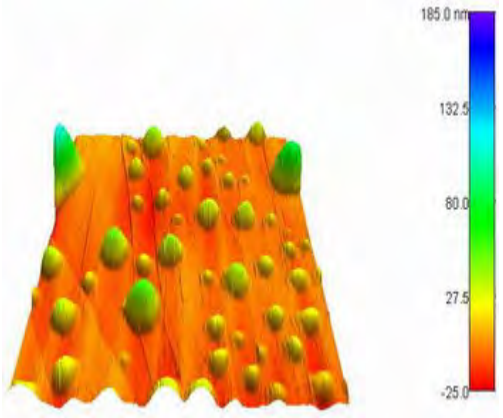

AFM images of nanobubbles on solid substrate

H. Elnaiem , D. Casimir, P. Misra and S.M. Gatica
Howard U
Work performed at the Howard Nanoscale Facility.